Characterisation of ACBD3 and PI4Kβ Expression in Breast Cancer and the Effects of ACBD3 Overexpression

A Thesis Submitted for the Degree of Doctor of Philosophy

By

Jack Houghton-Gisby

Declaration

I declare that the research presented for this thesis is my own work, except where otherwise stated and referenced and has not been submitted for any other degree.

Jack Houghton-Gisby

Acknowledgements

I would Firstly like to thank Breast Cancer Hope and Brunel University London who funded this work. Without them I would not be starting the career I have worked towards for the last 10 years.

This work would not have been possible without the support of many people. I would firstly like to thank my supervisor Dr Amanda Harvey whose insight has been invaluable and who allowed me to pursue questions I found interesting even if it meant straying from the plans we made, I am certainly a better scientist because of you. I must also give special mention to Dr Gudrun Stenbeck and Dr Manos Karteris who have also supported me in the lab and lent some of their vast expertise, thank you.

Thank you Stephen Hare for training me, for being a good friend, and from whom I inherited good practice and lab savvy. Thanks also to everyone else I have met at Brunel, in the lab, office, or otherwise many of whom have become friends and helped me through this project; especially Rachel (my IHC independent scorer), Dorothee, and Rooban, who have liberally shared both knowledge and materials and challenged my understanding of science.

To my partner Jess who supported me moving away to start this doctorate and who would later move her life to join me here, Thank you. We've had many adventures and seismic shifts since I started, and you are probably the person who is most familiar with the findings of this work after my lab group. I promise there is a day coming soon where you don't hear 'ACBD3'.

My Family have been very supportive of me through all of university and especially this PhD, my brother went as far as to read the abstract for a paper I wrote which is commendable given the content. Particularly I need to thank my grandmother Margaret who has been both interested and supportive of the work and is currently fighting breast cancer for the second time in her life. From you I have learnt about a side of breast cancer that cannot be discovered in a laboratory, this work is dedicated to you.

Abstract

Targeted breast cancer treatments are essential for increasing chemotherapy effectiveness whilst simultaneously reducing side effects and are the focus of a whole generation of drug development in cancer and elsewhere.

The *ACBD3* gene encodes an essential structural tether protein of the same name that has an unusually large number of cellular roles, diverse binding partners, and few redundancies. Chromosome 1q is frequently amplified in breast cancer and the *ACBD3* locus (1q42.12) was previously found to be amplified in multiple breast cell lines and primary breast tumours. Previous research found that *ACBD3* mRNA was upregulated in breast tumour tissue matched against adjacent normal tissue and that ACBD3 overexpression promoted cancer stem cell renewal and activated the Wnt/β-Catenin signalling pathway in breast cancer cell lines. Due to the broad functions of ACBD3 and its contextual role in cells it was hypothesised that ACBD3 expression may have other affects in breast cancer.

ACBD3 was overexpressed at the mRNA and protein level in breast cancer patient tumours compared to normal tissue and mRNA expression over the median value was detrimental for breast cancer patient survival, relapse free survival and distant metastasis free survival. IHC staining of breast cancer and normal breast tissue cores found that ACBD3 was highly expressed in epithelial ductal cells. ACBD3 mRNA and protein expression was higher in a panel of breast cancer cell lines compared to a normal like breast cell line and ER+ cell lines had the highest protein expression of ACBD3. ACBD3 mRNA and protein expression was upregulated in a previously engineered T47D everolimus chemotherapy resistant cell, the T47D breast cancer cell line was transfected with eGFP-ACBD3 but this did not affect everolimus resistance. ACBD3 overexpression did increase cell growth and there were also a number of expression changes to oncoproteins. A GOLD domain deletion mutant of ACBD3 was constructed and this led to more oncoprotein expression changes when expressed in the T47D cell line. Transcriptional and translational regulation are sensitive to cell density which has implications for all ex vivo study of ACBD3 and several compounds have been found that augment ACBD3 expression.

ACBD3 was hypothesised to be a marker of progression in breast cancer and may promote a Luminal B pathology over Luminal A. its overexpression increased growth in a Luminal A cell line, increased expression of proteins associated with inflammation and secretion and reduced immunogenic protein expression. Luminal B patients had the largest reduction in relapse free survival when *ACBD3* mRNA

expression was high. ACBD3 expression appears to be a biomarker for breast cancer patient outcomes and may have some validity in predicting response to therapy and was also associated with ER+ and signalling. New mechanisms by which ACBD3 might cause inflammation were determined in addition to known roles for ACBD3 in redox stress and in iron import. ACBD3 also reduced immunogenic proteins when overexpressed.

ACBD3 is certainly associated with worse outcomes and with progression in breast cancer and ACBD3 dependent pathways should be considered as a target for treatment in the future. The consensus of these results agree that ACBD3 expression in breast cancer is associated with characteristics of stemness and that ACBD3 may decrease immune system detection in addition to Wnt signalling.

Conference Presentations and Publications of this work

The research for this thesis was presented at a number of internal conferences. Plans to present this work externally were restricted by the COVID-19 pandemic which was most unfortunate.

A poster presentation of this work won 2nd prize at the 2018 College of Health and Life Sciences PhD Research Conference.

Sections from the introduction chapter of this thesis were used to write a review article that was published in Cancer Studies and Therapeutics. Full reference:

Houghton-Gisby, J. and Harvey, A.J., 2020. ACBD3, its Cellular Interactors, and its role in Breast Cancer. Cancer Studies and Therapeutics, 5(2), pp. 1-7.

Contents

List of Tables

Chapter 1 Introduction

Chapter 2 Materials and Methods

Chapter 5 Examining regulators of ACBD3 and PI4Kβ Expression in Breast Cancer Cell Lines

Chapter 6 ACBD3 Overexpression and Mutation in the T47D Breast Cancer Cell Line

List of Figures

Chapter 1 Introduction

Chapter 2 Materials and Methods

Chapter 3 ACBD3 Bioinformatics and Clinical Outcomes

Chapter 4 ACBD3 Expression in Breast Cancer Cell Lines and Breast Cancer

Chapter 5 Examining regulators of ACBD3 and PI4Kβ Expression in Breast Cancer Cell Lines

Chapter 6 ACBD3 Overexpression and Mutation in the T47D Breast Cancer Cell Line

Chapter 7 Discussion

Chapter 9 Appendix

Abbreviations

17βE2 – 17β-estradiol

1p – Chromosome 1 arm p

1q – Chromosome 1 arm q

3D – 3 dimensional

A – Alanine

aa – Amino acid

AC – Adenocarcinoma

ACB – Acetyl CoA binding

ACBD – Acyl CoA Binding Domain containing protein

ACBP – Acyl CoA binding protein

ACC – Adrenocortical carcinoma

***ACTB* –** beta actin (gene)

ACTH – Adrenocorticotropic hormone

ADP – Adenosine diphosphate

ALDH – Aldehyde dehydrogenase

APS – adapter protein with a pleckstrin homology and Src homology 2 domain

ATP – Adenosine triphosphate

ATP5B – Adenosine triphosphate synthase F1 subunit beta

AKT – Protein kinase B

ARF1 – Adenosine diphosphate-ribosylation factor 1

ATM – ataxia-telangiectasia mutated

Axl – anexelekto protein

BAD – Bcl-2-associated death promoter

BCL-x – B-cell lymphoma-extra large

BLCA – Bladder urothelial carcinoma

***BLZF1* –** Basic Leucine Zipper Nuclear Factor 1 (gene of GOLGIN45)

BOLERO – Breast cancer trials of oral everolimus

BPA – Bisphenol A

BRCA – Breast invasive carcinoma

BRCA1 – Breast cancer type 1 susceptibility protein

BRCA2 – Breast cancer type 2 susceptibility protein

C3G – Guanyl-nucleotide exchange factor, isoform L

CA^{2+} – Calcium

CamKII – Calcium/calmodulin-dependent protein kinase

cAMP – cyclic adenosine triphosphate

CAP – Catabolite activator protein

CBL – Castitas B-lineage lymphoma proto oncoprotein

CD34 – Cluster of differentiation 34 protein

CESC – Cervical squamous cell carcinoma and endocervical adenocarcinoma

CDH1 – Cadherin 1

CDK1 – Cyclin Dependent Kinase 1

cDNA – complementary deoxyribonucleic acid

CEACAM-5 – Carcinoembryonic antigen-related cell adhesion molecule 5

CEBPB – CCAAT Enhancer Binding Protein Beta)

CHEK2 – Checkpoint Kinase 2

ChIP-Seq – Chromatin immunoprecipitation Sequence

CHOL – Cholangiocarcinoma

c-MET – Mesenchymal epithelial transmission tyrosine kinase receptor

CMF – Cyclophosphamide, methotrexate, Fluorouracil

COAD – Colon adenocarcinoma

COPI – Coat protein I

CRISPR – Clustered regulatory interspaced short palindromic repeats

CSC – Cancer stem cell

cT – Cycle threshold

CTCF – CCCTC-binding factor

***CTNNB1* –** beta catenin (gene)

CVB3 – Coxsackie virus B3

CYC1 – Cytochrome C1

DBI – Diazepam binding inhibitor (also known as ACBD1)

***delins* –** Deletion insertion

DEXRAS1 – Dexamethasone-induced Ras-related protein 1

DLBC – Lymphoid neoplasm diffuse large B cell lymphoma

DMEM – Dulbecco's modified eagle's medium

DMFS – Distant metastasis free survival

DMSO – Dimethyl sulfoxide

DMT1 – Divalent metal transporter 1

DNA – deoxyribonucleic acid

E – Glutamic acid

ECI2 – Enoyl-CoA Delta Isomerase 2 (also known as ACBD2)

EcoRI – E.coli restriction enzyme 1

eGFP – Enhanced green fluorescent protein

EIF4A2 – Eukaryotic translation initiation factor 4A2

EMT – Epithelial to mesenchymal transmission

ER – Oestrogen receptor

***ERBB2* –** Human epidermal growth factor receptor 2 (gene)

ERK – Extracellular signal-regulated kinase

ESCA – Oesophageal carcinoma

ESRRG – Oestrogen related receptor gamma

EveR – Everolimus resistant

F – Phenylalanine

FASN – fatty acid synthase

FBS – Foetal bovine serum

FEC – Fluorouracil, epirubicin, cyclophosphamide

FEC-T – Fluorouracil, epirubicin, cyclophosphamide, docetaxel

FGR basic – Feline Gardner-Rasheed sarcoma

FOXA1 – Forkhead box A1

FOXA2 – Forkhead box A2

FOXC2 – Forkhead box C2

GABA – Gamma aminobutyric acid

GAP – GTPase-activating protein

GAPDH – Glyceraldehyde-3-Phosphate Dehydrogenase

GBM – Glioblastoma multiforme

GCP60 – Golgi Resident Protein 60 (alias for ACBD3)

GDI – GDP dissociation inhibitors

GDP – Guanosine diphosphate

GEPIA – Gene expression profiling interactive analysis

GNST – Genistin

GTP – Guanosine triphosphate

GI60 – Growth inhibition 60%

GLUT – Glucose transporter protein

GM130 – Golgin subfamily A member 2 (also known as GOLGA2)

GOLD – Golgi Dynamics

GOLGB1 – Golgin subfamily B member 1

***GORASP2* –** Golgi reassembly stacking protein 2 (gene of GRASP55)

GRASP – Golgi reassembly stacking proteins

GSEA – Genome set enrichment analysis

GSV – Glucose transporter type 4 storage vesicles

HD – Huntington's disease

HER2 – Human epidermal growth factor receptor 2

HIF1 – Hypoxia inducible factor 1

HIST2H2BE – Histone H2B type 2-E

HNSC – Head and neck squamous cell carcinoma

HO-1 – Haem oxygenase 1

HRT – Hormone replacement therapy

HTT – Huntingtin

I – isoleucine

IC50 – Inhibitory concentration 50%

ICAM-1 – Intracellular adhesion molecule 1

IDC – Invasive ductal carcinoma

IGF – Insulin like growth factor

IGF1R – Insulin like growth factor 1 receptor

IHC – Immunohistochemistry

IL – Interleukin

IL-2 RA – interleukin-2 receptor alpha

IMM – Inner mitochondrial membrane

IR – Insulin receptor

IRE – Iron response element

JEM1 – Also known as GOLGIN45

JUN – Ju-nana protein

K – lysine

K381_R528delinsXX – deletion of amino acids 381 to 528 two stop codons inserted

kDa – kilodalton

KDM2B – Lysine demethylase 2B

KICH – Kidney chromophobe

KIRC – Kidney renal clear cell carcinoma

KIRP – Kidney renal papillary cell carcinoma

KLF9 – Krüppel Like Factor 9

Kpn1 – *Klebsiella pneumoniae* nuclease 1

KQ117AA – lysine 117 and glutamine 118 mutation to alanine and alanine

LAML – Acute myeloid leukaemia;

LD50 – Lethal dose 50%

LGG – Brain lower grade glioma

LIHC – Liver hepatocellular carcinoma

LH – luteinizing hormone

LUAD – Lung adenocarcinoma

LUSC – Lung squamous cell carcinoma

MESO – Mesothelioma

mRNA – messenger ribonucleic acid

MEK1 – MAPK ERK kinase

MT1-MMP – Membrane type 1 matrix metalloprotease

mTOR – Mammalian target of rapamycin

MCP – Monocyte Chemoattractant Protein

MNDA – N-methyl-D-aspartic acid

MST1 – Macrophage stimulating 1

NBEC – Normal breast epithelial cells

NMR – Nuclear magnetic resonance

NMT – N-myristoyltransferase

nNOS – Neuronal nitric oxide synthase

NOX5 – NADPH oxidase

NRAS – Neuroblastoma cell rat sarcoma protein

N/S – Not significant

NUMBL – NUMB-like

OMM – Outer mitochondrial membrane

OS – Overall survival

OV – Ovarian serous cyst-adenocarcinoma

P450scc – (gene CYP11A1)

P53 – Tumour protein 53

PAAD – Pancreatic adenocarcinoma

PALB2 – Partner and localiser of BRCA2

PAP7 – PBR/PKA-RI-alpha-associated protein (alias for ACBD3)

PBS – Phosphate buffered Saline

PCR – Polymerase chain reaction

PCPG – Pheochromocytoma and paraganglioma

PDGF-AA – platelet derived growth factor-AA

PECAM-1 – Platelet And Endothelial Cell Adhesion Molecule 1

PH – Pleckstrin homology

PI – Phosphatidylinositol

PI3K – Phosphoinositide 3-kinase

PI(4)P – Phosphatidylinositol 4-phosphate

PI4Kβ – Phosphatidylinositol 4 kinase beta (also known as PI4KIIIβ)

PIP5K1A – Phosphatidylinositol-4-phosphate 5-kinase type 1 alpha

PIST – PDZ interacting specifically with TC10

PKA – Protein kinase A

PKCA – Protein kinase C alpha

PKN2 – PKC-related serine/threonine-protein kinase

PLK1 – Polio like kinase 1

polyHEMA – poly-2-hydroxyethyl methacrylate

PPNAD – primary pigmented nodular adrenocortical disease

PR – Progesterone receptor

PRAD – Prostate adenocarcinoma

PTEN – Phosphatase and tensin homolog deleted on chromosome 10

Q – Glutamine

QPCR – Quantitative polymerase chain reaction

QPS – Glutamine penicillin streptomycin

R – Arginine

RAB4 – Ras-related protein 4A

RAS – Rat sarcoma protein

RCN – Relative cell number

READ – Rectum adenocarcinoma

RET – Rearranged during transfection proto-oncogene

RFS – Relapse free survival

Rhes – Ras homolog enriched in striatum

RNA – ribonucleic acid

ROS – Reactive oxygen species

SacI – *Streptomyces achromogenes* restriction enzyme 1

SAM68 – SRC associated in mitosis of 68 kDa

SARC – Sarcoma

SCV – Salmonella-containing vacuoles

SD – Standard deviation

SDM – site directed mutagenesis

SDS-PAGE – sodium dodecyl sulfate - polyacrylamide gel electrophoresis

siRNA – short interfering ribonucleic acid

SIRT1 – Silent mating type information regulation 2 homolog

SKCM – Skin cutaneous melanoma

SLC35A1 - Solute carrier family 35 member A1

SMURF2 – SMAD specific E3 ubiquitin protein ligase 2

SPARC – Secreted protein acidic and cysteine rich

SPI-2 T3SS – Salmonella pathogenicity island 2 type III secretion system

SRB – Sulforhodamine B

SRSF2 – Serine and arginine rich splicing factor 2

Src – Sarcoma protein

SREBP – Sterol regulatory element binding protein

SseF – Secretion system effector F

SseG – Secretion system effector G

SSP – Signaling pathways project

STAD – Stomach adenocarcinoma

StAR – steroidogenic acute regulatory

START – (StAR)-related lipid transfer

STK11 – Serine/Threonine Kinase 11

TBC1D22 – TBC domain 1 containing protein 22

TBS-T – Tris buffered saline - Tween20

TC10α – Ras Homolog Family Member Q

TCF4 – Transcription factor 4

TF – Transferrin

TGCA – The cancer genome atlas program

TGCT – Testicular germ cell tumours

TGN – Trans Golgi network

THCA – Thyroid carcinoma;

THYM – Thymoma

Tie-2 - Angiopoietin receptor

TMED8 – trans-membrane p24 trafficking protein 8

TMEM41B – Transmembrane protein 41B

TNBC – Triple negative breast cancer

TNM – Tumour size, node invasion, metastasis (tumour grading system)

TOP1 – DNA topoisomerase 1

TSPO – transporter protein

TUG – Tether containing UBX domain for GLUT4

UBC – Ubiquitin C

UBX – Ubiquitin regulatory X protein

UCEC – Uterine corpus endometrial carcinoma

UCS – Uterine carcinosarcoma

UK – United Kingdom

UNC45A – Unc-45 myosin chaperone A

UVM – Uveal melanoma

VAPB – Vesicle associated membrane protein-associated protein B

VDAC1 – Voltage dependent anion channel 1

VEGF – Vascular endothelial growth factor

VPS36 - Vacuolar protein sorting 36 homolog

vRNA – Viral ribonucleic acid

XhoI – *Xanthomonas holcicola* restriction enzyme 1

Wnt – Wingless Int-1 protein

WT – wildtype

***YWHAZ* -** Tyrosine 3-Monooxygenase/Tryptophan 5-Monooxygenase Activation Protein Zeta (gene)

Chapter 1

Introduction

1.1 Breast Cancer

1.1.1 History

Breast cancer is one of the earliest cancers to be documented and was known to medicine over 5,000 years ago where it was acknowledged to be untreatable and fatal (Breasted 1930). Through the 1800s the practice of mastectomy: removal of the breast tissue, was refined and it became popular to cut away tissue to the extent that breast lymph, surrounding muscle and sometimes chest cavity wall would be excised following the hypothesis that to cut more would cure more (Halsted 1907). This radical mastectomy would be commonplace for nearly 100 years until it was shown that a radical mastectomy provided no benefit in survival rates over a lumpectomy. The lumpectomy or wide local excision surgery aimed to cut away only the tumour and a border of healthy breast tissue and keep as much breast as was feasible, this was combined with radiotherapy and is still standard practice when cancer is confined to the breast.

The subtyping of breast cancers and discovery that breast cancer cells can express: oestrogen receptors (ER), human epidermal growth factor 2 receptors (HER2), and progesterone receptors (PR) alone, in combination or not at all led to breakthroughs in targeted drug design and targeted therapies (Walt, AJ et al. 1976, Wei, Sheridan et al. 1987, Slamon, D. J., Clark et al. 1987). The monoclonal antibody drug trastuzumab against the HER2 receptor is one of these targeted therapies and can significantly shrink HER2+ breast tumours and cells at secondary sites by labelling them for immune destruction (Slamon, D. J., Leyland-Jones et al. 1998). This has led to increased survival for HER2+ breast cancer patients. Anti-hormone therapy pre- and post-surgery for oestrogen and progesterone receptor positive cancers also improved patient outcomes. Other drugs followed as the understanding of cancer evolved with the publication of the Hallmarks of Cancer being a turning point in how cancer is viewed and should be attacked pharmacologically (Hanahan, Weingberg 2000, Hanahan, Weinberg 2011). Many modern drugs were developed based on that understanding, including those that target the metabolic and signalling

pathways of cancer cells as well as DNA replication apparatus (Bjornsti, Houghton 2004, Kirchner, Meier-Wiedenbach et al. 2004, Saran, Foti et al. 2015).

Alongside drug advancement came the understanding that certain genetic mutations could increase susceptibility to certain cancers. Most well-known to the wider world are mutations of the genes *BRCA1* and *BRCA2*, either of which increase lifetime risk of breast cancer (72% and 69% rate of occurrence by age 80 respectively) (Kuchenbaecker, Hopper et al. 2017). This has helped tailor therapy regimes and assess the risk of recurrence. *BRCA1* and *BRCA2* mutant carriers are likely to have an earlier onset of breast cancer and benefit from full mastectomy over lumpectomy.

1.1.2 Statistics

Breast cancer is the most common cancer in women with one in eight developing breast cancer in their lifetime in the UK (Cancer Research UK 2017). Approximately 55,000 women and 350 men are diagnosed with invasive breast cancer in the UK each year. Breast cancer treatments have a large success rate (proportional to how early the cancer is discovered) with 78% of female patients surviving for over ten years but new treatments are in decline with triple negative breast cancer patients having little improvement in patient outcomes for decades (Won, Spruck 2020). Breast cancer incidence in the UK is increasing for females (25% over the last three decades, 6% in the last ten years) meaning that treatment of the same efficiency results in more total patient deaths now than ten years ago, without improved treatment there will be more deaths per year in the future. 11,563 deaths in the UK were attributed to breast cancer in 2016 and prevention is inarguably better than cure, approximately 23% of breast cancer occurrences are preventable with obesity and alcohol being the two largest modifiable risk factors (Brown, Rumgay et al. 2018, Cancer Research UK 2017). Tobacco smoking, lack of physical exercise, exposure to radiation, oral contraceptives and hormone replacement therapy (HRT) are also considered preventable risk factors for developing breast cancer (Cogliano, Baan et al. 2011, World Cancer Research Fund / American Institute for Cancer Research 2018).

1.1.3 Breast Cancer Subtypes and Pathology

Breast cancer prognosis and progression varies considerably based on the presence or absence of oestrogen receptor (ER), progesterone receptor (PR), and human epidermal growth factor 2 receptor (HER2), and on their pathology (Lamb, Vanzulli et al. 2019, Ross-Innes, Stark et al. 2012, Inic, Zegarac et al. 2014, Russo, Russo 2006, Won, Spruck 2020). Receptor status and pathology are used to divide breast cancers into distinct subtypes that offer robust prediction of effective treatments and outcomes.

The Luminal A subtype has a similar gene expression profile to luminal breast cells and are generally positive for ER and/or PR expression (Ciriello, Gatza et al. 2015). Luminal A has the best prognosis of all subtypes (Carey, Perou et al. 2006). Patients with Luminal B breast cancers have a worse prognosis than those with Luminal A, and tumours have a higher expression of proliferative markers but are otherwise similar to the luminal A subtype (Inic, Zegarac et al. 2014).

The HER2+ subtype expresses HER2 surface receptor and proteins in the HER2 pathway; patients with HER2+ subtype cancers have higher grade tumours and worse prognosis than patients with Luminal type cancers but also have effective specific therapies in the form of anti-HER2 antibodies and HER2 inhibiting drugs (Slamon, D. J., Leyland-Jones et al. 1998, Slamon, Dennis J., Leyland-Jones et al. 2001, Carey, Perou et al. 2006, Eiger, Agostinetto et al. 2021).

Basal-like breast cancers are often triple negative meaning they do not express ER, PR, or HER2. Patients with basal-like breast cancers have the poorest prognosis of breast cancer subtypes (Carey, Perou et al. 2006, Liu, Y., Tamimi et al. 2011). The expression profile of basal-like breast cancers is similar to basal epithelial breast cells with high levels of proliferative markers and the fewest targeted therapy options. Triple negative breast cancers (TNBC) are likely to be higher grade than other breast cancer types, tend to be more aggressive, and are more likely to metastasise and recur (Cancer Research UK 2020). Lack of receptor markers means that TNBC has the fewest targeted treatment options and means the tumours are not as dependent on exogenous endocrine stimulation so are more likely to be self-sustaining in proliferative signalling (a classic hallmark of cancer) (Won, Spruck 2020, Hanahan, Weinberg 2011). Patients are more likely to have TNBC if they are under 50.

Staging and grading of breast cancers follows the same definition as other cancers and is summarised in Table 1.1 and Table 1.2 (Cancer Research UK 2020, Amin, Edge et al. 2017).

Stage	features
0	Ductal carcinoma *in situ*. A pre-invasive cancer refined to the ducts that has not spread into surrounding breast tissue.
1	Small tumour located entirely within the breast tissue or local lymph node.
2	Cancer is located in the breast tissue and/or local lymph nodes.
3	Cancer that has spread from the breast to local lymph nodes and/or breast skin and/or the chest wall. This is a locally advanced cancer.
4	Breast cancer that has spread to more distant locations in the body (secondary cancers, metastasis). The lungs are the most common site of metastasis in patients with brain, bone, and liver also common.

Table 1.1 – A brief description of breast cancer features by stage.

Grade	Appearance
1	Slow growing cells that look similar to normal breast cells. Ductal cancers form small tubules whilst lobular cancers form cords. This grade is associated with best prognosis
2	Cells are less differentiated than grade 1 and do not resemble normal breast cells.
3	Cells are not differentiated and are faster growing. They do not resemble normal breast cells, they spread quickly and are associated with worse prognosis.

Table 1.2 – A brief description of breast cancer appearance by grade.

1.1.4 Treatment

In the United Kingdom breast cancer treatment will commonly involve surgery, either a lumpectomy where the tumour is excised along with a border of healthy breast tissue or a full mastectomy where all breast tissue is removed from one or both breasts. Patient genetics may inform this decision and *BRCA1* and *BRCA2* mutant carriers will benefit from full mastectomy of both breasts. For cancer in stages 0-2, surgery followed by radiotherapy of the breast may be the only treatment necessary

to achieve remission but patients with larger early stage cancers may have chemotherapy pre-surgery to shrink the tumour before excision and this is especially effective with trastuzumab treatment in HER2+ patients (National Institute for Health and Care Excellence 2018). Patients with ER+ or PR+ cancer usually have hormone therapy for at least five years after surgery and HER2+ presenting cancer patients will have at least one year of trastuzumab (given at three-week intervals). Other chemotherapy may be given if the tumour was larger than 1cm or was a high grade. A local sentinel lymph node biopsy will be carried out after surgery to rule out the spread of the primary tumour.

Stage 3 breast cancer treatment for non-inflammatory cancers is similar to lower stages but will most likely involve chemotherapy before and/or after surgery.. Inflammatory breast cancer patients will usually have neo-adjuvant chemotherapy prior to surgery to reduce swelling and destroy any metastatic cells. Mastectomy is most common for inflammatory breast cancer and is followed by radiotherapy.

For patients with stage 4 breast cancer, in addition to the treatments for previous stage, hormone therapy and antibody therapies can be effective at controlling secondary cancers if they express HER2 (trastuzumab) or ER (aromatase inhibitors, tamoxifen), (National Institute for Health and Care Excellence 2017). Chemotherapies may be used for hormone negative cancers and metastatic cancer of the lungs and liver, or if patients are not responsive to anti-hormone therapy. Radiotherapy is used for metastatic cancer of the brain, bone, and skin around the breast. Palliative care is also employed to ease the symptoms of advanced cancers.

According to the 2017 clinical guidelines for the management of breast cancer, standard breast cancer chemotherapy regime choices on the NHS in the UK include one of:

- Fluorouracil (600mg/m^2), Epirubicin (75mg/m^2) and Cyclophosphamide (600mg/m^2) for six cycles (FEC).
- Doxorubicin (60mg/m^2) and Cyclophosphamide (600mg/m^2) (AC).
- Fluorouracil (600mg/m^2), Epirubicin (75mg/m^2),Cyclophosphamide (600mg/m^2) for six cycles followed by Docetaxel (100mg/m^2) for two to three cycles (FEC-T).

When anthracyclines cannot be administered the following regimes are also approved:

- Cyclophosphamide (600mg/m^2), Methotrexate (40mg/m^2) and Fluorouracil (600mg/m^2) for six cycles (CMF).
- Docetaxel (75mg/m^2) and Cyclophosphamide (600mg/m^2) for four cycles.

Node positive patients should be considered for a taxane containing regime and palliative chemotherapeutics include: Capecitabine, Doxorubicin, Epirubicin, Paclitaxel, Taxotere, and Vinorelbine as single agents or in combination with Trastuzumab (for HER2+ cancers).

The antineoplastic drug everolimus may be given in conjunction with exemestane for first or second line treatment for post-menopausal metastatic breast cancer patients that are ER+ and HER2- (NHS England 2018, Hortobagyi 2015). Everolimus (brand name Afinitor) is an mTOR inhibitor rapalogue, initially approved as an immunosuppressant and later (2012) for use in breast cancer. The use of everolimus in breast cancer was evidenced by the BOLERO-2 (breast cancer trials of oral everolimus) phase III clinical trial that combined everolimus with exemestane for patients that had previously received letrozole or anastrozole. Patients treated with everolimus and exemestane in combination had significantly increased progression free survival (6.9-10.6 months), compared to exemestane with placebo treated patients (2.8-4.1 months) (Baselga, Campone et al. 2012, Beaver, Park 2012, Dorris, Jones 2014).

1.1.5 Breast Cancer Genetics

Familial history often influences screening for breast cancer but less than 30% of breast cancers identified through family history are found to have high penetrance alleles for breast cancer risk. Despite their rarity, these minor alleles can infer up to an 80% lifetime risk of breast cancer and are associated with earlier onset in many cases. In addition to the previously described *BRCA1* and *BRCA2* mutant alleles, *PTEN*, *P53*, *CDH1*, STK11, *ATM*, *PALB2*, and *CHEK2* all have rare alleles that confer risk to breast cancer with varying penetrance (Tung, Lin et al. 2016, Kuchenbaecker, Hopper et al. 2017, Filippini, Vega 2013, Ngeow, Sesock et al. 2017, Corso, Intra et al. 2016, Ciriello, Gatza et al. 2015, Petridis, Shinomiya et al. 2014, Masciari, Larsson et al. 2007, Lee, D. S., Yoon et al. 2012, Moran, Nikitina et al. 2017, Lipsa, Kowtal et al. 2019).

ERBB2, which encodes the HER2 receptor, has several common polymorphisms and some of these may affect risk of breast cancer and/or are differentially expressed in patients that are heterozygous for the *ERBB2* aa655 variants (Puputti, Sihto et al. 2006, Pinto, Vasconcelos et al. 2004, Montgomery, Gertig et al. 2003, Watrowski, Castillo-Tong et al. 2015). Women who were heterozygous or homozygous for the valine 655 allele over the isoleucine 655 allele had increased risk and earlier onset of breast cancer, and had less disease free survival when their breast cancer was HER2+ (Lee, S. C., Hou et al. 2008, Han, Diao et al. 2014, Krishna, Chaudhary et al. 2018). The cause of increased risk when HER2 carries this polymorphism is not known but HER2 is known to heterodimerise with IGF-2 to overcome anti HER therapies and HER2 mutations could affect binding affinity or specificity for IGF-2 or other transmembrane receptors (Chan, J. Y., LaPara et al. 2016, Lu, Y., Zi et al. 2001, Nahta, Yuan et al. 2005).

1.1.6 Chromosome 1 and Breast Cancer

Somatic gene mutations in patients and dysregulation of genes play a much larger role in the majority of breast cancers, which are not caused by high penetrance risk alleles. Some of this dysregulation can be attributed to chromosomal level changes and chromosome 1 in particular undergoes changes in breast cancer, typically deletions of 1p and amplification of 1q (Bièche, Champème et al. 1995, Orsetti, Nugoli et al. 2006, Tomasetto, Régnier et al. 1995, Goh, Feng et al. 2017).

Chromosome 1 arm q is frequently amplified in breast cancer and may even be the most common defining feature of these cancers (Soloviev, Esteves et al. 2013). *ARF1* and *RAB4* are located at 1q42.13 and were both found to be significantly overexpressed at the mRNA level in breast cancer. ARF1 (ADP-ribosylation Factor 1) and RAB4 (RAS related protein 4a) are both observed to have an effect in breast cancer. RAB4 in conjunction with RAB5 promotes and drives metastasis by facilitating the formation of cellular structures that make contact with and can degrade extracellular matrix (invadosomes) containing (MT1-MMP) and β3 integrin which together degrade the extracellular matrix, a process vital for cancer invasion and metastasis (Frittoli, Palamidessi et al. 2014). RAB4 is overexpressed in breast cancers and unsurprisingly associated with increased cell motility, it is one of many RAS related proteins that has clinical significance in cancer (Tzeng, Wang 2016). ARF1 is the most amplified gene of the ADP-ribosylation factor family in breast cancers and its amplification is associated with increased gene transcription and

worse prognosis for patients (Xie, Tang et al. 2016). ARF1 inhibition prevents metastasis of tumour xenografts in immunodeficient mice and is replicable in zebrafish models of breast cancer metastasis.

The *ACBD3* gene is located on chromosome 1 arm q (1q42.12) adjacent to *ARF1* and *RAB4* (1q42.13) in the middle of a large region of gain for breast cancers (Orsetti, Nugoli et al. 2006). Orsetti et al mapped the frequency at which regions of arm 1q were amplified or deleted in tumours and cell lines. The 1q42.12 locus was found to be amplified in eight different cell lines (BRCAMZ01, BT20, HCC2218, MDAMB436, MDAMB453, SUM149, ZR751 and ZR7530) and six out of twenty-five primary tumours (Orsetti, Nugoli et al. 2006). Loss of region 1q42.12 was seen only in one cell line (UACC812) where the terminal ~38 megabases of arm 1q were deleted and loss of 1q42.12 was not observed in any primary tumour samples. RNA expression levels of genes or groups of genes on arm 1q were analysed by a cDNA array to find regions of gain. 1q42.12 is located in the middle of a region of gain coined G7, the largest region of gain (in bases) on chromosome 1.

The function and cellular importance of ACBD3 are understudied compared to other proteins that make as many interactions, in as many pathways as ACBD3 does and ACBD3 overexpression has recently been associated with poor breast cancer patient prognosis and the renewal of cancer stem cells (Huang, Y., Yang et al. 2018). Huang et al (2018) propose that ACBD3 maintains the cancer stem cell pool in breast cancer and ACBD3 in known to participate in preventing differentiation. *ACBD3* proximity to *ARF1* and *RAB4* may confer a huge selective advantage to breast cancer cells with amplifications of this locus imbuing these cells with both survival and invasive advantages (Zhou, Atkins et al. 2007).

1.2 ACBD3

ACBD3 was first discovered as an interactor of GOLGB1, named GCP60 and independently found to be an interactor of the mitochondrial translocator protein TSPO and protein kinase A and named PAP7. ACBD3 has had several names, each of which captured a distinct aspect of its diverse function (Sohda, Misumi et al. 2001, Li, H., Degenhardt et al. 2001). Ultimately it was renamed as Acetyl CoA Binding Domain containing protein 3, or ACBD3, by the HUGO gene nomenclature committee reflecting its functional groups and protein family rather than any particular role, of which there are many (www.genenames.org). The ACBD family contains seven proteins (1-7) which all contain the Acyl-CoA binding (ACB) domain.

1.2.1 Functional Domains

In addition to the acyl CoA binding domain at its N-terminus, ACBD3 contains a Golgi dynamics (GOLD) and a glutamine rich Q domain as well as a proline rich region (Figure 1.1)(Klima, Tóth et al. 2016). The GOLD domain is found in Golgi proteins and lipid trafficking proteins and makes up the C-terminus of ACBD3 (aa384-526). It is a beta strand rich domain and is responsible for ACBD3 localization to the Golgi via direct interaction with GOLGB1 (Sohda, Misumi et al. 2001). ACBD3 is a largely unstructured or loosely structured protein, as many linkers are, and of all the recognisable domains only the GOLD domain structure has been solved by X-ray crystallography with the rest of ACBD3 being modelled by NMR and predictive modelling software (Figure 1.1).

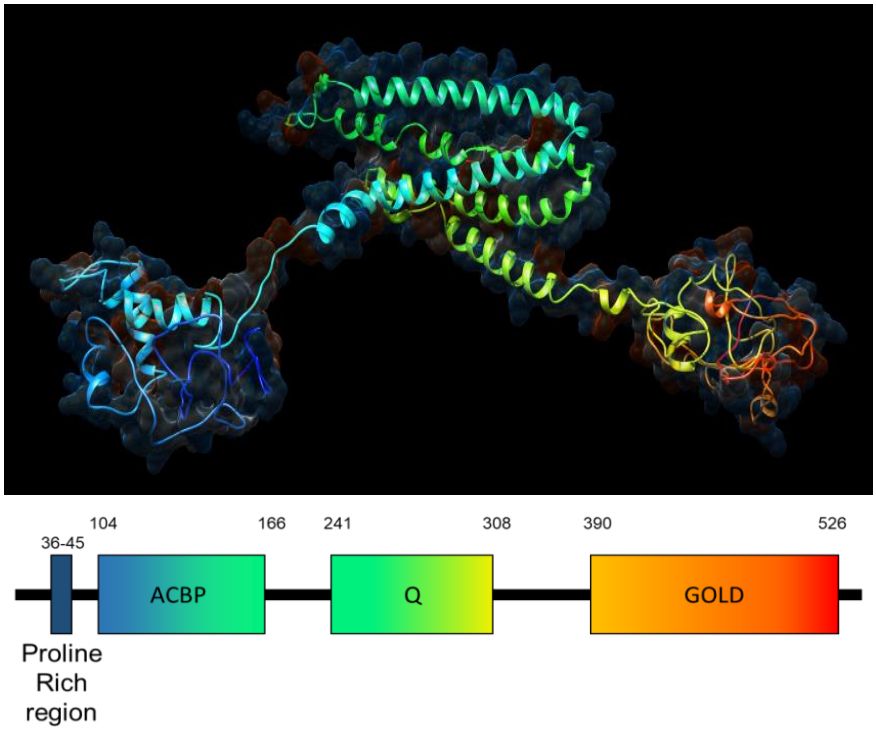

Figure 1.1 - Predicted 3D structure of human ACBD3. Modelled by Phyre2 software using the primary amino acid sequence which agrees strongly with crystal structures of individual ACBD3 domains and related proteins (Kelley, Mezulis et al. 2015). From the N-terminus in blue to the C-terminus in red ACBD3 clearly contains 3 domains: the ACBP domain, the Q domain and the Golgi dynamics (GOLD domain) respectively connected by flexible linkers. The N-terminus also contains a proline rich region and two cryptic nuclear localisation sequences ($ER_4E_4RERLQKE_3KR_3$) between the ACB and GOLD domains. Supporting the nuclear localisation motif there are also nine DNA binding motifs (E/DR_nED) between the ACB domain and Q domain (light blue) of ACBD3. The hydrophilic surface of acbd3 has been superimposed on ACBD3 showing the electrostatic charge of the protein model with red depicting negative charge and blue depicting positive charge.

The Q domain is a glutamine rich region (aa241-308) which forms a long loop made of alpha helices. The N-terminus of PI4KB extends through this loop to interact with ACBD3 at the Golgi membrane and is supported by Rab11 (Figure 1.1, Figure 1.2) (Klima, Tóth et al. 2016). The N-terminal ACB domain is part of a family that binds Acyl CoA and Palmitoyl CoA but the function of this domain in ACBD3 is unclear. To the N-terminus of the ACB domain is a proline rich region (aa21-60) which is indicative of protein-protein interaction sites and may complement the ACB domain which, as a family, is often found paired with protein-protein interaction domains such as the Pleckstrin homology domain (PH) and the Src homology domain.

ACBD3 has no reported function in the nucleus but is known to have a signalling role in mitosis (Zhou, Atkins et al. 2007). Despite this, human ACBD3 encodes two nuclear localisation signals that follow the motif: $ER_4E_4RERLQKE_3KR_3$ and nine individual DNA binding motifs: E/DR_nED (based on primary structure predictions).

1.2.2 ACBD3 in Breast Cancer

Chromosome 1 arm q contains many genes important in cancer progression or tumour suppression: *NRAS*, *JUN*, *MYCL*, *ESRRG*, *ARF1* and *RAB25* are amongst the best known. There are however many more 1q genes that are amplified in breast cancer with deletions strikingly rare despite common deletions in the p arm. Some of these genes (*PI4Kβ*, *PIP5K1A* and *HIST2H2BE*) have more recently been recognised as oncogenic with *ACBD3* being the latest 1q gene observed to affect breast cancer (Waugh 2014).

The *ACBD3* containing 1q42.12 locus was seen to be amplified in six breast cell lines (BRCAMZ01, BT20, HCC2218, MDAMB436, SUM149, ZR751) and eight out of twenty-five primary breast tumours in a breast cancer 1q amplification study (Orsetti, Nugoli et al. 2006). Loss of region 1q42.12 was seen in only one cell line (UACC812) and was not observed in any primary tumour samples.

There has only been one research article published to date concerning ACBD3 overexpression in breast cancer but its findings have wide ranging implications (Huang, Y., Yang et al. 2018). The relative quantity of ACBD3 in normal (n=111) and tumour (n=1099) tissue was analysed and ACBD3 protein was shown to have a higher mean average quantity and larger range of expression in the breast tumour sample group and ACBD3 mRNA was similarly upregulated in breast tumour tissue matched against adjacent normal tissue; all subtypes of breast cancer (basal-like, HER2,

Luminal A, Luminal B) showed a statistically significant level of ACBD3 mRNA upregulation compared to normal tissue. Protein levels of ACBD3 were upregulated in eight breast cancer cell lines (MDA-MB453, MDA-MB-415, BT549, MDA-MB-231, ZR-75-30, SKBR3, T47D and MCF7) compared with two normal breast epithelial cell lines (NBEC1 and NBEC2). The same was also true of ACBD3 protein levels in nine breast tissue samples compared to matched adjacent normal tissue. In some cases, the difference between normal and tumour expression of ACBD3 was vast with one of the nine matched samples having eleven times the relative quantity of ACBD3 in tumour tissue compared to the adjacent normal tissue and no matched tissue from patients or from breast cell lines showed exception to the trend that ACBD3 is upregulated at mRNA and protein level in breast tumour cells.

In a cohort of Chinese breast cancer patients Huang et al showed that ACBD3 protein expression increased as cancer stage became more advanced (using histoimmunochemical staining of fixed tissue) with the mean optical density of ACBD3 more than doubling from normal breast tissue to clinical stage I breast cancer (Huang, Y., Yang et al. 2018). This trend repeated itself between clinical stage I and II: ACBD3 increased to seven times the optical density of normal tissue between stage II and stage III and eight times the optical density between stage III and stage IV. This trend was also queried using the Kalpan-Meier plotter database and it was found that high levels of ACBD3 mRNA in breast tumour tissue predicted lower rates of patient survival and that this significance was less prominent in stages I and II but made a large difference in stage III and IV cancers with 60% probability of survival at 120 months when ACBD3 expression is low and less than 30% probability of survival when ACBD3 expression is high. Later clinical stage in cancer correlated with poorer survival. These results showed that ACBD3 is more abundant in later stages of cancer and that high ACBD3 mRNA correlates with poorer survival. Taken together this shows that ACBD3 upregulation contributes to poorer outcomes of patients in later cancer stages.

Gene set enrichment analysis (GSEA) showed that ACBD3 expression and cell cycle-activated gene signatures positively correlate (Huang, Y., Yang et al. 2018). Overexpression of ACBD3 caused increased side populations of stem-like cancer cells (measuring hoechst efflux by cells by flow cytometry) in cell cultures and inhibition of ACBD3 by siRNA reduced these side population cells significantly. When ACBD3 was overexpressed in mammospheres they became larger and more numerous in suspension cultures (Huang, Y., Yang et al. 2018). Conversely when

siRNA was used to silence ACBD3 fewer, smaller mammospheres were produced compared to controls in T47D and BT549 cell lines.

GSEA was further analysed to look at specific pathways activated by ACBD3 overexpression. It was found that CTNNB1 and TCF4 activated gene signatures both positively correlated with ACBD3 expression. *CTNNB1* encodes the beta catenin protein which in response to Wnt signalling accumulates in the cytoplasm and then translocates to the nucleus where it propagates the Wnt signal. Wnt interacts with NOTCH, NUMB mediates the inhibition of NOTCH and ACBD3 enables NUMB to mediate these effects (detailed further in section 1.7.1) (Cheng, Huber et al. 2008, Zhou, Atkins et al. 2007). ACBD3 overexpression led to an increase of beta catenin in the cytoplasm and nucleus compared to when ACBD3 expression was low (65% versus 20% nuclear and cytoplasmic localisation) (Huang, Y., Yang et al. 2018). TCF4 is a transcription factor for genes that code proteins in the Wnt signalling pathway. When TCF4 was knocked down the self-renewal ability of ACBD3-expressing cells was abolished and it was concluded that ACBD3 promoted cancer stem cell propagation via the Wnt/beta catenin signalling pathway.

ACBD3 makes interactions in diverse pathways including glucose import, steroidogenesis, neuronal cell fate, and redox stress which are described below. A protein involved in this many processes and with numerous binding partners including Protein kinase A could foreseeably have more involvement in breast cancer than just increasing β-catenin signalling. One promising line of inquiry is with ACBD3's most studied and semi-constitutive binding partner PI4Kβ, a phospholipid kinase that is implicated in breast cancer in its own right.

1.2.3 PI4Kβ in Breast Cancer and Interaction with ACBD3

Phosphatidylinositol 4 Kinase III beta (PI4Kβ) is a lipid kinase that converts phosphatidylinositol (PI) into phosphatidylinositol 4-phosphate PI(4)P (both of which are signalling molecules) and is implicated in breast cancers with 20% of primary tumours showing over expression of PI4Kβ (Tan, Brill 2014, Morrow, Alipour et al. 2014).

PI4Kβ is localised to the Golgi by ACBD3 where the rate of conversion of PI to PI(4)P is increased. ACBD3 does not affect the enzymatic activity of PI4Kβ but by tethering it to the Golgi membrane PI4Kβ is proximal to the PI substrate and does not rely on diffusion through the cytoplasm for its interaction with substrates (Klima, Tóth et al. 2016). Interaction between ACBD3 and PI4Kβ is achieved by extension of an

amphipathic helix at the N-terminus of PI4Kβ (aa44-64) through the Q domain alpha helices loop of ACBD3 (aa241-308). The small GTPase Rab11 binds PI4Kβ to support this interaction whilst ACBD3 is tethered by GOLGB1 bringing PI4Kβ close to the Golgi membrane with its kinase active site facing the PI substrate embedded in the lipid bilayer (Figure 1.2).

PI4Kβ is positioned on chromosome 1q, where amplification is common in breast cancers and may even be a defining feature (Orsetti, Nugoli et al. 2006). As *ACBD3* is also positioned on 1q, it is likely that both genes will have a high copy number in many breast cancers. The copy number of a gene and its oncogenicity are not always causal, instead only some genes that are amplified have a role in cancers; some of these (including *PI4Kβ*) are established oncogenes with a large body of literature (Waugh 2014) whilst others, including ACBD3, are just emerging (Houghton-Gisby, Harvey 2020).

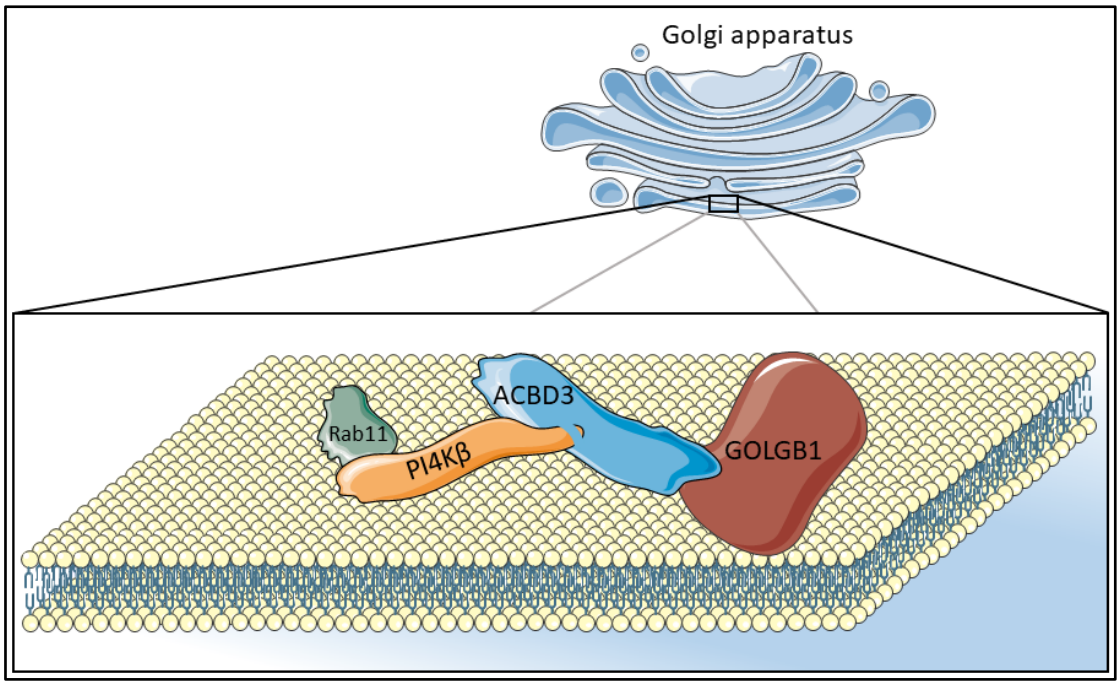

Figure 1.2 - ACBD3 tethers PI4Kβ to Golgi membranes. In conjunction with the Rab11 GTPase, ACBD3 maintains PI4Kβ in close and persistent contact with its PI substrate at the membrane which is then converted into PI(4)P (Klima, Tóth et al. 2016). The N-terminus of PI4Kβ which contains the amphipathic kinase helix protrudes through and binds to the Q domain loop of ACBD3. GOLGB1 binds to the GOLD domain of ACBD3 to tether it to the membrane.

PI4Kβ is reported to have increased gene copy number in 62% of 939 patient breast tumour samples (Waugh 2014), *PI4Kβ* expression in breast cancer correlates

with poor patient outcomes and its locus (1q21.3) is a biomarker for breast cancer (Morrow, Alipour et al. 2014, Goh, Feng et al. 2017). Evidence of PI4Kβ upregulation at the protein level in breast ductal carcinoma samples from the human protein atlas was also found by Waugh (Waugh 2014). Independent of its lipid kinase function, PI4Kβ also mediates indirect phosphorylation and activation of AKT (Protein kinase B), an important kinase in breast cancer signalling (Paplomata, O'Regan 2014, Morrow, Alipour et al. 2014). AKT dysregulation drives many breast cancers by promoting cell cycle progression and suppressing apoptosis, it is commonly overexpressed or constitutively active (Paplomata, O'Regan 2014).

The PI4Kβ substrate phosphatidylinositol (PI) and the product PI(4)P are cellular signalling molecules and docking sites on the membrane for other proteins including ARF1 (ADP-ribosylation Factor 1). ARF1 is essential for the formation of COPI vesicles and Golgi function including localisation of Golgin-160 to the Golgi and is encoded by a gene adjacent to *ACBD3* on chromosome 1 (1q42.13) (Liu, Yizhou, Kahn et al. 2014). ACBD3 is hijacked by some picornavirus viral proteins to form replication organelles, and recruits PI4Kβ to these sites to enrich them for PI(4)P (Sasaki, Ishikawa et al. 2012, Xiao, Lei et al. 2017). This is another example of how the role of ACBD3 is contextual and dependent on its cellular location, cell cycle position and binding partners. PI4Kβ has been found to be a target in malaria and drugs to inhibit PI4Kβ have already been developed (McNamara, Lee et al. 2013). PI4Kβ mutants that do not bind ACBD3 have been engineered and compounds that inhibit PI4Kβ enzymatic function are available which aids its study (Greninger, Knudsen et al. 2013, McNamara, Lee et al. 2013).

1.3 ACBD3 Related proteins

The Acyl CoA binding domain containing protein family contains seven proteins (ACBD1-7). The simplest are ACBD1 and ACBD7 which only contain the ACBD domain, ACBD1 was originally known as Acyl CoA binding protein (ACBP). All other members of the ACBD family contain extra functional domains or, at the least, unstructured tails. Long chain Acyl CoA concentration is tightly regulated in the cell and most is bound up in Acyl CoA binding proteins with free Acyl CoA in the 5-20nM range (Færgeman, Knudsen 1997). As well as being tightly regulated, Acyl CoA has regulatory roles of its own and is essential for secretory and membrane protein trafficking between the endoplasmic reticulum and the Golgi. At the mitochondria Acyl CoA esters inhibit the mitochondrial adenine nucleotide translocase protein which

catalyses the exchange of ATP and ADP across the IMM (inner mitochondrial membrane) known to be the rate limiting step in energy metabolism.

ACBD1 (known formally as diazepam binding inhibitor (DBI)) is a small ACBD family member at only 10kDa; it binds long chain Acyl CoA esters and is fairly ubiquitous between tissue types. It has been observed in the nucleus of rat liver cells where it influences transcription of genes related to Acyl CoA metabolism. DBI is known to have neurological roles including the balance of stem cell maintenance and clonal expansion in the post-natal brain by negatively regulating $GABA_A$ to promote stem cell proliferation (Dumitru, Neitz et al. 2017). DBI is a secreted protein in the brain, expressed mainly in astrocytes and binds to the GABA receptor complex directly (Guidotti, Forchetti et al. 1983, Khalil, Taïb et al. 2015). *ACBD1* knockout mice show reduced interest in socialising and increased repetitive grooming (Ujjainwala, Courtney et al. 2018).

ACBD2 (Enoyl-CoA Delta Isomerase 2 (ECI2)) contains the recognisable ACB domain at the N-terminus and an enoyl CoA isomerase/hydratase domain at the C-terminus which catalyses the conversion of 3 type double bonds into 2-trans form in a number of enoyl-CoAs (Geisbrecht, Zhang et al. 1999). ACBD2 has roles in unsaturated fatty acid metabolism and peroxisomal fatty acid metabolism some of which may be redundant pathways in the cell(van Weeghel, te Brinke et al. 2012). Like some other ACBD proteins ACBD2 is implicated in feeding behaviour and efficiency (Reyer, Shirali et al. 2017). ACBD2 also has a role in prostate cancer cell survival that promotes fatty acid degradation and its expression is a measure for mortality (Itkonen, Brown et al. 2017).

ACBD4 has an N-terminal ACBP domain and a long C-terminal region with no recognisable domains or function. It is a peroxisomal protein and interacts with vesicle associated membrane protein-associated protein B (VAPB) to promote association between peroxisomes and the endoplasmic reticulum (Costello, Castro et al. 2017a). ACBD4 may be a target of p53 as it was upregulated in cell lines treated with Inauhzin which inhibits SIRT1 to induce p53 (Liao, Jun-Ming, Zeng et al. 2012).

ACBD5 is similar in structure to ACBD4 and is closely related to it with a longer amino acid chain to the C-terminus of its ACBP domain. ACBD5 is also associated with peroxisomes and binds VAPB to tether them to the ER and its deficiency causes very long chain fatty acid metabolism defects (Ferdinandusse, Falkenberg et al. 2017, Costello, Castro et al. 2017b). An *ACBD5 RET* fusion gene has been observed in the papillary thyroid cancer of an atomic bomb survivor where the 3' tyrosine kinase

domain of *RET* has translocated and been ligated to the 5' of *ACBD5* (Hamatani, Eguchi et al. 2014). *RET* is a known proto oncogene and the RET/ACBD5 fusion protein was shown to cause tumours in nude mice and was therefore suggested to be causative of the thyroid cancer.

ACBD6 contains two C-terminal Ankyrin repeats and its N-terminal ACBP domain has preference for unsaturated long chain acyl-CoAs. *ACBD6* is expressed in placenta, cord blood, CD34 progenitors, bone marrow, spleen, and embryonic stem cells suggesting that it is involved in blood vessel formation and haematopoiesis (Soupene, Serikov et al. 2008).The N-myristoyltransferase enzymes NMT1 and NMT2 attach myristoyl-CoA onto glycine residues in proteins but lack specificity for only myristoyl-CoA. ACBD6 binds NMT1 and NMT2 to prevent competition between myristoyl-CoA and palmitoyl-CoA and allows N-myristoylation to proceed in the presence of abundant palmitoyl-CoA (Soupene, Kao et al. 2016). Chlamydia hijacks human ACBD6 to buffer Acyl-CoA levels in the bacterial replicative reticulate body in host cells to sustain bacterial acyltransferase activity and remodel host phosphatidylcholine (Soupene, Wang et al. 2014).

ACBD7 is a smaller paralogue of ACBD1 containing only an ACBP domain with a very similar amino acid sequence (Burton, Rose et al. 2005). Little has been published about ACBD7 possibly because it is much less ubiquitous than ACBD1, being expressed mainly in the brain, and it has yet to be observed to bind Acyl CoA. It is known to have a role in the leptin-melanocortin pathway that controls feeding behaviour and is expressed in response to leptin in arcuate nucleus neurons in the hypothalamus (Lanfray, Richard 2017, Lanfray, Caron et al. 2016).

There is also an isoform of ACBD1 known as endozepine-like peptide (ELP) expressed in the testis of most mammals but not primates, of which humans are included (Ivell, Balvers 2001, Pusch, Balvers et al. 1996). Like ACBD1, ELP binds mid to long chain Acyl CoAs but is also an essential part of spermatogenesis, expressed in post meiotic germ cell stages. Loss of ELP in primates follows a similar pattern to fertilin, another spermatozoon protein that is abundant in other mammals and it has been suggested that both of these proteins are at least in part responsible for relatively poor fertility in human males (Ivell, Pusch et al. 2000). ACBD3 also has a short isoform found in the testis of mice and other mammals but not in humans (Li, H., Degenhardt et al. 2001).

1.4 ACBD3 Roles at the Trans Golgi Network

1.4.1 The Golgi Apparatus

The Golgi apparatus receives newly synthesised secretory proteins from the endoplasmic reticulum and processes them, adding oligosaccharides to form glycoproteins. The Golgi also adds carbohydrates to lipids. Proteins processed by the Golgi are secretory and are either stored in the cell within vesicles/organelles or are excreted from the cell. This organelle is composed of a stack of cisternae that are generated from vesicles, in telophase at the centrosomes with coordination from microtubules, into distinctive flattened compartments that fragment again when mitosis is initiated (Mirinov, Beznoussenko 2011).

The formation of the Golgi stacks from Golgi vesicles is not fully mapped but it is known that Golgi reassembly stacking proteins (GRASPs) are responsible for the tethering of individual stacks, or ribbons, to form the mature organelle. GRASP65 and GRASP55 are two cytosolic peripheral Golgi protein homologs that tether membranes of the cis and trans Golgi network respectively (Shorter, Watson et al. 1999, Barr, Puype et al. 1997). These GRASP proteins form stable dimers on the cytosolic face of Golgi membranes and further oligomerise with GRASP proteins on adjacent Golgi ribbons to form distinctive stacks (Xiang, Wang 2010). Oligomerization is achieved through interaction of N-terminal GRASP domains but phosphorylation of these domains by CDK1 and PLK1 for GRASP65 and ERK/MEK1 for GRASP55 (all recognisable as kinases associated with mitotic cell cycle progression) prevents their interaction and catalyses the decoupling of Golgi ribbons allowing for COPI vesiculation during late G2 phase (Colanzi, Corda 2007, Truschel, Zhang et al. 2012, Tang, D., Yuan et al. 2012).

COPI is a protein complex that coats the vesicles that transport proteins between Golgi stacks from the cis Golgi through the medial stacks to the trans Golgi network (TGN), and between the Golgi and the endoplasmic reticulum (ER) (Cosson, Letourneur 1997). In prophase and prometaphase, the Golgi undergoes extensive COPI vesiculation following decoupling of GRASP proteins whilst vesicle fusion is inhibited. Fusion and reformation of the Golgi in telophase requires Golgin proteins including GM130, Golgin-160 and GOLGB1 (also known as Giantin) to capture vesicles and fuse them into Golgi ribbons in addition to the dephosphorylation of GRASP proteins to stack the ribbons.

1.4.2 ACBD3 at the Golgi

ACBD3 was first discovered from a pull-down experiment baited with GOLGB1 and it was found that they interact via their respective C-termini (Sohda, Misumi et al. 2001). GOLGB1's function in cells is not well understood but loss of function mutations in mice have been shown that it is vital for palate development (Lan, Zhang et al. 2016). At the Golgi GOLGB1 is likely to have an intracisternal function and may mediate the localisation of ACBD3 to the Golgi.

1.4.3 Golgin-160

ACBD3 interacts with Golgin-160, a cytosolic Golgi membrane protein that has a role in glucose transporter type 4 sorting in adipose cells (Belman, Bian et al. 2015). Golgin-160 is cleaved by caspases during apoptotic signalling to create seven possible fragments. The initiator caspase: caspase 2 cleaves Golgin-160 to produce fragment aa140-311 which reveals a hidden nuclear localisation sequence on this fragment (Mancini, Machamer et al. 2000, Sbodio, Hicks et al. 2006). Executioner caspases 3 and 7 also cleave Golgin-160 into alternate fragments in the execution stage of apoptosis. ACBD3 preferentially interacts with the caspase 2 generated fragment aa140-311 over full length golgin-160 or any of the alternate fragments and this interaction is dependent on the redox state of cysteine 463 on ACBD3 (Sbodio, Machamer 2007).

Golgi fragmentation is a key feature of apoptosis and mutant Golgin-160 that cannot be cleaved delays apoptosis and Golgi destruction in response to staurosporine. The aa140-311 fragment has been suggested to have a prosurvival function in the nucleus and when ACBD3 is overexpressed cells become more sensitive to apoptosis by staurosporine because the majority of the Golgin-160 aa140-311 fragments are bound to ACBD3 at the Golgi and cannot propagate a signal in the nucleus(Sbodio, Hicks et al. 2006). This is however in direct conflict with the observation that non cleavable Golgin-160 mutants reduce sensitivity to some apoptotic drugs, such as staurosporine, that cause endoplasmic reticulum stress or induce the ligation of death receptors (Maag, Mancini et al. 2005, Sbodio, Machamer 2007).

1.4.4 GLUT4

GLUT4 (glucose transporter type 4) allows the facilitated diffusion of glucose from the surroundings into cells via concentration gradient. GLUT4 is essential for the import of glucose into muscle and fat cells and its cell surface expression is regulated by insulin, a peptide hormone released in response to high glucose levels, typically following ingestion of carbohydrates (Li, j., Houseknecht et al. 2000). GLUT4 is sequestered into storage vesicles (GSVs) that are tethered to Golgi membranes by TUG (Tether containing UBX domain for GLUT4), Golgin-160 and ACBD3 when insulin is absent (Figure 1.3). This prevents cells from importing glucose and forms part of the glucose homeostasis mechanism (Govers 2014).

Circulating Insulin binds to and activates the insulin receptors (IR) of adipose and muscle tissue which causes phosphorylation of the Castitas B-lineage lymphoma proto oncoprotein (CBL) on tyrosines 700 and 774 (via recruitment by APS which is first activated by tyrosine-618 phosphorylation by IR). Phosphorylated CBL translocates to lipid raft subdomains of the plasma membrane, via the CBL constitutive partner CAP, and sequesters the CRK adapter protein with its constitutively associated partner C3G, a Rap guanine nucleotide exchange factor (Baumann, Ribon et al. 2000, Fecchi, Volonte et al. 2006). These events bring C3G into proximity with TC10α, a G protein on the lipid raft of the plasma membrane, and activates TC10α. PIST (PDZ interacting specifically with TC10) is the cytoplasmic effector of active TC10α and mediates cleavage of acetylated TUG (Bogan, Rubin et al. 2012). PIST binds to Golgin-160 and interacts with TUG but not GLUT4 (Figure 1.3).

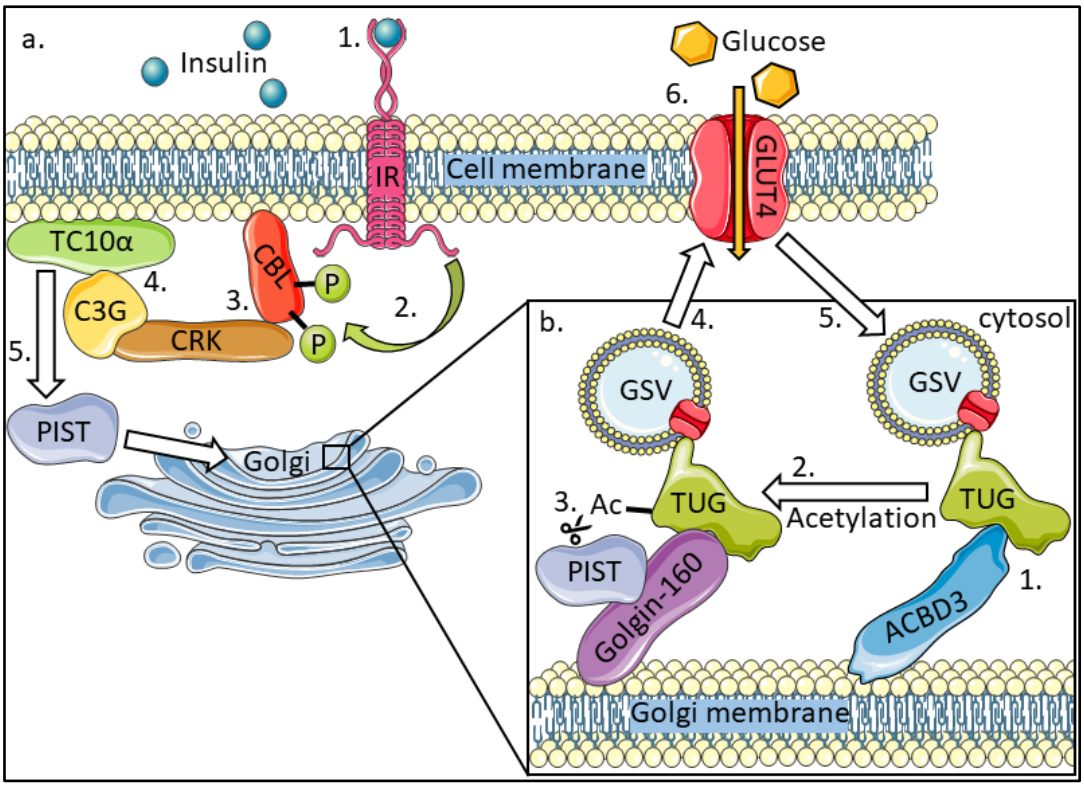

Figure 1.3 - The effect of insulin on TUG, the interaction between TUG and ACBD3, and the recycling of GLUT4 storage vesicles to regulate glucose import (Bogan, Rubin et al. 2012, Belman, Bian et al. 2015, Fecchi, Volonte et al. 2006). a) (1) Extracellular insulin binds the transmembrane insulin receptor (IR) causing receptor activation. **(2)** The active IR tyrosine phosphorylates CBL inside the cell. **(3)** Phosphorylated CBL recruits the CRK-C3G complex to the membrane lipid raft sub domain facilitating interaction of C3G and TC10α. **(4)** C3G activates TC10α which subsequently activates its effector: PIST. **(5)** PIST relocates to the Golgi causing the release of GSVs with embedded GLUT4 transporter which fuse with the cell membrane **(6)** allowing glucose to enter the cell. GLUT4 is continuously cycled away from the membrane in GSVs creating a fast on and off switch for insulin dependent glucose import.

b) (1) ACBD3 interacts with TUG and is dependent on the acetylation state of TUG. **(2)** Acetylation of TUG on lysine 549 causes TUG to preferentially bind Golgin-160 over ACBD3. **(3)** PIST, activated by the insulin receptor signalling cascade, also binds Golgin-160 and catalyses the cleavage of acetylated TUG causing GSVs to be released into the cytoplasm to fuse with the cell membrane **(4)**. **(5)** GLUT4 is continuously cycled away from the cell membrane embedded in GSVs and is sequestered back to the Golgi where they bind TUG.

ACBD3 binds TUG to sequester it at Golgi membranes initially in the absence of insulin. ACBD3 bound TUG can be acetylated on lysine 549 which increases its affinity for Golgin-160 over ACBD3 (Belman, Bian et al. 2015). TUG binds GSVs to

tether them at Golgi membranes and in response to insulin, the subsequently activated PIST binds Golgin-160 and stimulates acetylated TUG cleavage. This releases GSVs allowing them to integrate with the plasma membrane where GLUT4 forms a channel for glucose import (Mohan, Sheena et al. 2010). GLUT4 is continuously cycled away from plasma membranes back into GSVs to increase the on/off response of insulin sensitive cells when insulin is not present. ACBD3 binds the cleaved TUG keeping it at Golgi membranes to be acetylated again and bind another GSV which is then released to the surface again by PIST activity. This process cycles for as long as the insulin signal persists (Figure 1.3). GLUT4 exocytosis is regulated by tankyrase 1 as are several other ACBD3 related processes discussed below including Golgin45 expression and the promotion of beta catenin transcription in the Wnt signalling pathway (Guo, H., Zhang et al. 2012, Huang, S. A., Mishina et al. 2009). Tankyrase 1 and 2 are currently being targeted as cancer therapeutics because of their interactions in carcinogenic pathways(Lu, H., Lei et al. 2013, Seimiya, Muramatsu et al. 2005, Haikarainen, Krauss et al. 2014, Kim, M. K. 2018). Tankyrase also targets Axin for degradation leading to increased Wnt signalling which is known to be aberrant in breast cancers and may be influenced by ACBD3(Huang, Y., Yang et al. 2018, Howe, Brown 2004).

1.4.5 Golgin45

Golgin45 (also known as JEM1 and BLZF1) is a Golgi scaffold protein that binds the GOLD domain of ACBD3 via its coiled coil domain. ACBD3 has been shown to greatly increase Golgin45 localisation to the Golgi and forms a cisternal adhesion complex with ACBD3, GRASP65 and TBC1D22 (a Rab33b GTPase specific activator (GAP)) (Xihua, Mengjing et al. 2017). The function of Golgin45 is not fully known but beyond its Golgi structural functions Golgin45 also has a leucine zipper motif and is theoretically capable of homo and heterodimerisation to form a nuclear factor (Duprez, Tong et al. 1997). Golgin45 has been suggested as an ACBD3 docking site that is distinct from GOLGB1 as Golgin45 is ubiquitous at the Golgi relative to GOLGB1 which is localised mainly around the Golgi rim (Koreishi, Gniadek et al. 2013, Xihua, Mengjing et al. 2017). This supports observations that ACBD3 has a structural role in the Golgi and that loss of ACBD3 causes unstacking of the Golgi. *Golgin45* is located on chromosome 1(q24) the same arm of the same chromosome as *PI4Kβ* and *ACBD3*, and is regulated by tankyrase, another Golgi associated protein, which promotes ubiquitination and degradation of targets (Zhang, Y., Liu et al. 2011). Golgin45 is shown to be downregulated in hepatocellular carcinomas and

in acute promyelocytic leukaemia cell line NB4 (Tong, Fant et al. 1998, Huang, Y., Yang et al. 2018). Golgin45 forms dimers *in vivo* with the structural Golgi protein GRASP55 (Zhao, Li et al. 2017).

1.4.6 GTPases

Rab (small Ras like) GTPases serve important roles at the Golgi, providing anchoring sites for Golgi proteins, regulating structure and taking part in retrograde transport on endoplasmic reticulum/Golgi vesicles (Moyer, Balch 2001). Rab GTPases are commonly chaperoned and recruited to membranes by specific binding partners and these interactions are mediated by GDP dissociation inhibitors (GDIs) (Ullrich, Stenmark et al. 1993). The combination of chaperones, resident membrane protein partners and GDIs ensures that different Rab proteins are recruited to their respective membranes/organelles in a location specific and tissue specific manner.

Several of the ACBD3 interactors discussed in this thesis, as well as ACBD3 itself, bind Rab GTPases or regulate their activities and in addition to the structural role of these Golgi proteins, the GTPases themselves appear to have a vital role in Golgi dynamics (Liu, Shijie, Storrie 2012, Stenmark 2009). The Golgin45/GRASP55 complex at the medial Golgi binds Rab2 and is the effector for transport and structural functions of the Golgin45/GRASP55 complex (Short, Preisinger et al. 2001). This is supported by knockdown of Golgin45 which disrupts Golgi structure and by *in vitro* experiments with non-hydrolysable GTP analogues which promote the stacking of Golgi ribbons, presumed now to be by their constitutively activating effect on Rab2 and other Rab GTPases (Rabouille, Misteli et al. 1995).

ACBD3 binds the Rab33b GTPase activating protein TBC1D22 and localises it to the Golgi in a complex with the Golgin45/GRASP55 dimer (Xihua, Mengjing et al. 2017). TBC1D22 activates Rab33b which has a role in Golgi transport to the endoplasmic reticulum and in nanoparticle trafficking (Panarella, Bexiga et al. 2016, Tregei, Yi et al. 2010). PI4Kβ is an important ACBD3 binding partner with roles in maintaining the PI4P pool at the Golgi membrane (Klima, Tóth et al. 2016). PI4kβ interacts with the GTP bound form of Rab11 and is required for Rab11 localisation at the Golgi. PI4Kβ in turn is recruited by ACBD3 and this complex, possibly with GOLGB1, promotes PI4P production (Figure 1.2) (Clayton, Minogue et al. 2013).

Dexras1 is a small GTPase known to interact with ACBD3 at the Golgi (Cheah, Kim et al. 2006). Rhes is another GTPase protein very closely related to Dexras1 expressed exclusively in the corpus striatum and is also a known interactor of ACBD3

(Falk, Pierfrancesco et al. 1999). Rhes is heavily implicated in Huntington's disease progression and ACBD3 has been shown to mediate Huntington's disease neurotoxicity (Baiamonte, Lee et al. 2013, Sbodio, Paul et al. 2013).

1.5 ACBD3 at the Mitochondrial Membrane

ACBD3 is often considered a resident Golgi protein due its structural role and interactions with other structural and functional components but it can also be found at other membranes including the cytosolic cell membrane and at the outer mitochondrial membrane (OMM). ACBD3 does not have any enzymatic activity of its own but serves as a tether and adapter for other molecules to build and retain complexes involved in cholesterol import and redox stress.

1.5.1 Steroidogenesis

ACTH (Adrenocorticotropic hormone) and LH (luteinizing hormone) activate G protein-coupled receptors in adrenal, leydig and ovarian cells causing the activation of intracellular adenylyl cyclase which in turn raises cytosolic cAMP concentration (Miller 2013). cAMP accumulation leads to protein phosphorylation and lipid and protein synthesis in the cell which all influence steroid production. Cholesterol forms the building block for steroids and must be transported to the OMM (outer mitochondrial membrane) of mitochondria to sustain steroid synthesis and is sourced from plasma membranes, lipid droplets, and by de novo synthesis within the endoplasmic reticulum (Shen, Azhar et al. 2015, Murphy, Martin et al. 2009).

ACBD3 interacts with TSPO (previously the peripheral-type benzodiazepine receptor) on the cytosolic outer mitochondrial membrane (OMM) which stimulates cholesterol transport from the OMM to the IMM (Figure 1.4a) (Krueger, Papadopoulos 1990, Li, H., Degenhardt et al. 2001). TSPO is anchored at the OMM by the voltage dependent anion channel VDAC1 and makes up approximately 2% of OMM proteins. TSPO tethers cytosolic ACBD3 to the OMM which subsequently recruits protein kinase A (PKA) via the PKARIα subunit. This brings PKA into proximity with one of its substrates: the steroidogenic acute regulatory (StAR) protein which is phosphorylated on residues S57 and S195 by PKA (Arakane, King et al. 1997). StAR then facilitates cholesterol import from the OMM to the IMM.

StAR binds cholesterol via a hydrophobic sterol binding pocket (SBP) at the cytosolic OMM causing a conformational change of StAR that is essential for

cholesterol to cross the OMM (Rajapaksha, Kaur et al. 2013). At the IMM P450scc (CYP11A1) carries out the first reactive step in the conversion of cholesterol to steroid hormones, using its electron transfer partners: ferredoxin reductase and ferredoxin to produce pregnenolone (Miller, Auchus 2011). P450scc is located at the inner mitochondrial membrane (IMM) and determines the net steroidogenic capacity of the cell and is the chronic regulator of steroidogenesis (Strushkevich, MacKenzie et al. 2011, Elustondo, Martin et al. 2017). The rate determining step in steroidogenesis is the transport of cholesterol from the OMM to the IMM and the ACBD3 protein is essential for this step.

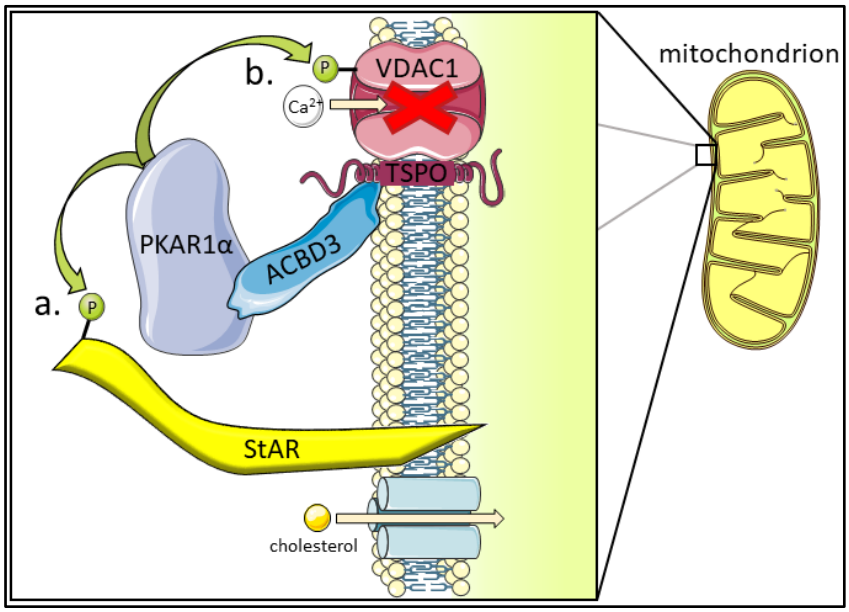

Figure 1.4 – ACBD3 has functions at the mitochondria. At the Outer Mitochondrial membrane (OMM) ACBD3 is essential for mediating interactions between PKA holoenzyme (via direct tethering with the PKAR1α subunit shown) and its substrates: StAR and VDAC1.

a) The phosphorylation state of StAR determines whether cholesterol can cross the IMM and be converted to pregnenolone, the basic building block of all steroid hormones in mammals. Cholesterol import is the rate limiting step in steroidogenesis and ACBD3 is indispensable for this process.

b) VDAC1 is a Ca^{2+} ion import channel at the OMM and phosphorylation by PKA closes this channel to prevent calcium import. Mitochondrial import of Ca^{2+} forms part of the calcium homeostasis mechanism in the cell, closing the VDAC1 ion channel causes cytosolic Ca^{2+} concentration to rise in the cell which leads to redox stress and local inflammation. Again, ACBD3 is essential for localising PKA to the mitochondria where it can then phosphorylate the VDAC1 substrate.

Pregnenolone is transported to the endoplasmic reticulum where the final steroid products are synthesised (Strushkevich, MacKenzie et al. 2011, Sewer, Li 2008, Miller, Auchus 2011). This is the process by which all steroids are made in the hormone producing organs of mammals. These are comprised of six groups: Androgens (testosterone and dihydrotestosterone), oestrogens (oestradiol), glucocorticoids (cortisol and corticosterone), mineralocorticoids (aldosterone), progestins (progesterone) and calciferols (1,25-dihydroxy vitamin D) which are all tissue specific hormones synthesised from pregnenolone (Shen, Azhar et al. 2015, Acconcia, Marino 2016). ACBD3 overexpression increases chorionic gonadotropin induced steroid production (Liu, J., Rone et al. 2006).

PKAR1α is a tumour suppressor and is important in primary pigmented nodular adrenocortical disease (PPNAD) nodule formation and tumorigenesis in mice and humans. Mutation of PKAR1α leads to hyercortisolism that drives tumorigenesis, and high ACBD3 expression in steroidogenic tissues (of which the adrenal cortex is one) may contribute to the overexpression/over activity of mutant PKAR1α. PPNADs are characterised by a resistance to apoptosis which in itself contributes to cancer occurrence and is a major hallmark of cancer (Hanahan, Weinberg 2011). The first publication to suggest any link between ACBD3 and cancer demonstrated that ACBD3 follows the same expression profile as PKAR1α in PPNAD tissue and speculated that in tumorigenesis this could lead to deregulation of steroid synthesis (Liu, Jun, Matyakhina et al. 2003). PKA is a kinase with a huge range of targets and is controlled by a range of subunits that form distinct holoenzymes with different specificities. The inactivating mutations of PKARIα that lead to PPNAD cause increased PKA activity, PKA activates the mTOR pathway leading to phosphorylation of targets such as the proapoptotic BAD protein, inactivating it and contributing to apoptotic resistance (de Joussineau, Sahut-Barnola et al. 2014). mTOR is in itself an effector in many important signalling pathways and causative or accelerative in many cancers including breast cancer; in breast cancer mTOR dysregulation is common to the extent that several generations of chemotherapeutic rapalogues have been developed to inhibit it (Hare, Harvey 2017).

Steroidogenic acute regulatory (StAR)-related lipid transfer (START) domain containing proteins, of which StAR was the first to be identified, play key roles in cholesterol metabolism at the mitochondria by binding cholesterol and other lipids (Alpy, Tomasetto 2005). ACBD3 tethering of PKA to the mitochondria is essential for StAR induced cholesterol import into intermembrane mitochondrial space and subsequent conversion to pregnenolone for steroid synthesis (Rajapaksha, Kaur et

al. 2013). Other START domain containing proteins also play important roles in cholesterol trafficking and membrane transport which control cholesterol availability to the mitochondria. StARD3 (previously MLN64) is one such START domain containing protein which shares 37% amino acid sequence identity with StAR of which the C-terminal lipid binding domains are most conserved (50%) (Moog-Lutz, Tomasetto et al. 1997). StARD3 is not a known interactor of ACBD3, as StAR is not, but shares homology with StAR protein, the activation of which is dependent on ACBD3. StARD3 is upregulated in breast and ovarian cancer, as ACBD3 appears to be, and may contribute to the dysregulation of androgen production and signalling of these cancers (Tomasetto, Régnier et al. 1995).

Whilst there is no direct link between StarD3 and ACBD3, it is very possible that ACBD3 will be found to influence steroidogenesis in cancers. As evidenced by the correlation of ACBD3 and PKA (RIα subunit) expression in PPNAD tissue, the increased steroid production in chronic gonadotropin when ACBD3 is overexpressed and the indispensable role of ACBD3 for steroid synthesis (Liu, Jun, Matyakhina et al. 2003, Liu, J., Rone et al. 2006).

1.5.2 Redox Stress

Interestingly, and in a separate process, TSPO tethered ACBD3 recruits PKA to phosphorylate VDAC1 and prevent Ca^{2+} import into the mitochondria (Figure 1.4b) (Gatliff, East et al. 2017). VDAC1 is important in Ca^{2+} homeostasis, especially mitochondrial Ca^{2+} homeostasis which controls the metabolism of mitochondria and therefore energy availability in the cell (Shoshan-Barmatz, Krelin et al. 2018). VDAC1 is an ion channel permeable to Ca^{2+} and permits Ca^{2+} to enter the mitochondria along its concentration gradient; this imbues mitochondria with the ability to buffer intracellular Ca^{2+}.

ACBD3 can bind TSPO at the mitochondria to recruit the PKA complex via direct interaction with PKARIα (Figure – 1.4) (Li, H., Degenhardt et al. 2001). Unlike steroidogenesis, which is under hormonal control, this complex can also be localised to the mitochondria by increased TSPO expression induced by glutamate, a signalling molecule that is known to cause acute neurotoxicity (Gatliff, East et al. 2017, Atlante, Calissano et al. 2001). At the mitochondrial membrane PKA can then phosphorylate VDAC1 which prevents it from allowing Ca^{2+} transport into the mitochondria. This causes Ca^{2+} accumulation in the cytosol which signals redox stress via the calcium sensing CamKII and its effector NADPH oxidase (NOX5) leading to inflammation by

increased reactive oxygen species (ROS). This is particularly relevant to neuro-inflammation and associated cytotoxicity where TSPO is not expressed in healthy brain tissue but can accumulate later, in age related degenerative disease or after traumatic stress, and may contribute to neurodegeneration (Kumar, Muzik et al. 2012). This is another example of ACBD3 being part of multiple disparate functions within a single niche (in this case the OMM).

Redox stress and ROS promote inflammation, and long-term inflammation can promote cancer and inflammation is common in the tumour microenvironment (Deshmukh, Srivastava et al. 2019, Hanahan, Weinberg 2011). Elevation of cellular ROS have been detected in the majority of cancers including breast cancer (Storz 2005, Toyokuni, Okamoto et al. 1995). ACBD3 upregulation and overexpression may contribute to a tumour promoting microenvironment by increased redox stress and ROS production.

1.5. Lipid Metabolism

Lipid metabolism defects are linked to diabetes, neurodegeneration and cancer (Menendez, Lupu 2007, Spell, Kölsch et al. 2004, Ferré, Foufelle 2007). Sterol regulatory element binding proteins (SREBPs) are transcription factors that maintain homeostasis of fatty acids and cholesterol in the body. Overexpression of ACBD3 inhibits SREBP1 sensitive fatty acid synthase (FASN) activity, is observed to block SREBP1 maturation by direct binding and inhibits its nuclear form (Chen, Patel et al. 2012). ACBD3 overexpression was also shown to reduce FASN and *de novo* palmitate synthesis pathways at the protein and transcription level and both of these appear to be mediated by the N-terminal region of ACBD3 containing the ACBP domain (Figure 1.1). The N-terminal region was implicated by deletion of amino acids 1-171 which abolished much of ACBD3s influence of SREBP1 expression whereas deletion of C-terminal amino acids did not. The two nuclear localisation sequences on human ACBD3 are located between amino acids 199 and 228 so were present in the N-terminal deletion mutant (Fan, Liu et al. 2010).

1.6 Iron Transport

ACBD3 was found to be an interactor of Divalent metal transporter 1 iron responsive element (DMT1 IRE) by yeast 2 hybrid screening and it was demonstrated that siRNA silencing of ACBD3 prevented iron uptake into cells and downregulated

protein levels of DMT1 (Okazaki, Ma et al. 2012). Increasing iron in rat diets was shown to downregulate ACBD3 protein levels at the duodenum. These findings implicate ACBD3 as a regulator of iron transport in DMT1 (IRE) expressing cells and conversely ACBD3 is also regulated by dietary iron. The regulatory function of ACBD3 is further evidenced by Choi et al who discovered that, in the brain, ACBD3 binds Dexras1 and DMT1 (Rhes and DMT1 in the corpus striatum) (Choi, Bang et al. 2013). ACBD3 and Dexras1 co-transfection into HEK293T cells enhanced iron uptake into cells whilst Dexras1 alone caused only a small change inferring that ACBD3 mediates the positive effect of Dexras1 on iron uptake by DMT1. This is in agreement with intestinal iron uptake (in rats) where low ACBD3 expression results in low protein levels of DMT1 (Okazaki, Ma et al. 2012).

DMT1 is a membrane resident cotransporter of protons and divalent metal ions including iron. DMT1 has several isoforms and DMT1(IRE) (iron responsive element isoform I) is: essential for dietary iron absorption at the brush border membrane of the duodenum (small intestine), important in iron uptake in neuronal cells, and may have an iron transport role in other cells. DMT1 imports free iron directly through the plasma membrane into cells as well as transferrin bound iron via endosomes (Figure 1.5) (Richardson, Ponka 1997, Cheah, Kim et al. 2006). Transferrin binds transferrin receptors on the cell surface and cause DMT1, the transferrin receptor and transferrin to be endocytosed. The transferrin endosomes then undergo acidification to release iron from transferrin whereby the free iron then enters the cytoplasm through the embedded DMT1 transporter (Dautry-Varsat, Ciechanover et al. 1983).

ACBD3 is an adapter between DMT1 and its positive regulator Dexras1 and tethers Dexras1 to DMT1 at the cytosolic plasma membrane. In the brain N-methyl-D-aspartic acid (NMDA) glutamate receptor activation causes activation of nNOS which s-nitrosylates Dexras1 to a more active form. Active Dexras1 then activates DMT1 via the ACBD3 adapter causing iron transport into the cytoplasm (Cheah, Kim et al. 2006).

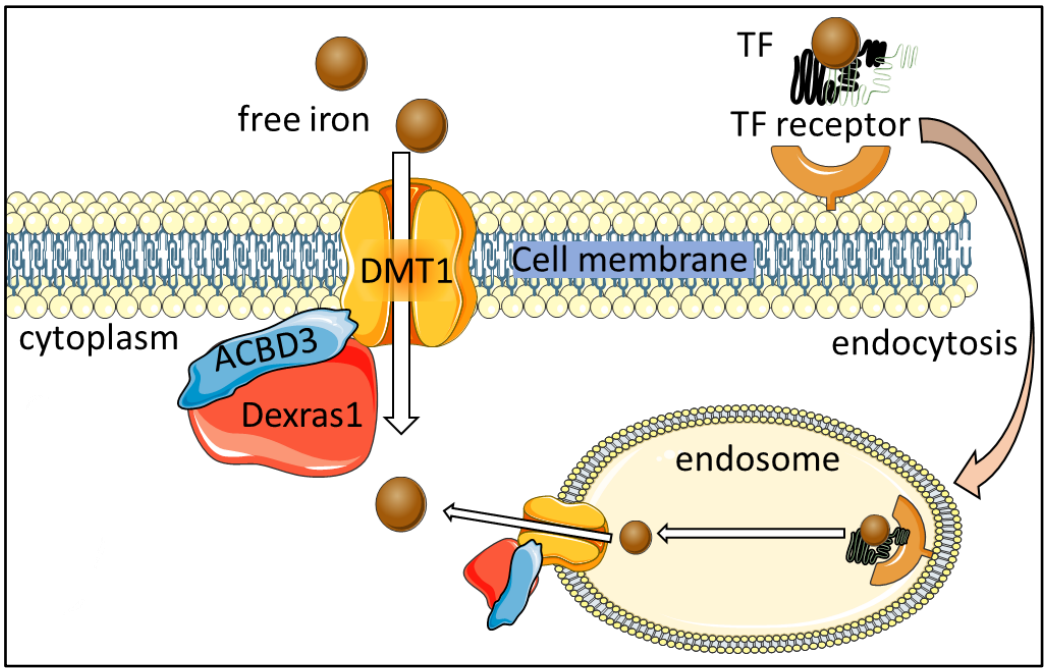

Figure 1.5 – ACBD3 binds Dexras1 and DMT1 promoting cellular import of iron. The DMT1 metal transporter facilitates the import of both free iron and transferrin (TF) into cells of the small intestine and the brain. ACBD3 binds DMT1 at the cell membrane and Dexras1 to stimulate DMT1 activity to import free iron. TF binds the transferrin receptor which is then endocytosed with DMT1 into an endosome. The endosome is then acidified causing release of iron from TF. DMT1 is stimulated by Dexras1, tethered to DMT1 by ACBD3, to pump iron from the endosome into the cytoplasm. In the brain Dexras1 is s-nitrosylated to a form of increased activity by nNOS in the NMDA signalling cascade (not shown). In the corpus striatum, Rhes replaces the role of Dexras1 (adapted from (Choi, Bang et al. 2013)).

1.7 ACBD3 in Signalling

1.7.1 NUMB

Mammalian NUMB, an endocytic adapter protein, is involved in cytosolic signalling and is segregated asymmetrically into one daughter cell during the mitosis of neural progenitor cells with its protein partner NOTCH (Artavanis-Tsakonas, Rand et al. 1999). This asymmetric distribution of NUMB results in one identical pluripotent daughter cell to maintain the population of neuronal precursors and one differentiated neuron cell. This balances the need to create neurons and maintain the pool of precursor cells in embryonic neurogenesis. Loss of function mutations in NUMB and the NUMB-like paralog in mice (NUMBL) results in overproduction of neurons but causes premature depletion of the progenitor pool whereas depletion of only one gene shows no change, alluding to a redundant pathway in neurogenesis between NUMB and NUMBL in mammals (Petersen, Zou et al. 2002).

High levels of NUMB protein in one new daughter cell maintains an undifferentiated pluripotent cell phenotype the same as the parent cell whereas the other daughter cell, with low levels of NUMB, undergoes differentiation to become a neuronal cell, a mechanism that is conserved between drosophila and mammals (Uemura, Shepherd et al. 1989, Verdi, Schmandt et al. 1996). In drosophila NUMB specifies cell fate by inhibiting NOTCH, a transmembrane receptor that mediates intercellular signalling in development, however, it is not certain that this is conserved in mammals. NUMB alone however is not enough to specify a pluripotent cell fate as the daughter cell that does not receive NUMB starts to produce and accumulate NUMB protein early in G_1 phase and NUMB is actually required for the cell to differentiate into a neuron (Zhou, Atkins et al. 2007).

ACBD3 has been identified as a NUMB binding partner after it was observed that ACBD3 cytosolic release in mitosis and cellular location are paired with NUMB mediated cell fate (Zhou, Atkins et al. 2007). ACBD3 is bound to Golgi/mitochondrial membranes through most of the cell cycle and only binds NUMB during mitosis when the breakdown of the Golgi releases ACBD3 into the cytosol. Constitutively cytosolic ACBD3 inhibits neurogenesis in mouse embryos and results in less neurons. This suggests that permanently cytosolic ACBD3 is preventing differentiation in otherwise neuronal fated cells and that it achieves this by binding NUMB outside of mitosis. This explains how a protein level increase of NUMB in a NUMB deprived daughter cell still leads to neuronal differentiation after mitosis because ACBD3 is membrane bound,

whereas in a NUMB rich daughter cell during mitosis ACBD3 is cytosolic and free to bind NUMB (Figure 1.6).

The ACBD3 interacting region on NUMB is essential for NUMB activity and interaction with ACBD3 increases NUMB activity (Zhou, Atkins et al. 2007). The C-terminus of ACBD3 binds with the N-terminus of NUMB, and NOTCH also binds the N-terminus of NUMB (Guo, M., Jan et al. 1996). NUMB is still the effector protein of this signalling pathway as ACBD3 alone cannot prevent differentiation of neural progenitors (in drosophila). Cytosolic ACBD3 expression leads to inhibition of NOTCH suggesting that NOTCH inhibition by NUMB is conserved from drosophila to mammals and it can be concluded that ACBD3 and NUMB are both required to specify cell fate in neural progenitors. NOTCH signalling in the differentiating daughter neuron cell (Figure 1.6e) also has intercellular signalling capabilities causing lateral inhibition of NOTCH signalling in adjacent progenitor cells to prevent neighbours becoming neurons as well, this creates the familiar mosaic/chequered pattern of neurons and progenitors in the developing brain.

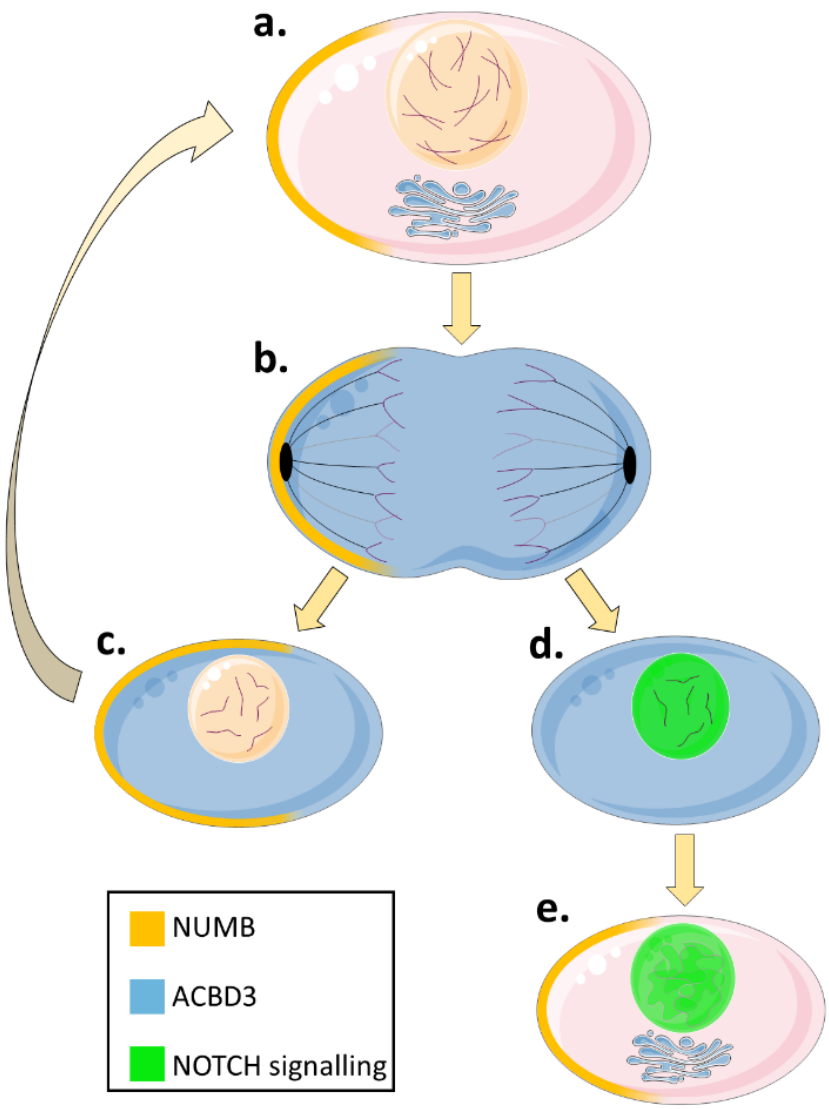

Figure 1.6 – The differential regulation of NOTCH signalling by ACBD3 and NUMB in neurogenesis (Zhou, Atkins et al. 2007). Cytosolic NUMB (yellow shading) acts synergistically with cytosolic ACBD3 (blue shading) to inhibit NOTCH signalling (represented by a green nucleus) and specifies progenitor cell fates during mitosis.

a) NUMB accumulates asymmetrically in one half of a progenitor cell before mitosis. ACBD3 is bound to the Golgi apparatus and other organelles (not shown) and does not interact with NUMB. **b)** During mitosis the Golgi apparatus fragments into vesicles and ACBD3 is released into the cytosol where it can interact with asymmetrically distributed NUMB. **c)** One of the daughter cells will contain NUMB and cytosolic ACBD3. ACBD3 increases the ability of NUMB to bind and inhibit NOTCH. Without NOTCH signalling the daughter cell remains a progenitor cell to maintain the pool of neuronal precursors. **d)** The second daughter cell will contain cytosolic ACBD3 but no NUMB protein meaning that NOTCH is not inhibited and enters the nucleus signalling to the cell to differentiate. **e)** NUMB protein is produced in the differentiating cell in G_1 but at this time the Golgi has reformed and ACBD3 is no longer free in the cytoplasm and cannot interact with NUMB and so cannot inhibit NOTCH signalling.

1.8 ACBD3 and Disease

ACBD3 has been implicated in diseases such as Huntington's disease and breast cancer and is essential for infection of some viruses and salmonella. Due to the large number of cellular processes that ACBD3 is involved in, some literature hints at a role of ACBD3 in other cancers and we explore this possibility as broadly as possible.

1.8.1 Huntington's Disease

Rhes is closely related to the protein Dexras1 which interacts with ACBD3 (Harrison 2012, Falk, Pierfrancesco et al. 1999, Sbodio, Paul et al. 2013). Based on this observation it was discovered that Rhes also interacts with ACBD3 and It has been found that ACBD3 mediates this cytotoxicity in Huntington's disease (HD) mouse models and also that knockdown of ACBD3 abolishes the cytotoxicity in those models (Sbodio, Paul et al. 2013). It was further shown that Huntingtin (HTT) protein and disease causing mutant HTT protein (mHTT) bind ACBD3 and Rhes to form a ternary complex. ACBD3 is upregulated in HD mouse models and patients with HD show a 2.5-fold increase in ACBD3 expression based on striatal samples. Golgi stress has been shown to be important in the physiological process of cytotoxicity and the mechanism by which cytotoxicity is induced in HD is thought to be by initial endoplasmic reticulum stress, leading to Golgi stress and toxicity which in turn induces ACBD3 expression. The upregulated ACBD3 may then perpetuate the cycle by binding Rhes. It is proposed that binding of Rhes and mHTT to ACBD3 at the Golgi may be the initial cause of this stress (Lunkes, Mandel 1998, Baiamonte, Lee et al. 2013, Sbodio, Paul et al. 2013).

Whilst HD is thought of as a strictly neurodegenerative disease, caused by degradation of the corpus striatum; the testes of HD patients, and of mouse models, undergo severe degradation as the disease progresses (Van Raamsdonk, Murphy et al. 2007). It is noteworthy that the Rhes protein to which HTT binds is not found in the testes, but ACBD3 the speculative mediator of mutant huntingtin induced cytotoxicity, is abundant in the testes and the mHTT-ACBD3 interaction in these tissues merits further study. Linking ACBD3 further to HD is ACBD3s roles in iron homeostasis which has been reviewed in chapter 1.6 – iron transport. The ACBD3-Rhes interaction is involved in the process of iron uptake and, possibly causally, iron transport is largely dysregulated in HD (Rosas, Chen et al. 2012, Okazaki, Ma et al. 2012).

1.8.2 Coxsackie Virus

Coxsackie virus is one of the leading causes of aseptic meningitis and Coxsackie virus B3 (CVB3) can induce inflammation of muscle, degeneration of brain, pancreas, heart, muscle and fat pads (in mice) (Alexander, Chapman et al. 1993, Yin-Murphy, Almond 1996). Conflicting studies have shown that ACBD3 expression is either essential or dispensable for enteroviruses including Poliovirus, Aichi virus and Coxsackie virus. It is not controversial that 3A viral protein recruits ACBD3 to viral replication organelles, but the function of ACBD3 at replication organelles has been up for debate (Sasaki, Ishikawa et al. 2012). The viral 3A protein is present in many human pathogen members of the family picornavirus, genus enterovirus, and in host cells 3A inhibits protein transport and stimulates vRNA production by sequestering Golgi proteins to create viral replication organelles (Wessels, Notebaart et al. 2006).

Using CRISPR to edit *ACBD3* out of the genome and cause complete knockout, cells become resistant to CVB3 infection as the virus can no longer replicate (Kim, H. S., Lee et al. 2018). All previous studies into the role of ACBD3 in viral replication used siRNA and it is postulated that incomplete knockdown of ACBD3 may account for the contradicting results where researchers found ACBD3 to be essential or dispensable for viral infection in a number 3A expressing enteroviruses. It is further suggested that viral replication may only require very low levels of ACBD3 which is why viral replication still occurred in Dorobantu's observations although this is conjectural (2014).

1.8.3 Salmonella

Not dissimilarly to viruses, *Salmonella enterica serovar typhimurium* bacteria replicates within host cells in membrane-bound compartments termed Salmonella-containing vacuoles (SCVs). Following infection of epithelial cells, the SCV localises itself close to the host Golgi using SseF and SseG bacterial effector proteins which are part of the Salmonella pathogenicity island 2 type III secretion system (SPI-2 T3SS). This secretion system translocates other effectors across the vacuole membrane onto the SCV surface, surrounding microtubules and the cytoplasm. SseF was found to bind to ACBD3 by the yeast 2 hybrid system and this binding was dependent on SseG (Yu, Liu et al. 2016).

1.9 Other Oncoproteins that Interact with ACBD3 Pathways

Due in part to *ACBD3*s original classification as at least three different genes, its functions are rarely unified with papers tending to focus on one of ACBD3s many roles. This may be why it has taken so long to recognise *ACBD3* as a potential protooncogene which whilst far from established is beginning to emerge (Huang, Y., Yang et al. 2018). For the most part current literature on ACBD3 shows that it interacts with many known oncogene products and participates in an unusually large number of major cellular processes that, when deregulated, form essential hallmarks for cancer initiation and progression.

1.9.1 PI3K/AKT/mTOR

AKT is a kinase and the effector of PI3K in the PI3K/AKT/mTOR signalling pathway that stimulates cellular growth and survival. AKT has a broad range of targets including many of the ACBD3 binding partners, of which, PI4Kβ and Rhes also have regulatory effects on AKT (Bang, Steenstra et al. 2012, Paplomata, O'Regan 2014). AKT, PI3K, mTOR and their activities are all implicated in progression of cancer and are targets for current or future therapies (Paplomata, O'Regan 2014, Hare, Harvey 2017).

1.9.2 Krüppel Like Factor 9 (KLF9)

KLF9 is a basic transcription element binding protein that can supress or promote the expression of different genes depending on whether the promoter has one GC box (inhibition) or tandem repeats of the GC box (activation). KLF9 binds DNA via its C2H2 type zinc finger domain and is important in neural development, endometrial uterine proliferation, differentiation and adhesion and in pregnancy. KLF9 also appears to have tumour suppression activity where it prevents invasion and depletes (cancer) stem cell populations. An analysis by Simmen and Frank (2008) on the targets of KLF9 shows that ACBD3 is suppressed by KLF9 and KLF9 is downregulated in invasive breast cancers where NOTCH and ACBD3 have roles, specifically in cancer stem cell maintenance as we discuss below (Hare, Harvey 2017).

KLF9 is significantly down regulated in invasive breast cancers, endometrial carcinoma, glioblastoma and colorectal cancer and its expression can inhibit growth of tumour xenografts from glioblastoma neurospheres (Ying, Tilghman et al. 2014,

Limame, de Beeck et al. 2014). It is thought that the role of KLF9 in depleting cancer stem cells reduces the number of cancer cells in the microenvironment that can metastasise and that inhibiting KLF9 increases the population of these stem cells. It has been shown that the inhibition of NOTCH1 by KLF9 is important in tumour suppression and that KLf9 supresses neurosphere formation by 60% in controls but only by 33% when NOTCH1 expression is constitutively active (Ying, Tilghman et al. 2014). Whilst KLF9 is only a small part of the story in tumour suppression there may be more tumour suppressive targets for this transcription factor which explains why NOTCH1 expression only recovered 27% of neurosphere formation capacity.

1.10 Project Aims

The current understanding of breast cancer biology is better than most other cancers with several receptors known to play key roles, several alleles known to be risk factors, and many oncoproteins known to drive the disease. The picture however is not complete and there are potentially many more factors and roles left to uncover that have differing degrees of importance in breast cancer progression and therefore treatment. Targeted treatments are essential for increasing efficacy of chemotherapies whilst simultaneously reducing off target effects and are the focus of a whole generation of drug development in cancer and elsewhere.

ACBD3 is located on chromosome 1q whose locus is often amplified in breast tumours and in breast cancer cell lines. ACBD3 is involved in a large number of disparate cellular processes, has few known redundancies for its functions, and during the project ACBD3 overexpression was independently found to result in worse patient outcomes. This makes *ACBD3* a logical gene to study in breast cancer, and in general ACBD3 is not well characterised.

This work sought to determine whether ACBD3 expression affected breast cancer cell behaviour using breast cancer cell lines and breast cancer patient data. PI4Kβ activity is dependent on ACBD3 binding and is known to have a role in breast cancer, so was also studied throughout this work. Despite the limited information about ACBD3 regulation, efforts were made to find stimuli and compounds that regulated ACBD3 expression. Phenotypical and protein level changes were also measured when ACBD3 was overexpressed or mutated in breast cancer cell lines.

The aims were to:

1) find and collate data on ACBD3 mRNA and protein expression in human tissue, specifically healthy and cancerous breast tissue to assess ACBD3 as a breast cancer biomarker and to compare this with breast cell lines to use as models for breast cancer in the laboratory.
2) examine factors that affect ACBD3 expression in breast cancer cell lines and to trial some of these for therapeutic potential.
3) Examine the impact of ACBD3 overexpression on breast cancer cell phenotype and protein expression profile.

To achieve these aims I:

- Used many available bioinformatics resources and databases to characterise ACBD3 expression in healthy and cancerous tissue.
- Assayed a range of different types of breast cell lines for ACBD3 mRNA and protein expression.
- Used immunohistochemical techniques to determine ACBD3 protein expression in human breast and breast cancer cores/samples.
- Used the literature on ACBD3 binding partners and related cellular processes to screen for compounds or conditions that might affect ACBD3 expression.
- Created mutants of the *ACBD3* gene, engineered a cell line that overexpressed wildtype and mutant *ACBD3*, and measured phenotypical and proteomic changes to this cell line.

Chapter 2

Materials and Methods

2.1 Materials

2.1.1 products and manufacturers

Product	Manufacturer	Address
RPMI 1640 cell medium	Gibco (Life Technologies)	Carlsbad, California, USA
RPMI DMEM/F12 cell medium		
TriplE express		
Foetal Bovine Serum	Biosera	Marikina, Manila, Philippines
Cholera Toxin	Sigma-Aldrich	St. Louis, Missouri, USA
Human Epidermal Growth Factor		
Hydrocortisone		
SigmaFast protease inihibtor cocktail tablets		
T25 and T75 cell culture flasks	Nunc	Roskilde, Denmark
ACBD3 monoclonal antibody	Abcam	Cambridge, Cambridgeshire, UK
Beta-actin monoclonal antibody		
Histone H2B polyclonal antibody		
PI4KB monoclonal antibody		
Anti-mouse polyclonal antibody conjugated to HRP reporter enzyme	Dako	Santa Clara, California, USA
Anti-rabbit polyclonal antibody conjugated to HRP reporter enzyme		
Brilliant blue R-250	Bio-rad	Hercules, California, USA
RNeasy mini kit	Qiagen	Hilden, North Rhine-Westphalia, Germany
dNTPs	Invitrogen (Life Technologies)	Carlsbad, California, USA
Human Recombinant Insulin		

Lipofectamine 3000 and P3000		
Random primers		
Ribonuclease inhibitor		
Superscript II reverse transcriptase		
ACBD3 QPCR custom primers	Primer Design	Chandler's Ford, Hampshire, UK
PI4Kβ QPCR custom primers		
BrightWhite 96 well plates		
GeNorm QPCR kit		
PrecisionPlus 2X QPCR master mix with SYBR GREEN		
Precision nanoscript2 reverse transcription kit		
ACBD3 siRNA	Dharmacon	Lafayette, Colorado, USA
DharmaFECT1 transfection reagent		
Jetprime transfection reagent	Poly-plus transfection	New York, New York, USA
KLD enzyme mix and buffer	New England Biolabs	Ipswich, Massachusetts, USA
Q5 polymerase		
Lysis Buffer 17	R&D Systems	Minneapolis, Minnesota, USA
Proteome profiler XL Oncology array		
Breast core tissue array slides	US Biomax	Rockville, Maryland, USA

Table 2.1 - Sources and details of manufactures for the reagents and consumables used in this project. Abbreviations: dNTPs = deoxy N(Adenosine / Cytidine / Guanidine / Thymidine) triphosphates, HRP = Horse Radish Peroxidase, ACBD3 = Acyl-Coa Binding Domain protein 3, PI4KB = Phosphatidylinositol 4 Kinase Beta, RPMI = Roswell Park Memorial Institute , DMEM = Dulbecco's Modified Eagle Medium , QPCR = quantitative polymerase chain reaction.

2.1.2 Compound Reagent Preparations

Below are details for preparing all reagents, buffers, and materials that were not premanufactured. The use of these materials is detailed throughout chapter 2.2 methods.

Laemmli cell lysis buffer	
Reagent	**quantity**
1M TRIS pH 6.8	1ml
Glycerol	2ml
10% (w/v) SDS	4ml
B-mercaptoethanol	0.5ml
Bromophenol blue	Very little, enough to colour solution
dH_2O	Up to 10ml

Table 2.2 – Reagents to make up laemmli lysis buffer for lysing cells and preserving protein.

10X SDS-PAGE running buffer	
Reagent	**quantity**
TRIS base	30.3g
glycine	144.4g
SDS	10g
dH_20	Make up to 1000ml

Table 2.3 - Reagents to make up 10X SDS buffer. Working buffer (1X) was made by adding 100ml of 10X buffer to 900ml of dH_2O.

SDS-PAGE acrylamide gel				
Per gel	**Stacking layer**	**Resolving layer**		
		8%	**10%**	**12%**
dH_2O	2.1ml	4.6ml	4ml	3.3ml
30% acrylamide	0.5ml	2.7ml	3.3ml	4ml
1.5M TRIS (pH 8.8)		2.5ml	2.5ml	2.5ml
1M TRIS (pH 6.8)	0.38ml			
10% SDS	40µl	100µl	100µl	100µl
10% (w/v) ammonium persulfate	40µl	100µl	100µl	100µl
TEMED	4µl	6µl	4µl	4µl

Table 2.4 - Reagents used to make the stacking and resolving layers for one acrylamide protein separating gel. This preparation makes approximately 3ml of stacking layer gel and 10ml of resolving layer gel. dH_2O, 30% acrylamide, TRIS, and 10% SDS for the stacking and resolving layer may be prepared in parallel, ammonium persulphate and TEMED should only be added immediately prior to casting the gel.

Coomassie staining reagents		
Reagent	**Stain solution**	**Destain solution**
Methanol	500ml	500ml
Acetic acid	400ml	400ml
dH_2O	100ml	100ml
Brilliant blue R-250	1g	

Table 2.5 – reagents to make up Coomassie stain for total protein staining of acrylamide gels and destain. Stain solution should be stirred until coomassie is completely dissolved, stain can be recovered after staining and renewed with additional coomassie brilliant blue (1g per litre). Destain can be recovered by filtering paper to remove brilliant blue.

10X TOWBIN buffer	
Reagent	**quantity**
TRIS base	24.1g
Glycine	112.5g
dH_20	Up to 1000ml

Table 2.6 - Reagents to make up 10X TOWBIN buffer. Working buffer (1X) was made by adding 700ml dH_2O, 100ml of 10X Towbin transfer buffer, and 200ml methanol and making up to 1000ml total with dH_2O.

10X TBS	
Reagent	**Quantity**
TRIS base	24.1g
NaCl	88g
dH_20	Up to 1000ml

Table 2.7 - Reagents to make up 10X TRIS buffered saline. Working solution (1) was made by adding 100ml of 10X solution to 900ml dH_2O.

Electrochemiluminescence reagents	
ECL A	**ECL B**
2.5 ml 100mM TRIS	2.5ml 100mM TRIS
55µl luminol (250mM)	3µl hydrogen peroxide
22µl coumaric acid (90mM)	

Table 2.8 - Reagents for electrochemiluminescence (ECL) components A and B. solution A and B are made separately and mixed by pouring from one tube to the other, several times, directly prior to adding to the antibody-stained nitrocellulose membrane. Luminol and coumaric acid were solubilised in DMSO.

2.1.3 DNA Plasmids

The pEGFP-C3 empty vector was kindly donated to us by Dr Annabelle Lewis (Division of Biosciences, Brunel University London, UK) and the pEGFP-*ACBD3* C3 vector was kindly donated to us by Professor Carolyn Machamer (Department of Cell

Biology, The Johns Hopkins University School of Medicine, Baltimore, Maryland, USA) (Sbodio, Hicks et al. 2006) (Figure 2.1), plasmids were transformed into competent DH5α *E.coli* to grow my own stocks as described in 2.2.9. All mutants of the *ACBD3* gene were engineered in and derived from the pEGFP-*ACBD3* C3 vector.

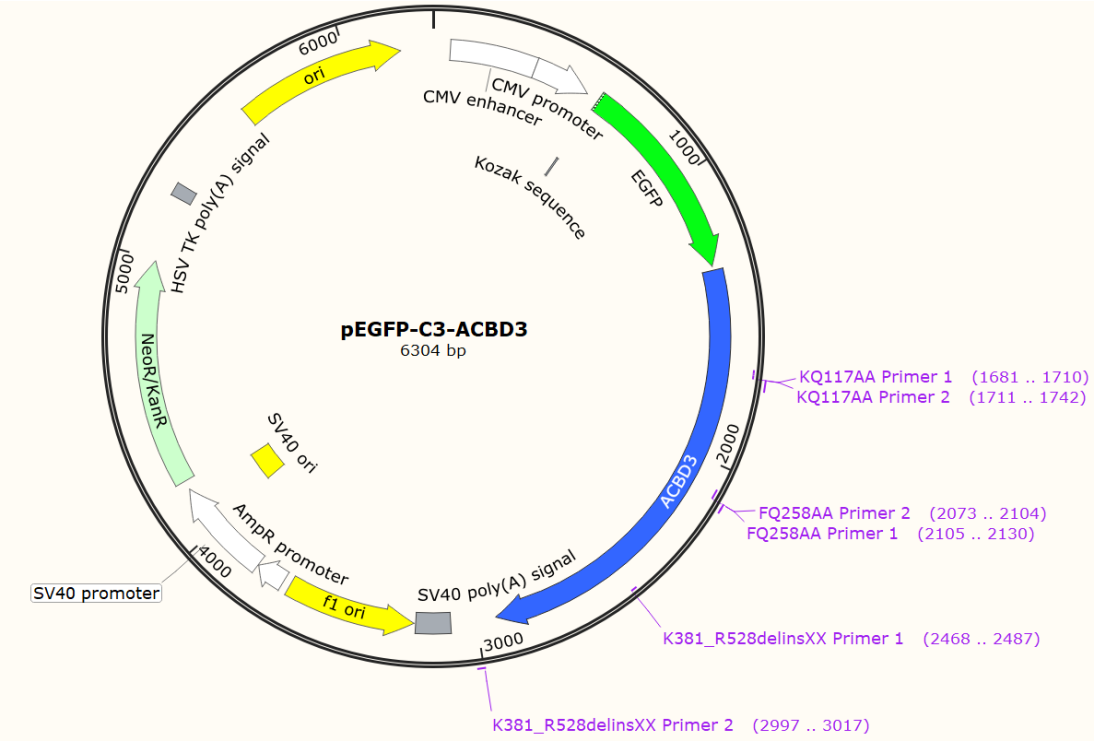

Figure 2.1 – *pEGFP-C3-ACBD3* plasmid map deduced by sanger sequencing using universal C3 plasmid primers (figure created in snapgene). The *ACBD3* gene is in frame with the *EGFP* gene meaning they are expressed as one transcript resulting in GFP tagged fluorescent ACBD3 protein. Primer pairs for engineering mutants are displayed on the map.

2.2 Methods

2.2.1 Cell lines

Various cell lines were used throughout this project as models for healthy and cancerous breast tissue and their characteristics are summarised in Table 2.9. All cell lines, except for the PMC42 line, were purchased from the American Tissue Culture Collection (ATCC), Manassas, VA, USA.

Cell line	Tissue/Cancer type	ER status	PR status	HER2 status	Pathology
MCF12A	Luminal/ epithelial	-	-	-	Normal/fibrocystic
BT20	Basal	-	-	-	IDC
MDA-MB-231	Claudin low	-	-	-	AC
MDA-MB-436	Basal B	-	-	-	IDC
SKBR3	HER2	-	-	+	AC
MDA-MB-361	Epithelial	+	-	+	AC / brain metastasis
PMC42	Basal	+	+	-	Not specified
T47D	Luminal A	+	+	-	IDC
BT474	Luminal B	+	+	+	IDC

Table 2.9 – Breast cancer type, receptor status and pathology of cell lines used in this work. Oestrogen receptor (ER), progesterone receptor (PR) and human epidermal growth receptor 2 (HER2) expression is given as either positive or negative for each cell line. Pathology abbreviations: AC = Adenocarcinoma; IDC = infiltrating ductal carcinoma. (Holliday and Speirs 2011, Chavez et al 2012, Whitehead et al 1984, Neve et al 2006). Cell lines were ordered by normal followed by cancerous, then ER status, then PR status, then alphabetical order.

The **MCF12A** cell line is derived from a mammoplasty reduction from a 60-year-old female with fibrocystic breast disease, it immortalised spontaneously and is non-cancerous. MCF12A cells were used in Chapter 4 as a normal like control for relative ACBD3 and PI4Kβ expression at the mRNA and protein level (Figures 4.3, 4.4, 4.5 and 4.6).

MDA-MB-231 cells were derived from the triple negative adenocarcinoma of a 51-year-old female in 1973, MDA-MB-231 is a very fast growing low maintenance cell line and was often used for experiments requiring large cell numbers (Cailleau, Olivé

et al. 1978). Cells were used to determine ACBD3 and PI4Kβ expression at the mRNA and protein level in a triple negative cell line (Chapter 4 – Figures 4.3, 4.4, 4.5, and 4.6), to visual multiple bands of ACBD3 staining by appropriate antibody (Chapter 4 – Figure 4.7), and to determine the efficacy of treatment with speculative ACBD3 regulators (iron or BQR695 PI4Kβ inhibitor, Chapter 5 – Figures 5.1, 5.2, 5.4 and 5.5). MDA-MB-231 cells were chosen to study the effects of ACBD3 regulators on growth as triple negative breast cancers currently have the fewest targeted treatment options.

MDA-MB-436 cells were used a model for Basal B type breast cancer and are a type of triple negative breast cancer. They were derived from a 43-year-old female in the mid-1970s (Cailleau, Olivé et al. 1978). These cells were chosen to determine ACBD3 and PI4Kβ expression at the mRNA and protein level in another triple negative breast cancer cell line and compare to MDA-MB-231 cells (Chapter 4 – Figures 4.3, 4.4, 4.5 and 4.6).

BT20 cells were derived from a 74-year-old female in 1958 (Lasfargues, Etienne Y., Ozzello 1958). BT20 cells were used to determine and compare ACBD3 and PI4Kβ expression at the mRNA and protein level in another basal type triple negative breast cancer cell line (Chapter 4 – Figures 4.3, 4.4, 4.5 and 4.6).

PMC42 cells were derived from the pleural effusion of a metastatic breast cancer of a 68-year-old female in the late 1970s (Whitehead, Bertoncello et al. 1983). PMC42 cells were used as to determine ACBD3 and PI4Kβ protein expression in another basal type breast cancer but that were not triple negative (Figure 4.6).

BT474 cells were derived from a ductal carcinoma in a 60-year-old female in 1978, are of Luminal B subtype, and positive for ER, PR, and HER2 expression (Lasfargues, E. Y., Coutinho et al. 1978). BT474 cells were used to determine *ACBD3* and *PI4Kβ* mRNA expression in Luminal B type breast cancer cells (Chapter 4 – Figures 4.3, 4.5, and 4.6).

SKBR3 cells were used as a model for HER2 type breast cancer derived from the adenocarcinoma of a 43-year-old female in 1970. Cells were used to determine *ACBD3* mRNA expression in a HER2 type breast cancer cell line (Chapter 4, Figure 4.3). Due to low expression, *PI4Kβ* mRNA for this cell line could not be included. Further complications with bacterial infection prevented this cell line being included in protein level expression of ACBD3 or PI4Kβ. The results of ACBD3 mRNA expression were included as SKBR3 was the only HER2+ ER- cell line reasonably available.

MDA-MB-361 cells were derived from a breast tumour that metastasised to the brain in a 40 year old female patient. They were used to determine ACBD3 and PI4Kβ expression at the mRNA and protein level in a HER2+ and ER+ breast cancer cell line (Chapter 4 – Figures 4.3, 4.4, 4.5, 4.6) and were also transfected to stably overexpress ACBD3, unfortunately the transfected cells did not recover.

T47D cells were derived from the pleural effusion of an invasive ductal carcinoma in a 54 year old female (Keydar, Chen et al. 1979). The T47D breast cancer cell line were used throughout this work to determine PI4Kβ expression at the mRNA and protein level in an ER+ Luminal A type cell line (Chapter 4 – Figures 4.3, 4.4, 4.5, and 4.6) and determine the effect of cell density on expression (Chapter 5 – Figures 5.9, 5.10, 5.11, 5.12, and 5.13).The T47D-EveR (everolimus resistant) cell line was previously engineered from T47D cells by long term treatment with everolimus in medium (Hare 2018). ACBD3 and PI4Kβ was compared between the T47D and T47D-EveR cell line at the mRNA and protein level to determine if either were altered (Chapter 5 – Figures 5.7, 5.8, 5.9, 5.10, 5.11, 5.12, and 5.13). The rate of growth was also compared between these line (Chapter 5 – Figure 5.14). ACBD3 was upregulated in the T47D-EveR cell line so ACBD3 was stably transfected into the T47D cell line to determine if this augmented resistance to everolimus (Chapter 6 – Figures 6.3, 6.4, 6.13, 6.14, and 6.15). The effect of overexpression on anoikis resistance was also examined when ACBD3 was overexpressed (Chapter 6 – Figure 6.15) and oncoprotein expression level changes were also examined (Chapter 6 – Figures 6.17).

2.2.2 Cell culturing

All cell work was carried out in a laminar flow cabinet under sterile conditions that were maintained by cleaning with 70% industrial methylated spirit (IMS) before and after every use as well as regular deep cleaning with chemgene cleaning agent in addition to IMS. Plasticware and disposables entering the cabinet were pre-sterilised and packaging was also sterilised using IMS. Water baths used to incubate medium and samples were cleaned at least weekly and filled with dH_2O. Cell incubators were cleaned regularly with chemgene and IMS and humidity was maintained using heat treated dH_2O.

2.2.3 Sub-culturing Cells from Cryostorage

Cell line stocks were stored in liquid nitrogen in 1.5ml cryo tubes in 1ml of the recommended medium with 10% Dimethyl sulfoxide (DMSO) as a cryoprotectant. Cells to be thawed were transferred, on ice, from liquid nitrogen to a 37°C water bath and once fully thawed were added to 9ml of pre-warmed medium. They were then centrifuged at 1000 *g* for 5 minutes (to remove DMSO) and the pellet was resuspended in 5ml of medium at 37°C and then transferred to a T25 culture flask. The cells were then incubated at 37°C, 5% CO_2, 95% humidity, for 24 hours followed by a medium change or passaging of cells if confluence had reached 80%.

Cell line	Base Medium	Additives
MCF12A	DMEM/F12 with glutamine	5% Foetal Bovine Serum, 20ng/ml Epidermal Growth Factor, 10µg/ml insulin, 0.5µg/ml hydrocortisone, 100ng/ml Cholera toxin.
BT20, BT474, PMC42, SKBR3, T47D, T47D-EveR, MDA-MA-231, MDA-MA-361, MDA-MB-436	RPMI 1640	10% Foetal Bovine Serum, 20µg/ml L-glutamine, 100U/ml penicillin, 100µg/ml streptomycin.
T47D, T47D-EveR, and MDA-MB-361 stably transfected cell lines	RPMI 1640	10% Foetal Bovine Serum, 20µg/ml L-glutamine, 400µg/ml G418 sulphate.
T47D-EveR Maintenance media	RPMI 1640	10% Foetal Bovine Serum, 20µg/ml L-glutamine, 100U/ml penicillin, 100µg/ml streptomycin. Everolimus 100100µM

Table 2.10 – Base medium and additives used for different breast cancer cell lines.

Cells were passaged, whenever confluence reached 80%, by removing medium, washing twice with 5-10ml of phosphate buffered saline (PBS) and detached from the flask surface by incubation at 37°C with TriplE express (1ml for T25 flasks, 2ml for T75 flasks) until cells could be seen to detach from the flask (2-6 minutes). TryplE treated cells were then passaged into new T25 flasks or from T25 flasks into T75 flasks. The dilution factor varied between cell lines but was generally a 1/3 or 1/4 dilution. Once passaged, appropriate medium (at 37°C) was added, which also deactivated TriplE, and cells were incubated at 37°C, 5% CO_2, 95% humidity. Details

of medium used for each cell line can be viewed in Table 2.9. T47D everolimus resistant cells (EveR) were grown in the standard medium with the addition of 100nM everolimus for 48-72 hours every 3 passages.

2.2.4 Cryopreservation

Once cell numbers had been expanded for experimental use, aliquots were taken to replace those taken from cryostorage. The medium was removed from 1 T75 flask and the cells were washed twice with 10ml of PBS. 2ml of 37°C TripleE express was added and the flask was incubated at 37°C until cells detached from the flask surface. 5ml of appropriate medium was added to the flask and the contents of the flask were centrifuged at 1000 *g* for 5 minutes with a low deceleration speed to avoid pellet displacing from the bottom of the tube. The pellet was then resuspended in 2ml of appropriate medium (see Table 2.10) with 10% DMSO then aliquoted into 2 1.5ml cryo-tubes. These were then transferred to the vapour phase of a liquid nitrogen tank for at least three hours, and then lowered into the liquid phase for storage.

2.2.5 Cell Imaging

All cellular imaging was undertaken on the FLoid cell imaging station (Thermo Fisher Scientific) at 460X magnification using either white light or the green light filter.

2.2.6 Cell Growth Curves

Cells were grown to 80% confluence and then detached as previously described. 5ml PBS was added and cells were transferred to a 15ml falcon tube and centrifuged at 1000 *g* for 5 minutes. The supernatant was discarded and the pellet was resuspended in a known volume of medium (usually 10ml). Cells were counted by adding 25µl of cell suspension to each end of a haemocytometer and counting the total number of cells in 3 4X4 grids (top left, bottom left, bottom right) then dividing by 3 and multiplying by 10,000 to determine for the number of cells per ml of suspension. The suspension was then diluted to the desired concentration and 2ml was added to each of a total of 18 wells in 6 well plates (6 plates each with cells in 3 wells). At 24, 48, 72, 96, 120, and 168 hours a plate was washed twice in PBS and cells were detached in 300µl TriplE per well. Cells were then counted by haemocytometer as before and the total cells were recorded. Cell number was plotted as the mean average cells for the 3 wells with standard deviation.

2.2.7 Anoikis Resistance Assays

Poly-2-hydroxyethyl methacrylate (PolyHEMA) powder was dissolved in 98% ethanol to a final concentration of 20mg/ml and agitated overnight in a 50ml tube. 1ml of this solution was then added to each well of a 6 well plate in a sterile hood and the lids were left off allowing the ethanol and water to evaporate for 2 to 3 hours. This was then repeated with another 1ml of solution and then lids were placed onto plates which were sealed in polypropylene bags and stored at 4°C until use. Cells were seeded onto polyHEMA coated plates at $2X10^5$ cells in 2ml of appropriate medium and incubated for 24 hours at 37°C, 95% humidity and 5% CO_2. The medium and cells were then extracted, the cells were pelleted and resuspended in 400µl TriplE and incubated at 37°C for 7 minutes. 30µl of the suspension was then added to 10µl of trypan blue dye (v/w 0/4%) and incubated for 3 minutes. Cell death was calculated as the number of blue stained cells divided by the total number of cells counted.

2.2.8 Cell Transfection with siRNA

ACBD3 ON TARGETplus smartpool siRNA was used in conjunction with DharmaFECT 1 transfection reagent to transfect breast cell lines. Cells were seeded at 50,000 per well in 12 well plates with 1ml of medium and incubated for 18 hours. After 18 hours wells were washed with antibiotic free and serum free medium and

then 800µl of antibiotic-free medium (containing 10% serum) was added to each well. No treatment, transfection reagent only, and transfection reagent with non-targeting siRNA were used as negative controls. Transfection reagent with previously verified siRNA that targets *PRKCA* was used as a positive control, and all transfections were carried out in duplicate in addition to the target siRNA (Table 2.11). For each condition (in duplicate) 2µl of transfection reagent was added to 198µl of serum and antibiotic free medium, concurrently, appropriate siRNA was added to serum and antibiotic free medium to a total volume of 200µl and both solutions were incubated for 5 minutes at room temperature. The transfection reagent and the siRNA containing medium were then mixed by gentle pipetting and inversion and incubated at room temperature for 20 minutes. 200µl of transfection medium was then added dropwise to the appropriate well. This was repeated after 24 hours where media was changed and new transfection medium was added. Samples were then collected either 24, 48 or 120 hours after the second transfection by removing medium and adding hot laemmli lysis buffer directly to the well and scratching the well with the tip, pipetting up and down to lyse the cells and suspend the contents. Untreated cells were expected to grow faster than those treated with transfection reagent and were seeded in quadruplicate, 2 wells were harvested in the same volume of lysis buffer as treated cells and 2 wells were harvested in 150% the volume of lysis buffer to account for a possible higher cell number.

Untreated cells	Untreated cells	Transfection reagent only	Transfection reagent only
Non-targeting siRNA	Non-targeting siRNA	Positive control siRNA	Positive control siRNA
ACBD3 siRNA	ACBD3 siRNA	Untreated cells	Untreated cells

Table 2.11 – 12 well plate layout for siRNA transfection assays.

2.2.9 Bacterial Transformation

50µl of chemically competent DH5α were removed from -80°C storage and thawed on ice for 30 minutes, then 10-25ng plasmid DNA was added and gently mixed by inversion. This DH5α were then incubated on ice for 1 hour, heat shocked at 42°C for 45 seconds, and placed on ice for 5 minutes. 950ul of antibiotic-free LB medium was added and the DH5α incubated at 37°C on a shaker for 1 hour. 950µl was then spread onto a selection LB agar plate and the remaining solution was diluted by a factor of 20 in 950µl LB medium and spread onto a second selection plate. For pEGFP

C3 vector and derivatives there of the selection drug was Kanamycin (50µg/ml). Plates were incubated at 37°C for 18-48 hours until single colonies were visible. Individual colonies were picked and grown in 5ml LB medium with 50µg/ml Kanamycin at 37°C in a shaker for 24 hours. Plasmid DNA was then extracted using centrifugal spin columns following standard protocols.

2.2.10 Cell Transfection with Plasmid DNA

Plasmid was transfected into breast cell lines using lipofectamine 3000. One day before transfection, cells from a T75 at or just over 80% confluency were detached and transferred to a 24-well plate at 10^5 cells per well in 500µl antibiotic free medium. The next day 25µl medium and 1µl lipofectamine 3000 (per well) were added to 1 eppendorf and 25µl medium (per well), 500ng plasmid (per well) and 1µl P3000 reagent (per well) were added to a second Eppendorf. The contents of these tubes were then mixed by pipetting and inversion and incubated at room temperature for 15 minutes. 50µl of transfection mixture was then added to each well. No treatment and lipofectamine 3000 only were used as negative controls and SiGLO siRNA was used as a positive transfection control as it is easy to visualise at 24 and 48 hours post transfection and is not reliant on being transcribed. G418 was the appropriate selection antibiotic for the EGFP C3 vector and several assays were undertaken to find the optimal concentration for different cell lines. It was found that 400µg/ml G418 effectively abolished viable T47D parental, T47D everolimus resistant, and MDA-MB-361 cell lines within 10 days. G418 was added to the transfected and control wells and was replaced with new medium every 72 hours. Controls were kept until all cells died at which point medium was changed to standard medium and incubated for 10 days to ensure no viable cells remained.

2.2.11 Site Directed Mutagenesis (SDM)

SDM was carried out on the pEGFP-*ACBD3* C3 vector to make specific base changes in the *ACBD3* open reading frame that resulted in protein level residue changes. Primer design and mutant development is described in chapter 7 but briefly primers were designed with non-complementary bases at the centre of one primer and at least 9 complementary bases either side of the non-complementary bases. A second primer was designed to be fully complementary to the other DNA strand immediately after the 5' of the first primer creating an origin of replication for PCR. Normal considerations for primer design were also considered such as GC content,

unique sequence, primer dimers, primer hair pinning, and ensuring at least three out of the five 3' bases are a G or C. Q5 high fidelity polymerase was used to extend the primers and amplify the entirety of the plasmid, introducing the mutation encoded on the first primer following the program in Table 2.12.

1µl of PCR product was then treated with NEB KLD (kinase, ligase, DNAse) enzyme mix to phosphorylate blunt ends of the PCR product, ligate the linear product into a circular plasmid, and digest the template DNA (the DNAse targets only methylated DNA, the template DNA used in all cases was harvested from DH5α which methylates DNA). 5µl of the KLD mix was then used to transform competent DH5α and transfect cell lines as described in sections 2.2.9 and 2.2.10.

Process	Temperature	Time	Cycles
Initial denaturation	95°C	30 seconds	1
Denaturation	95°C	10 seconds	25
Annealing	Primer dependent	20 seconds	
Extension	60°C	180 seconds	
Hold	4°C	indefinite	1

Table 2.12 - Program for SDM PCR, annealing temperatures for individual primer pairs are detailed in chapter 6.

2.2.12 Sanger Sequencing of the C3 Vector

Purified plasmid DNA from *E.Coli* transformations was sent to Genewiz (Essex, United Kingdom) for Sanger sequencing, in the first instance to confirm the *ACBD3* wildtype sequence and subsequently to confirm successful mutations had been introduced to *ACBD3* by SDM. In all instances the universal C3 primers were used to analyse *ACBD3* from both ends of the gene (Table 2.13). DNA was diluted to 1µg in 20 ul dH_2O and posted in Eppendorf tubes. Sequencing data was analysed in clustal omega multiple sequence aligner both for the DNA sequence and the amino acid sequence (derived using ExPasy translate) (Madeira, Park et al. 2019, Gasteiger, Gattiker et al. 2003).

Primer	Sequence
EGFP-C-Forward	5'- CATGGTCCTGCTGGAGTTCGTG -3'
EGFP-C-Reverse	5'- GTTCAGGGGGAGGTGTG -3'

Table 2.13 – Universal C3 primers used to sequence inserts in the multiple cloning site of the eGFP-C3 vector from upstream into the insert (forward primer) and downstream into the insert (reverse primer).

2.2.13 Cell Line Drug Treatments

96 well plates were seeded and incubated with appropriate medium for 24 hours to allow cells to attach. After 24 hours drug treatment was made up to 1000X of final concentration in suitable carrier (DMSO for everolimus and BQR695, complete medium for ammonium citrate and ammonium iron citrate) and 5µl of 1000X solution was added to 495ul medium. 11µl of this solution was then added to wells and cells were incubated as described for 72 hours (medium only, no cells, wells were also present). Each treatment concentration was assayed in sextuplet per plate and each experiment was carried out independently 3 times.

2.2.14 MTT Cell Viability Assay

MTT (3-(4,5-Dimethylthiazol-2-yl)-2,5-diphenyltetrazolium bromide) assays were carried out in 96 well plates; the MTT tetrazolium dye is reduced to insoluble formazan crystals by mitochondrial succinate dehydrogenase activity and is therefore a relative measure of the quantity of viable cells (Berridge, Tan 1993). MTT assays were used to assess cell growth with different concentrations of ferric ammonium citrate, ammonium citrate and BQR695 PI4Kβ inhibitor. Formazan is purple and absorbs light of 500nm to 600nm strongly (peak absorbance of 590nm but this varies depending on biological material in the sample). Formazan was measured at 540nm and the background absorbance at 630nm was used as a baseline.

After 72 hours of treatment the MTT reagent was made up in medium to a final concentration of 2.5mg/ml, the plates were washed twice with PBS and 100µl of medium/MTT solution was added to each well. Plates were then incubated for 2.5 hours at 37°C, 5% CO_2, 95% humidity. After incubation, the medium/MTT solution was removed and 100µl of acidified isopropanol (0.04*N* HCL) was added and pipette tips were used to dislodge and dissolve the formazan crystals that adhere to the plate.

Plates were incubated for a further 15 minutes before absorbance was taken using a Biotek ELx808 plate reader.

The 630nm mean background reading was subtracted from the 540nm reading of each well to remove nonspecific absorbance. To allow for comparison of results from individual experiments relative cell number was calculated as the mean absorbance value for each concentration divided by the mean absorbance of the control carrier reagent (no treatment) only.

Ferric ammonium citrate concentrations were calculated by the effective iron concentration in mass per volume but were converted to molarity concentration to make direct comparisons between ferric ammonium citrate and ammonium citrate which have different molecular weights. The conversion from mass per volume to molarity is detailed in Table 2.14.

Iron concentration (ng/ml)	Ammonium Iron(III) Citrate molarity (nM)
0	0
10	1.7907
50	8.9534
100	17.907
500	89.534
1,000	179.07
5,000	895.34
10,000	1790.68
50,000	8953.4
100,000	17906.8
500,000	89534
1,000,000	179068

Table 2.14 - Iron concentration in ng/ml used for MTT experiments and equivalent molarity used to make valid comparisons with ammonium citrate controls at equivalent concentration in cell medium.

2.2.15 Sulforhodamine B assay (SRB)

The MTT assay was not suitable for testing dose responses to everolimus as everolimus inhibits mTOR which affects mitochondrial activity and MTT is insolubilised by mitochondrial succinate dehydrogenase activity. The SRB assay was chosen instead as a colorimetric assay with comparable sensitivity and works by staining total protein and therefore equates to relative total cell number for a given cell line.

After 72 hours of treatment cells were fixed by the gentle addition of 25µl ice cold 50% (w/v) trichloroacetic acid to each well (without removing medium) and

incubated for 1 hour at 4°C. Plates were then rinsed 4 times in a large container of tap water and air dried. Fixed cells were stained with 50µl 0.4% (w/v) SRB in 1% acetic acid and incubated for 20 minutes at room temperature. The SRB dye was tipped out and wells were washed 4 times with 200µl 1% acetic acid and air dried. SRB was then solubilised in 100µl 10mM TRIS base solution and mixed by pipetting up and down and scraping the well with the tip. Plates were read at 405nm and 550nm absorbance using a BMG Labtech clariostar plate reader. The 405nm mean background reading and 550nm medium only mean reading were subtracted from the 550nm reading of each well to remove nonspecific absorbance.

Relative cell number was calculated as the mean absorbance value for each concentration divided by the mean absorbance of the DMSO only absorbance value.

2.2.16 Lysing Cells for SDS-Polyacrylamide Gel

Cells were detached from flasks as previously stated and counted using a haemocytometer then centrifuged at 1000 *g* for 5 minutes with a low spin down speed and lysed in hot 1ml laemmli buffer per 10^7 cells, separated into 50µl aliquots and stored at -20^{o}C.

2.2.17 SDS-PAGE

Polyacrylamide gels were made with a stacking and resolving layer to separate proteins by molecular weight (Table 2.3). dH_2O, acrylamide, TRIS and SDS were mixed in a 15ml falcon tube, ammonium persulfate and TEMED were added immediately prior to casting each respective layer of the gel and left to set for 20 minutes. Approximately 5.5ml of resolving gel and 2.5ml of stacking gel was used per gel cast. Page ruler plus prestained protein ladder was used to visualise separation and cell lysate was added to wells in equal quantities (approximately 10^5 cells per well in most cases), electrophoresis was carried out at 40 milliamps per gel in SDS buffer (Table 2.4).

2.2.18 Coomassie staining

New samples run of SDS-page gels were stained with coomassie blue to indicate loading and as a control prior to western blotting and staining for loading control protein (Table 2.5). SDS-page gel was transferred to a lidded container and

approximately 20ml of coomassie stain was added and incubated for 3 hours at room temperature on a rocker. After 3 hours, the stain was poured away, the container and gel were rinsed with water and destain solution was added and incubated on a rocker for 10 minutes. Destain was then removed and replaced with new destain and incubated on a rocker overnight or until the gel background staining was reduced and protein bands were visible on the gel. Image J software was then used to approximate relative loading and adjustments to loading were made as necessary for SDS-page for western blotting.

2.2.19 Western blotting

Separated proteins in the acrylamide gel were transferred to a nitrocellulose membrane by wet electrophoresis in Towbin transfer buffer (Table 2.6) at 300 volts for 1 hour. The nitrocellulose membrane was then blocked in 5% reconstituted powdered cows milk in Tris-buffered saline with 0.1% tween-20 (TBS-T), or undiluted UHT soya milk with 0.1% tween-20, for 1 to 2 hours at room temperature on a rocker at 30 RPM. To detect proteins of interest, the membrane was then incubated with primary antibody (diluted in 0.1% tween-20 milk, 3ml total) overnight at 4°C on a rocker at 30RPM. The membrane was then washed in TBS-T, 3 times for 10 minutes each on a rocker prior to incubation with secondary antibody (diluted in TBS-T milk) for 1 to 2 hours in a sealed plastic envelope on a rocker at room temperature. The membrane was then washed 3 times in TBS-T 0 for 10 minutes per wash. Concentrations of antibodies and working concentrations for incubations are detailed in Table 2.15.

Antibody	concentration	dilution	Working concentration
Rabbit anti ACBD3 primary	1.021g/l	1:1000	1.021µg/ml
Rabbit anti PI4KB primary	1.671g/l	1:1000	1.671 µg/ml
Mouse anti β-actin primary		1:5000	
Goat anti rabbit HRP conjugated secondary	0.25g/l	1:1000	0.25 µg/ml
Rabbit anti mouse HRP conjugated secondary		1:2000	

Table 2.15 - Concentration of antibodies used and working concentration for western immunoblot incubations.

Visualisation of antibodies was carried out using light sensitive film and electrochemiluminescence solution (Table 2.8). 1 minute exposures were carried out followed by longer or shorter exposures as necessary.

2.2.20 RNA extraction

Cells were detached from their flasks and centrifuged as described in section 2.2.3. RNA extraction was carried out on cell pellets immediately after centrifugation. Several methods, including centrifugal spin columns and magnetic beads were used for RNA extractions using the standard protocols. Briefly, cell pellets were lysed and centrifuged to remove debris and aggregates. For spin columns, supernatant was transferred to the column and centrifuged, flow through was discarded followed by several wash centrifugations with decreasing ethanol. RNAse free dH_2O was then added to the column and incubated for 2 minutes before centrifugation to elute the RNA from the column.

For magnetic bead RNA extraction, pellets were lysed in the supplied buffer including proteinase K and mixed carrier RNA and magnetic beads. A magnetic rack was used to retain the beads with bound RNA whilst samples were washed with buffer containing 80% ethanol. RNA was then detached from the beads with RNAse free dH_2O. magnetic bead extraction was found to give lower yield of RNA compared to spin columns.

RNA was eluted in dH_2O and was pipetted to aid suspension before reading RNA concentration at 260nm using a Nanodrop 2000 spectrophotometer (Thermo scientific). The 260/280 absorbance ratio was to determine the RNA:DNA ratio. A ratio of at least 2.00 was considered acceptable. The RNA was also separated on a 1% denaturing agarose gel at 100V on ice to check the quality of the RNA product mainly by visual conformation of 18s and 28s RNA bands and absence of smearing. RNA was kept on ice at all points following elution and stored at -80°C.

2.2.21 Reverse Transcription of RNA and cDNA Synthesis

Reverse transcription (RT) of RNA to cDNA was performed using Superscript II to achieve first strand synthesis. a small amount of RT was carried out using Nanoscript2 RT kit from Primer Design when superscript II was not available. In both cases, standard protocols were used starting with a known quantity of RNA as follows: 1µg RNA, 1µl random primers (150ng/µl), 1µl dNTP mix (10mM ATP, 10mM TTP,

10mM GTP, 10mM CTP) were mixed and made up to 12µl with nuclease free dH_2O and heated at 65°C for 5 minutes. The reaction mixture was then placed back on ice and 4µl first strand buffer, 2µl 0.1M DTT, 1µl ribonuclease inhibitor was added to each tube which was then incubated at 25°C for 2 minutes. 1µl of reverse transcriptase (200U/µl nanoscript from primer design or superscript II from Invitrogen) was then added and tubes were placed in a thermocycler using the program in Table 2.16.

Temperature	Time
25°C	10 minutes
42°C	50 minutes
70°C	15 minutes
4°C	Hold/indefinite

Table 2.16 - Thermocycler program for RNA reverse transcription reaction. The thermocycler should use a heated lid of 80°C (10°C above maximum temperature of reaction) and the program can be stopped as soon as the temperature reaches 4°C or left overnight.

2.2.22 Quantitative Polymerase Chain Reaction (QPCR)

All QPCR reactions were carried out in 96-well brightwhite plates using the applied biosystems Quant Studio 7 Flex real-time PCR system. All reactions used carried a total volume of 20µl using 10µl precisionPLUS 2X master mix, 1µl of primers, 8.5µl of nuclease free dH_2O and 0.5µl cDNA. cDNA concentration was not measured directly but in all cases was made from the reverse transcription of a known quantity of RNA (1µg) using the same programme and thermocycler. QPCR was then carried out using the program detailed in Table 2.17 where data collection was carried out at 60°C followed by melt curve analysis. Three independent biological experiments (three biological replicates) were tested per condition and each biological replicate was measured in triplicate.

The primers used to validate reference genes for chosen cell lines and subsequently used as reference genes were provided in the commercial primer design geNorm kit. The primer sequences for chosen reference genes are detailed in Table 2.16. *ACBD3* and *PI4Kβ* primers were custom ordered from primer design and the sequences were proprietary.

Process	Temperature	Time	Cycles
Denaturation	95°C	120 seconds	1
Denaturation	95°C	10 seconds	40
Annealing and extension (Data collection)	60°C	60 seconds	
Melt curve	variable	-	1

Table 2.17 - Program for QPCR for all samples and GeNorm analysis using the applied biosystems Quant Studio 7 Flex.

2.2.23 Reference Gene Assessment

Reference genes that were most stable between 8 cell lines were found by QPCR using the 12 gene GeNorm kit from Primer design. Two replicates for BT20, BT474, MCF10a, MDA-MB-231, MDA-MB-436, PMC42, SKBR3 and T47D cell lines were used, and the data was analysed by Qbase+ software (Biogazelle). For the 12 reference genes, an M and V value was calculated to give expression stability of the genes and an optimal number of reference genes to use in QPCR assays. Comparisons between the T47D parental, T47D everolimus resistant, and MDA-MB-361 cell lines and derivatives thereof were made using YWHAZ and TOP1 reference gene primers as these had previously been established to be the best choice by earlier GeNorm analysis (Hare 2018).

Qbase+ software was used to analyse QPCR results of GeNorm assays. All other analysis was carried out in Microsoft Excel using self-made templates and equations using the $2^{-\Delta\Delta Ct}$ method. Briefly, the mean Ct for each set of technical replicates was taken to give a Ct value for each biological replicate. The geometric mean of the reference gene Ct values was then calculated for each biological replicate to calculate the normalisation factor. The gene of interest Ct was then subtracted from the normalisation factor to give the ΔCt of the gene. The ΔCt was then subtracted from the reference sample ΔCt (usually the first sample alphabetically or the lowest seeding density or control) to give the $\Delta\Delta$Ct value. The relative quantity was then calculated as $2^{-\Delta\Delta Ct}$, this is further summarised in Equation 2.1 below.

$$2^{-(sample(Ct_{(gene\ of\ interest)} - Ct_{(normalisation\ gene)})) - (reference(Ct_{(gene\ of\ interest)} - Ct_{(normalisation\ gene)}))}$$

Equation 2.1 – Relative quantity of the gene expression in a sample relative to the quantity of the same gene in a reference sample. The relative quantity of the gene of interest in the reference sample will always equal 1 as the ΔCt is subtracted from itself equalling 0 and 2^{-0} equals 1.

2.2.24 Proteome Profiler Oncology Antibody Array

The R&D systems XL oncology array consisted of a membrane with fixed antibodies for many key oncoproteins, tumour suppressors and markers of cancer. It was used to assess proteome changes when cell lines were stably transfected with an ACBD3 expressing vector compared to an empty control vector.

Cells were detached from culture flasks and pelleted as previously described and lysed in R&D lysis buffer 17 (90%) and 10X sigma-fast protease inhibitor cocktail (10%) at 100µl per 10^6 cells. lysates were rocked for 30 minutes at 4°C, centrifuged at 14,000 x g for 5 minutes and the supernatant was retained in a new tube and stored at -80°C.

Per membrane, 2ml of array buffer 6 was added to 1 well of the supplied 4 well plate, the membrane was added and placed on a rocker for 1 hour at room temperature. Up to 0.5ml of sample was added to 0.5ml of array buffer 4 and adjusted to a total volume of 1.5ml with array buffer 6. When comparing samples, the same amount (whichever sample had the least volume) of each sample was added to minimise loading differences. Array buffer 6 was aspirated from the 4 well plate and 1 sample was added to each well/membrane and incubated at 4°C overnight.

Membranes were placed into individual plastic trays and washed 3 times with 1X wash buffer (supplied) for 10 minutes each. The 4 well plate was washed thoroughly with dH_2O and air dried and the membranes were returned to the same wells of the plate. Per membrane 30µl of detection antibody cocktail was mixed with 1.5ml of array buffer 4/6 (1 part array buffer 4 and 2 parts array buffer 6) and 1.5ml was added to each membrane. The plate was then incubated on a rocker at room temperature for 1 hour, the membrane and plate were then washed as described previously. Streptavidin-HRP was diluted according to the batch specification (1:2000) in 2ml of array buffer 6 per membrane, membranes were placed in the 4 well plate and incubated with 2ml diluted streptavidin-HRP for 30 minutes at room temperature on a rocker. Membranes were then washed again as described and then

partially dried by touching the side of the membrane to blue roll to wick away the wash buffer. To process: the membranes were placed on individual polypropylene sheets and 1ml of chemi reagent was added to each membrane. Membranes were covered with polypropylene sheet and incubated at room temperature for 2 minutes and the reagent was removed by wicking the edge against blue roll. The arrays were then placed into a fresh polypropylene sheet inside a dark box and exposed to hyperfilm for 1 minute, 2 minutes, and 10 minutes, (and 3 hours for membranes where less than 250µl of lysate was added). Films were then developed, fixed, and scanned at 600 dots per inch for analysis.

The arrays were analysed in ImageJ software using a circle sampler to measure mean grey pixel density. This was then inverted by subtraction from 255 and the background (negative control dots on the array) was also subtracted. Reference samples were used to normalise results between arrays and the normalisation factor was calculated as the mean average of an array reference spots / by the other array reference spots, the pixel density of reference spots was measured at 1 minute exposure. All other spots were measured on the film with the lowest exposure time where all dots were visible with the naked eye (not including the negative control).

2.2.25 Immunohistochemistry

Arrays of breast core samples were stained for ACBD3 protein using anti-ACBD3 primary antibody (from rabbit), the specificity of which was verified by use in western blots producing a band of expected size (Chapter 4 – Figure 4.6) Augmentation of ACBD3 expression also altered that intensity of ACBD3 staining by western blot, further validating the antibody (Chapter 6).

Breast core arrays of breast cancer, adjacent, and normal adjacent tissue were purchased from Biomax US, in all cases the slides were stained in the same way. The protective paraffin layer was removed by washing in coplin jars of histoclear and ethanol as outlined in Table 2.18, all reagents were a total of 50ml. wash was wicked from the slide between every step.

Wash	Time
Histoclear	2 X 5 minutes
1:1 Histoclear:Ethanol	3 minutes each
100% Ethanol	
95% Ethanol	
70% Ethanol	
50% Ethanol	
dH_2O	1 minute

Table 2.18 – Wash steps to remove paraffin from array slides.

The slide was then placed in a tray of 50ml of hot 22µM sodium citrate and was heated in a microwave at medium power (90 seconds on, 30 seconds off) for a total of 10 minutes. The slide was left to cool in solution and was then washed twice in PBS with 0.025% Triton-X. the slide was then wicked for excess wash and incubated in a coplin jar with 3% hydrogen peroxide-PBS for 15 minutes. The slide was then washed 3 times in PBS Triton X then 200µl 5% bovine serum albumin (BSA) in PBS was added directly to the top of the slide to cover the core array and parafilm was placed on top to spread the BSA and cover the slide. The slide was then incubated in a humidity chamber at room temperature for 1 hour.

BSA was removed from the slide by wicking onto blue roll, ACBD3 primary antibody was then diluted in 5% BSA (1:100 for array BC08032a, 1:75 for other arrays) and 200µl of diluted antibody was added to the slide, covered with parafilm and incubated in a humidity chamber at 4°C overnight. The next day the slide was washed 3 times in PBS Triton-X, wicked dry and then 3 drops of Zytochem Plus kit secondary antibody was added to the slide, spread with parafilm, and incubated for 1 hour in a humidity chamber at room temperature. The slide was then washed 3 times in PBC Triton-X, wicked dry, and 3 drops of streptavidin-HRP was added to the slide, spread with parafilm and incubated for 45 minutes in the humidity chamber at room temperature. The slide was washed 3 times in PBC Triton-X, wicked dry, and 200µl of zytochem plus DAB solution was added to the slide, spread with parafilm and incubated for 2 to 10 minutes (until visible red-brown colour change).

Slides were then washed in dH_2O for 5 minutes, wicked dry, stained with haematoxylin (200µl for 30 seconds), then immediately rinsed with dH_2O added

dropwise to on end of the slide. The slide was then placed in 0.1% sodium bicarbonate (w/v in dH_2O) for 60 seconds and wicked dry. The slide was then dehydrated following the steps in Table 2.17 in reverse (50% ethanol to histoclear). Finally, 50µl of DPX mounting glue was added to a cover slip and the slide was lowered face down onto the coverslip and gently pushed against the cover slip until the glue covered the array and cover slip. The slide was then picked directly upwards to avoid moving the cover relative to the samples and was left to dry face up at 4°C overnight.

Cores were analysed manually using a microscope. Cores were looked at 1/3 at a time (upper left, upper right, bottom centre) and scored for intensity of brown (DAB) staining against blue background (Haematoxylin nuclear stain). Scores were given as in Table 2.19 and scoring was repeated for each array 3 times on sequential days. The mean average of each 1/3 core was taken and then the mean average of all 3 days was calculated to give the final score. Scores were then compared to available data about each patient that the core was derived from.

Score	% DAB staining intensity
0	0-10
1	10-25
2	25-50
3	50-75
4	75-100

Table 2.19 - Percentage of DAB staining intensity represented by staining score for breast core arrays.

2.2.26 Bioinformatics Resources

Expression of ACBD3 was validated by the gene expression profile interactive analysis resource (GEPIA) (http://gepia.cancer-pku.cn/) using the GTEx and TCGA databases (40).

Copy number variation and mutations were retrieved from the TCGA cohort pan-cancer data with the cBIO portal resource (http://www.cbioportal.org/) (41, 42). Gene variants and upstream intergenic variants were retrieved from the genome wide association studies catalogue (https://www.ebi.ac.uk/gwas/) and from genehancer (https://www.genecards.org/) (43, 44). pan-cancer analysis data sampled: ACC, adrenocortical carcinoma; BLCA, bladder urothelial carcinoma; BRCA, breast

invasive carcinoma; CESC, cervical squamous cell carcinoma and endocervical adenocarcinoma; CHOL, cholangiocarcinoma; COAD, colon adenocarcinoma; DLBC, lymphoid neoplasm diffuse large B cell lymphoma; ESCA, oesophageal carcinoma; GBM, glioblastoma multiforme; HNSC, head and neck squamous cell carcinoma; KICH, kidney chromophobe; KIRC, kidney renal clear cell carcinoma; KIRP, kidney renal papillary cell carcinoma; LAML, acute myeloid leukaemia; LGG, brain lower grade glioma; LIHC, liver hepatocellular carcinoma; LUAD, lung adenocarcinoma; LUSC, lung squamous cell carcinoma; MESO, mesothelioma; OV, ovarian serous cyst-adenocarcinoma; PAAD, pancreatic adenocarcinoma; PCPG, pheochromocytoma and paraganglioma; PRAD, prostate adenocarcinoma; READ, rectum adenocarcinoma; SARC, sarcoma; SKCM, skin cutaneous melanoma; STAD, stomach adenocarcinoma; TGCT, testicular germ cell tumours; THCA, thyroid carcinoma; THYM, thymoma; UCEC, uterine corpus endometrial carcinoma; UCS, uterine carcinosarcoma and UVM, uveal melanoma.

Methylation data were retrieved from TCGA and MET500 OMICs data using the UALCAN resource (http://ualcan.path.uab.edu/) (45).

Predicted protein structures were modelled by the Phyre2 protein fold recognition server (www.sbg.bio.ic.ac.uk/~phyre2/) and the subsequent 3D models were analysed in Chimera X software (https://www.cgl.ucsf.edu/chimerax/) (46, 47).

Breast cancer patient relapse free survival, overall survival, and distant metastasis free survival data were retrieved and analysed into Kaplan-Meier survival curves in the KMplotter resource using the jetset data set (https://kmplot.com/) (48, 49). ACBD3 expression data in breast cancer patient responders and non-responders to therapies were retrieved from ROCplotter using the jetset dataset (http://www.rocplot.org/) (50).

ACBD3 binding factors and transcription factors were found using the signalling pathways project resource (https://www.signalingpathways.org/) to probe manually curated ChIP-Seq and transcriptomic data (51).

ACBD3 protein data were retrieved from the human protein atlas (https://www.proteinatlas.org/) (52). Association data for protein interactions and co-expression were carried out using geneMANIA (genemania.org) (53).

2.2.27 Statistical Analysis

Mean averages of data were taken across independent experiments and unpaired T-tests were performed to calculate statistical significance. Significant data were defined by $P<0.05$ and confidence intervals were defined as * = $P<0.05$, ** = $P<0.01$, *** = $P<0.001$.

Chapter 3

ACBD3 Bioinformatics and Clinical Analysis

3.1 Introduction

Increased *ACBD3* mRNA expression has previously been found to correlate with poor breast cancer patient prognosis and *ACBD3* was overexpressed in breast cancer cell lines based on observations in the TGCA database and 253 breast core samples from Chinese breast cancer patients (Huang, Y., Yang et al. 2018). *ACBD3* overexpression in T47D and BT549 breast cell lines caused increased, bulkier, mammosphere formation in suspension cultures whilst silencing of *ACBD3* with siRNA reduced the size and number of mammospheres (Huang, Y., Yang et al. 2018). Similarly, *ACBD3* overexpression increased side populations of cell lines inferring that ACBD3 promoted self-renewal and maintained cancer stem cell (CSC) populations (Huang, Y., Yang et al. 2018). It was concluded that ACBD3 activated the Wnt/β-catenin signalling pathway and that this was causative of CSC side population maintenance and malignant mammosphere formation.

The mechanism by which ACBD3 promotes CSCs and worsens patient outcomes is not understood and may be much broader than activation of the Wnt/β-catenin signalling pathway (Huang, Y., Yang et al. 2018). The role of ACBD3 is highly contextual depending on partners and cellular location and ACBD3 has a lack of known redundancies for many of its functions (Fan, Liu et al. 2010, Yue, Qian et al. 2019). ACBD3 has many interactors, some of which are implicated in breast cancer in their own right (Houghton-Gisby, Harvey 2020, Rostoker, Abelson et al. 2015, Garrido, Osorio et al. 2015, Morrow, Alipour et al. 2014, Stylianou, Clarke et al. 2006, Colaluca, Tosoni et al. 2008, Zhang, J., Shao et al. 2016, Garcí-a-Heredia, Verdugo Sivianes et al. 2016, Acharya, Xu et al. 2016). Several ACBD3 roles could arguably promote the hallmarks of cancer including dysregulating cellular energetics, sustaining proliferative signalling, replicative immortality and tumour-promoting inflammation (Hanahan, Weingberg 2000, Hanahan, Weinberg 2011, Belman, Bian et al. 2015, Liu, Jun, Matyakhina et al. 2003, Arakane, King et al. 1997, Zhou, Atkins et al. 2007, Gatliff, East et al. 2017).

As cancer treatments become more specialised and regimes become more personalised there is a need to profile gene and protein expression in tumours. Different types of cancer can have very distinct mRNA and protein expression profiles

and within cancer types, subtypes also have defining expression patterns. In breast cancer, tumours are subtyped based on oestrogen receptor, progesterone receptor, and epidermal growth factor receptor status, in addition to the allele variant of *BRCA1*, *BRCA2,* and mutations in genes such as *P53* (Walt, AJ et al. 1976, Wei, Sheridan et al. 1987, Slamon, D. J., Clark et al. 1987, Kuchenbaecker, Hopper et al. 2017, Filippini, Vega 2013, Lee, D. S., Yoon et al. 2012). Chromosome 1 is commonly amplified in breast cancers and increased copy number increases transcription of many chromosome 1q genes (Waugh 2014, Orsetti, Nugoli et al. 2006, Bièche, Champème et al. 1995), The location of *ACBD3* on arm q of chromosome 1 locus (1q42.13) may be important because of this (Orsetti, Nugoli et al. 2006).

It is imperative to study any genes that may influence therapy options or present as biomarkers for risk, progression, or patient prognosis in breast cancer. Genes may be overexpressed by a number of mechanisms including copy number increase or changes in transcription regulation including transcription factors or DNA methylation. For genes causative or promotive of cancer, inhibiting expression uses different strategies depending on the mechanism of upregulation. Protein coding mRNA that is not translated has no known effects in cancer, but increased mRNA often leads to increases in protein level expression. Protein expression increases can have a wide range of effects and targeting oncogenic proteins, or their interactors forms the core of modern chemotherapeutic design.

3.2 Chapter Aims

The aim of this thesis was to determine whether ACBD3 is overexpressed in breast cancer, to investigate whether its expression impacts patient survival and therapeutic outcomes and to consider the broader implications of ACBD3 expression in terms of its interactions. As direct evidence for the mechanisms that correlate ACBD3 expression and cancer prognosis are very limited, bioinformatic resources were searched to build a more comprehensive picture of ACBD3 expression, regulation, and mutation in healthy and cancerous breast tissue. In addition, databases were queried to investigate the link between ACBD3 expression and survival, relapse and metastatic outcomes for patients divided by receptor status, breast cancer subtype and response to chemotherapeutic agents. Finally, string analysis was used to identify potential novel ACBD3 binding partners.

3.3 Results

3.3.1 ACBD3 Expression In Tumours and Normal Tissue

To investigate the difference in *ACBD3* expression between normal and tumour tissues, the gene expression profiling interactive analysis tool (GEPIA) was queried for *ACBD3* transcription levels in different tissues, and most normal tissues were found to have lower expression of *ACBD3* than their paired tumour samples (Figure 3.1).

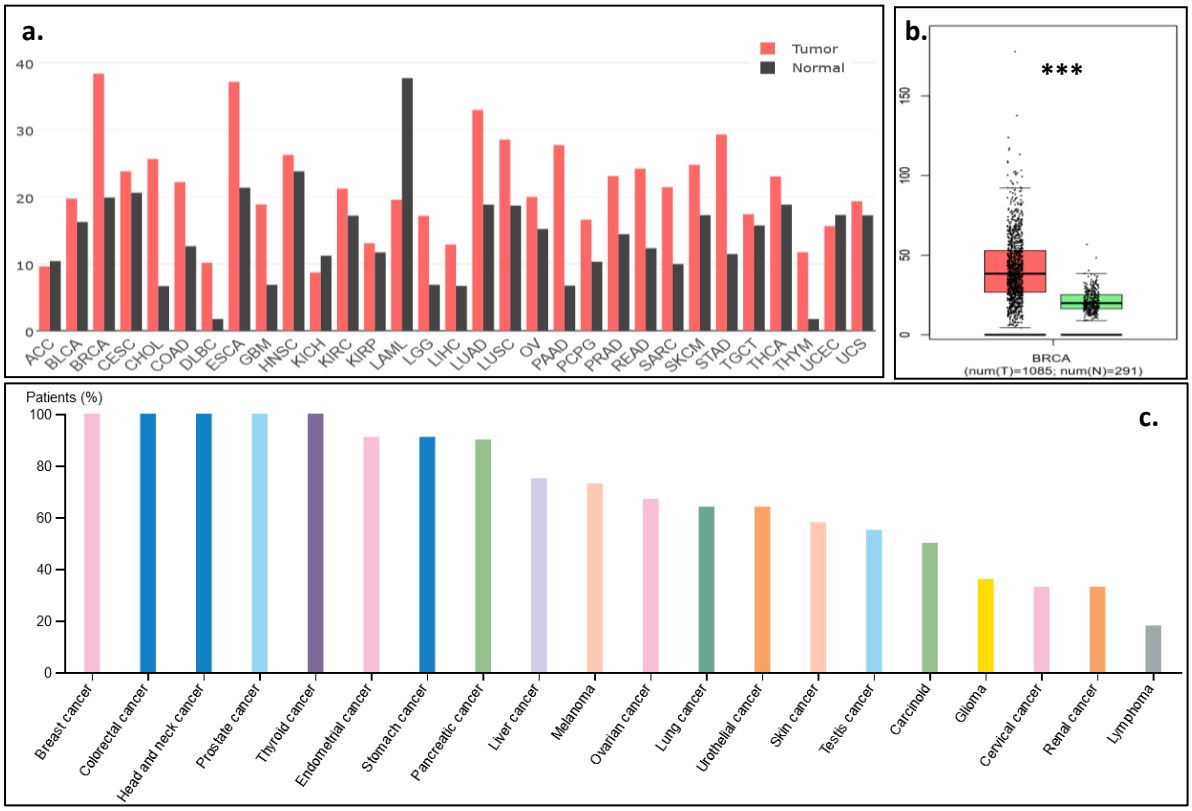

Figure 3.1 - a) Median *ACBD3* mRNA expression in transcripts per million of different tumours and matched normal tissue (Tang, Z., Li et al. 2017). **b)** *ACBD3* mRNA in breast tumour samples (red) and paired normal breast tissue (green) (**P* value < 0.001, Log_2FC cutoff = 0.75). *ACBD3* expression was 93.06% higher in cancerous breast tissue and samples also had a larger range of expression than normal tissue. **c)** Protein levels of ACBD3 measured by antibody staining.

The highest levels of *ACBD3* mRNA were found in in invasive breast carcinoma with 38.38 transcripts per million (TPM), higher than in any other cancer or paired healthy tissue (Figure 3.1a) (Tang, Z., Li et al. 2017). By comparison *ACBD3* mRNA was expressed at 19.88 TPM in paired normal breast tissue, meaning that *ACBD3* expression was increased almost 2-fold in tumours compared with normal breast

tissue. Expression also varied more between the breast cancer samples than in the paired normal breast tissue with a much larger interquartile range, smaller minimum value, higher maximum value, and more numerous and distant outliers beyond the maximum range (Figure 3.1b).

Conversely, *ACBD3* mRNA expression in acute myeloid leukaemia was lower than its paired normal tissue (37.71 vs 19.56 TPM), a very close inverse to the breast *ACBD3* expression profile, potentially suggesting differences in role or context of ACBD3 function between solid and haematopoietic tumours. Three other tumour types: adrenocortical carcinoma, kidney chromophobe, and uterine corpus endometrial carcinoma showed downregulation of *ACBD3* mRNA expression compared to matched normal tissue.

To investigate whether high expression of ACBD3 protein were also found in cancers, and if these correlated with *ACBD3* mRNA expression, the human protein atlas was queried. Whilst a direct correlation was not expected, it was reassuring that tissues with higher mRNA expression levels such as prostate and colon cancer as well as head and next carcinoma samples also had higher protein levels. Breast cancer had one of the highest levels of ACBD3 protein expression by the methodology used (11 out of 11 patient samples had medium levels of ACBD3 staining) (Figure 3.1c).

3.3.2 *ACBD3* Amplification and Mutation in Cancer

The cBIO portal for cancer genomics was used to examine the amplification of the *ACBD3* gene in tumours as well as determine the frequency of mutations and fusions (Cerami, Gao et al. 2012, Gao, Aksoy et al. 2013). Mutation frequency was generally low across all the cancers examined (Figure 3.2) Breast cancers were found to have the highest proportion of *ACBD3* gene amplifications at 8.76% and a low percentage of mutations relative to other cancers such as uterine and prostate (Figure 3.2), but interestingly ovarian cancer had no *ACBD3* mutations. In breast cancer, *ACBD3* mutations occurred in 5 out of 1084 patients, one each of: E212Q, E226K, E348Q, R523T mutation, and a E348Nfs*21 frame shift deletion (Figure 3.3). Whilst the highest of the cancers examined, the *ACBD3* amplification rate in breast cancer was less than expected based on the *ACBD3* transcriptional upregulation observed with the GEPIA tool (Figure 3.1) and the commonality of chromosome 1q amplification in breast cancer (Orsetti, Nugoli et al. 2006).

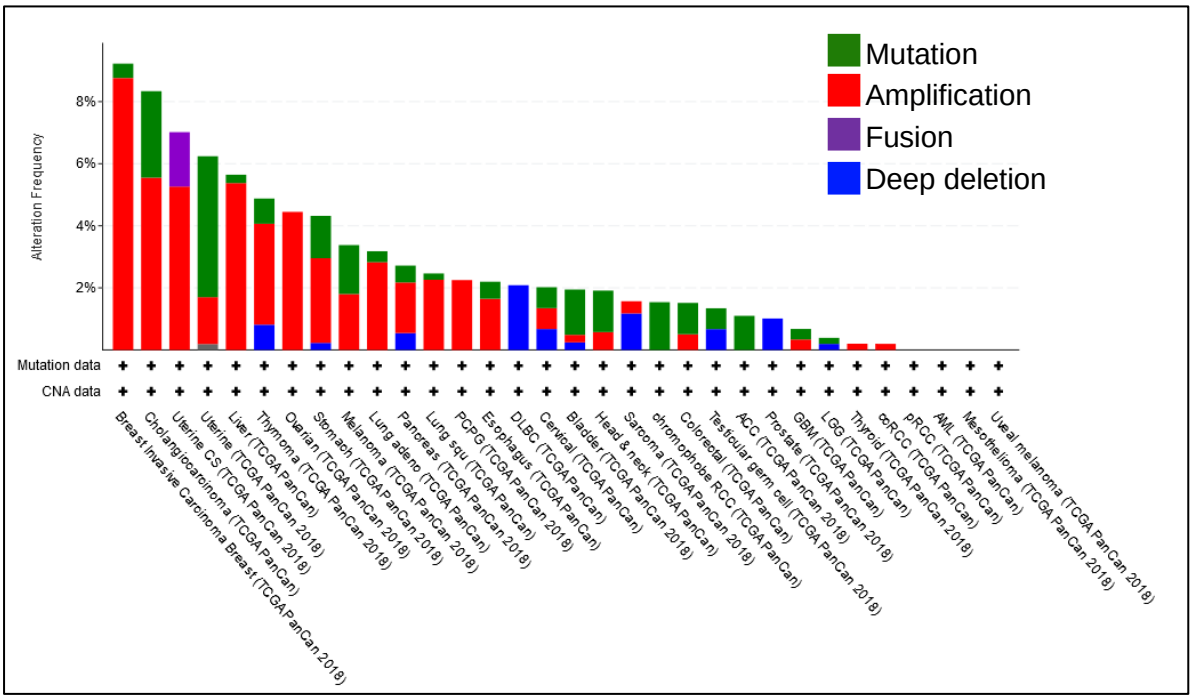

Figure 3.2 – Frequency of ACBD3 alterations in different cancers. There was a higher frequency of ACBD3 alteration in breast cancer (first bar) than in any other cancer. ACBD3 was mutated infrequently (green) but underwent gene amplification (red) more in breast cancer than in any other cancer. ACBD3 was most frequently mutated in adrenocortical carcinoma. Acute myeloid leukaemia samples had no alteration frequency. Data was accessed from cBIOportal (Cerami, Gao et al. 2012).

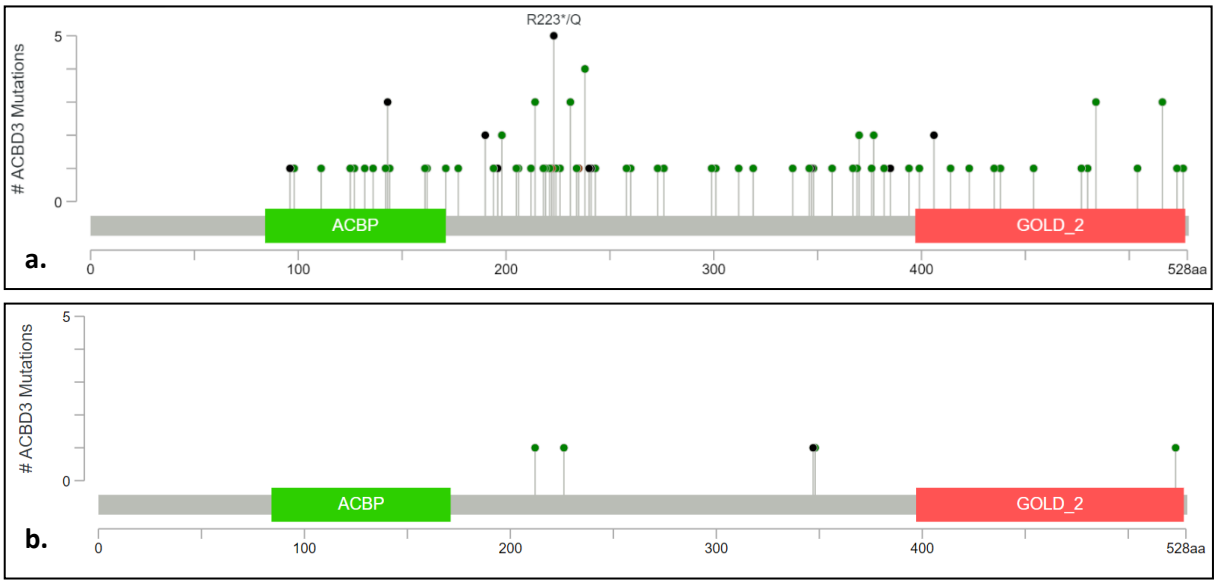

Figure 3.3 – Position and frequency of mutations in ACBD3 that resulted in amino acid changes for a.) all cancers, and b.) breast cancers. ACBD3 somatic mutation frequency in breast cancers was 0.5%, green circles represent single amino acid level changes, black circles represent missense mutations (Cerami, Gao et al. 2012).

The four *ACBD3* breast cancer mutants with base changes were cross referenced with the literature and it was found that none of the single amino acid change mutants had been engineered previously or studied *in vivo* or *in vitro* so any functional changes caused by the codon changes are unknown. The fifth mutation identified, the E348Nfs*21 deletion, results in early termination of transcription and encodes a truncated ACBD3 protein that terminates at aa367. This protein would be missing the entirety of the Golgi dynamics (GOLD) domain making it very unlikely that this mutant protein would localise to the Golgi or interact with any Golgi resident proteins (Horova, Lyoo et al. 2019). All other instances of mutation occurred in the flexible linkers, outside of known domains. To better understand how the mutants might affect the structure of ACBD3 the Phyre2 protein fold recognition server was used to model the mutant proteins but results were inconsistent with the same input sequence providing different output structures (data not shown) (Kelley, Mezulis et al. 2015). ACBD3 is a flexible protein and X-ray crystal structures have only been produced and solved for the GOLD domain suggesting that the protein has many conformations of equivalent stability and that this did not allow Phyre2 to model one definitive structure (Klima, Chalupska et al. 2017).

ACBD3 minor alleles and intergenic variants were queried in the Genome Wide Association Studies catalogue for phenotypic risk association (Buniello, MacArthur et al. 2019). It was found that five DNA variants upstream of *ACBD3* (three intergenic variants and two regulatory region variants) were associated with core binding factor acute myeloid leukaemia risk (Lv, Zhang et al. 2017). There was one other risk variant but this was not linked to cancer but rather behaviour which is not that surprising given several other ACBD family proteins are known to influence behaviour in animals (Ujjainwala, Courtney et al. 2018, Lanfray, Caron et al. 2016, Lanfray, Richard 2017). The Genehancer database was also searched corroborating that the same five *ACBD3* variants were associated with core binding factor acute myeloid leukaemia risk and, additional *ACBD3* regulatory region variants were found that enhanced the red blood cell distribution width (a measure of red blood cell volume variation), and that were associated with plateletcrit: (the percentage of blood volume occupied by platelets) (Fishilevich, Nudel et al. 2017). Another *ACBD3* regulatory region variant was associated with DNA methylation.

3.3.3 Copy Number Variation and Promoter Methylation of *ACBD3* in Breast Cancer

As *ACBD3* was found to be upregulated in many cancers, with the highest expression in breast cancers, and gene amplification events were relatively low, the UALCAN resource was queried to determine the mechanisms underlying this upregulation. Methylation of the *ACBD3* promoter region was examined using TCGA and MET500 databases (Chandrashekar, Bashel et al. 2017), as variations in methylation of gene promoters are linked with transcriptional regulation, typically repression (Baylin, Herman 2000, Smiraglia, Plass 2002, Laird 2003, Yang, Park 2012, Bouras, Karakioulaki et al. 2019, Achinger-Kawecka, Valdes-Mora et al. 2020). Tumour sample *ACBD3* promoter methylation was not found to be significantly different from paired normal tissue methylation (*P = 0.86) and methylation was observed to be very low in both cases (Figure 3.4). This suggests that the ACBD3 reading frame is constitutively open and accessible in healthy and cancerous breast tissue and that methylation is not a major regulator of the *ACDB3* gene expression. *ACBD3* promoter methylation was similarly low in all other tissues examined (data not shown).

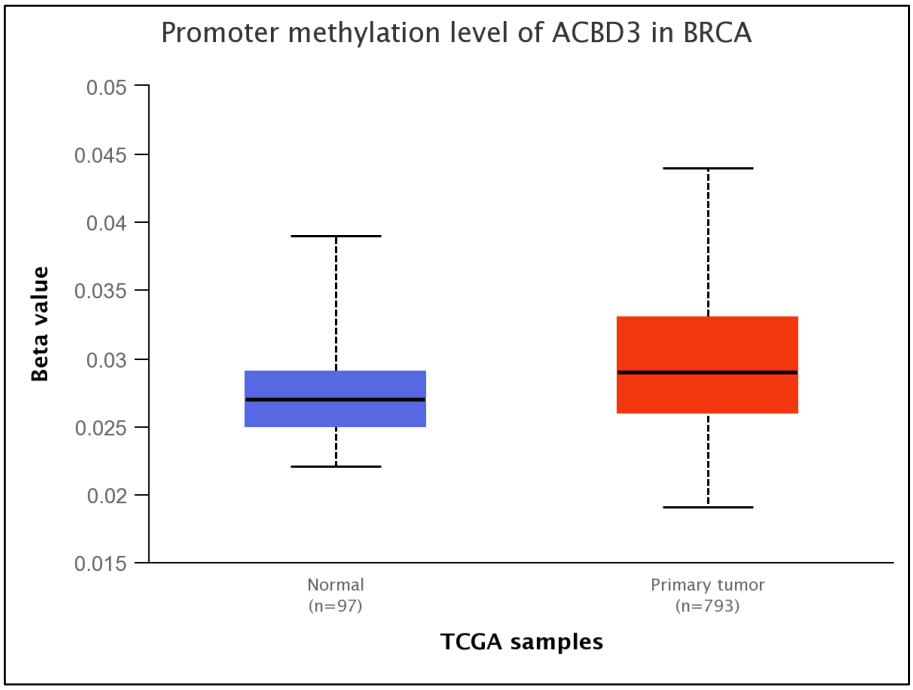

Figure 3.4 – *ACBD3* promoter methylation in normal breast tissue (blue) and breast tumour tissue (red). a low beta value represents low methylation and therefore low inhibition of transcription. A beta value below 0.3 is considered hypomethylation.

3.3.4 *ACBD3* Transcription Factors in Breast Tissue

Both methylation and amplification of *ACBD3* were low in breast cancer samples compared to the level of *ACBD3* upregulation, therefore the signalling pathways project (SPP) ChIP-seq database was used to find *ACBD3* binding factors in normal tissue that may be important in breast cancer (Ochsner, Abraham et al. 2018). A large number of factors were discovered that bind within 10,000 bases of the *ACBD3* transcription start site across all tissues and some of these stand out as having roles in breast cancers including NOTCH1-NICD, CDK9, CTCF, and CEBPB (Stylianou, Clarke et al. 2006, Reedijk, Odorcic et al. 2005, Schlafstein, Withers et al. 2018, Brisard, Eckerdt et al. 2018, McLaughlin, He et al. 2019, Aulmann, Bläker et al. 2003, Docquier, Kita et al. 2009, Mustafa, Lee et al. 2015, Oh, Oh et al. 2017, Damaschke, Gawdzik et al. 2020, Grimm, Rosen 2003, Zahnow 2009, Kurzejamska, Johansson et al. 2014). The transcriptomics function of the SPP was used to find regulators of *ACBD3* expression that caused a fold change of two or more for all tissues (Figure 3.5a). Amongst those identified across tissue types were the oestrogen receptor (when stimulated with Bisphenol A), the insulin receptor, the vitamin D receptor, FOXA1 and a number of viral transcription factors.

In breast tissue specifically, the insulin receptor pathway-related X10 ligand and the FOXA1 transcription factor were shown to increase *ACBD3* transcription by 2-fold or more (Figure 3.5b).

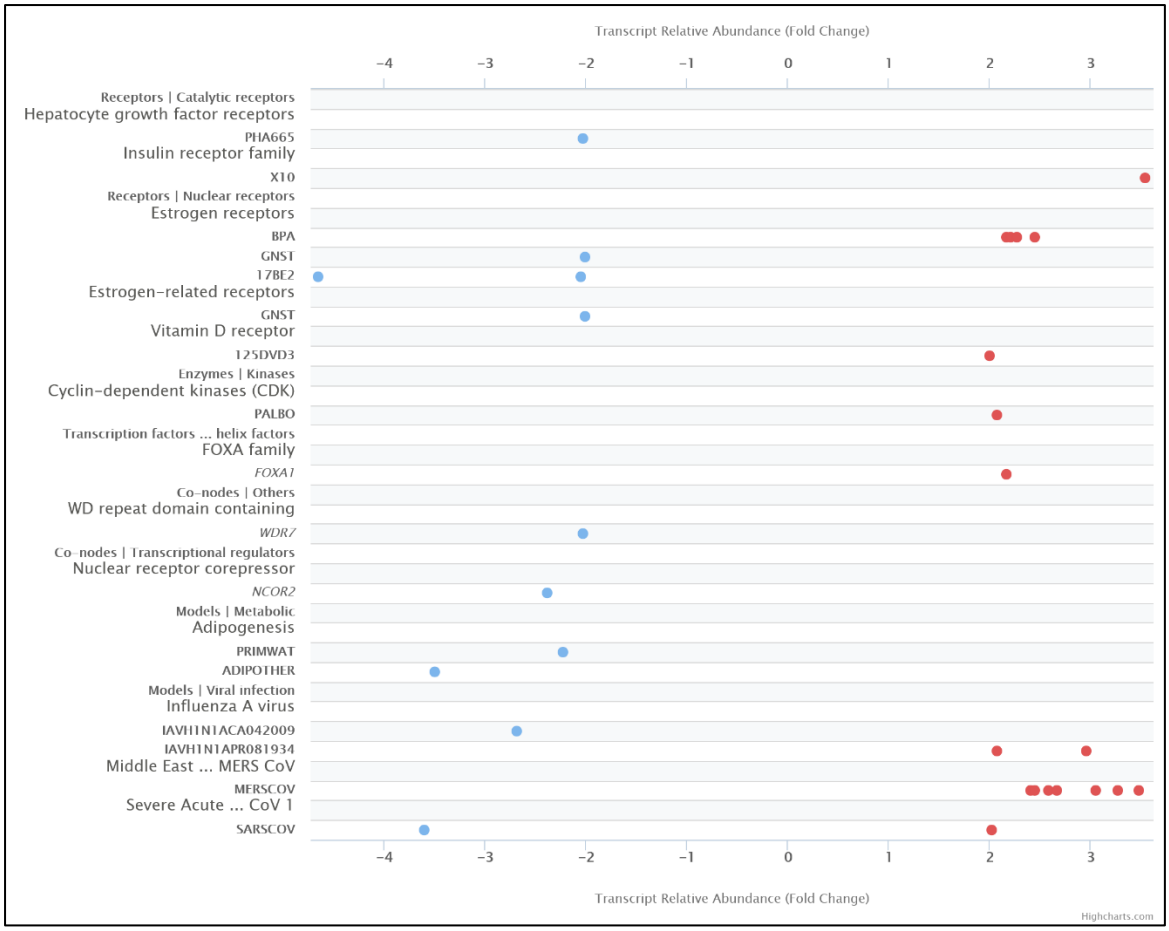

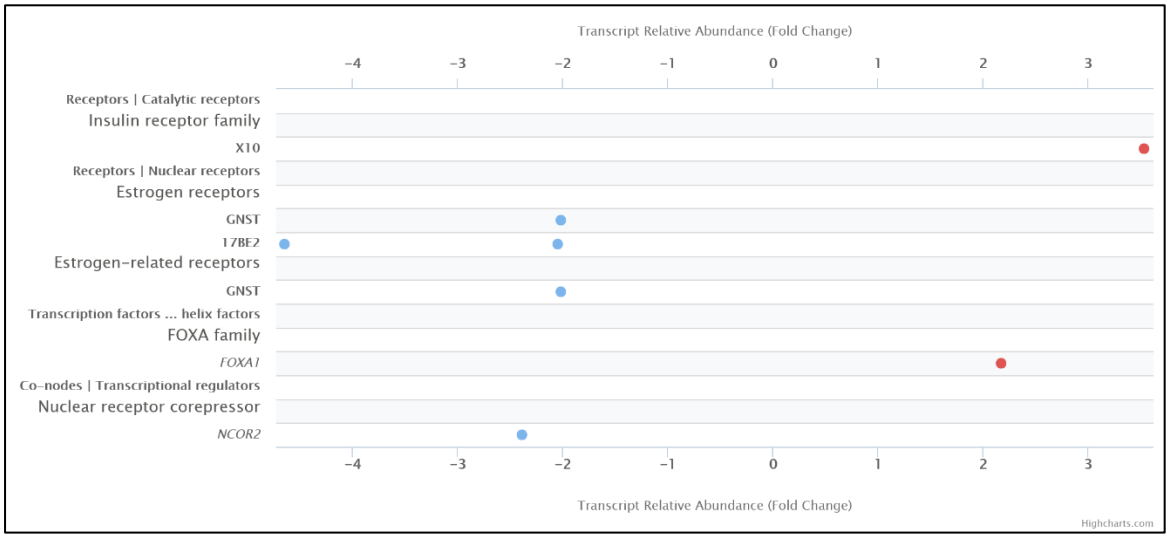

Figure 3.5 – Transcription factors that change *ACBD3* transcription in: a) all tissues and b) normal breast tissue. blue dots show repression of *ACBD3* transcripts, red dots show promotion of *ACBD3* transcripts (*$P < 0.001$).

3.3.5 *ACBD3* mRNA Expression and Breast Cancer Patient Prognosis

Previously high *ACBD3* tumour expression was correlated with poorer overall survival for breast cancer patients irrespective of clinical stage (Huang, Y., Yang et al. 2018), but little is known about the impact of ACBD3 expression in the different breast cancer subtypes, or on either relapse free or distant metastasis free survival. The KMplotter breast cancer mRNA gene chip database was used to look at differences in survival, relapse and distant metastasis in breast cancer patients based on whether mRNA levels of ACBD3 were above or below the median expression level in their breast tumour (Nagy, Lánczky et al. 2018). The patient cohort overall and subgroups were analysed and results with a significant difference were recorded.

Higher *ACBD3* levels were associated with earlier relapse, more probable distant metastasis and lower survival. When exploring subgroups and tumour subtypes, high *ACBD3* expression was associated with a higher probability of relapse and distant metastasis in patients with ER+, HER2- and Luminal B tumours. High tumour *ACBD3* was also associated with less overall survival in ER+ and HER2- tumours (Figure 3.6).

3.3.6 Relapse Free Survival is Worse When Tumour *ACBD3* Expression is Above the Median

Relapse free survival (RFS) was less likely when *ACBD3* tumour expression was above the median level in breast cancer patients, median survival was 229 months when *ACBD3* was below the median and 173 months when *ACBD3* expression was above the median (Figure 3.6a). RFS was not significantly different when HER2+ patients were divided by *ACBD3* expression but was significantly lower in HER2- patients with *ACBD3* expression above the median level (43 months) compared to below the median (74 months) (Figure 3.6b). RFS was not significantly different when triple negative breast cancer patients were divided by median *ACBD3* but both ER+ and ER- negative groups had less RFS when tumour *ACBD3* was expressed above the median (Figure 3.6c and 3.6d). RFS was also not significantly different when PR+ and PR- patients were divided by *ACBD3* expression. Luminal B breast cancer patients were found to have the largest difference in RFS of all intrinsic subtypes when divided by ACBD3 expression (Figure 3.6e).

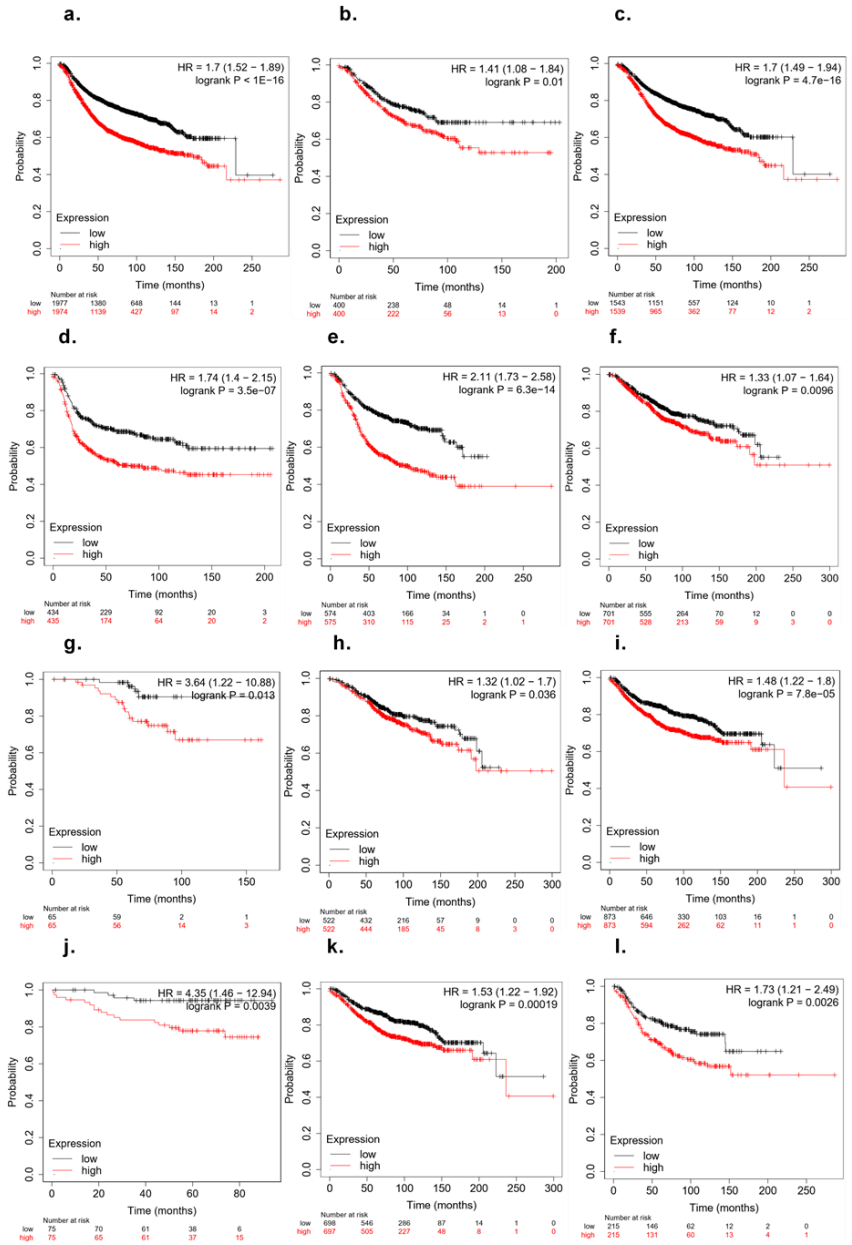

Figure 3.6 – Kaplan Meier plots for patient prognosis when divided by *ACBD3* mRNA expression. Black data points represent patients whose breast tumours had *ACBD3* mRNA expression below the median level. Red data points represent patients whose breast tumours had *ACBD3* mRNA expression above the median level.

(a-e) Relapse free survival when ACBD3 is high or low for: **a)** breast cancer patient cohort overall, **b)** HER2- breast cancer patients, **c)** ER+ breast cancer patients, d) ER-breast cancer patients, e) Luminal B breast cancer patients.

(f-h) Overall survival when tumour ACBD3 is high or low for: **f)** the breast cancer patient cohort overall, **g)** HER2- breast cancer patients, **h)** ER+ breast cancer patients.

(i-l) Overall distant metastasis free survival when tumour *ACBD3* was high or low for: **i)** the breast cancer patient cohort overall, **j)** HER2- breast cancer patients, **k)** ER+ breast cancer patients, **l)** intrinsic type luminal B breast cancer patients.

3.3.7 Overall Survival is Worse When Tumour *ACBD3* Expression is Above the Median

The probability of overall survival (OS) was reduced in breast cancer patients with tumour *ACBD3* expression above the median level (Figure 3.6f). Upper quartile survival was 126 months for patients when *ACBD3* was below the median level and 82 months when *ACBD3* was above the median level. HER2-, and ER+ patients had less OS when *ACBD3* expression above the median (*$P < 0.05$) (Figure 3.6g and 3.6h) but these changes were not as large as those seen in RFS differences (Figure 3.6b and 3.6c). ER+ patients had an upper quartile survival of 144 months when *ACBD3* expression was below the median and 105 months when *ACBD3* was expressed above the median level. OS in Luminal B patients was not significantly different between patients divided by *ACBD3* expression. *ACBD3* expression was not a predictor for OS in Luminal B breast cancer patients.

3.3.8 Distant Metastasis Free Survival is Worse When *ACBD3* Expression is Above the Median

Distant matastasis free survival (DMFS) was less likely when *ACBD3* expression was high, the uper quartile DMFS was 138 months for the cohort as a whole when *ACBD3* was expressed below the median level in breast tumour and 68 months when *ACBD3* was expressed above the median (Figure 3.6i). HER2- patients were at greater risk of distant metastasis when *ACBD3* was high in their tumours (Figure 3.6j). ER+ patients were more likely to have distant metastasis if tumour *ACBD3* was above the median level, upper quartile DMFS was 75 months when *ACBD3* was high and 143 months when *ACBD3* was low (Figure 3.6k). Luminal B breast cancer patients had less DMFS when *ACBD3* was expressed above that median level, upper quartile DMFS was 107 months when *ACBD3* was below the median level and 38 months when ACBD3 was above the median (Figure 3.6l). These findings in breast cancer patients indicate that high *ACBD3* mRNA expression negatively effects survival, relapse risk and distant metastasis risk.

3.3.9 *ACBD3* Expression in Responders and Non-Responders to Chemotherapy in Breast Cancer

Given *ACBD3* expression over the median was found to predict less relapse free survival, less overall survival and less distant metastasis free survival for patients in many subgroups, it appears that *ACBD3* could be predictive of patient outcomes. ROCplotter was queried to determine whether *ACBD3* expression had an impact on therapeutic outcomes (Fekete, Győrffy 2019). *ACBD3* expression was higher in patients who had pathological complete response to combination chemotherapy regimens (FAC, FEC, CMF), as well as to individual agents such as ixabepilone, Taxane, and anthracycline (Figure 3.7a). This observation is a strong contrast to data in Figure 3.6 where high ACBD3 expression had consistently negative patient outcomes. *ACBD3* expression was not significantly different between those that had 5 years relapse-free survival and those that relapsed before 5 years following chemotherapy (Figure 3.7b).

The picture for patients with HER2+ cancer was slightly different. Here, those who had complete pathological response to chemotherapy had lower *ACBD3* RNA expression than those who did not respond (Figure 3.7c). Patients who responded to trastuzumab did not have significantly different *ACBD3* expression but those treated with lapatinib anti-HER2 therapies had significantly lower *ACBD3* expression than those who did not respond (Figure 3.7d and 3.7e). Anthracycline treatment appeared to be more effective when *ACBD3* expression was significantly lower (Figure 3.7f). Patients taking trastuzumab who were relapse free for 5 years did not have significantly different tumour *ACBD3* RNA expression from those that relapsed before 5 years (data not shown).

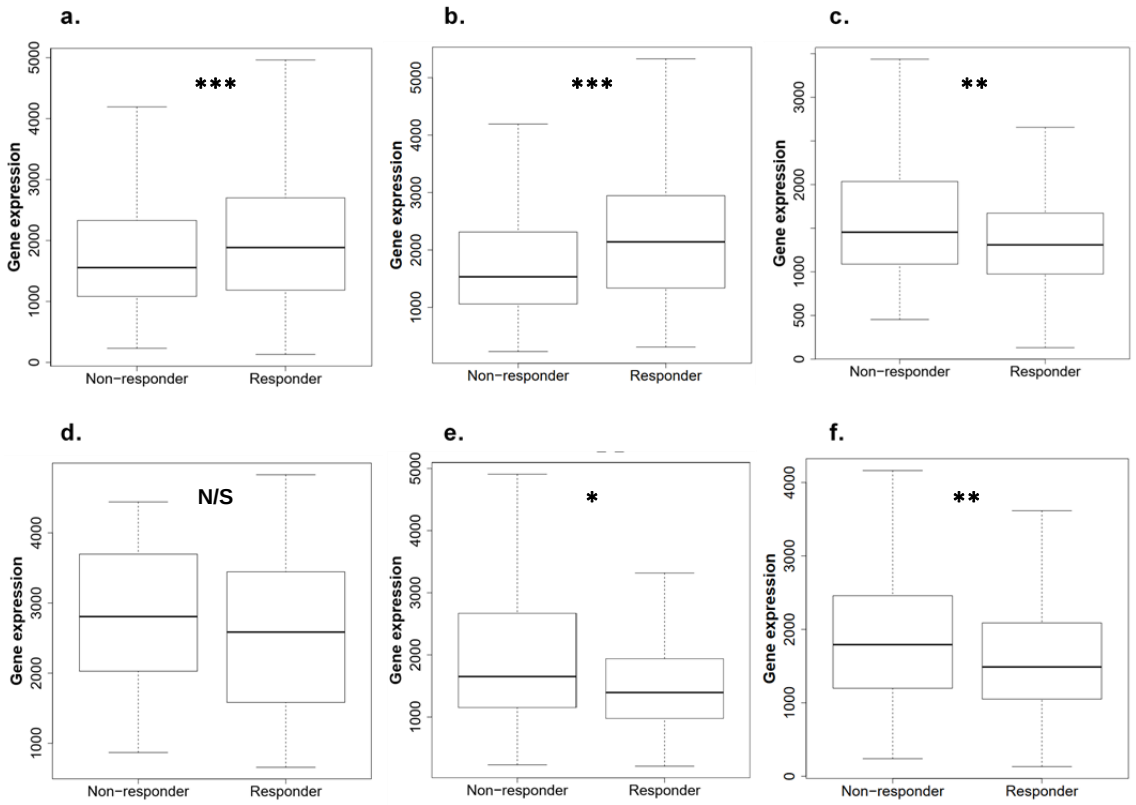

Figure 3.7 – a) *ACBD3* expression in breast chemotherapy responders and non-responders. *ACBD3* is 1.1-fold higher in responders than in non-responders to chemotherapy overall in breast cancer (*P** = 0.0000014). **b) *ACBD3* expression in HER2+ chemotherapy responders and non-responders**. *ACBD3* mRNA expression is 1.2-fold higher in HER2- responders to chemotherapy (*P** < 0.000001). **c) *ACBD3* expression in HER2- responders and non-responders to any chemotherapy.** *ACBD3* is 1.2-fold higher in HER2+ non responders to chemotherapy (*P** = 0.007). **d) *ACBD3* expression in responders and non-responders to trastuzumab.** There was no significant difference in *ACBD3* expression between responders and non-responders to trastuzumab. **e) ACBD3 expression in responders and non-responders to lapatinib.** ACBD3 was 1.2-fold higher in non-responders to lapatinib (*P** = 0.025). **f) ACBD3 expression in HER2+ responders and non-responders to anthracycline.** ACBD3 was 1.2-fold higher in HER2+ non-responders to anthracycline (*P** = 0.0056).

3.3.10 Novel ACBD3 Protein Interactions

There are to date only a modest number of publications concerning ACBD3 and there are limited known ACBD3 interactors despite several essential cellular roles. The GeneMANIA network was queried to determine if there are more protein

interactors of ACBD3 as well as proteins that co-localise or co-express. GeneMANIA collates data from primary studies found in protein interaction databases, including BioGRID and PathwayCommons, physical interactions were defined as two gene products found to interact in a protein-protein interaction study. *ACBD3* was queried in GeneMANIA and many novel interactions were found including The VPS36 endosomal sorting complex protein and SLC35A1 Golgi membrane protein (Figure 3.8). Of particular interest to cancer study were the interactions with UNC45A (encodes a regulatory component of the progesterone receptor/heat shock protein 90 chaperoning complex), PKN2 (PKC-related serine/threonine-protein kinase) and KDM2B (histone lysine demethylase).

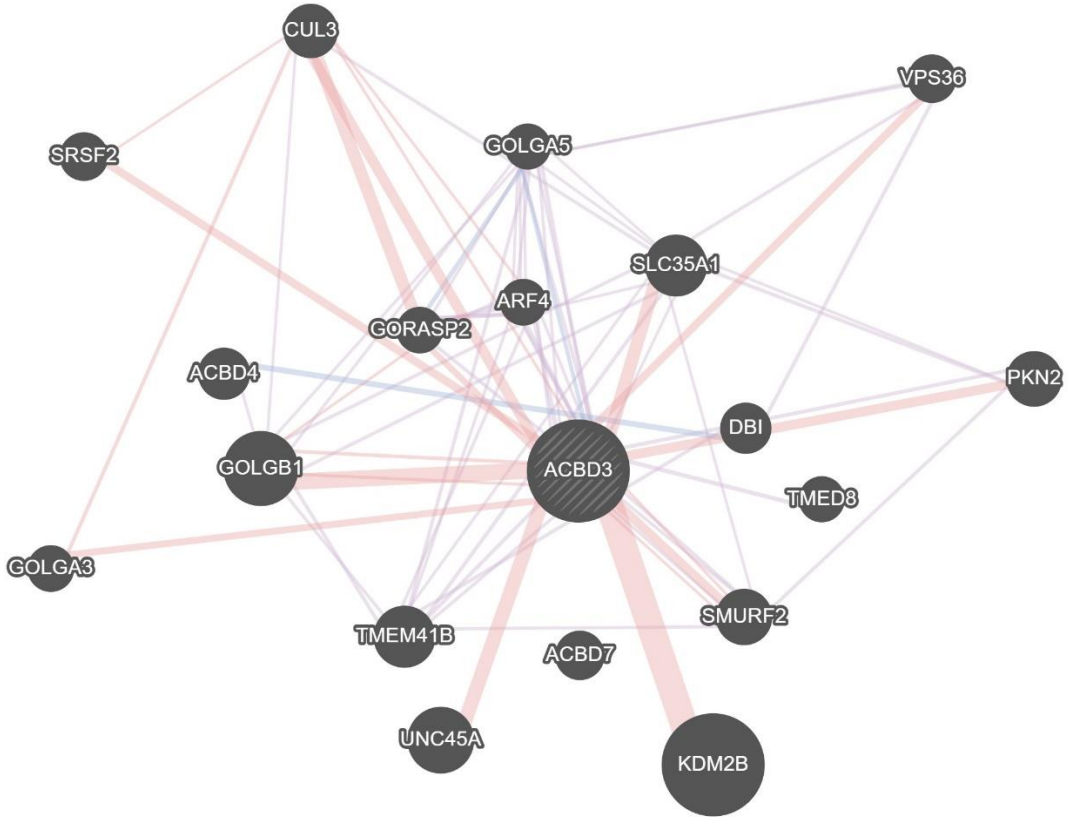

Figure 3.8 – GeneMANIA protein association data for interactions with ACBD3. Physical interactions between gene products are represented by pink lines between genes, co-expression is represented by purple lines between genes and co-localization in blue. Thicker lines indicate more evidence (publications) supporting the interaction.

Another nuclear protein, SRSF2, was found to interact with ACBD3 and ACBD3 has previously been reported to have both nuclear import signals (Fan, Liu et al.

2010). SRSF2**,** a member of the serine/arginine rich family of pre-mRNA splicing factors, was also found to interact with ACBD3.

Co-expression of genes was also queried in geneMANIA and the genes of several novel protein interactors of ACBD3 are also co-expressed. These include: *SMURF2*, *GORASP2*, *PKN2* and *SLC35A1*, increasing the validity of the interaction data. Other co-expressing genes include, *ARF4*: encodes ADP ribosylation factor 4, *TMEM41B*: encodes transmembrane protein 41B, and *TMED8*: encodes trans-membrane p24 trafficking protein 8, a paralogue of *ACBD3*.

3.4 Discussion

Bioinformatic databases were used to determine whether ACBD3 is overexpressed in breast cancer, and to search for leads in regulating ACBD3 in breast cell lines and to search for possible mechanisms by which ACBD3 might affect breast cancer. These results showed that *ACBD3* was widely expressed in different tissue types, and, in many cases, expression was increased in tumour samples when compared with normal tissue. Expression was highest in breast cancer, with a large difference in expression between normal samples and tumour samples. Acute myeloid leukaemia was the only cancer with a notable downregulation of *ACBD3*. The data support a potential role for ACBD3 in tumour development in a wide range of cancers including breast cancer; however, gene amplification and mutation rates were relatively low compared to other more well-known oncogenes such as *p53* which is mutated in over 30% of breast cancers (Filippini, Vega 2013, Lee, D. S., Yoon et al. 2012, Duffy, Synnott et al. 2018) . Additionally, analysis of copy number variation and promoter methylation revealed that changes in expression are not related to increased copy number or changes in methylation patterns suggesting that other mechanisms were responsible for *ACBD3* over expression.

ACBD3 was more highly expressed in breast cancer than in any other cancer or matched normal tissue. Copy number variation and promoter demethylation could not account for the 93% upregulation of *ACBD3* mRNA in breast cancer. FOXA1, Bisphenol A, and calcitriol were discovered as *ACBD3* positive transcriptional regulators; oestrogen receptor and insulin receptor-related agonists were found to be either repressors or promoters of *ACBD3* transcription. ACBD3 protein was also upregulated in breast cancer and several novel ACBD3 binding partners were found,

including nuclear proteins and the progesterone receptor co-chaperone UNC45A. *ACBD3* expression over the median level in breast cancer tissue resulted in reduced relapse free overall, and distant metastasis free survival for breast cancer patients as a whole with some differences observed between subtypes. *ACBD3* tumour expression was higher in HER2+ patients that did not respond to anti HER2 therapies, or anthracycline chemotherapies.

It was hypothesised that over expression of *ACBD3* was most likely linked to upregulation of, or increased activation of, transcription factors. The analysis showed that several transcription factors, already linked to breast cancer could increase *ACBD3* expression (Figure 3.5a and 3.5b).

ACBD3 was previously predicted to enter the nucleus as it was proposed to have 2 nuclear import signals and 9 DNA binding motifs (Fan, Liu et al. 2010); ACBD3 has not however been observed in the nucleus. It is interesting then to find a potential interaction of ACBD3 with two nuclear proteins in high throughput studies, SRSF2: a spliceosome and RNA export protein and KDM2B: a histone lysine demethylase which promotes breast cancer stem cell renewal and higher expression is associated with poor prognosis for TNBC patients (Zheng, Fan et al. 2018, Kottakis, Foltopoulou et al. 2014, Fraile, Chavdoula et al. 2020, Yan, Yang et al. 2018) (Figure 3.8). This may be the first step in a decade toward finding an ACBD3 function in the nucleus, or, as with Src and Sam68 (Roche, Fumagalli et al. 1995, Resnick, Taylor et al. 1997, Fumagalli, Totty et al. 1994, Taylor, Shalloway 1994), it is possible that the interaction occurs during mitosis when the nuclear envelope breaks down. KDM2B inhibits senescence and, like ACBD3, is implicated in CSC self-renewal and Wnt/β-Catenin signalling in breast cancer (Pfau, Tzatsos et al. 2008, Lu, L., Gao et al. 2015, Huang, Y., Yang et al. 2018). The finding that they physically interact in protein interaction studies is interesting and merits further study as it provided further evidence that implicates ACBD3 in the Wnt signalling pathway, and an additional ACBD3 association with CSC-maintaining proteins in breast cancer. This could explain why breast cancer patient relapse is more likely when *ACBD3* expression is high.

Interaction with UNC45A was the novel protein interaction with the most likely impact in breast cancer. UNC45A Is a regulatory component of the progesterone receptor/heat shock protein 90 chaperoning complex, which functions in the assembly and folding of the progesterone receptor. The encoded protein is thought to be essential for normal cell proliferation, and for the accumulation of myosin during

development of muscle cells (Chadli, Graham et al. 2006a). UNC45A expression in cancer correlates with progression, grade, and metastasis and downregulation of UNC45A also downregulates the mitotic kinase NEK7 (Chadli, Graham et al. 2006a, Eisa, Jilani et al. 2019, Guo, W., Chen et al. 2011, Bazzaro, Santillan et al. 2007, Epping, Meijer et al. 2009). UNC45A is not essential for normal breast development but is important in breast cancer cell proliferation where siRNA silencing of UNC45A causes cell cycle arrest and cell death in the Hs578T cell line (Guo, W., Chen et al. 2011, Eisa, Jilani et al. 2019).

PKN2 is a PKC-related serine/threonine-protein kinase and Rho/Rac effector protein that participates in the regulation of cell cycle progression (Schmidt, Durgan et al. 2007), actin cytoskeleton assembly and cell adhesion (Calautti, Grossi et al. 2002), cell migration and tumour cell invasion (Lachmann, Jevons et al. 2011), embryogenesis (Danno, Kubouchi et al. 2017), and insulin responsiveness in skeletal muscle (Ruby, Riedl et al. 2017). KDM2B is a histone lysine demethylase that is expressed ubiquitously and has ubiquitin ligase activity (Saritas-Yildirim, Pliner et al. 2015). KDM2B inhibits cell senescence (Pfau, Tzatsos et al. 2008), promotes cell proliferation (He, Kallin et al. 2008), and promotes cell migration (Zacharopoulou, Tsapara et al. 2018). Like ACBD3, KDM2B is involved in stem cell renewal, and has functions in cancer development including a role in breast cancer where it is implicated in CSC self-renewal (Yan, Yang et al. 2018, Kottakis, Foltopoulou et al. 2014). KDM2B regulates Wnt/β-Catenin signalling by controlling turnover of nuclear β-Catenin in Xenopus (Lu, L., Gao et al. 2015).

3.4.1 ACBD3, Oestrogen Receptor Status, and Signalling

The oestrogen receptor has a long-established link to breast cancer development with the majority of breast cancers being ER-positive (Lamb, Vanzulli et al. 2019) and modulation of oestrogen receptor has been key to declining mortality from breast cancer for over 30 years. There was significantly less survival, more relapse, and more distant metastasis in ER+ patients when divided by *ACBD3* expression, and *ACBD3* overexpression appears to be universally detrimental to breast cancer prognosis.

Tumour *ACBD3* above the median level equated to patient relapse 4 years and 8 months earlier than patient with tumour *ACBD3* below the median (24% decrease

in relapse free time). It is a testament to the quality of treatment for breast cancer that we were not able to produce median time values for any subgroup of patients or for the cohort when looking at overall survival and distant metastasis free survival. This is because so many patients stay relapse free, metastasis free, and survive, that with almost 25 years of data the median threshold for these metrics has not been reached and we therefore only have upper quartile values for some other metrics. 75% of patients survived for 126 months when *ACBD3* was below the median level compared to 82 months when *ACBD3* was above the median level (a 35% decrease in upper quartile survival time). Even more strikingly 75% of patients stayed distant metastasis free for 138 months when *ACBD3* was below the median but only for 68 months if *ACBD3* was above the median (a 51% decrease in upper quartile distant metastasis free time). The increased risk of, and decreased time to, relapse and metastasis support a role for *ACBD3* in cancer stem cell formation and maintenance. By extension, the metastases risk decreases overall survival as 90% of cancer deaths are caused my metastatis (Peitzsch, Tyutyunnykova et al. 2017).

FOXA1 is a forkhead DNA binding protein transcription factor and can be tumour-suppressive or tumour-promoting depending on the cancer. It is essential for oestrogen receptor-α expression and is involved in breast morphogenesis (Bernardo, Lozada et al. 2010). FOXA1 is itself associated with low tumour grade, ER expression and positive outcomes in breast cancer but its overexpression has also been associated with invasiveness, and FOXA1 mutations were found in endocrine therapy resistant breast tumours (Thorat, Marchio et al. 2008, Ciriello, Gatza et al. 2015, Razavi, Chang et al. 2018, Rheinbay, Parasuraman et al. 2017). FOXA1 expression is commonly coordinated with ER expression in breast metastases and FOXA1 has been shown to mediate ER binding reprogramming (Ross-Innes, Stark et al. 2012). FOXA1 protein expression is downregulated when BRCA1 is downregulated and both proteins regulate the CDC inhibitor p27 (Williamson, Wolf et al. 2006).

FOXA1 was found to be a positive *ACBD3* transcription factor in normal breast tissue and FOXA1 is associated with ER expression in breast cancer (Thorat, Marchio et al. 2008). FOXA1 induces both *ERα* and *ACBD3* expression, but GNST and 17βE2 (activators of ER signalling pathway) were found to repress *ACBD3* transcription by at least 2-fold. It is conceivable that ER signalling negatively regulates ACBD3 expression in breast cancer, but that FOXA1 expression contributes to the reprogramming of ER binding and signalling in breast cancer (Ross-Innes, Stark et

al. 2012), cancelling out the negative impact of GNST- and 17βE2-mediated ER transcriptional repression of ACBD3. This would explain why decreased distant metastasis-free survival was observed in ER+ patients when *ACBD3* expression was high.

3.4.2 ACBD3, the HER2 Receptor, and Insulin Signalling in Breast Cancer

HER2 signalling through alternate pathways, and upregulation of HER2 downstream signalling pathways are two of the main mechanisms for anti-HER2 therapy resistance (Pohlmann, Mayer et al. 2009). *ACBD3* levels were found to be statistically higher in non-responders to anti-HER2 therapy and *ACBD3* transcription to be induced by X10, an insulin analogue that activates the IGF and insulin receptors. IGFIR can phosphorylate and activate the HER2 receptor to negate the effects of anti HER2 therapies in breast cancer cell lines and anti IGFIR drugs re-sensitize trastuzumab resistant cell lines to trastuzumab (Lu, Y., Zi et al. 2001, Lu, Y., Zi et al. 2004, Nahta, Yuan et al. 2005). Higher expression of *ACBD3* in non-responders to anti-HER2 therapies may be an indicator of the increased IGF signalling that sustains HER2 activation and signalling.

X10, also known as ASPB10, is a potent artificial insulin analogue where aspartic acid substitutes the histidine-B10 residue of insulin to prevent hexamer formation and increase uptake and availability. It is an agonist of both the insulin like grown factor (IGF) receptor and the insulin receptor (IR). The insulin and IGF1 receptors have important roles in breast cancer; IGF signalling is important in mammary gland development and metastatic pathways, and its receptor is overexpressed and hyperphosphorylated in breast cancer, the insulin receptor is now being explored as a target for therapy (Chan, J. Y., LaPara et al. 2016, Papa, Gliozzo et al. 1993, Resnik, Reichart et al. 1998, Rostoker, Abelson et al. 2015, Chan, Jie Ying, Hackel et al. 2017). These pathways are both linked to breast cancer development where IGF1R is an activator of metastatic pathways and the IR is often overexpressed or constitutively active increasing glucose import to propagate the Warburg effect (Milazzo, Sciacca et al. 1997, Chan, J. Y., LaPara et al. 2016, Svendsen, Winge et al. 2013, Resnik, Reichart et al. 1998, Rostoker, Abelson et al. 2015, Hvid, Blouin et al. 2013, Barbosa, Martel 2020).

Glucose transporter 1 is classically associated with the Wahlberg effect but glucose transporter 4 should not be overlooked as its downregulation impairs growth and causes remodelling of metabolism in breast cancer cells (Acharya, Xu et al. 2016, Garrido, Osorio et al. 2015). ACBD3 is involved in glucose transporter 4 vesicle cycling and subsequent glucose import in response to insulin, it would therefore be logical that the insulin signalling pathway regulates *ACBD3* expression (Belman, Bian et al. 2015, Bogan, Rubin et al. 2012) . Although an artificial and potent insulin analogue, X10 strongly upregulated *ACBD3* transcription in healthy breast tissue. it is conceivable that an increase in Golgi localised ACBD3, induced by IGF1R signalling, would increase the pool of available GLUT4 containing vesicles and therefore increase glucose import and energy for the proliferating cancer cells. X10 is reported to cause breast cancer in Sprague-dawley rats and had a mitogenic effect in MCF7 cells (Milazzo, Sciacca et al. 1997, Drejer 1992, Svendsen, Winge et al. 2013). X10 has also been seen to increase the growth of MC38 colon cancer allografts on obese mice and increased mammary tumour occurrence in rats (Hvid, Blouin et al. 2013).

Overall, the work in this chapter has validated the choice to study ACBD3 expression in the context of breast cancer. High *ACBD3* mRNA expression was found in breast cancer and was associated with worse patient outcomes in relapse, metastasis and survival. ACBD3 was also high at the protein level in breast cancer and several novel protein interactors were found. The mechanism by which ACBD3 was upregulated could not be determined by the techniques used but binding factors and regulators of transcription have been discovered which has informed work in subsequent chapters. Finding that several activators of oestrogen receptor signalling were also repressors of ACBD3 was interesting, especially when it is considered that FOXA1 was found to promote both ER and ACBD3 expression in breast tissue. ER expression is one of the most important markers in breast cancer determining both therapies and, to a certain extent, outcomes. If ER signalling is a repressor of ACBD3 then it is prudent that ACBD3 expression be determined in ER+ and ER- breast cancer cell lines and patient samples.

Now that the correlation between high tumour *ACBD3* expression and poorer prognosis has been corroborated, this work can focus on determining if ACBD3 is affecting breast cell behaviour directly or if it is a marker of other changes such as

FOXA1 signalling and associated ER reprogramming, or of PI4Kβ expression/activity. The next step will be to compare cell line models to the data here, to use these results and the literature to uncover ACBD3 regulators and to design ACBD3 mutants based on literature and mutants found in patient breast tumours.

Chapter 4

ACBD3 Expression in Breast Cancer Cell Lines and Breast Cancer

4.1 Introduction

The purpose of this thesis was to examine whether ACBD3 is biologically important in breast cancer occurrence and/or progression and if ACBD3 expression is a reliable biomarker for breast cancer characteristics and/or patient outcomes. The introduction provides lines of evidence as to the functions of ACBD3 in normal cellular processes and highlights the functions that are implicated in, or may be relevant in, cancer. The results of chapter 3 reinforced assertions that ACBD3 has a role in breast cancer and corroborates previously published work (Huang, Y., Yang et al. 2018). *ACBD3* was found to be commonly upregulated in breast cancers and expression above the median level correlated with worse patient prognosis when relapse free survival, overall survival and distant metastasis free survival were considered. There were also small but statistically significant differences in *ACBD3* expression between subgroups of breast cancer patients who did, or did not, respond to chemotherapies; particularly *ACBD3* was increased in HER2+ patients that did not respond to anti HER2+ therapies. The human protein atlas also showed that ACBD3 protein expression was high in breast cancers, but this sample was limited to eleven breast cancer cores with no normal tissue control.

To study ACBD3 expression in breast cancer further, models for breast cancer were needed and these took the form of breast cell lines. A number of factors informed the choice of cell lines including existing literature where amplification of 1q loci, including the *ACBD3* loci (1q42.12), was analysed in breast cell lines and primary tumour samples (Orsetti, Nugoli et al. 2006).

Relative mRNA expression analysis was performed by QPCR, and comparison of protein levels carried out by western blotting. In addition to *ACBD3*, *PI4Kβ* expression was also of interest as it encodes an important binding partner of ACBD3 and, as a gene, is implicated in breast cancer in its own right (Sasaki, Ishikawa et al. 2012, Orsetti, Nugoli et al. 2006, Goh, Feng et al. 2017). Using QPCR, relative

quantity (RQ) of these genes between cell lines and relative quantities, or ratios, in respect to each other (within and between cell lines) were recorded.

In addition to work on cell lines, breast cancer arrays of embedded breast core samples were stained for ACBD3 protein to determine any correlations between ACBD3 protein levels and patient data such as age, pathology of tumour and receptor status. This was important as it allowed links to be made between the findings of *in vitro* cell line models and patient samples and allowed for the analysis of hundreds of individual patient tumours rather than relying only on a limited number of cell lines. It also allowed for a direct comparison of ACBD3 protein expression between healthy and cancerous breast tissue which was not possible using the methodology in chapter 3.

4.2 Chapter Aims

The aim of this chapter was to detect levels of ACBD3 and PI4Kβ in my chosen breast cancer models and examine any correlation between levels of transcription and translation of these genes and their protein products. The results from these models were then compared to patient sample cores where correlations between ACBD3 expression and tumour characteristics were analysed.

4.3 Results

4.3.1 Validation of Reference Genes

Quantitative polymerase chain reaction (QPCR) is a comparative method of quantifying mRNA transcripts. mRNA quantity of a target gene is given relative to a reference gene to normalise for cell number and total amount of cDNA. Common reference genes such as *ACTB* and *GAPDH* are not always suitable loading controls when studying cells, especially cancer cells where transcription and translation are dysregulated. Proteins that are stably expressed do not always have correspondingly stable expression of mRNA. Because of these factors, the expression of twelve house-keeping genes in eight breast cancer cell lines were analysed to find which were most stably expressed between the cell lines to make quantification of target mRNA (*ACBD3* and *PI4Kβ*) comparable between cell lines. Multiple reference genes are used to reduce variation and normalise to multiple controls. To achieve this the

GeNorm kit from primer design was used to perform QPCR on cDNA from breast cell lines in conjunction with Qbase+ software; the GeNorm kit contains primers for 12 reference/housekeeping genes for use with qPCR and the Qbase+ software then analyses the results using an algorithm to determine the stability of expression (the M value) and how many reference genes should be used to validate results (V value) (Figures 4.1 and 4.2). Qbase+ uses a proprietary algorithm and software but briefly the M value is an arbitrary unit of the stability of expression of each reference gen across all cell lines (Figure 4.1). the V value indicates pairwise variation of an increasing number of reference genes between 2 sequential normalisation factors (Figure 4.2). A high variation (lower V value) indicates that adding a reference gene has a significant positive effect on calculating a reliable normalisation factor for QPCR analysis.

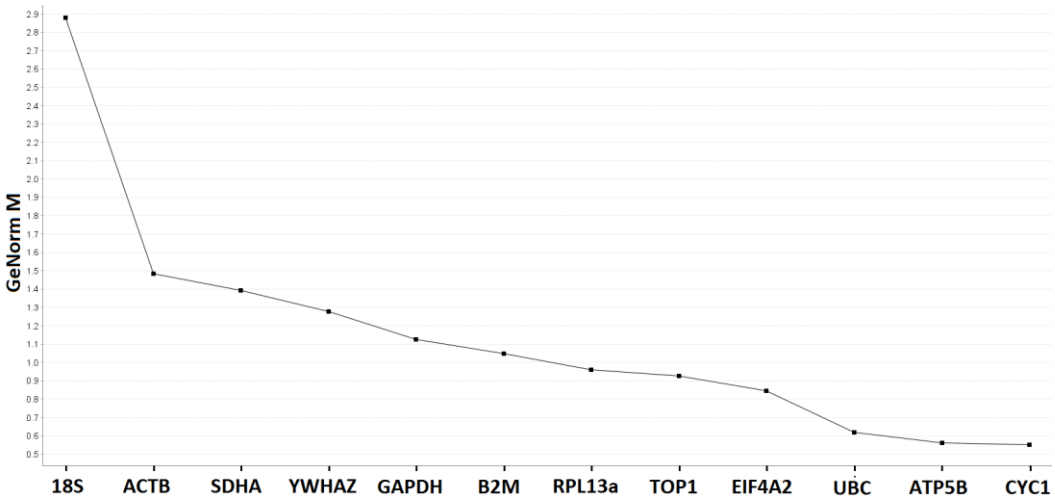

Figure 4.1 - The M value of each reference gene, or the mean average stability of expression of each reference gene over 8 different breast cell lines. M represents the discrepancy in expression between samples where the smallest M value represents the most stable expression between samples. The order of stability increases from left to right (increasing M value) with *CYC1* being most stably expressed gene between cell lines.

It was found that the optimal number of genes to use as reference genes is 5 but this value is subject to available sample and costs. The experiment was undertaken twice and the 5 most stably expressed genes were *CYC1*, *ATP5B*, *UBC*, *EIF4A2* and *TOP1* in descending order (figure 4.1 and figure 4.2). It was decided that 3 reference genes would be used as a compromise between cost, availability and validity and because an initial GeNorm qPCR experiment (not shown) with

contamination in the non-template controls showed similar results but with *TOP1* and UBC exchanging stability ranking in M value. It was decided that *CYC1* and *ATP5B* reference genes would be used as the two genes with the most stable expression between cell lines and *EIF4A2* would be used as it was the fourth most stably expressed gene across two GeNorm experiments.

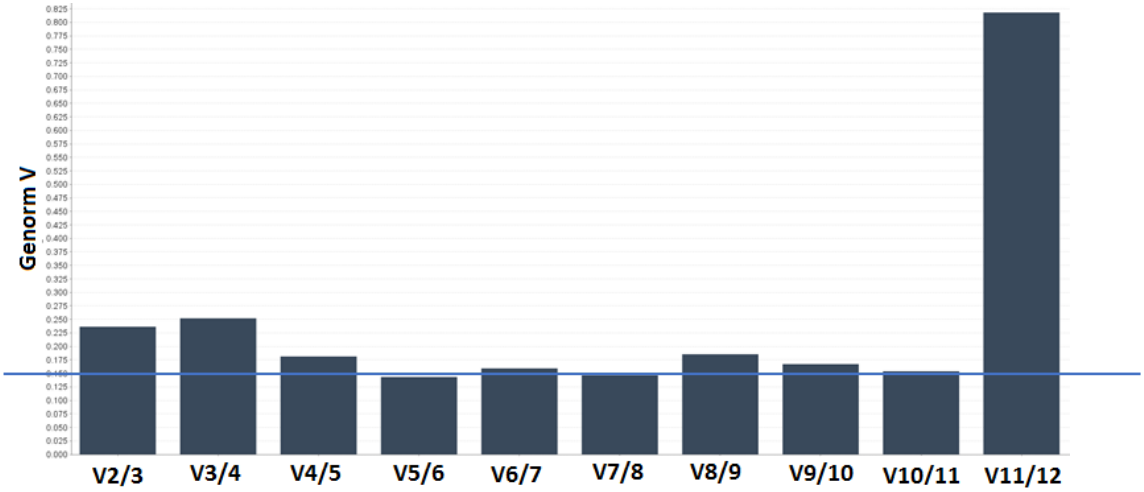

Figure 4.2 - The V value as determined by the Qbase+ software. V represents the pairwise variation between different numbers and combinations of reference genes to standardise results from QPCR experiments. Below 0.15 V the addition of extra reference genes does not increase the validity of results. In this case V5/6 is the least number of reference genes in combination below the 0.15 V threshold (blue line). The number of reference genes that are ultimately used is based on other factors such as cost and available sample material which may be limiting factors. The results for subsequent QPCR assays will use these reference genes: *CYC1*, *ATP5B* and *EIF4A2*, considered to be a balance between reference stability, cost and sample availability.

4.3.2 mRNA expression of *ACBD3* in breast cell lines

The cell lines were grown to 80% confluency and RNA was immediately extracted from them. From this cDNA was produced and 3 biological replicates per cell line were assayed for gene expression using the reference genes identified in section 4.3.1.

ACBD3 mRNA expression was significantly higher in all breast cancer cell lines tested compared to the non-cancerous breast cell line MCF12A (Figure 4.3). The SKBR3 breast cancer cell line, derived from a HER2+ invasive ductal carcinoma, had that highest level of *ACBD3* mRNA (506% higher compared to MCF12A, *P =

0.000556) followed closely by the triple negative invasive ductal carcinoma derived BT20 cell line (480% higher compared to MCF21A, *P = 0.000978). The BT20 and SKBR3 cell lines are both negative for ER and PR receptors but share little else in common. There was no statistically significant difference between *ACBD3* expression in the breast cancer cell lines overall when divided by PR status or ER status suggesting that *ACBD3* overexpression was not related to breast cancer receptor status. There were also no statistical differences when cell lines divided by pathology, subtype or HER2 receptor status. The breast cancer cell lines with the highest level and lowest level of *ACBD3* expression were both triple negative cell lines (BT20 and MDA-MB-231 respectively).

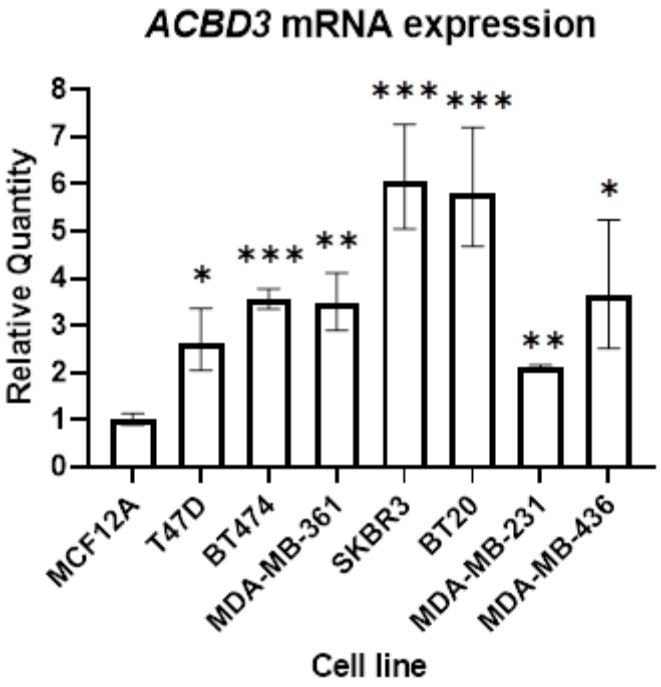

Figure 4.3 – *ACBD3* mRNA was increased in breast cancer cell lines relative to the MCF12A normal-like breast cell line. Cell type from left to right: MCF12A - normal-like, T47D - Luminal A, BT474 - Luminal B, MDA-MB-361 and SKBR3 - HER2+, BT20, MDA-MB-231, and MDA-MB-436 - triple negative. SKBR3 cells had the highest expression at 6.06 times the RQ of MCF12A expression. mRNA levels were measured by QPCR, each cell line was measured from 3 independent samples and each sample was measured 3 times (n=3). error bars represent the standard deviation, Asterisks represent confidence interval of expression difference relative to the MCF12A cell line.

MDA-MB-436 *ACBD3* expression was 263% higher (*P = 0.01504), BT474 256% higher (*P = 0.000323), MDA-MB-361 245% higher (*P = 0.002138), T47D 162% higher (*P = 0.012792), and MDA-MB-231 111% higher (*P = 0.001866), all relative to MCF12A expression. Statistical analysis was performed on the ΔΔCt per biological replicate as the relative quantity (RQ) is a log value and does not follow a normal distribution.

4.3.3 mRNA expression of *PI4Kβ* in breast cell lines

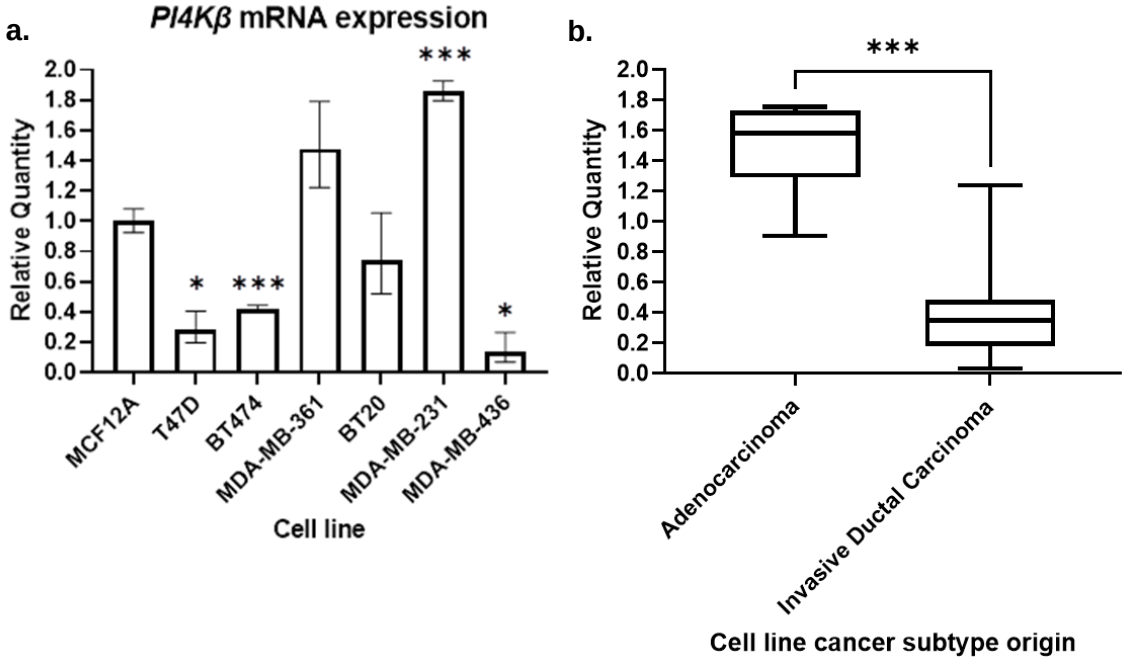

Figure 4.4 – Relative quantity of *PI4Kβ* mRNA transcripts in different breast cell lines. **a)** Cell type from left to right: MCF12A - normal-like, T47D - Luminal A, BT474 - Luminal B, MDA-MB-361 and SKBR3 - HER2+, BT20, MDA-MB-231, and MDA-MB-436 - triple negative. *PI4Kβ* expression was significantly higher in the MDA-MB-231 breast cancer cell line compared to the non-cancerous normal like MCF12A breast cell line. The BT474, MDA-MB-361 and T47D breast cancer cell lines had significantly lower relative *PI4Kβ* expression than the MCF12A cell line. error bars represents the standard deviation. **b)** *PI4Kβ* RQ in Adenocarcinoma and Invasive Ductal Carcinoma cell lines was significantly different. Adenocarcinoma derived cancer cell lines (MDA-MB-231 and MDA-MB-361) had significantly higher *PI4Kβ* expression than Invasive Ductal Carcinoma derived cell lines (BT20, BT474, MDA-MB-436, and T47D). Quantity in each case is relative to MCF12A cell line expression in 4.4a (*P = 0.000391).

mRNA expression of the ACBD3 binding partner PI4Kβ was also examined, and it was found that *PI4Kβ* expression was significantly different in four breast cancer cell lines compared to the MCF12A control (Figure 4.4a). *PI4Kβ* expression was significantly higher in the adenocarcinoma derived MDA-MB-231 breast cancer cell line (86%, **P* = 0.000881) and significantly lower than the control in the invasive ductal carcinoma derived BT474 (58%, **P* = 0.000405), MDA-MB-436 (86%, **P* = 0.022517) and T47D (72%, **P* = 0.014182) cell lines. *PI4Kβ* expression data for the SKBR3 cell line was not included as variance between technical replicates was high and overall expression very low suggesting that *PI4Kβ* expression in this cell line was very low. SYBR green chemistry used to perform these QPCR experiments has difficulty in detecting very low-level late cycle exponential amplification of targets according to the manufacturer (email correspondence with PrimerDesign, Southampton, UK, 2019).

The relative quantity (RQ) of all adenocarcinomas (ACs) biological replicates was compared to the invasive ductal carcinomas (IDCs) biological replicates and it was found that *PI4Kβ* expression was statistically significantly lower in the invasive ductal carcinomas, the median average RQ of the IDCs was 0.35 compared to 1.58 for the ACs relative to the MCF12A cell line (Figure 4.4b).

4.3.4 The Relationship Between *ACBD3* and *PI4Kβ* Gene Expression

Due to the functional interaction between ACBD3 and PI4Kβ proteins and their location on chromosome 1 arm q, it was decided to examine any correlation between the expression of the two genes. *PI4Kβ* mRNA expression was lower than *ACBD3* mRNA expression in all cell lines (*PI4Kβ* was amplified at a later cycle than *ACBD3* during QPCR in all cases relative to the reference genes). Overall, there was no clear relationship between the expression of *ACBD3* and *PI4Kβ* with no correlation for individual biological replicates of all cell lines (MCF12A, BT20, BT474, MDA-MB-231, MDA-MB-361, MDA-MB-436, T47D) (Figure 4.5a).

All breast cancer cell lines had a lower *PI4Kβ* to *ACBD3* ratio than the normal MCF12A control cell line and, as with *PI4Kβ* expression status, the adenocarcinoma-derived cell lines had a higher ratio than the invasive ductal carcinoma cell lines (Figure 4.5b). The *PI4Kβ/ACBD3* ratio did not correlate with any receptor status, just as expression of either gene in isolation could not, the ratio did follow a similar pattern

to *PI4Kβ* mRNA expression alone. The MDA-MB-231 cell line had the lowest expression of *ACBD3* of the breast cancer cell lines and the highest *PI4Kβ* expression.

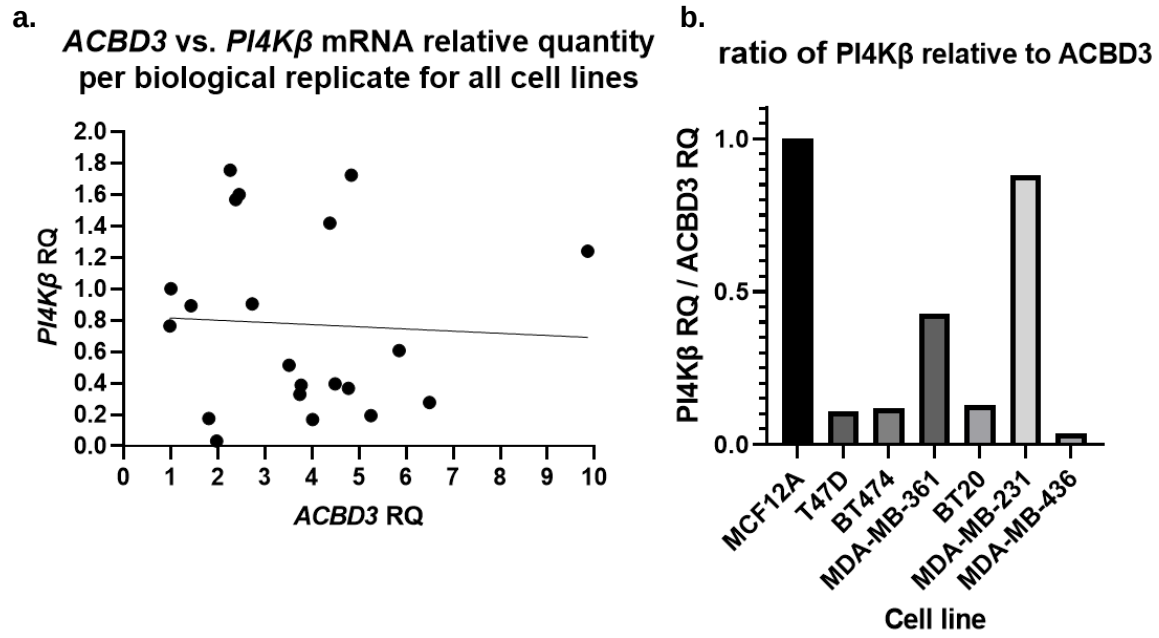

Figure 4.5 – The relationship between ACBD3 and *PI4Kβ* expression. a) *PI4Kβ* RQ was plotted against ACBD3 RQ for each biological replicate of all cell lines. There was no correlation between *ACBD3* expression level and *PI4Kβ* expression level (slope of trendline =0.06181, deviation from 0 was not significant (**P* = 0.8249). The ratio of ACBD3 to *PI4Kβ* was not a predictor for any breast cancer cell line characteristic. **b)** *PI4Kβ*/*ACBD3* expression as a ratio for each cell line. All breast cancer cell lines had a lower *PI4Kβ*/*ACBD3* ratio than the normal like MCF12A cell line and the ratios of cancer cell lines closely matched *PI4Kβ* expression alone (except for the MCF12A cell line) (Figure 4.4a).

4.3.5 ACBD3 and PI4Kβ protein expression in breast cell lines

ACBD3 and PI4Kβ protein expression was examined for breast cell lines as mRNA and protein expression can be very different. Whilst there was a large amount of data available for mRNA expression in breast cancer (Chapter 3, throughout), data for protein expression were limited (Chapter 3, Figure 1c). Breast cell lines were grown to 80% confluency and lysed directly in laemli buffer for analysis by western blot. ACBD3 and PI4Kβ protein expression was then compared by western blot and β-actin expression was also measured as a loading control (in addition to cell counting prior to lysis) .

As with mRNA expression, ACBD3 protein levels were lowest in the MCF12A breast cell line and there was considerable variance between breast cancer cell lines (Figure 4.6). The ER+ and PR+ PMC42 And T47D cell lines had the highest ACBD3 levels followed by the ER+ MDA-MB-361 cell line. The MDA-MB-436 cell line had the least ACBD3 expression of the cancer cell lines, and MCF12A, BT20 and MDA-MB-231 cell lines all showed multiple banding suggesting post translational changes to ACBD3.

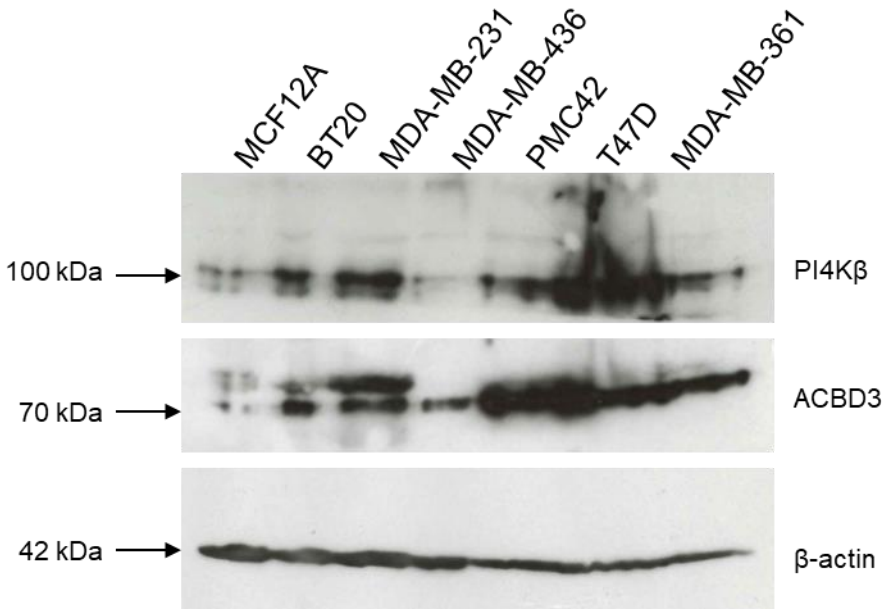

Figure 4.6 – ACBD3 protein expression is higher in breast cancer cell lines than the normal like MCF12A cell line, PI4Kβ protein expression is also higher in 5 out of 6 breast cancer cell lines compared to the MCF12A cell line. From left to right: MCF12A has 3 distinct bands of staining of ACBD3, BT20 and MDA-MB-231 have 2 bands, MDA-MB-436, PMC42, T47D, and MDA-MB-361 have 1 band of ACBD3 staining. Most cell lines have 2 bands of staining for PI4Kβ and PI4Kβ protein expression was lower in the MDA-MB-436 cell line compared to the MCF12A cell line. β-actin was stained as a loading control, exposure = 10 seconds, ACBD3 exposure = 2 minutes, PI4Kβ exposure = 1 minute, representative of n=2.

The same blot was also used to detect PI4Kβ protein levels and showed a similar expression pattern to ACBD3 except that MDA-MB-436 cell line which had lower PI4Kβ expression than the MCF12A normal-like cell line. This is in line with the mRNA expression data where MDA-MB-436 had the lowest relative quantity of *PI4Kβ*. The PI4Kβ protein expression profile does not follow the mRNA expression profile,

instead PI4Kβ protein expression closely matches ACBD3 protein expression in each cell line. It should be noted that the cell lines used for protein analysis are not the same as the cell lines used for mRNA analysis in all cases.

4.3.6 ACBD3 Undergoes Posttranslational Modifications to Different Extents in Different Cell Lines

Multiple bands of ACBD3 protein on westerns blots were observed for some cell lines (Figure 4.6) and so the lysates of 3 independent biological replicates of the MDA-MB-231 cell line were separated on a 12% polyacrylamide gel to better visualise multiple bands of ACBD3. 4 different bands at approximately 62kDa, 70kDa, 80kDa and 90kDa were found. MDA-MB-231 cells were enriched for highest weight ACBD3 form with less intense lower-weight ACBD3 bands and minimal 62kDa ACBD3 (Figure 4.7). This suggests that ACBD3 undergoes posttranslational modifications and the spacing between bands of approximately 8kDa possible indicates ubiquitination of the protein as ubiquitin subunits are 8.5kDa each. Whilst there is literature and structural information to support the notion that ACBD3 is phosphorylated at multiple sites, there is currently no evidence of ubiquitination of ACBD3 *in vivo*.

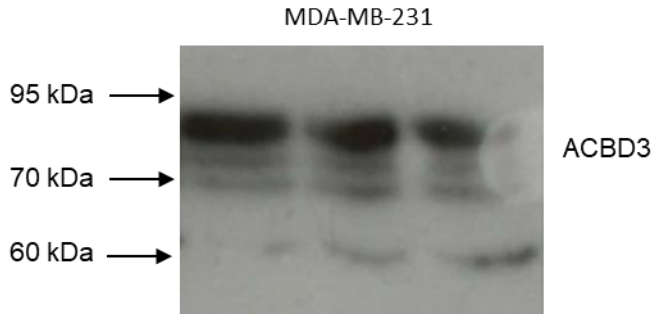

Figure 4.7 – Western blot of 3 biological replicates of the MDA-MB-231 cell line with high separation between 60kDa and 90kDa. In all lanes a band is visible corresponding to 62kDa which is the predicted weight of ACBD3. There are then 3 distinct bands of higher molecular weight. MDA-MB-231 is enriched for the highest weight band and the band of expected size is the least prominent. Loading control was measured by coomassie staining and all lanes appear to be equally loaded. The spacing between bands is 8-10kDa with the lowest conferring to 62kDa, then 70Da and 80kDa and 90kDa (all approximate values). It is unlikely that the bands show intermediary breakdown products of ACBD3 as full length ACBD3 has a mass of 62kDa, the approximate size of the lowest weight band.

4.3.7 Immunohistochemical Staining of Breast Cancer Patient Breast Sample Cores

Breast core tissue arrays were incubated with ACBD3 antibody, which was detected with a biotin-labelled anti-rabbit secondary antibody and streptavidin-HRP, to examine ACBD3 protein levels in breast cancer patient tissue. staining. Each core was scored per 1/3 core as: 0-10% staining=0, 10-25% staining=1, 25-50% staining=2, 50-75% staining=3, 75-100% staining=4; all cores were scored on 3 sequential days and the mean score for all days was taken.

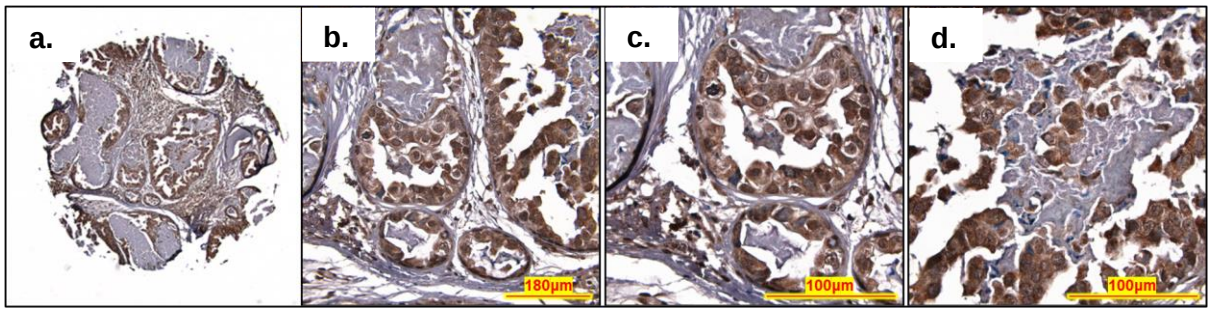

Figure 4.8 – An ACBD3 antibody-stained invasive carcinoma tissue core observed at various magnifications. An invasive carcinoma from a 39-year-old female, stage IIA, ER-PR- HER2 2+ reveals a pattern of differential ACBD3 staining (brown), haematoxylin was used a as a nuclear stain (blue). **a)** low magnification image of entire core, fibrous interlobular tissue has a low level of ACBD3 staining whilst breast duct acini have high levels of ACBD3 staining. **b)** medium magnification of regular and irregular duct acini. **c)** high magnification of regular small acini have high ACBD3 staining of luminal epithelial and basal myoepithelial cells. **d)** high magnification of an irregular large acini. Luminal epithelial and basal myoepithelial cells are both highly stained for ACBD3 but cells within the acini, possibly a ductal carcinoma *in situ* have a moderate to low level of ACBD3 staining, with some embedded cells with high levels of ACBD3, possibly luminal epithelial cells.

Figure 4.8 shows a 1mm core from the BR1008b array with ACBD3 typical staining patterns. There are areas of higher staining at the ducts or lobules with surrounding tissue showing low or no staining for ACBD3 (Figure 4.8a). At 40X magnification, individual cells of both regular and irregular lobules can be seen; luminal epithelial cells that line of the lobules have strong staining for ACBD3 as do the myoepithelial basal layer of cells beneath (Figure 4.8b). At 60X magnification the regular acini (Figure 4.8c) and irregular acini with invasive cells (Figure 4.8d) can be seen at a cellular level. Fibrous surrounding tissue has low staining for ACBD3 whilst

the invasive cells have cells of epithelial appearance and high ACBD3 staining embedded within cells with low or no ACBD3 staining.

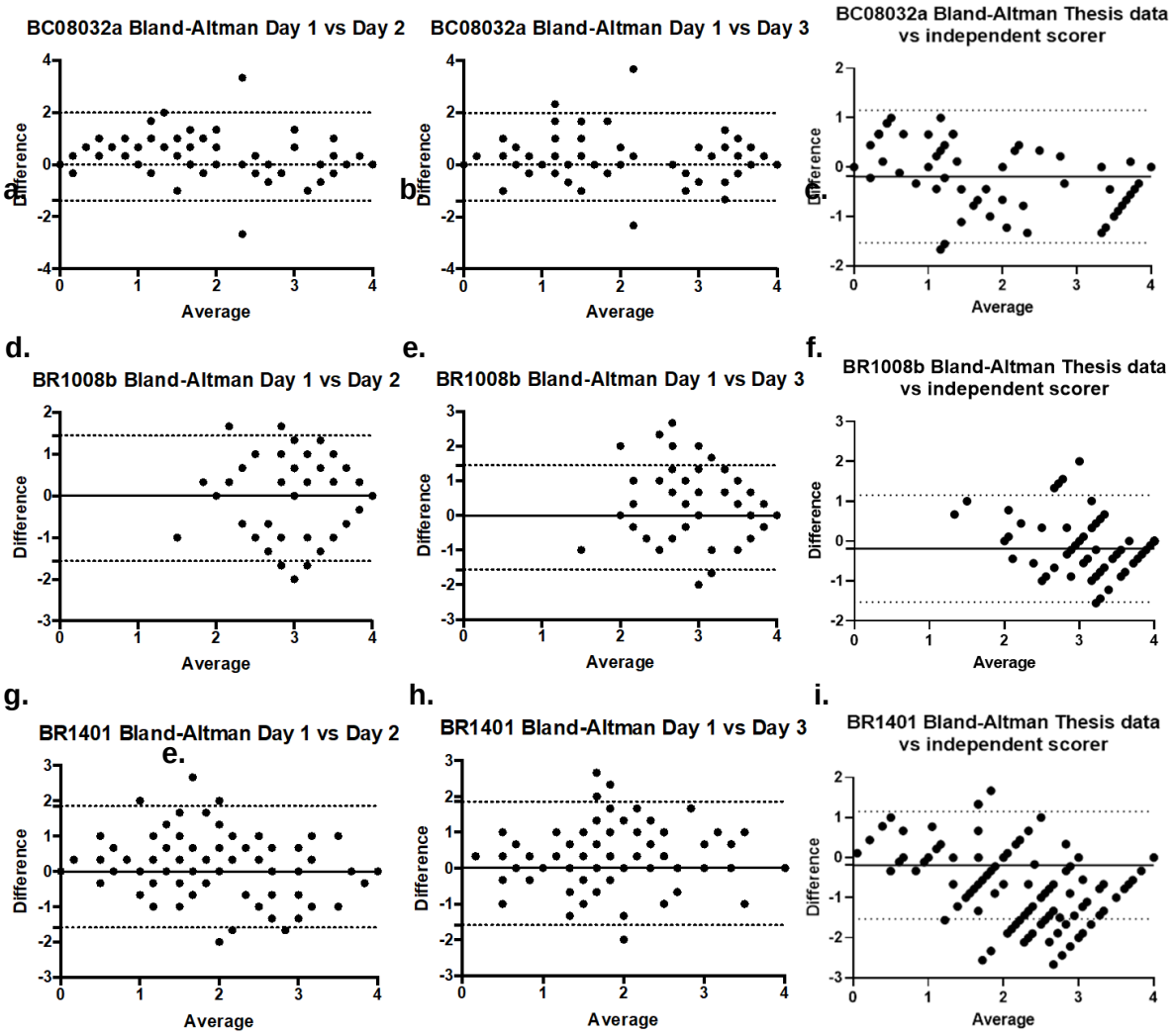

Figure 4.9 – Bland Altman plot comparing difference in ACBD3 intensity scoring on different days and between two scorers. Day 1 scores compared to day 2 and day 3, and mean score for data presented compared to score from an independent observer with experience in the technique used for: **a-c) BC08032a array, d-f) BR1008b array, g-i) BR1401 array.** The average score per core on 2 days is plotted on the x axis and the difference between scores is plotted on the y axis. The solid line represents the bias value, and the dotted lines represent 95% limits of agreement.

Scores for ACBD3 staining on independent days were analysed for each array and presented as Bland Altman plots (Figure 4.9) (Altman, Bland 1983). In all cases the bias value (the average of the difference in score) was very small indicating that

scores were not biased between days and were therefore equally valid. Difference in ACBD3 staining score between days was smallest at high score value (4 out of 4) for all 3 arrays. The +/- 95% limit of agreement and hence the difference was smaller between the data presented here and the data generated by an independent scorer than the difference between repeated measurements by me on sequential days. This highlights the importance of taking a mean average of repeated measurements and also suggests the techniques between myself and an experienced tissue core scorer were consistent. The bias was very low between myself and the other scorer but my scores were consistently slightly higher across all arrays (Figure 4.9c, f, and i).

There was a clear trend in the BR18008b array where difference in score between days was highest for scores of 3, decreasing for lower or higher scores (Figure 4.9d and e). This suggests that scoring cores around 75% ACBD3 staining intensity was the least consistent and most susceptible to ambiguity. This array also had fewer low ACBD3 intensity scored cores (minimum mean score = 1.3).

To a lesser extent there was also a trend in the BR1401b array towards larger differences between days around scores of 2, but there was a more even distribution of scores overall (Figure 4.9g and i). Larger differences between days for scores between 2 and 3 may be down to the heterogeneity of samples and therefore ACBD3 staining making it harder to consistently score cores with middling overall ACBD3 protein staining.

The relatively thick cores (5 micron) prevented automatic reading of the arrays by computer as the reader could not focus on cores consistently. Overall the scoring was not biased from day to day, but there was some ambiguity in scoring. The identity of the individual cores was not known until after all scoring was complete and scores from previous days were not observed when repeating measurements.

The interclass correlation coefficient (ICC) was also calculated for the data compared in Figure 4.9. Firstly the ICC was calculated using the two way mixed effects model to measure consistency between the scorers (myself and an independent scorer model: ICC(3,k)) (Koo, Li 2016). The ICC score between scorers for the BC08032a array slide was 0.923 meaning reliability between scores was excellent. For the BC1008b array the ICC was 0.741 indicating moderate reliability bordering good reliability. The ICC score for the BR1401 array equalled 0.733, very similar to the score for the BC1008b array.

The ICC between days of scoring was then calculated. As this was undertaken by 1 scorer (myself) then the test type was test/retest, the model was the same but the ICC score dictates absolute agreement and not consistency. ICC between repeated measures of the BC08032a array was 0.913 indicating excellent agreement between repeated scoring. The ICC score for BC1008b 0.699 indicating moderate agreement between days, as in the bland-altman plots (Figure 4.9d and e) there was clearly more discrepancy in score for this array than in others. The ICC value for the BR1401 scoring was 0.822 indicating that there was good agreement between scores on different days.

4.3.8 ACBD3 Protein Expression in Malignant, Cancer Adjacent, and Normal Adjacent Breast Tissue

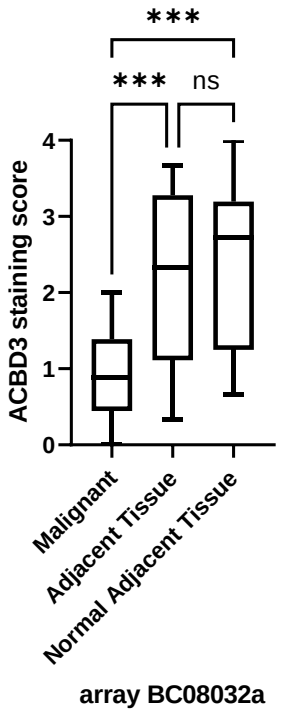

Figure 4.10 – ACBD3 staining score of the BC08032a US biomax tissue array. ACBD3 protein levels are significantly lower in malignant tissue compared to either cancer adjacent tissue or normal adjacent tissue.

Breast core array BC08032a consisted of 64 cores: 1 adrenal cortex control core plus equal parts malignant breast tissue, cancer adjacent breast tissue and

normal adjacent breast tissue. Array BC08032a was chosen to make direct comparisons between normal and cancerous breast tissue, and to analyse any significant differences between breast cancer pathologies within the sample of 31 breast cancer tissue cores.

Contrary to previous reports (Huang, Y., Yang et al. 2018), ACBD3 protein staining results for this array slide found ACBD3 protein staining to be statistically significantly lower in malignant breast cancer tissue compared to adjacent tissue or normal adjacent tissue (Figure 4.10). The mean average ACBD3 staining for malignant tissue was 0.92/4 compared to 2.14/4 for adjacent tissue (*$P < 0.001$), and 2.31 for normal adjacent tissue (*$P < 0.001$). There was no significant difference in staining between the cancer adjacent and normal adjacent breast tissue samples. Comparing breast core staining by receptor status, subtype, grade, stage or TNM score did not produce any differences that reached statistical significance within this limited sample.

ACBD3 antibody was diluted to 1:100 for slide array BC08032a and staining was weaker than expected overall. To avoid a loss in dynamic range of staining in subsequent array slides, ACBD3 antibody was incubated at 1:75 on subsequent array slides meaning that ACBD3 staining of breast cancer cores cannot be directly compared between this slide and the two subsequent slides. The core diameter on this slide is also larger at 1.55mm diameter compared to 1mm diameter for subsequent slides (the core thickness remained at a consistent stated 5µm although many cores across all array slides required adjustment of microscope focus suggesting discrepancies in core thickness). The pattern of staining of different cell types within cores was consistent across all arrays.

4.3.9 ACBD3 Protein Expression in Malignant Breast Tissue and Metastatic Lymph Node Tissue

Array BR1008b consisted of 101 cores: 1 adrenal cortex control core, 50 cores of malignant non-metastatic breast cancer tissue of various stage, grade, and receptor status. 40 cores were of breast cancer metastasis into lymph node tissue, and 10 cores were of normal adjacent tissue. Array BR1008b was chosen to analyse differences in ACBD3 protein expression between malignant non-metastatic breast tissue, metastatic breast cancer in lymph node tissue and normal adjacent breast

tissue. Unfortunately, multiple cores from this slide were completely lost during staining and many more were partially lost, including complete loss of 7 normal adjacent tissue cores and partial loss of the remaining 3. It has been previously noted informally by other researchers that loss of cores is more likely with smaller (1mm diameter) cores and that normal tissue cores are more likely to be lost than malignant cores (Kerslake, 2021 Personal Communication). Therefore, the analysis focussed on differences between in situ and invasive samples and on differences in ACBD3 expression when patient samples were divided by receptor status.

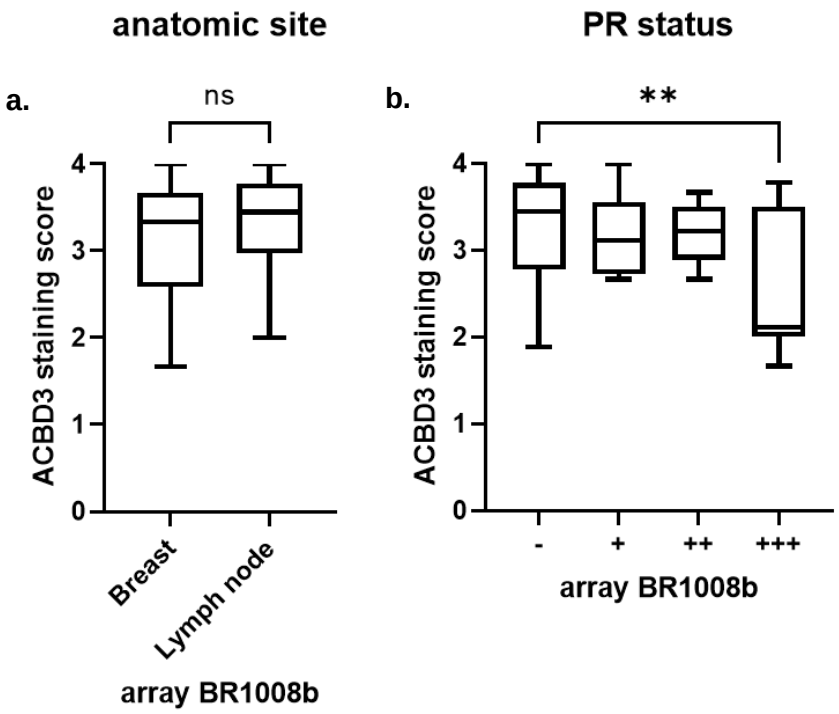

Figure 4.11 – ACBD3 staining score of the BR1008B US BIOMAX array. a) There was no statistical difference in ACBD3 staining between malignant breast tissue (n=48) and metastatic breast cancer of the lymph node (n=38). **b)** ACBD3 protein expression was significantly higher in PR negative breast cancer cores (n=50) compared to PR 3+ cores (n=9) (malignant breast tissue and metastatic lymph tissue, $*P = 0.0067$), but there was no statistical difference between PR- samples compared to all grades of PR+ core (not shown).

There was no statistical difference between ACBD3 protein expression between malignant breast tissue and metastatic breast cancer in lymph node (Figure 4.11a). High ACBD3 expression has previously been associated with more advanced stage tumours and with cancer stem cells and so it was unexpected to find no

statistical difference between non-metastatic and metastatic breast tissue (Huang, Y., Yang et al. 2018). ACBD3 protein levels were significantly higher in PR- breast cancers (mean=3.296) compared to breast cancers with high expression of PR (PR 3+) (mean=2.642) (*P = 0.0067) (Figure 4.11b). this included both non-metastatic and metastatic (lymph node) breast cancer samples and this trend did not extend to PR- breast cancer samples when compared to samples with lower PR expression (PR 1+, PR 2+). Although most normal adjacent tissue cores detached during staining, 3 partial cores were scored and had a mean score of 2.70; whilst this small sample size could not reach any statistical conclusions, it is was lower than the mean average for the breast cancer tissue cores overall (3.25) which is in keeping with previous literature but contradictory to the results of Figure 4.11 where ACBD3 protein expression was higher in breast cancer cell lines than a normal like breast cell control (Huang, Y., Yang et al. 2018).

Overall, breast cancer cores in the BR1008b array had increased ACBD3 staining compared to the BC08032a array which has been attributed to the increased concentration of ACBD3 antibody at 1:75 dilution (Compared to 1:100 for the BC08032a array). The BR1401b array however was also stained with 1:75 ACBD3 antibody and has a more dynamic range of core scoring with many cores scored as 4 but also many scored as <1.

4.3.10 ACBD3 Protein Expression in Malignant Breast Tissue of Multiple Subtype Receptor Status and Pathology

Array B1401b consisted of 141 cores: 1 adrenal cortex control core, and 140 cores of breast cancer tissue of various stage, grade, receptor status and pathology. This array was chosen to analyse differences in ACBD3 protein expression between breast cancers with different features with a large enough sample size to determine statistical significance between breast cancer subgroups. This array contained cores the same size as array BR1008b and was stained in parallel, very few cores were lost from this array during staining and there were an acceptable number of partial core losses.

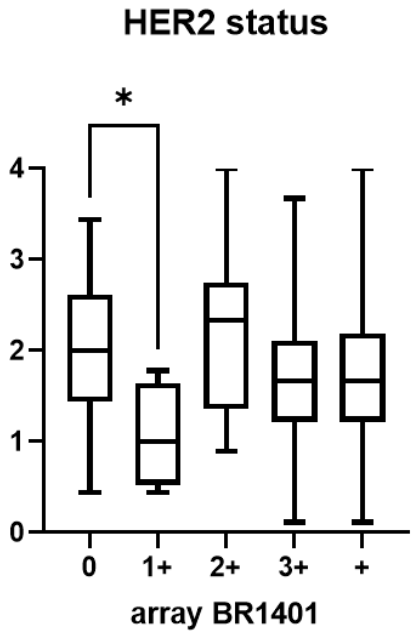

Figure 4.12 – ACBD3 staining score of the BR1401 US biomax array. There was a statistically significant difference between HER2- (grade 0) breast cancer samples and HER 1+ samples, *P = 0.0107.

In spite of the sample size of array BR1401, there were no cases of breast cancer with PR 3+ receptor status so the results from Figure 4.11b could not be corroborated in a larger sample size. HER2- breast cancer samples had significantly higher ACBD3 protein expression than HER2 1+ breast cancer samples (2.038, n=49, versus 1.055, n=4, respective mean averages, *P = 0.0107) (Figure 4.12). there was no significant difference between HER2- (0) breast cancer samples and HER2+ samples of any grade or between HER2 1+ and HER2 2+ breast cancer samples. The BR1008b array had no breast cancer samples with HER2 1+ staining and so this result could also not be corroborated between arrays.

No other statistically significant changes were found between subgroups of the sample including by age, TNM score, grade, stage, pathology, or other receptor status (data not shown).

4.3.11 Examination of Histology and Patterns of ACBD3 Staining in Breast Cancer Tissue Cores

There were not many clear differences in ACBD3 staining based on patient pathology other than those described above (Figure 4.10, 4.11, and 4.12). There were, however, consistent and repeated patterns of staining of cores based on cell type and local structure (Figure 4.13). The 1.55mm cores of array BC08032a stained in a consistent and structure specific manner for cancer adjacent tissue, normal adjacent tissue and breast cancer tissue, Figure 4.13 shows some typical patterns of ACBD3 staining at 10X and 40X magnification from this core.

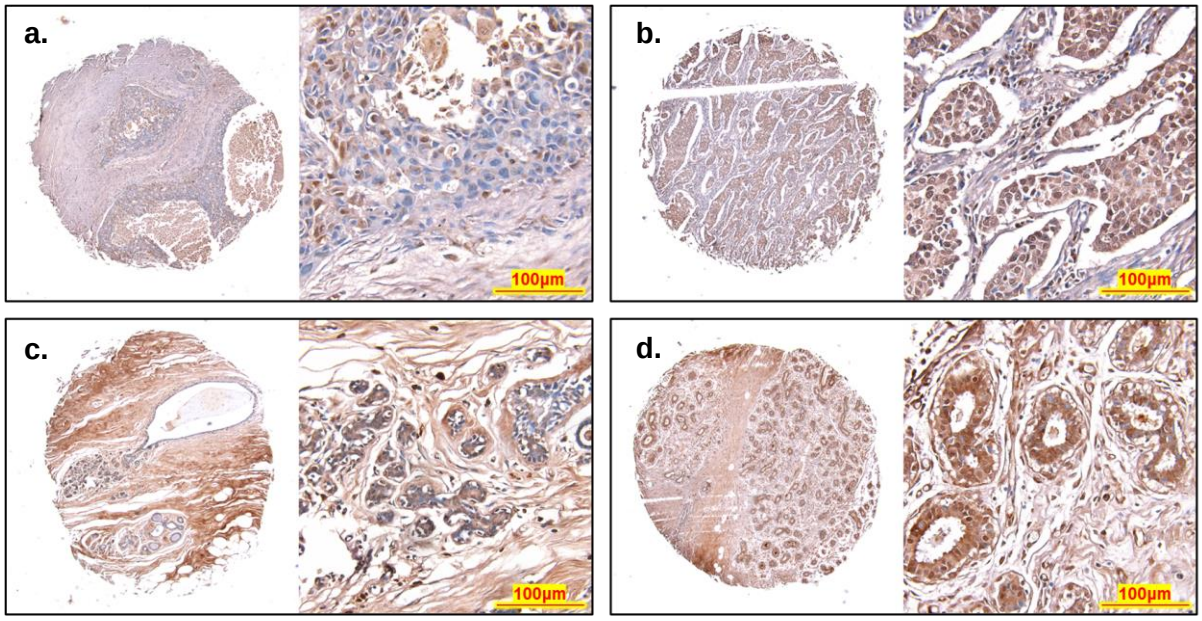

Figure 4.13 – Histology of ACBD3 stained breast cores at 10X and 40X magnification. ACBD3 staining was detected by 3,3′-Diaminobenzidine (DAB) in brown, nuclei were stained by haematoxylin in blue. **a)** invasive ductal carcinoma of a 47-year-old female. Stage IA, grade 3, T1N0M0 scored as 1.1 overall for ACBD3 staining. **b)** invasive ductal carcinoma of a 50-year-old female. Stage IIA, Grade 2, T2N0M0 scored as a 2 overall for ACBD3 staining. **c)** normal adjacent breast tissue with ductal ectasia of a 41-year-old female, scored 2.9 overall. **d)** cancer adjacent tissue (adenosis) of a 39-year-old female, scored 1.7 overall.

Figure 4.13a shows a core from an invasive ducal carcinoma, ACBD3 protein staining (brown) overall is low despite high coverage of haematoxylin nucleus staining (blue). At higher magnification of the central duct there is a mix of cells with high and low expression of ACBD3 with moderate to low expression of ACBD3 in fibrous tissue

at the bottom of the high magnification image (pink hue). The core in Figure 4.13b is also from an invasive ductal carcinoma and contains many more small ducts and, in this case, invasive cells in the ducts have higher staining of ACBD3 compared to the surrounding tissue. Invasive cells are tightly packed and have a uniform amount of ACBD3 staining. Fibrous tissue appears to have low ACBD3 staining overall.

Figure 4.13c shows a normal adjacent breast tissue core from a 41-year-old female with ducal ectasia. Adipose cells are visible at the lower right of the core and ACBD3 staining cannot be seen here in sharp contrast to the surrounding fibrous tissue where ACBD3 staining is higher. Increased magnification of the small ductal acini showed that staining was low in the benign ectasia cells blocking the ducts with some staining of ACBD3 at the basal myoepithelial cells. Figure 4.13d shows a core of cancer adjacent tissue with benign adenosis (enlarged more numerous lobules). Epithelial and myoepithelial cells lining the ducts have high levels of ACBD3 staining with moderate staining of the surrounding tissue.

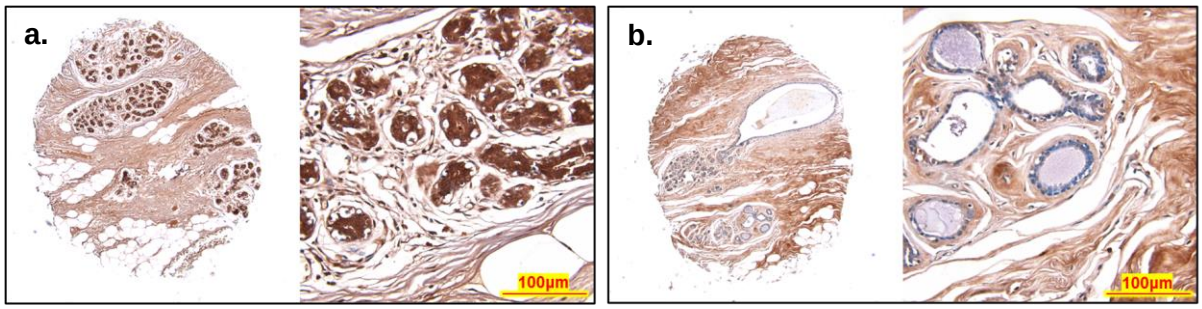

Figure 4.14 – Less typical ACBD3 staining in breast cores. a) 53-year-old female cancer adjacent breast tissue, Adipose cells have no ACBD3 staining in agreement with other observations whilst multiple small acini have very strong ACBD3 staining of luminal epithelial cells that are densely packed. Fibrous interlobal tissue has a moderate to high level of ACBD3 staining typical of AT cores. **b)** 41-year-old female normal adjacent breast tissue, ACBD3 staining is low in the acini including the luminal epithelial cells and what appear to be invasive cells within the ducts, this in direct contrast to most normal and cancerous cores where there is strong ACBD3 staining of luminal epithelial cells. The fibrous interlobal moderately high in the fibrous interlobal tissue which is typical of NAT cores.

ACBD3 staining was high in the luminal epithelial and basal myoepithelial cells of breast duct acini in both healthy breast and breast cancer samples but there were some exceptions (Figure 4.14). ACBD3 was moderate in fibrous interlobular tissue and stroma. Less normal appearing ducts that were small and closed had high levels

of ACBD3 staining (Figure 4.14a). Occasionally cores were found to have no ACBD3 staining of luminal epithelial or basal myoepithelial cells of the ducts (Figure 4.14b) and occasionally ducts were also full of cells despite being normal tissue samples. ACBD3 staining was not detectable in adipose tissue.

4.4 Discussion

The work in this chapter has determined basal mRNA and protein expression in breast cancer cell lines and was in agreement with the results of chapter 3, validating these cells as appropriate breast cancer models. These models also found that there was positive correlation between ACBD3 protein expression and ER positivity. As available protein expression data was limited breast cores were stained by IHC techniques and correlations between ACBD3 expression and receptor status were found. PI4Kβ expression was also queried as it is a known interactor of ACBD3 with a role in breast cancer, and to determine whether the expression of ACBD3 and PI4Kβ correlated in any way.

ACBD3 expression was increased in breast cancer cell lines compared to the MCF12A normal-like breast cells at the mRNA and protein level and this supported the hypothesis that ACBD3 has a role in breast cancer and corroborated the bioinformatic results from patient samples in chapter 3 (Figure 3.1b and c). This also validated breast cell lines as a viable model for studying ACBD3 in breast cancer. There was particular difficulty in achieving equal loading between all 7 cell lines for western blot due at least in part to different cell size and therefore different total cell number at 80% confluency. The blot is representative of what was observed in two biological replicates of each cell line, but the second set of biological replicates could not be presented on one blot.

4.4.1 PI4Kβ Expression in Breast Cancer Cell Lines and Relationship with ACBD3 Expression

At the mRNA level there was a clear and statistically significant difference in *PI4Kβ* expression between cell lines derived from adenocarcinomas (high expression) and cell lines derived from invasive ductal carcinomas (low expression) (Figure 4.4b). *PI4Kβ* expression was previously found to be a marker for breast cancer recurrence

and is upregulated in 20% of breast tumours (Goh, Feng et al. 2017, Tan, Brill 2014, Morrow, Alipour et al. 2014). mRNA levels of *PI4Kβ* varied between the cell lines and expression was lower in several breast cancer lines (BT474. MDA-MB-436, T47D) compared to the normal-like breast cell line (Figure 4.4a). Only the MDA-MB-231 cell line had higher *PI4Kβ* expression to a statistically significant level.

Contrary to mRNA expression data, PI4Kβ protein levels were higher in breast cancer cell lines compared to the normal-like control, with the exception of the MDA-MB-436 cell line which had lower PI4Kβ protein expression. The MDA-MB-436 cell line also had the lowest *PI4Kβ* mRNA expression.

Unlike *PI4Kβ* mRNA expression*, ACBD3* mRNA expression did not correlate with any particular characteristics of the cell lines. At the protein level, breast cancer cell lines with high levels of ACBD3 protein also had high levels of PI4Kβ protein (Figure 4.6). The PI to PI(4)P conversion activity of PI4Kβ is not dependent on ACBD3 protein, but ACBD3 localises PI4Kβ to PI-containing membranes and by association greatly increases PI4Kβ activity. The overexpression of ACBD3 protein may lead to overexpression of PI4Kβ as, without ACBD3, PI4Kβ activity is low regardless of expression but there is no direct evidence for a causal relationship here (Klima, Tóth et al. 2016, McPhail, Ottosen et al. 2017, Lyoo, van der Schaar, Hilde M. et al. 2019, Sasaki, Ishikawa et al. 2012). It is also possible that PI4Kβ overexpression leads to overexpression of ACBD3 for the same reason.

The positive correlation between PI4Kβ and ACBD3 protein expression was absent at the mRNA level. *ACBD3* mRNA levels also did not correlate well with ACBD3 protein levels: T47D and MDA-MB-361 cells had high levels of ACBD3 protein expression but second and third lowest expression of *ACBD3* mRNA respectively, (not including the normal like MCF12A line). Also, *ACBD3* mRNA expression varied between different breast cancer cell line and was 2.1-fold to 5.8-fold higher in breast cancer cell lines compared to the MCF12A cell line. This suggests that ACBD3 protein levels are regulated post transcriptional and/or post translation and this is supported by chapter 3 (Figure 3.4) showing that the ACBD3 reading frame is hypomethylated and not regulated by methylation at the stage of transcription in normal breast or breast cancer.

4.4.2 ACBD3 expression in breast cell lines and ER status

ACBD3 protein expression was highest in ER+ cell lines. PMC42 and T47D are both ER+ PR+ HER2- whilst the MDA-MB-361 cell line is ER+ PR- HER2+. This association was not found at the mRNA level (Figure 4.3). In chapter 3 it was hypothesised that ACBD3 mRNA expression may be a marker for oestrogen receptor remodelling and it was found that oestrogen related pathways were associated with ACBD3 transcription repression (Chapter 3 – Figure 3.5). Despite this, high ACBD3 protein levels were associated with breast cancer cell lines that expressed the oestrogen receptor which further suggests ACBD3 expression could be a marker of a remodelled oestrogen receptor signalling pathway that no longer represses *ACBD3* transcription. Core staining of array BR1401 found that the highest mean ACBD3 protein scoring was found in ER+, PR-, HER2-, breast cancer patients, but this difference did not reach statistical significance compared to patients with other combinations of receptor status.

The ACBD3 antibody used throughout this project was found to give multiple bands in some, but not all cell lines, in western blots, ruling out the possibility of non-specific binding, and all of the prominent bands are of a size larger than the size of ACBD3 (62 kDa). We were unable to determine the cause of the multiple banding but one candidate was poly-ubiquitination as bands have equal spacing of around 8.5 kDa (Figure 4.7) and ACBD3 was found to interact directly with KDM2B which has known ubiquitin ligase activity (Chapter 3 – Figure 3.8). The triple negative BT20 and MDA-MB-231 cell lines showed the clearest evidence of multiple ACBD3 banding, if these multiple bands are from poly-ubiquitination then this may be a mechanism of regulation in these cell lines that have lower expression of ACBD3 compared to the ER+ lines.

4.4.3 ACBD3 expression in breast cancer patient samples

It was unexpected to find that ACBD3 scoring was much lower for the cancers compared to either adjacent tissue. It does not match the findings in cell lines, bioinformatics, or previous publications (Huang, Y., Yang et al. 2018). The fibrous and connective tissue in the adjacent tissues had more ACBD3 staining and, as the bulk of many cores were made up of this, they scored highly. Fibrous tissue of the malignant cores had low to moderate staining with invasive cells that themselves had

varying and sometimes strong staining for ACBD3. It is possible that the level of ACBD3 protein is negatively affected by tissue disruption and links between ACBD3 overexpression and extracellular proteins are found later in chapter 6. A possible explanation is that ACBD3 protein expression was high in cancerous cells (as evidenced by high staining of irregular ductal epithelial cells and invasive cells of the duct) but that in the context of a whole core including normal tissue and adipose tissue, ACBD3 was not increased. ACBD3 may even be the target of downregulation in response to breast cancer that cancerous cells do not respond to but that normal cells surrounding them do. There is some precedent for this as ACBD3 was found to be supressed by ER signalling but is highest in ER+ cell lines suggesting that repressors of ACBD3 may be reprogrammed in breast cancer. ACBD3 staining was significantly higher in PR- breast cancer cores compared to PR 3+ cores on one slide and significantly higher in HER2- cores compared to HER2 1+ cores on another slide but this result could not be cross corelated between slides because only one slide had PR 3+ breast cancer patients and that same slide had no HER2 1+ patients.

A common feature of normal and cancerous tissue was high ACBD3 staining of luminal epithelial and myoepithelial basal cells of ducts. As many breast cancers originate from myoepithelial basal cells, that may be why ACBD3 protein levels were higher in breast cancer cell lines but ACBD3 expression did not appear high when viewed in the context of whole breast cores with cancer in part of as opposed to the whole core. As a protein that is strongly associated with Golgi function, it would be logical to find increased ACBD3 in the cells of the breast duct which are secretary and ACBD3 expression may be required for secretion from these cells.

Unfortunately, the adjacent tissue samples on other arrays were destroyed/displaced during the staining process and this has anecdotally been referred to as common on large (100 or more core) arrays where the core samples are smaller in diameter (Kerslake, 2021 Personal Communication).

There was no significant difference in ACBD3 staining between malignant non-metastatic breast cancer cores and cores from metastatic breast cancer of the lymph node suggesting that ACBD3 expression does not correlate with metastasis (Figure 4.11a). ACBD3 overexpression in breast cancer cell lines promotes the formation of cancer stem cells(Huang, Y., Yang et al. 2018), and these are often slower growing more dormant cells and so an association between ACBD3 expression and lymph

node invasion was not necessarily expected. It was observed with invasive ductal carcinomas that there were often many invasive cells in the lobules that had low staining for ACBD3 but some cells embedded in them had very high staining, and this could be, in effect, staining cancer stem cells or cells that may become them as the heterogenous tumour evolves.

ACBD3 interacts with the progesterone receptor chaperone UNC45A, a regulatory component of the progesterone receptor/heat shock protein 90 chaperoning complex, which functions in the assembly and folding of the progesterone receptor (Chadli, Graham et al. 2006b). An ACBD3-UNC45A interaction could have a negative effect on PR nuclear expression, and it is possible that PR signalling-dependent breast cancers may be under selection pressure to downregulate ACBD3 protein relative to PR- breast cancers.

In summary, the breast cancer cell lines chosen as models for this project all had higher levels ACBD3 mRNA and protein than a normal like breast cell control and ACBD3 expression varied between cancer cell lines. There was positive correlation between ACBD3 and PI4Kβ protein levels in breast cell lines. These results serve as a baseline for work in subsequent chapters and informed which cell lines should be used for different experiments.

ACBD3 protein expression in patient tumour core samples were found to be higher in normal breast tissue compared to breast cancer tissue, conflicting with results found in breast cell lines in this chapter, with bioinformatic analysis in chapter 3, and previously published results. It was also found that in breast cancer patient samples, ACBD3 expression positively correlated with PR negativity and HER2 positivity.

Chapter 5

Examining regulators of ACBD3 and PI4Kβ Expression in Breast Cancer Cell Lines

5.1 Introduction

ACBD3 is essential for embryogenesis, is causative of disease progression in mouse models of Huntington's disease, is essential for CBV3 viral infection, and has no known redundancies for its functions (Zhou, Atkins et al. 2007, Sbodio, Paul et al. 2013, Kim, H. S., Lee et al. 2018, Lyoo, van der Schaar, Hilde M. et al. 2019). Despite its importance in normal cell function and in disease, there are few experimentally confirmed regulators of ACBD3 at the protein level and none at the mRNA level (Okazaki, Ma et al. 2012, Okazaki, Glass 2017).

Chapter 4 confirmed that ACBD3 is overexpressed in breast cancer cell lines at the mRNA and protein level, and ER+ breast cancer cell lines had the highest expression of ACBD3 protein (Chapter 4 – Figure 4.6). In patient sample core analysis, it was found that ACBD3 protein levels were higher in HER2- breast cancer patients than HER2 1+ breast cancer patients (Chapter 4 – Figure 4.11a) and higher in PR- breast cancer patients than PR 3+ breast cancer patients (Chapter 4 – Figure 4.10). Chapter 3 uncovered potential factors that affect *ACBD3* transcription levels (Chapter 3 – Figure 3.5), found that *ACBD3* was overexpressed in breast cancer patient tumours (Chapter 3 – Figure 3.2) and found novel ACBD3 interactors and co-expressors (Chapter 3 -Figure 3.8). From the cumulative results of chapters 3 and 4 it was hypothesised that ACBD3 is either directly involved in breast cancer occurrence/progression with differential effect depending on receptor status (ER, PR, HER2) or that ACBD3 could be a biomarker for cellular changes that occur in breast cancer.

If ACBD3 has a direct role in breast cancer, then finding regulators of its expression are important as these could form part of a breast cancer treatment (or prevention) regime in the future. In the shorter-term, finding regulators of ACBD3 in breast cancer will provide evidence as to how ACBD3 is upregulated and what consequence that upregulation might have for breast cancer patients. As *ACBD3* is an essential gene that is expressed in all tissues, direct silencing or inhibition of its functions may not be desirable and instead targeting one or more of its known

interactors, such as PI4Kβ, may have more efficacy as a treatment option (Yue, Qian et al. 2019, Klima, Tóth et al. 2016).

To find out how ACBD3 expression might be regulated in breast cancer, I started with the one of two experimentally confirmed regulators of ACBD3 in any tissue: iron in the duodenum (Okazaki, Ma et al. 2012). ACBD3 interacts with the iron transporter DMT1 and its positive regulator Dexras1 to facilitate free iron and transferrin bound iron cellular import. This process is dependent on ACBD3 protein expression and is experimentally confirmed to also take place in the brain (Okazaki, Ma et al. 2012, Choi, Bang et al. 2013). Iron levels in the cells of the gut regulate ACBD3 protein levels by providing negative feedback which reduces ACBD3 protein and therefore prevents further iron import.

It was decided to target PI4Kβ activity as it is a key binding partner of ACBD3 and PI4Kβ was found to be upregulated at the protein level in the BT20, MDA-MB-231, PMC42, T47D, and MDA-MB-361 breast cancer cell lines compared to the non-cancerous MCF12A breast cell line (Chapter 4 – Figure 4.6). Breast cancer cell lines with the highest ACBD3 protein expression also had the highest PI4Kβ protein expression and this relationship could be causal with the expression of one affecting the expression of the other. As direct Inhibition of ACBD3 might not be desirable, inhibition of its binding partners may provide a more effective and specific treatment option for breast cancers.

PI4Kβ expression is associated with breast cancer but its inhibition in breast cancer has not been studied experimentally (Goh, Feng et al. 2017, Tan, Brill 2014, Morrow, Alipour et al. 2014, Waugh 2014). The MDA-MB-231 cell line was chosen to study the effects of a PI4Kβ inhibitor as it is the only breast cancer cell line in this project to express *PI4Kβ* mRNA to a significant level above the expression of the normal-like MCF12A cell line (chapter 4 - Figure 4.4a) and MDA-MB-231 cells have a high level of protein expression (relative to the MCF12A cell line, chapter 4 - Figure 4.6). The MDA-MB-231 cell line is also derived from a triple negative breast cancer and these tumours have the fewest treatment options and are associated with the worst prognosis for patients meaning evaluating novel treatment options for triple negative breast cancers is especially important (Won, Spruck 2020).

This chapter covers broad factors in a search for regulators of ACBD3 and their effect on breast cancer cell growth. The lack of relationship between these factors represents the gaps in current knowledge about ACBD3, its regulation in

general, and especially its regulation in breast cancer. The exploration of some compounds, such as a PI4Kβ inhibitor and iron, have a clear rationale whilst other findings came from experimental observations in relation to inconsistent results. mRNA expression of *ACBD3* was tested in a previously engineered everolimus resistant T47D breast cancer cell line (Hare 2018, Hare, Harvey 2017) and expression was found to be increased in some biological replicates but not others. Other inconsistencies in mRNA measurements led to further inquiries into a relationship between *ACBD3* expression and the seeding density of cell lines in culture.

Everolimus is an mTOR inhibitor and rapamycin analogue originally approved as an immunosuppressant for organ transplant patients (Kirchner, Meier-Wiedenbach et al. 2004, Beaver, Park 2012, Baselga, Campone et al. 2012). It was later approved as a second line treatment for breast cancer patients who are ER+ and have previously had aromatase inhibitor therapies. Whilst there are currently no published cases of acquired resistance to everolimus in breast cancer patients, it was considered important to determine what changes occur in cells with engineered everolimus resistance in an attempt to pre-empt any future acquired resistance in patients. Changes in mTOR related genes were found in the resistant cells as well as changes in the expression of several oncoproteins but the mechanism of resistance was not fully concluded (Hare 2018). ACBD3 expression changes in the everolimus resistant cell line and ACBD3 expression changes following everolimus treatment expands on the previous research and this is taken further in chapter 6. PI4Kβ expression in the T47D parental and T47D everolimus resistant cell line was also analysed.

5.2 Chapter Aims

The aim of this chapter was to discover regulators of ACBD3 expression in breast cancer cell lines and to examine whether ACBD3 expression changes correlated with changes in PI4Kβ expression. Based on these discoveries, the factors that regulate ACBD3 expression were analysed for efficacy as breast cancer treatments.

5.3 Results

5.3.1 Iron Treatment of the MDA-MB-231 Breast Cancer Cell Line

Iron is one of the few known negative regulators of ACBD3 protein expression (Okazaki, Ma et al. 2012). Inorganic iron is insoluble, so ferric ammonium citrate was used as the most suitable soluble form of iron as it is soluble in water and water-based solvents such as PBS and cell culture medium. The availability of ammonium citrate was also a factor as it allowed for the use of effective controls. Ferric ammonium citrate was solubilised in PBS at the concentrations indicated below, added to cell culture medium, and the effect on ACBD3 protein expression was measured by western blot in the MDA-MB-231 breast cancer cell line. Ferric ammonium citrate containing media was formulated in weight per volume but converted to molarity to make direct comparisons between an ammonium citrate control and because the molarity of the iron in ferric ammonium citrate would be equal to the molarity of the ferric ammonium citrate. A table of conversion between molarity and weight per volume can be found in chapter 2 – section 2,2.14 (Table 2.14).

5.3.2 ACBD3 Protein Expression in Response to Ferric Ammonium Citrate Supplementation

Initially the effects of ferric ammonium citrate on ACBD3 expression were compared to a PBS control. Ferric ammonium citrate in medium at 0.179μM and 89.53μM concentrations resulted in increased ACBD3 protein expression compared to PBS only control after 72 hours (Figure 5.1). Following 447.7μM ferric ammonium citrate treatment, ACBD3 was downregulated at the protein level compared to the 0.179μM and 89.53μM added ferric ammonium citrate conditions. There were multiple bands of staining with ACBD3 antibody (as in chapter 4 - Figure 4.6) and these bands appeared at first as two bands but were found to be four bands in the two close couplets that can be best visualised in lane one (PBS control) and lane five (447.7μM ferric ammonium citrate). The higher and lower weight bands of ACBD3 protein were differentially expressed with all bands upregulated compared to the no iron control following 0.179μM and 89.53μM ferric ammonium citrate treatment. Following 447.7μM ferric ammonium citrate treatment the lower weight couplet of bands were slightly upregulated compared to the PBS control and the higher weight couplet of bands were downregulated. After 89.53μM ferric ammonium citrate treatment or

higher, cell pellets were visibly orange indicating that iron was being taken up by the cells.

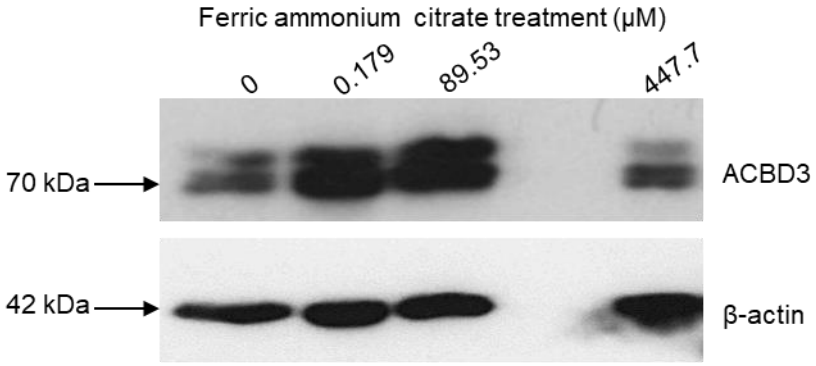

Figure 5.1 – ACBD3 protein expression is upregulated in response to ferric ammonium citrate treatment in the MDA-MB-231 cells. ACBD3 protein levels were increased after 72 hours of treatment with 0.179μM and 89.53μM ferric ammonium citrate compared to PBS only control. ACBD3 was slightly upregulated in the 447.7μM ferric ammonium citrate treated cells (combined floating and adherent cells) compared to control. There were multiple bands of ACBD3 staining and these were differentially expressed between different treatments. Exposure time for ACBD3 bands was 2 minutes. β-actin protein staining was used as a loading control in addition to cell counting before lysis (10 second exposure). Blot is representative of results from n=2.

5.3.3 MDA-MB-231 Cell Growth in Response to Iron Supplementation

ACBD3 protein levels were upregulated in response to 0.179μM and 89.53μM ferric ammonium citrate supplementation suggesting that iron does not negatively regulate ACBD3 protein levels in breast cancer. Increased ACBD3 expression in breast cancers could increase the cells' capacity to import iron, and cellular iron levels are linked to redox stress which can drive inflammation. An inflammatory microenvironment can promote cancer (Deshmukh, Srivastava et al. 2019, Hanahan, Weinberg 2011) but there is a limit to how much redox stress cells can tolerate(Townsend, He et al. 2008, Wang, J. B., Erickson et al. 2010, Perillo, Di Donato et al. 2020). If ACBD3 overexpression increases cellular iron, then breast cancers may be more sensitive to further increases in iron as a treatment than normal cells. The MDA-MB-231 cell line was again chosen to study the effect of iron on cell growth measured by MTT assay to calculate relative cell number.

Ferric ammonium citrate or ammonium citrate were added to medium at equivalent molarity for direct comparison. Supplemented medium was added to cells in 96 well plate format and treated for 72 hours. Cell viability was measured by MTT assay to determine cell growth relative to untreated cells (media + PBS carrier).

Ferric ammonium citrate increased mean relative cell number (RCN) above the level of untreated cells up to 1.79μM, with a maximum RCN of 124% for cells treated with 17.907nM ferric ammonium citrate compared to controls (Figure 5.2a). Mean RCN decreased above 1.79μM ferric ammonium citrate and the reduction in RCN compared to controls reached statistical significance at and above 17.907μM ferric ammonium citrate treatment.

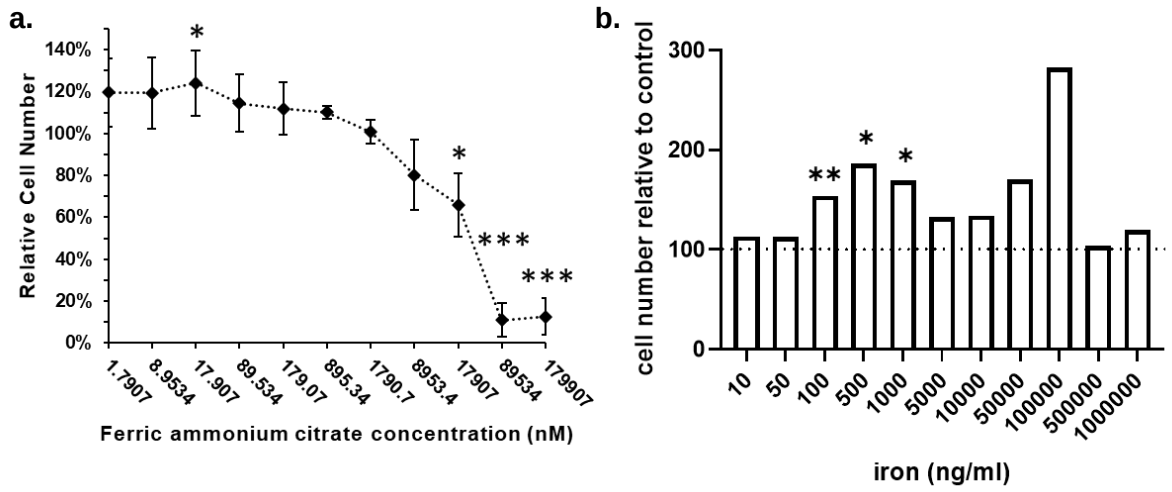

Figure 5.2 – a) Relative cell number after 72 hour ferric ammonium citrate treatment. 17.91nM ferric ammonium citrate treatment significantly increased relative cell number in the MDA-MB-231 cell line, MDA-MB-231 are tolerant to high levels of ferric ammonium citrate treatment. Ammonium citrate alone yielded no growth advantage relative to the PBS only control and ammonium citrate treatments had a lower mean relative cell number than ferric ammonium citrate treatment up to 17.907μM equivalent treatments. Relative cell number was measured by MTT assay after 72 hours of treatment with ammonium iron citrate or ammonium citrate compared to PBS only control**.** Data are plotted as mean plus/minus standard deviation error bars. All data were collected in sextuplet per assay and the assay was repeated three times independently (n=3). **b) 72-hour iron treatment increases MDA-MB-231 relative cell number between 100-1000ng/ml.** To find the specific effect of iron on cell growth, ammonium iron citrate treatment was normalised against ammonium citrate treatment at equal molarity. The dotted line represents 0% increased cell number compared to control *P values represent significant difference in relative cell number compared to the control for the same reagent.

Cells treated with ammonium citrate (without iron) showed no increase in RCN at any concentration in medium compared to controls but caused statistically significant decreases in RCN at 17.907nM, 179.07nM, 8.9534µM, 17.907µM, 89.534µM, and 179.07µM. It is possible that the ammonium citrate in the ferric ammonium citrate treatments was responsible for the decreasing RCN at high concentrations (>1.79µM) but as iron is insoluble without a suitable ligand this cannot be tested directly. Treatments were measured in moles rather than concentration by weight per volume to allow for direct comparisons between ammonium citrate and ferric ammonium citrate as they have different molecular weights.

To separate the effects of the iron from the effects of the ammonium citrate ligand as much as is possible, the RCN for ferric ammonium citrate treatments was normalised against the RCN for ammonium citrate treatments at equivalent molarity (Figure 5.2b); however, this cannot rule out the direct interplay between iron and ammonium citrate, which is mildly acidic. Iron supplementation did not decrease RCN at any concentration compared to equivalent ammonium citrate controls. 100ng/ml iron treatment (17.907nM) led to a 54.05% RCN increase (*P = 0.009271), 500ng/ml iron treatment 86% increase (*P = 0.031142) and 1µg/ml iron treatment 70.29% increase (*P = 0.015492) (Figure 5.2b). The largest difference was seen at 100µg/ml iron (182.66% increase) but, as can be seen in Figure 5.2a (17,907nM equivalent molarity), RCN for both conditions was small and the difference did not reach statistical significance (*P = 0.264012).

5.3.4 PI4Kβ inhibition in the MDA-MB-231 Breast Cancer Cell Line

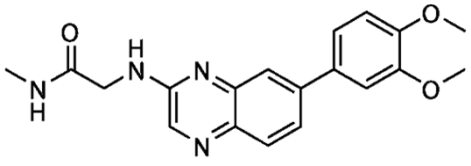

Figure 5.3 – The molecular structure of BQR695, a PI4Kβ specific inhibitor with sub-micromolar affinity (McNamara, Lee et al. 2013).

BQR695 is a PI4Kβ specific small molecule inhibitor from the Novartis compound library with a reported IC50 of 90nM; it is soluble in DMSO and insoluble in water (McNamara, Lee et al. 2013). BQR695 binds the ATP-binding pocket of PI4Kβ and

this binding is competitive with ATP. BQR695 is a quinoxaline compound with a central benzene ring and pyrazine ring and molecular formula: $C_{12}H_{20}N_4O_3$. Its structure is represented in Figure 5.3.

5.3.5 Treatment of MDA-MB-231 Cells with BQR695

BQR695 was found to be a PI4Kβ specific inhibitor whilst studying malaria infection and has not been tested for any therapeutic effect in cancers in spite of the evidence for a PI4Kβ role in cancer (Waugh 2014, McNamara, Lee et al. 2013, Goh, Feng et al. 2017, Tan, Brill 2014, Orsetti, Nugoli et al. 2006, Morrow, Alipour et al. 2014). The MDA-MB-231 cell line was treated with 50nM to 100μM BQR695 for 72 hours and the cell number was then measured relative to controls by MTT assay.

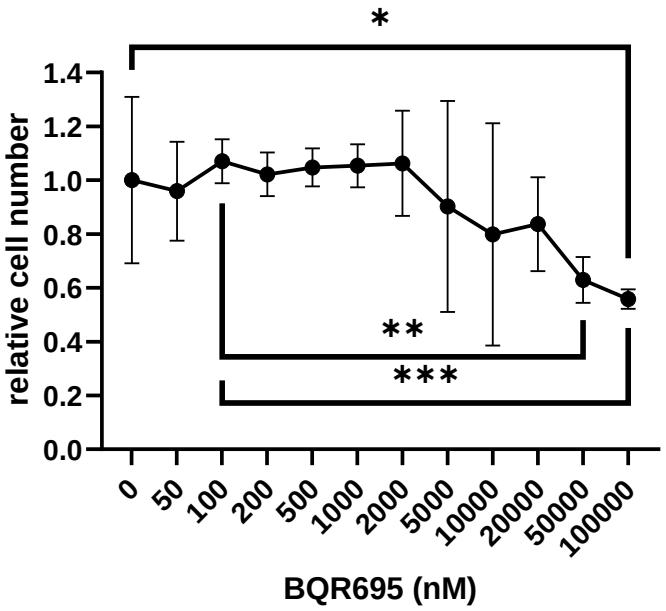

Figure 5.4 –MDA-MB-231 relative cell number after 72 hours of BQR695 treatments relative to the DMSO only (0nM BQR695) control. There was a significant difference between 0nM treatment and 100,000nM treatment (*P = 0.019771), 100nM and 50,000nM treatment (*P = 0.001398), and 100nM and 100,000nM (*P = 0.000138). 0nM BQR695 = DMSO only control (0.1% DMSO), all other treatments had a final concentration of 0.1% DMSO. MTT experiment was carried out three times independently (n=3) and each experiment was measured in sextuplet, error bars represent the standard deviation.

BQR695 treatment up to 2μM did not have a negative effect on MDA-MB-231 cell growth relative to the DMSO only control, based on mean relative cell number (RCN) (Figure 5.4). Only the 100μM BQR695 treatment had a statistically significant difference in RCN compared to the control (44.2% decrease in cell number, P = 0.019771). The 100nM treatment was close to the reported IC50 for PI4Kβ activity inhibition(90nM) and had no statistically significant effect on RCN compared to the control (McNamara, Lee et al. 2013). The 50μM and 100μM treatments had significantly lower RCN compared to the 100nM treatment (41.3% cell number decrease *P = 0.001398, and 47.8% cell number decrease *P = 0.000138 respectively).

5.3.6 ACBD3 Protein Expression in Response to BQR695 treatment

ACBD3 protein and PI4Kβ protein expression were found to positively correlate with each other (chapter 4 – Figure 4.6), and it was hypothesised that expression or activity of one may affect expression of the other. It has already been found that PI4Kβ activity is dependent on protein expression of ACBD3 although even low levels of ACBD3 protein (post *ACBD3* siRNA treatment) allow for PI4Kβ activity (Kim, H. S., Lee et al. 2018, Lyoo, van der Schaar, Hilde M. et al. 2019, Dorobantu, Cristina M., van der Schaar et al. 2014).

PI4Kβ was inhibited in the MDA-MB-231 cell line to find out if ACBD3 protein expression was dependent on the activity of PI4Kβ. MDA-MB-231 cells were seeded at 100,000 cells per well in six well plates. After 24 hours, cells were treated with double the IC50 of BQR695 inhibitor (180nM) in media for 24 hours and then lysed for analysis by western blot (n=3). ACBD3 was found to be upregulated at the protein level in one of three biological replicates treated with 180nM BQR695 in DMSO carrier compared to cells treated with DMSO only (Figure 5.5). There was variance in ACBD3 expression in all biological replicates and two BQR695 biological replicates had very similar or possibly lower ACBD3 expression than the controls. The BQR695 treated cells showed stronger higher weight banding of ACBD3 as visible in lane six of Figure 5.5 that is most apparent in the top panel (ACBD3 five-minute exposure).

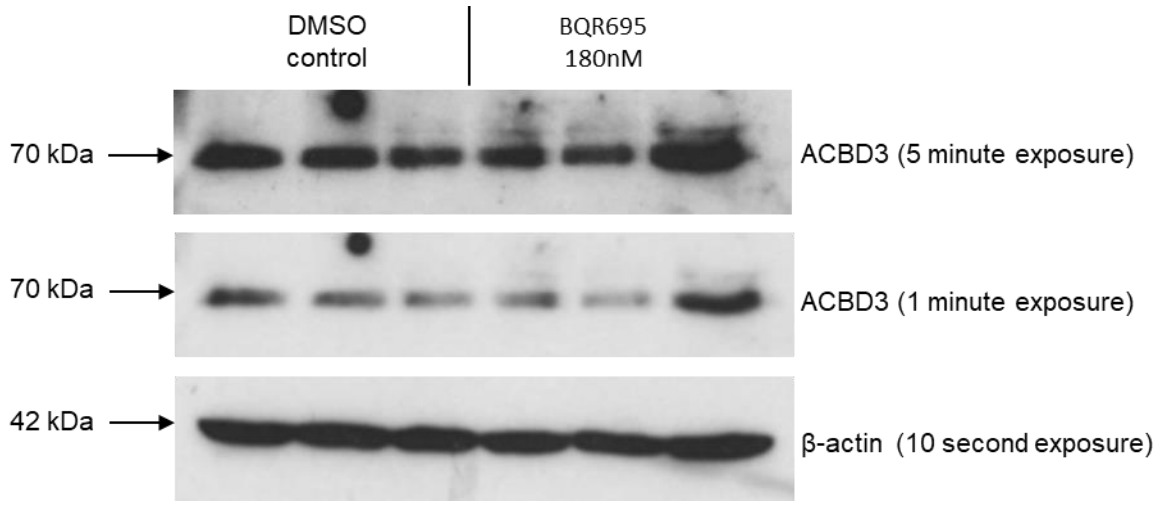

Figure 5.5 – Western blot of lysates from MDA-MB-231 cells treated with 2X IC50 of BQR695 (180nM) compared to DMSO only control treatment. 5 minute and 1 minute exposure western blot of ACBD3 protein expression, β-actin protein staining was used as a loading control in addition to cell counting before lysis (10 second exposure). Each lane contains the lysate of an independent biological experiment (n=3 per condition).

Multiple banding was previously observed in the MDA-MB-231 breast cancer cell line and other cell lines and had differential intensities. Inhibition of PI4Kβ activity appears to have increased the prevalence of the highest weight band of ACBD3 and it is possible that this represents a post translational modification to the ACBD3 protein when PI4Kβ is not active.

Upregulation of ACBD3 was observed in one sample of 180nM BQR695 treated cells and the experiment was repeated, this time with 10 times the IC50 of BQR695 (900nM). At this concentration of treatment there was still no definite upregulation of ACBD3 (Figure 5.6) and, overall, it cannot be concluded that PI4Kβ inhibition has a consistent effect on overall ACBD3 protein levels in the MDA-MB-231 cell line. At 900nM BQR695 treatment there was a less obvious effect on the proportion of higher weight ACBD3 bands.

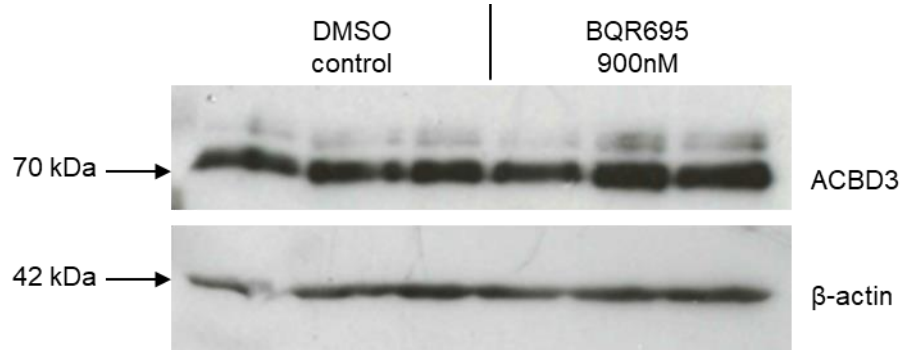

Figure 5.6 – Western blot detecting ACBD3 protein expression in MDA-MB-231 cells treated with 10X IC50 of BQR695 (900nM) compared to DMSO only control treatment. 1 minute exposure of ACBD3 staining. β-actin protein staining was used as a loading control in addition to cell counting before lysis (10 second exposure).

5.3.7 *ACBD3* and *PI4Kβ* mRNA Expression in an Everolimus Resistant T47D Breast Cancer Cell Line

An everolimus resistant T47D breast cancer cell line (T47D-EveR) was previously established to investigate any mechanism that might cause everolimus resistance (Hare 2018). *ACBD3* mRNA expression was measured by QPCR in the T47D naïve parental cell line and T47D everolimus resistant cell line. As a separate GeNorm analysis had been performed to find suitable reference genes for the T47D parental and T47D-EveR cell lines (Hare 2018), that analysis was referred to and the *YWHAZ* and *TOP1* reference genes were used in place of the reference genes described for previous QPCR experiments (Chapter 4 – 4.2.1). The relative quantity of several mTOR related proteins were also measured, *RICTOR* and *mTOR* expression matched previous mRNA expression results (not shown) (Hare 2018). *RAPTOR* was found to have approximately a 3-fold increase in expression where fold changes in expression were not found previously by Hare (2018), Hare did find RAPTOR to be upregulated at the protein level in the T47D-EveR cell line.

5.3.8 *ACBD3* is Upregulated in the T47D Everolimus Resistant Cell Line

ACBD3 mRNA was found to be 155% higher in the T47D-EveR cell line relative to the parental T47D cell line but only one biological replicate was tested (not shown). When this was repeated with three biological replicates the fold change disappeared and there was high variance between biological replicates. It was hypothesised that

ACBD3 mRNA expression may be cell density dependent in breast cell lines as was reported by Okazaki et al 2012, but their data were not shown in the paper. A third QPCR experiment to compare the expression of *ACBD3* between the T47D parental and T47D-EveR cell lines was carried out that controlled for cell density, cells were seeded at $5.33X10^4$ cell/cm^2 in T75 flasks and then harvested for RNA extraction after 24 hours (n=3). This density was chosen as it approximates 60-70% confluency for this cell line and cells would be in log growth whilst also being a large enough cell number to minimise errors in counting and distributing (4 million cells per 75cm^2 flask).

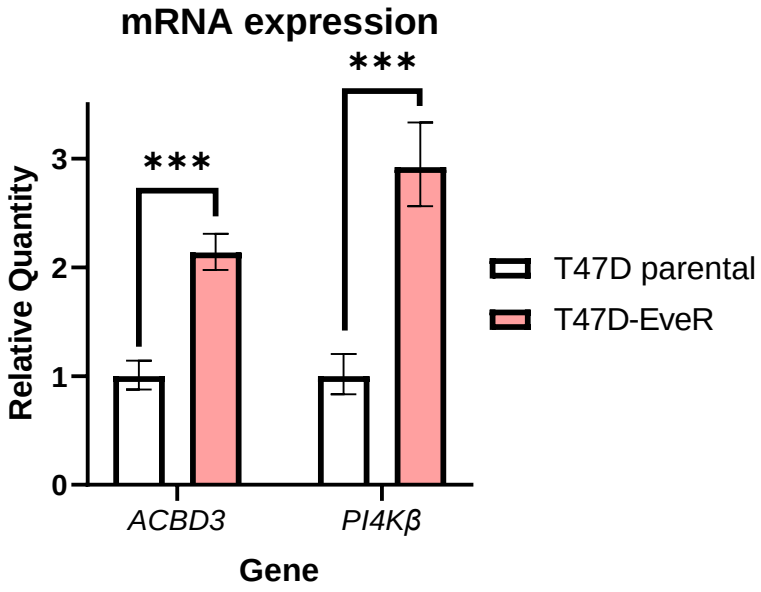

Figure 5.7 –*ACBD3* and *PI4Kβ* are more highly expressed in the everolimus resistant T47D cell line (T47D-EveR pink) than the T47D parental cell line (white). *ACBD3* expression was increased 2.56-fold in the everolimus resistant cell line and *PI4Kβ* expression was increased 2.92-fold. mRNA quantity is relative to the quantity in the parental cell line for each respective gene and was measured by QPCR. Error bars represent the standard deviation of the biological replicates (n=3). Each biological replicate was tested 3 times (3 technical replicates) per gene and normalised to *TOP1* and *YWHAZ* relative expression.

It was found that *ACBD3* was 113% higher in the T47D-EveR line (**P* = 0.000472) and *PI4Kβ* expression was 192% higher (**P* = 0.000553) compared to the parental cell line (Figure 5.7). This upregulation of *ACBD3* was similar to the initial single biological replicate finding for the everolimus resistant cell line. Taken

together, these results suggest that *ACBD3* expression is higher in the T47D-EveR cell line and also that expression of *ACBD3* might be dependent on cell density.

5.3.9 Everolimus Treatment Does Not Affect *ACBD3* mRNA Expression in the T47D Cell Line

The T47D-EveR cell line has undergone multiple changes compared to the T47D parental line including a slower reported growth rate and upregulation of β-catenin protein expression (Hare 2018). During routine culture the T47D-EveR cell line was treated with 100nM everolimus in media for 72 hours every third passage to maintain resistance. To determine whether *ACBD3* upregulation was a consequence of the everolimus treatment, the parental cell line was treated with 100nM everolimus for 24 hours and then RNA was harvested. As with the results in Figure 5.7, cells were seeded at $5.33X10^4$ cells/cm^2. Treatment medium was made up to a final concentration of 100nM everolimus in DMSO (0.002% DMSO final concentration) and control media contained 0.002% DMSO. Each condition was assayed 3 times, independently and in parallel (n=3).

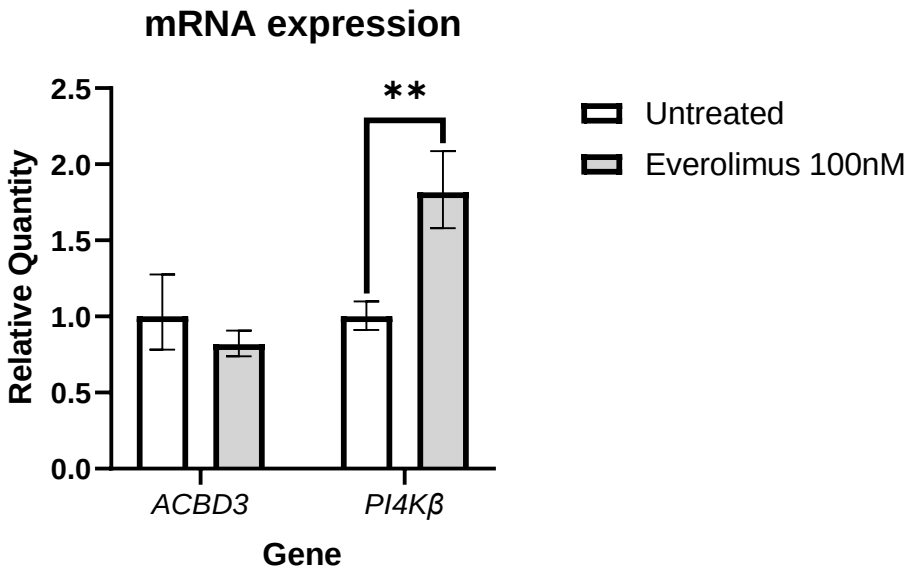

Figure 5.8 – mRNA expression of *ACBD3* and *PI4Kβ* in the T47D breast cancer cell line after 24 hours treatment with 100nM everolimus. *PI4Kβ* was 1.82-fold upregulated following everolimus treatment (**P* = 0.006794), *ACBD3* expression was not significantly different. Error bars represent standard deviation, n=3.

ACBD3 mRNA expression in the T47D parental cell line was not significantly different after 24 hours everolimus treatment compared to the DMSO-only control (untreated) despite being upregulated in the T47D-EveR cell line (Figure 5.8); however, *PI4Kβ* expression was upregulated by almost two-fold (81.6% upregulation) following 24 hours of everolimus treatment.

5.3.10 Everolimus Treatment Does Not Affect ACBD3 Protein Expression in the T47D Cell Line

The T47D-EveR cell line resistance to everolimus was maintained with one passage of 100nM everolimus complete media every three passages. The everolimus resistant cell line overexpressed *ACBD3* at the mRNA level but everolimus treatment did not affect ACBD3 mRNA levels in the T47D cell line. T47D cells were again treated with everolimus and samples were taken at multiple time points to determine if everolimus had an effect on ACBD3 protein levels independently of mRNA expression changes.. Parental cells were seeded into seven wells of six well plates at $2X10^4$ cells/cm^2 and after 24 hours media was changed to 100nM everolimus complete media for three of the wells and fresh complete control media (equivalent amount DMSO 0.002%) to three others. The seventh well was harvested simultaneously to treatment, by addition of hot laemmli buffer directly to the plate, followed by scraping with a pipette for a time 0 sample. After 6 hours, one treated and one untreated sample was harvested, and again at 24 hours and 72 hours. This was repeated for two experiments (n=2) and the results gained were consistent.

ACBD3 protein expression was not different at any time point for the everolimus treated cells but was upregulated at 6 hours and 72 hours after DMSO only control treatment (untreated) (Figure 5.9). PI4Kβ protein expression also increased overtime in the control samples at 6 and 72 hours compared to time and at 72 hours in the 100nM everolimus-treated cells.

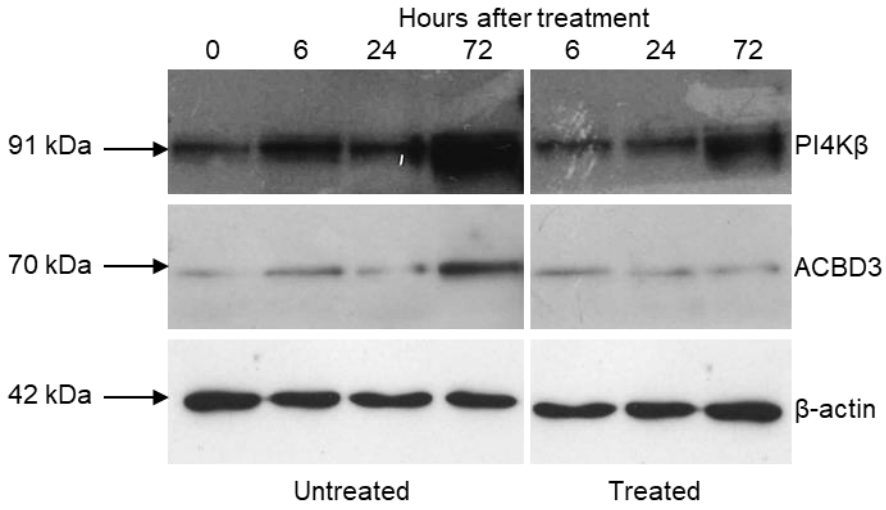

Figure 5.9– ACBD3 protein did not change over time following everolimus treatment in the T47D cell line but did increase over time in the DMSO only controls. PI4Kβ protein expression increased at 72 hours everolimus treatment but also increased over time in the controls**.** β-actin protein staining was used as a loading control in addition to cell counting before lysis. β-actin exposure = 10 seconds, ACBD3 exposure = 2 minutes, PI4Kβ exposure = 1 minute. Representative blot from n=2. (Panels are from a single blot that has been cropped to better interpret the results, the original uncropped blot image in the appendix - Figure 9.1).

The everolimus resistant cell line grew slower in everolimus containing medium and I had previously hypothesised that ACBD3 expression may be dependent on cell density. It is possible that ACBD3 protein levels did not increase over time in the everolimus treatment group because growth was largely inhibited meaning that cell density changed very slowly whilst in the control group cell density increased more rapidly in the same time.

5.3.11 ACBD3 and PI4Kβ Expression in Response to Cell Seeding Density

Initial QPCR results for baseline *ACBD3* expression were inconsistent when looking at T47D breast cell lines under different conditions. The loading control for QPCR was previously taken at the point of RNA extraction with cDNA synthesis based on RNA concentration. Cells were taken from a T25 or T75 flask at 80% confluency leaving some variability in the total cell number / cell density. ACBD3 protein expression was previously reported to be 2-fold greater in the K562 leukaemia cell

line when grown at $2.5X10^5$ cells/ml than in the same cell line grown at four times that density (the data were not shown in the paper) (Okazaki, Ma et al. 2012). Despite this observation being in suspension culture, because ACBD3 protein levels were also found to increase over time for untreated T47D cells (Figure 5.9), I hypothesised that this could also be due to increasing cell density. These three factors formed the hypothesis that ACBD3 expression in breast cancer cell lines is dependent on the density of the cells. As PI4Kβ is one of the main binding partners of ACBD3, PI4Kβ expression was also measured.

5.3.12 *ACBD3* mRNA Expression

Cells were grown to 80% confluency in 75cm^2 flasksand then seeded at 10^6, $2X10^6$, $4X10^6$, or $6X10^6$ in a 75cm^2 flask ($1.33X10^4$, $2.66X10^4$, $5.33X10^4$, or $8X10^4$ cells/cm^2 respectively). The T47D parental cell line and the T47D-EveR cell line were both tested as I was interested in *ACBD3* expression changes between these cell lines as well as for *ACBD3* expression changes in response to cell density. The *TOP1* and *YWHAZ* reference genes were used for QPCR again as they had previously been validated as appropriate references for the T47D and T47D-EveR cell lines as in Figure 5.7 and Figure 5.8 and by Hare 2018, each condition was assayed 3 times independently for n=3.

ACBD3 mRNA expression followed a similar pattern as cell density changed in both the T47D parental and T47D-EveR cell lines. In both cases ACBD3 was low at $1.33X10^4$ cell/cm^2 and increased greatly at $2.66X10^4$ cell/cm^2, there was only a small change in quantity between $2.66X10^4$ cell/cm^2 and $5.33X10^4$ cell/cm^2 for both cell lines (Figure 5.10). In the T47D-EveR cell line *ACBD3* mRNA expression decreased sharply between $5.33X10^4$ cell/cm^2 and $8X10^4$ cell/cm^2 but this did not occur in the parental cells.

Changes to *ACBD3* expression in the parental cell line depending on cell density did not reach statistical significance. In the T47D-EveR cell line, fold change differences in *ACBD3* expression were larger between cell density conditions than the parental cell line and reached statistical significance in most instances.

T47D-EveR cells seeded $2.66X10^4$ cell/cm^2 or $5.33X10^4$ cells/cm^2 had higher *ACBD3* expression than cells seeded $1.33X10^4$ cell/cm^2. *ACBD3* expression was

significantly decreased when T47D-EveR cells were seeded at 8X10^4 cells/cm^2 compared to 2.66X10^4 cell/cm^2 and 5.33X10^4 cell/cm^2 seeding densities.

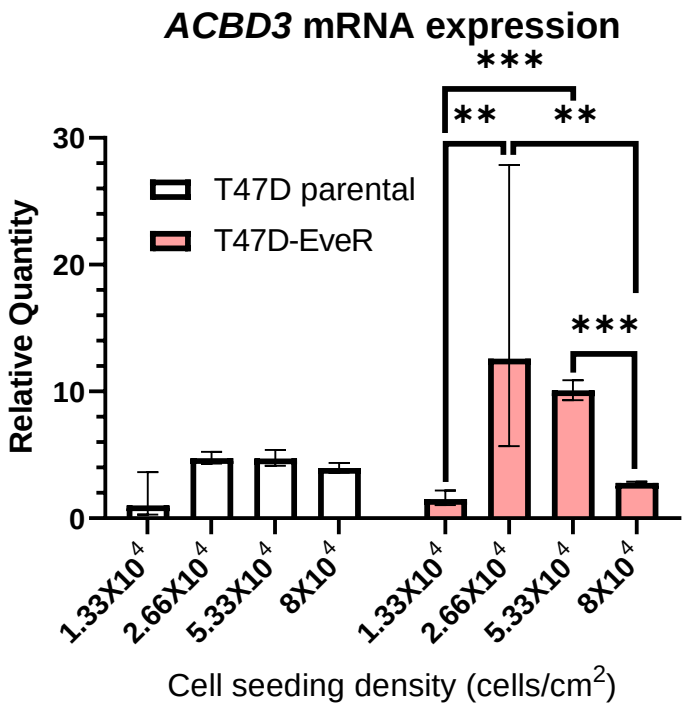

Figure 5.10 – *ACBD3* mRNA expression in the T47D parental and T47D-EveR cell lines when seeded at different densities. There were no statistically significant changes to *ACBD3* expression in the T47D parental cells (white) when seeded at different densities. In the T47D-Ever cell line (pink), *ACBD3* was significantly upregulated at 2.66X10^4 cell/cm^2 (RQ = 12.59, **P* = 0.006824) and 5.33X10^4 cell/cm^2 (RQ = 10.08, **P* = 0.000458) compared to at 1.33X10^4 cell/cm^2 (RQ = 1.50). in the T47D-EveR cell line, *ACBD3* was significantly upregulated at 2.66X10^4 cell/cm^2 (RQ = 12.59, **P* = 0.004422) and 5.33X10^4 cell/cm^2 (RQ = 10.08, **P* = 0.000059) compared to at 8X10^4 cell/cm^2 (RQ = 2.80). All values are relative to the T47D parental cell line seeded at 1.33X10^4 cell/cm^2, error bars represent the standard deviation, n=3 per condition and each biological replicate was assayed 3 times.

ACBD3 mRNA expression between the T47D parental and T47D-EveR cell line were also compared at equivalent densities. The comparison at 5.33X10^4 cell/cm^2 was previously reported in Figure 5.7 where ACBD3 was upregulated in the T47D-EveR cell line to a statistically significant level (2.13-fold increase, (**P* = 0.000236). At 1.33X10^4 cell/cm^2 there was no statistical difference in *ACBD3* expression between the cell lines (**P* = 0.554878). There was also no statistical

difference at 2.66X10^4 cell/cm^2 (*P = 0.060729) despite a 2.59-fold increase in mean *ACBD3* expression in the T47D-EveR cell line. *ACBD3* expression was downregulated 1.41-fold in the T47D-EveR cell line at 8X10^4 cell/cm^2 compared to the parental cell line, a small but statistically significant change (P = 0.000723).

5.3.13 *PI4Kβ* mRNA Expression

PI4Kβ mRNA expression was measured simultaneously to *ACBD3* expression in the T47D parental and T47D-EveR cell lines in the same samples with the same methodology (n=3). Expression of *PI4Kβ* in the T47D parental cell line seeded at 1.33X10^4 cell/cm^2 was only reliably detectable in one of the three biological replicates (RQ = 0.576, relative to the parental cells seeded at 2.66X10^4 cell/cm^2) and so was excluded. As stated in chapter 4 – 4.2.3, there are limitations to low level gene detection using SYBR green QPCR chemistry and linearity of amplification is lost resulting in high variance. All expression values were therefore given relative to *PI4Kβ* expression in the T47D parental cell line seeded at 2.66X10^4 cell/cm^2.

In the T47D parental line, *PI4Kβ* mRNA expression was highest in cells seeded at 2.66X10^4 cell/cm^2 (RQ = 1) and by comparison was lower to a statistically significant level when cells were seeded at 5.33X10^4 cell/cm^2 (RQ = 0.68, *P = 0.045865) and when seeded at 8X10^4 cell/cm^2 (RQ = 0.57, *P = 0.010594) (Figure 5.11). There was no significant difference in expression between cells seeded at 5.33X10^4 cell/cm^2 and 8X10^4 cell/cm^2.

In the T47D-EveR cell line, *PI4Kβ* mRNA expression was lowest at the lowest cell density (RQ = 0.22). Expression was comparatively higher at all other seeding densities to a statistically significant level (2.33X10^4 cell/cm^2 RQ = 1.07, 4.70-fold upregulated, *P = 0.027576; 5.33X10^4 cell/cm^2 RQ = 1.98, 8.73-fold upregulated *P < 0.00001; 8X10^4 cell/cm^2 RQ = 0.62, 2.75-fold upregulated, *P = 0.00811). *PI4Kβ* mRNA expression was not statistically different between T47D-EveR cells seeded at 2.66X10^4 cell/cm^2 and cells seeded at 5.33X10^4 cell/cm^2. There was a 3.17-fold difference in expression between cells seeded at 5.33X10^4 cell/cm^2 and cells seeded at 8X10^4 cell/cm^2 (*P = 0.000752).

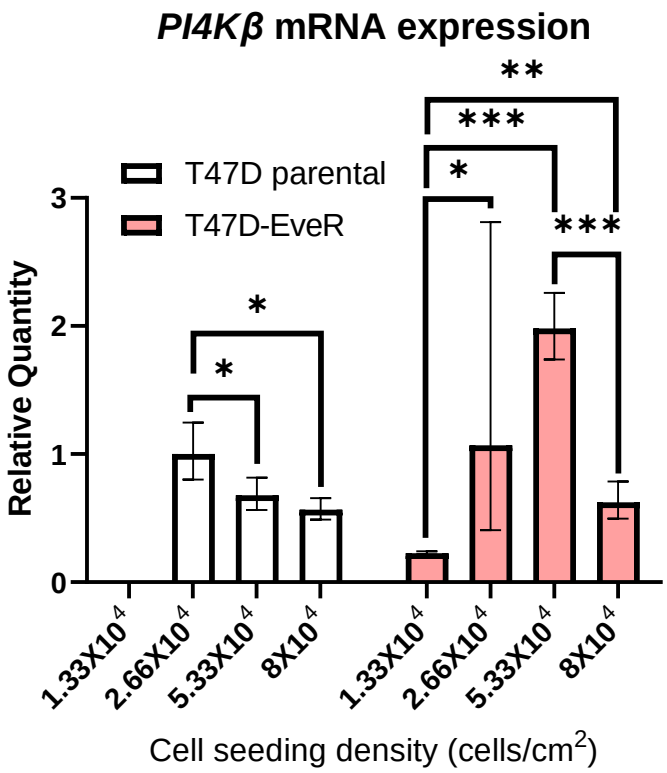

Figure 5.11 - *PI4Kβ* mRNA expression in the T47D parental and T47D-EveR cell lines when seeded at different densities. all values are relative to the T47D parental cell line seeded at 2.66X10^4 cell/cm^2, error bars represent the standard deviation, n=3 per condition and each biological replicate was assayed 3 times.

Overall, *PI4Kβ* mRNA expression in the T47D parental cell line trends downwards as cell density increases from 2.33X10^4 cell/cm^2 upwards. In the T47D-EveR line, *PI4Kβ* mRNA expression trends upwards as cell density increases to a maximum of 8.73-fold and then expression reduces at 8X10^4 cell/cm^2 down to a level that is intermediary compared to expression at 1.33X10^4 cell/cm^2 and 2.66X10^4 cell/cm^2 seeding densities.

Expression was not significantly different between cell lines at equivalent densities when seeded at 2.66X10^4 cell/cm^2 or at 8X10^4 cell/cm^2 but was statistically upregulated in the T47D-EveR cell line when seeded at 5.33X10^4 cell/cm^2 (*P = 0.000553). *ACBD3* mRNA expression was also statistically different between these two cell lines at 5.33X10^4 cell/cm^2 seeding density.

5.3.14 ACBD3 and PI4Kβ Protein Expression

The mRNA expression of *ACBD3* and *PI4Kβ* were found to be sensitive to cell seeding density which has implications for all cell line work that studies these genes. It was decided that any changes at the protein level should also be assessed as mRNA and protein levels do not always correlate and this was already found to be true of baseline ACBD3 and PI4Kβ expression (Chapter 4). T47D parental cells were seeded at the same cell density as in previous experiments (Figures 5.10 and 5.11) and incubated for 24 hours before being lysed for protein analysis by western blot.

There was no difference in ACBD3 expression in T47D cells seeded at different cell densities after 24 hours (Figure 5.12). This is in contrast to mRNA data where *ACBD3* expression increased 4 to 4.7-fold between $1.33X10^4$ and higher seeding densities (Figure 5.10).

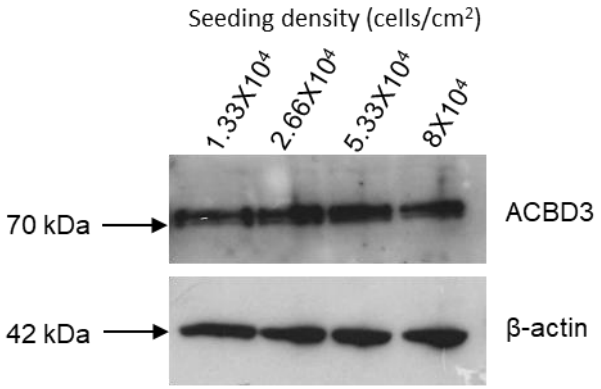

Figure 5.12 – ACBD3 protein expression in the T47D parental cell line when seeded at different densities did not change within 24 hours. ACBD3 did not change after 24 hours of seeding at different densities (5 minute exposure time), β-actin was stained as a loading control (10 second exposure time).

In a previous experiment looking at the effect of everolimus treatment on ACBD3 protein expression over time it was found that ACBD3 expression increased in the control group (Figure 5.9). Based on this it was hypothesised that ACBD3 protein expression does change depending on cell density but that 24 hours might not be enough time to see these changes. To test this, the T47D parental and T47D-EveR cell line were seeded at 100,000 cells in 6-well plates for a starting density of $1.042X10^4$ cells/cm^2 and lysates were collected every 24 hours for 96 hours total. In both cell lines ACBD3 protein expression increased over time which was inferred to

be due to increasing cell density (Figure 5.13). In the T47D parental cell line ACBD3 expression increased between 24 hours and 48 hours, and then decreased relative to 48 hours at 72 hours. In the T47D-EveR cell line ACBD3 protein expression increased between 24 hours and 48 hours and then did not substantially change for the rest of the time points.

PI4Kβ protein expression also increased over time in both cell lines. In the parental cell line PI4Kβ expression increased between 24 hours and 48 hours to its maximum level, then reduced to an intermediary level at 72 and 96 hours. In the T47D-EveR cell line PI4Kβ expression increased between 24 hours and 48 hours. Between 48 and 72 hours, samples had similar PI4Kβ expression and expression reduced to an intermediary level at 96 hours. ACBD3 protein expression and PI4Kβ protein expression were upregulated in the T47D-EveR cell line at all time points relative to the parental cells.

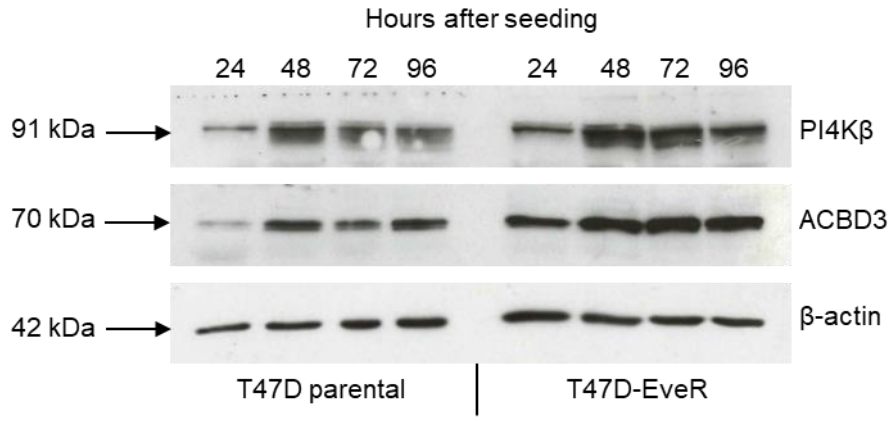

Figure 5.13 – ACBD3 and PI4KB protein expression changes over time starting at 1.042X10^4 cells/cm^2 cell seeding density. ACBD3 protein increased between 24 hours and 48 hours after seeding in the T47D parental cell line. PI4Kβ protein expression increased between 24 hours and 48 hours and then reduced slightly at 72 hours and 96 hours after seeding. PI4Kβ expression followed the same pattern of increase in the T47D-EveR cell line and expression was higher in the T47D-EveR cell line at all time points. ACBD3 expression increased between 24 hours and 48 hours in the T47D-EveR cell line and remained stable up to 96 hours post seeding, ACBD3 expression was higher in the T47D-EveR cell line at all time points. β-actin protein staining was used as a loading control in addition to cell counting before lysis. β-actin exposure = 10 seconds, ACBD3 exposure = 2 minutes, PI4Kβ exposure = 1 minute. Representative blot from n=2.

Cells for protein expression analysis were seeded at $1.33X10^4$ cells/cm^2 and then collected at 24-hour intervals. In order to make comparisons between mRNA and protein expression at equivalent densities, growth curves of the T47D parental and T47D-EveR cell lines were measured (Figure 5.14), the equation of the curve was calculated, and this was used to approximate the cell density at all time points in Figure 5.13. The doubling time for the T47D parental cell line was 37 hours, within the range of previously reported doubling times of 33 hours and 38.5 hours (Figure 5.14) (Finlay-Schultz, Jacobsen et al. 2020, Cailleau, Olivé et al. 1978). The doubling time for the T47D-EveR cell line was 31 hours, a higher growth rate than the parental line and faster than previous reports for this engineered cell line (Hare 2018).

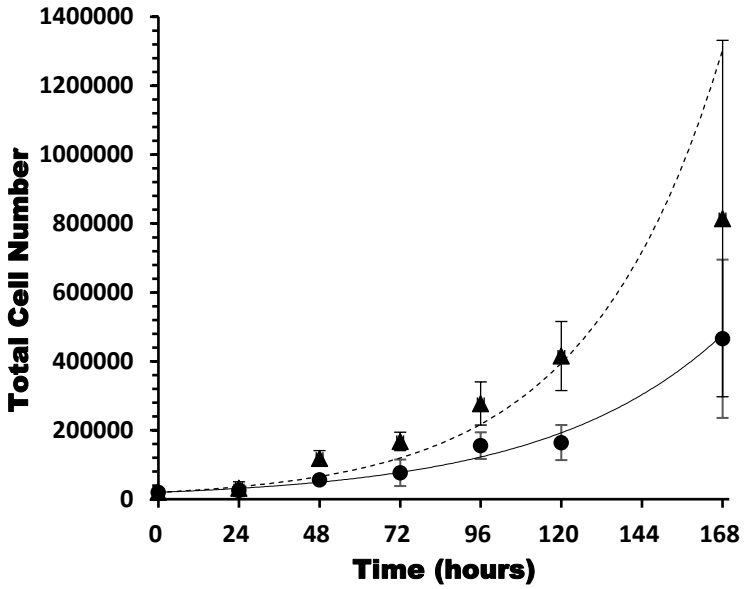

Figure 5.14 – Growth curves of the T47D parental (circle markers, solid trendline) and T47D-EveR (triangle markers, dotted trendline) cell lines over 7 days (168 hours) starting from 20,000 cells seeded in 9.6cm^2 wells. Cells were counted before seeding and then the cells of one well were detached and counted in triplicate for n=3 per day per cell line. Error bars represent the standard deviation. T47D parental growth curve equation y=20,000e(0.0189x), T47D-EveR growth curve equation y=20,000e(0.0249x).

The equation of the growth curve trendline in Figure 5.16 was used to calculate approximate cell number in protein samples of Figure 5.15. For example, the T47D-parental cells were seeded at 100,000 cells,

$$cell\ number = initial\ cells\ seeded \times e^{(0.0187 \times hours\ after\ seeding)}$$

= 100,000$e^{(0.0187*24)}$ = 156,643 cells.

The area of the well was 9.6cm^2 so the density after 24 hours = 156,643/9.6 = 1.63X10^4 cells/cm^2. This was repeated for other time points and for the T47D-EveR cell line using the equation of the growth curve for that cell line (Figure 5.16). The actual density for the mRNA data in Figure 5.12 and Figure 5.13 after 24 hours was also calculated and together these allow for comparison between the mRNA and protein level data. These densities are summarised in Table 5.1. Protein samples were collected every 24 hours from an initial fixed seeding density meaning that the difference in cell density between the T47D-EveR and T47D parental line increased over time.

Protein data (western blot)				
Time after seeding (hours)	24	48	72	96
T47D parental cell density	1.63X10^4	2.56X10^4	4X10^4	6.27X10^4
T47D-EveR cell density	1.78X10^4	3.05X10^4	5.22X10^4	8.94x10^4

Table 5.1 – Actual seeding density of samples at time of collection from results in Figure 5.13 based on growth rate calculated in Figure 5.14. The T47D-EveR cell line grows faster than the parental line causing a large difference in cell density between cell lines for protein level results 72 hours and 96 hours after seeding.

5.4 Discussion

The purpose of the work in this chapter was to determine potential regulators of ACBD3 expression in breast cancer cells based on the literatire and assess their suitability as a treatment. ACBD3 was found to be overexpressed in breast cancer cell lines in chapter 4 and high expression was found to confer to worse breast cancer patient outcomes, making ACBD3 a possible target for therapy. As ACBD3 does not have any enzymatic function to target, known regulators in other tissues and protein binding partners were targeted.

ACBD3 protein expression was upregulated in the MDA-MB-231 cell line following 179nM and 89.53μM Ferric Ammonium citrate treatment and 17.9nM treatment was found to increase relative cell number (RCN) in culture compared to controls. the effect of ferric ammonium citrate on cell number was normalised against ammonium citrate at equivalent molarity to deduce the effects of iron, iron was found to increase RCN at 100ng/ml, 500ng/ml, and 1000ng/ml and was not detrimental to RCN at any concentration.

The PI4Kβ inhibitor BQR695 did not consistently affect the protein expression of ACBD3 in the MDA-MB-231 cell line suggesting that PI4Kβ activity is not a regulator of ACBD3 protein expression. Inhibition of PI4Kβ was assayed as an inhibitor of MDA-MB-231 cell growth and treatment only resulted in a statistical reduction in cell number at 50μM and 100μM (555-fold and 1111-fold the reported IC50 respectively). Without data for the LD50 of BQR695 in any models it is not possible to say if these concentrations would be within physiologically tolerable limits and therefore a viable treatment option but these concentrations are very high and it is unlikely.

ACBD3 expression was upregulated at the mRNA and protein level in the T47D everolimus resistant cell line (T47D-EveR) compared to the parental T47D cell line from which it was derived. Everolimus treatment of the parental cell line did not affect ACBD3 mRNA or protein expression directly and it was hypothesised that ACBD3 could have a role in everolimus resistance. During these experiments it was found that there was some discrepancy in mRNA level results and that untreated control cells had increasing ACBD3 protein expression over time forming another hypothesis that ACBD3 expression may be dependent on cell density. It was found that mean *ACBD3* expression changed in the T47D cell line depending on seeding density, but this did not reach statistical significance. In the T47D-EveR cell line, *ACBD3* expression changed by a larger amount between different seeding densities and there was statistical significance between results. Overall, it was found that *ACBD3* expression increases from low to medium cell density (low density equivalent to 15% confluency, medium density equivalent to 30-70% confluency). ACBD3 expression then decreased at high density (equivalent to 85%+ confluency). Similarly, ACBD3 protein expression was found to increase over time from a fixed seeding density in the T47D parental and T47D-EveR cell lines and was higher in the T47D-EveR cell line at all equivalent time points.

PI4Kβ mRNA expression was also increased in the T47D-EveR cell line compared to parental cells and by a larger fold change than for ACBD3 expression. PI4Kβ protein expression increased following 72 hours of everolimus treatment but expression also increased in the untreated control cells at the same time point. Cell density also affected PI4Kβ expression at the mRNA and protein level. mRNA expression changes at different seeding densities followed a different pattern between the T47D parental and EveR cell lines, protein expression was approximately positively correlated with ACBD3 protein expression when measuring protein expression over time from a fixed seeding density.

5.4.1 Iron

Iron was an appealing choice to study as a regulator of ACBD3 protein expression as it is a naturally occurring product and a popular supplement that is well tolerated in the diet. Iron is an essential part of haemoglobin and women who are iron deficient are often anaemic. Iron deficiency is more common in women at approximately 30% of reproductive aged females compared to only 12.7% of men, and this percentage reduces for post-menopausal women (McLean, Cogswell et al. 2009, Wu, Y., Ye et al. 2020). Increased iron deficiency prevalence in reproductive aged women is thought to be related to menstruation, a regular loss of haemoglobin (Percy, Mansour et al. 2017). This means that iron deficiency is less common in the age group of women who are most likely to develop breast cancer (over 50) and it also means that iron levels are likely to be lower in young women, who are in turn more likely to develop breast cancers that are triple negative (Cancer Research UK 2017).

ACBD3 is directly involved in iron transport into the cell where it binds DMT1 iron transporter and the positive regulator Dexras1, and ACBD3 protein expression is downregulated by high levels of iron in the duodenum via negative feedback to maintain iron homeostasis (Okazaki, Ma et al. 2012, Okazaki, Glass 2017). There is no direct evidence for negative feedback in other tissues but ACBD3 is also required for iron import in the brain, even in the corpus striatum where the positive regulatory role of Dexras1 is replaced by Rhes but ACBD3 maintains its role (Cheah, Kim et al. 2006, Harrison 2012, Falk, Pierfrancesco et al. 1999, Sbodio, Paul et al. 2013). In Huntington's disease, ACBD3 protein is overexpressed in the corpus striatum and

iron levels are also dysregulated suggesting that ACBD3 is not negatively regulated by iron in the brain (Sbodio, Paul et al. 2013, Rosas, Chen et al. 2012). ACBD3 overexpression has been shown to increase iron import, and resultant redox stress may even form a positive feedback loop that exacerbates Huntington's disease (Rosas, Chen et al. 2012, Sbodio, Paul et al. 2013, Falk, Pierfrancesco et al. 1999). Any feedback loop that increases redox stress has implications in cancer as redox stress can cause inflammation which can promote a tumour microenvironment (Hanahan, Weinberg 2011). ACBD3 can also induce redox stress by promoting phosphorylation of VDAC1 at the mitochondria which prevents mitochondrial calcium import (Gatliff, East et al. 2017).

Isoforms of DMT1 are present in most tissues and it would be unexpected if ACBD3 did not have a similar role in other tissues and therefore be similarly regulated (Lis, Barone et al. 2004). It was unexpected then to find out that supplementing iron in cell culture medium actually increased ACBD3 protein expression at 1µg/ml and 500µg/ml iron concentration in the MDA-MB-231 cell line compared to no iron control (Figure 5.1). This means that intracellular iron is not negatively regulating ACBD3 in this breast cancer cell line. The breast cancer cells were extremely tolerant of iron supplementation and ferric ammonium citrate increased growth in cell culture up to 1.79µM (Figure 5.2). Whether this was an effect of the iron alone or the combination of iron and ammonium citrate is impossible to be certain of but there was no increase in RCN when cells were treated with ammonium citrate at equivalent molarity (Figure 5.2b). I would conclude from this that iron would be a poor therapeutic option for breast cancers based on this and certainly if ACBD3 has a role in breast cancer then iron does not target its action.

It should be noted that whilst the RPMI-1640 medium does not contain iron, the foetal bovine serum that it is supplemented with does contain iron. By adjusting for the approximate quantity of FBS already present, an adjusted distribution is produced. Iron in FBS is predominantly in the form of transferrin and may not be comparable to the iron chelated in ferric ammonium citrate. The iron levels of 12 commercial FBS serums were available, and it was found that iron levels are between 1.56 and 3.37µg/ml with a mean of 2.40 ± 0.63µg/ml which is equal to 0.043µM (Kakuta, Orino et al. 1997). Cell culture medium contained 5% FBS and would have a final concentration of 120ng/ml based on the mean average stated above. Concentrations of iron that had a statistically significant increase compared to

ammonium citrate only controls ranged from 100-1000ng/ml added iron and so total iron was closer to 220-1220ng/ml for these conditions.

5.4.2 PI4Kβ Inhibition

PI4Kβ has previously been found to have a role in breast cancer but treating MDA-MB-231 cells with the reported IC50 of a PI4Kβ specific inhibitor had no statistical effect on cell growth, it took a much larger dose of the treatment to cause significant cell number decrease (50-100μM). The 0nM treatment had large variance making it hard to perform statistical analysis against it. It is not known what the LD50 would be in humans or animals as there has been very limited study of this compound, but 50% cell viability (CC50) was found here to be between 50μM and 100μM in the MDA-MB-231 cell line. This is much higher than the reported IC50 which is sub-micromolar at 90nM and could result in many harmful off target effects if ever used at GI50 concentration in patients. It's possible that as a combined therapy that BQR695 could have a value in breast cancer treatment but would appear to be a poor candidate as a single treatment due to the high dose required to reach the GI50 in the MDA-MB-231 breast cancer cell line.

PI4Kβ activity is dependent on the presence of ACBD3 *in vitro*, and it was hypothesised that this relationship could be reciprocal with PI4Kβ activity affecting ACBD3 expression (Klima, Tóth et al. 2016). ACBD3 protein was upregulated in one of three samples of MDA-MB-231 cells treated with 180nM BQR695 compared to controls and there was no difference seen in cells treated with 900nM BQR695 compared to controls. A treatment-independent variance in ACBD3 expression was seen between samples in both the control and treated cells and this, and several other discrepancies in ACBD3 expression in repeated measures of breast cancer cell lines, led to studying ACBD3 expression in response to cell density.

5.4.3 Cell Density

Mean ACBD3 mRNA expression was different in the T47D cell line depending on cell seeding density but these differences fell just short of statistical significance. At the protein level there was a clear increase in ACBD3 between 24 and 48 hours after seeding followed by fluctuation between 48 and 96 hours after seeding. In a

T47D cell line with engineered everolimus resistance (T47D-EveR) there were much larger changes in ACBD3 mRNA expression and those changes did reach statistical significance at several seeding densities. Protein levels of ACBD3 in the T47D-EveR cell line also changed over time from a fixed initial seeding density where ACBD3 increased between 24 hours and 48 hours and then remained stable for the rest of the time course. From this it could be concluded that ACBD3 expression is dependent on cell density, especially in the T47D-EveR cell line and this same conclusion was previously made in a chronic myeloid leukaemia suspension cell line (Okazaki, Ma et al. 2012). Larger changes in this cell line may be because it was later found that the T47D-EveR cell line has a faster growth rate than the parental line (Figure 5.14) and so they reached a higher maximum density than the parental cells ($8X10^4$ cells/cm^2 condition for mRNA and 96 hours for protein, summarised in Table 5.2).

It is especially difficult to make conclusions about how cell density findings might be translated to a tumour environment. At the least, these results show that, when studying ACBD3 and PI4Kβ at both mRNA and protein level, cell density should be accounted for and ideally controlled for. If the time and resources were available then certainly this would have been repeated for all of the cell lines used in the thesis. All cell line mRNA data in chapter 4 were collected at sub confluency (70-80%) in order to measure cells in log growth phase and *ACBD3* mRNA expression was found to change least between medium confluency levels (30-65% confluency) in both the T47D parental and EveR cell lines. Further to this the T47D parental cell line did not show a significant decrease in ACBD3 expression at high seeding density.

Beyond the proof of a need for additional controls when studying ACBD3 and PI4Kβ in cell lines, changes in transcription with density could be related to other observations in the cell lines. It has been demonstrated that breast cancer cell lines have lower invasiveness at high cell densities, where matrix metalloproteinase (MMP) and tissue inhibitor of metalloproteinases (TIMP-1) are negatively regulated by Activator protein 1 (AP-1), NF Kappa B (nuclear factor kappa-light-chain-enhancer of activated B cells), and cAMP response element-binding protein (CRE), all transcription factors (Bachmeier, Vené et al. 2005, Bachmeier, Albini et al. 2005).

This presents cell density as a major mechanism of control for invasiveness and that cell density affects a range of cancer related pathways. Low cell density is mostly associated with expression of genes that facilitate more aggressive behaviour such as invasion, proliferation and activation or angiogenic pathways. Not

dissimilarly, I found in the T47D-EveR cell line that *ACBD3* expression was highest at the medium cell seeding densities and decreased at the highest density. *ACBD3* overexpression has previously been shown to increase mammosphere formation and activate Wnt signalling (Huang, Y., Yang et al. 2018). ACBD3 is also associated with cancer stem cell formation; these are cells that are generally slower growing and are not as invasive or proliferative as other cancer cells(Peitzsch, Tyutyunnykova et al. 2017). This also supports my observation that ACBD3 protein expression was lowest at the lowest cell densities. These less dense populations may have increased signalling of proliferative and invasive pathways whereas ACBD3 promotes a stem cell like side population phenotype that becomes more prevalent at higher cell densities.

5.4.4 The Everolimus Resistant T47D Cell Line

Whilst changes in ACBD3 expression varied between the T47D parental and everolimus resistant cell lines, ACBD3 expression was either higher or not different at the mRNA level in the T47D-EveR cells at all densities and higher at the protein level at all time points after seeding. Increased expression of ACBD3 suggested that it could have a role in promoting or maintaining everolimus resistance in these cells. Direct upregulation of *ACBD3* by everolimus treatment was ruled out by treating T47D cells with everolimus, but *PI4Kβ* expression was significantly upregulated following everolimus treatment in the same samples. This led to the hypothesis that ACBD3 upregulation might contribute to the everolimus resistance and this is explored in chapter 6. Work by a previous student who engineered the T47D-EveR cell line found that β-catenin protein was upregulated in that cell line (Hare 2018) combined with the knowledge that ACBD3 overexpression in breast cancer has been shown to increase β-catenin activity (Huang, Yang et al. 2018), provides a further possible link between ACBD3 and everolimus resistance in breast cancer.

There were also large changes in PI4Kβ expression found between cells seeded at different densities, and between the parental and everolimus resistant cell lines. *PI4Kβ* was expressed at a lower level in the T47D (parental) cell line relative to the normal like MCF12A cell line (Chapter 4 – Figure 4.4a); at the protein level, PI4Kβ was higher in the T47D cell line compared to the same control (Chapter 4 – Figure 4.6). The results for PI4Kβ expression in this chapter have not been

overlooked but instead there will be a larger discussion of the PI4Kβ findings throughout this thesis in the final discussion chapter (Chapter 7) to separate PI4Kβ results from the primary objective of characterising ACBD3 in breast cancer.

Chapter 6
ACBD3 Overexpression and Mutation in the T47D Breast Cancer Cell Line

6.1 Introduction

Previous chapters found *ACBD3* expression to be higher in breast cancer than other cancers and that expression was higher in breast cancer than normal breast tissue. ACBD3 was upregulated at the mRNA and protein level in seven breast cancer cell lines compared to a normal like control cell line. Ferric ammonium citrate/iron and cell density both altered expression of ACBD3, and ACBD3 was upregulated in an everolimus-resistant T47D breast cancer cell line.

Chapters 3 and 5 sought to determine how ACBD3 might be regulated in breast cancer and how its upregulation might be altered. New information about ACBD3 was found, but the small base of information available has made it difficult to expand those findings in the laboratory. Instead, it was decided that ACBD3 expression should be manipulated directly, using siRNA to downregulate ACBD3 or a vector to stably overexpress ACBD3.

ACBD3 knockdown by siRNA has been achieved several times, mostly in research concerning viral infection. The first publication to knockdown ACBD3 found that siRNA silencing prevented Aichi virus replication, and this was also the first publication to find that ACBD3 and PI4Kβ interact (Sasaki, Ishikawa et al. 2012). Subsequent papers on Aichi viruses had conflicting results with some finding that ACBD3 silencing did not supress virus replication, a criticism of these papers was that ACBD3 protein may not be fully knocked down and some residual ACBD3 protein expression can be seen on western blot figures in these papers (Dorobantu, Cristina M., van der Schaar et al. 2014, Dorobantu, C. M., Ford-Siltz et al. 2015). Ultimately, ACBD3 deletion by CRISPR-CAS9 found that complete deletion of ACBD3 prevents Aichi virus replication and incomplete knockdown of ACBD3 using siRNA is cited as an explanation for the previous conflicting results (Kim, H. S., Lee et al. 2018, Lyoo, van der Schaar, Hilde M. et al. 2019, Horova, Lyoo et al. 2019, Shin, Ku et al. 2021). It could be inferred that ACBD3 can still carry out its roles when expressed at low levels.

ACBD3 overexpression experiments have been conducted several times, including the overexpression of mutant constructs (Lyoo, van der Schaar, Hilde M. et al. 2019). The first ACBD3 overexpression experiment was carried out in HeLa cells using an eGFP-C3-ACBD3 vector and found that ACBD3 preferentially binds caspase generated fragments of Golgin-160 over the full-length protein (Sbodio, Hicks et al. 2006). Overexpression of ACBD3 also sensitized cells to apoptosis by staurosporine. Multiple subsequent publications where human ACBD3 was overexpressed used the construct created by Sbodio et al (Sbodio, Machamer 2007, Sbodio, Paul et al. 2013). The ACBD3 protein has also been mutated at various positions on the Q domain where single or combination substitutions of amino acids between 256 and 259 to alanine resulted in partial or full loss of PI4Kβ binding (Greninger, Knudsen et al. 2013, McPhail, Ottosen et al. 2017, Klima, Tóth et al. 2016). FQ258AA was the smallest substitution that led to complete loss of PI4Kβ binding (McPhail, Ottosen et al. 2017).

Mutation of the Acetyl-CoA binding domain (ACBD) of ACBD3 has not been published before and it is not certain which CoAs ACBD3 binds. Other members of the ACBD family (1-7) bind enoyl-CoA and parmityl-CoA, they have conserved residues in the domain associated with CoA binding and also conservation with the ACB domain of ACBP (Geisbrecht, Zhang et al. 1999, Soupene, Serikov et al. 2008).

Substitution mutations have also been engineered in the Golgi dynamics (GOLD) domain of ACBD3 which had no effect on PI4Kβ binding but LWR514AAA mutation caused greatly diminished ACBD3 Golgi localisation (Greninger, Knudsen et al. 2013, Horova, Lyoo et al. 2019). Chapter 3 (Figure 3.3b found one breast cancer patient where tumour ACBD3 contained a frame shift deletion (E348Nfs*21) resulting in a truncated ACBD3 protein missing the GOLD domain. The GOLD domain is responsible for ACBD3 localisation to the Golgi and for many ACBD3-Golgi-protein interactions including Golgin-160. ACBD3 is essential for proper Golgi formation, structure, and function and knockdown causes fragmentation of the Golgi in HeLa cells (Liao, J., Guan et al. 2019) (see Chapter 1 - 1.4 ACBD3 Roles at the Trans Golgi Network).

Chemotherapeutic drug efflux from the cell by efflux pump proteins, such as P-glycoprotein 1 are a major cause of chemoresistance in cancer and, as surface proteins, efflux pumps are processed by the Golgi apparatus (Molinari, Cianfriglia et al. 1994, Ughachukwu, Unekwe 2012, Nanayakkara, Vogel et al. 2019, Chintamani,

Singh et al. 2005). ACBD3 expression was found to be upregulated by a small but statistically significant amount in breast cancer patients that did not respond to some chemotherapies including anthracyclines (Chapter 3 – Figure 3.7). It is therefore possible that ACBD3 protein expression may influence the availability, or rate of production, of efflux pump proteins and therefore chemotherapy resistance.

In chapter 5 it was found that ACBD3 was upregulated in a T47D everolimus resistant cell line, but ACBD3 could not be induced by everolimus directly suggesting that ACBD3 upregulation could have a role in the everolimus resistance of these cells. This could be either by increasing Golgi size via a structural role, or by recruiting more Golgi associated protein to increase activity, to process or export surface proteins. Alternately ACBD3 might increase everolimus resistance by an as yet undetermined mechanism.

6.2 Chapter Aims

The aim of this chapter was to determine if ACBD3 upregulation was causative of everolimus resistance in the T47D-EveR cell line, and if so, were ACBD3 mutants able to elicit the same resistance. This was achieved by overexpression of ACBD3 in the parental T47D cell line. Further to this, other phenotypical changes were measured including growth rate and anoikis resistance when ACBD3 was overexpressed. As ACBD3 has many roles and is understudied, I sought to determine which oncogenic proteins, if any, underwent changes in expression when ACBD3 was overexpressed.

6.3 Results

6.3.1 *ACBD3* Knockdown

Prior to treating cells with ACBD3 siRNA, several transfection reagents were tested. DY-547 fluorescently labelled SiGLO was used to determine the effectiveness of Dharmafect formula 1 and Jetprime transfection reagents for transfecting the T47D and MDA-MB-231 cell lines. Transfection was carried out twice per well on consecutive days in both cases. It was found that SiGLO treatment with Dharmafect formula 1 produced more numerous fluorescent cells that also had a more fluorescent

appearance and therefore greater efficiency than SiGLO treatment with Jetprime (Figure 6.1).

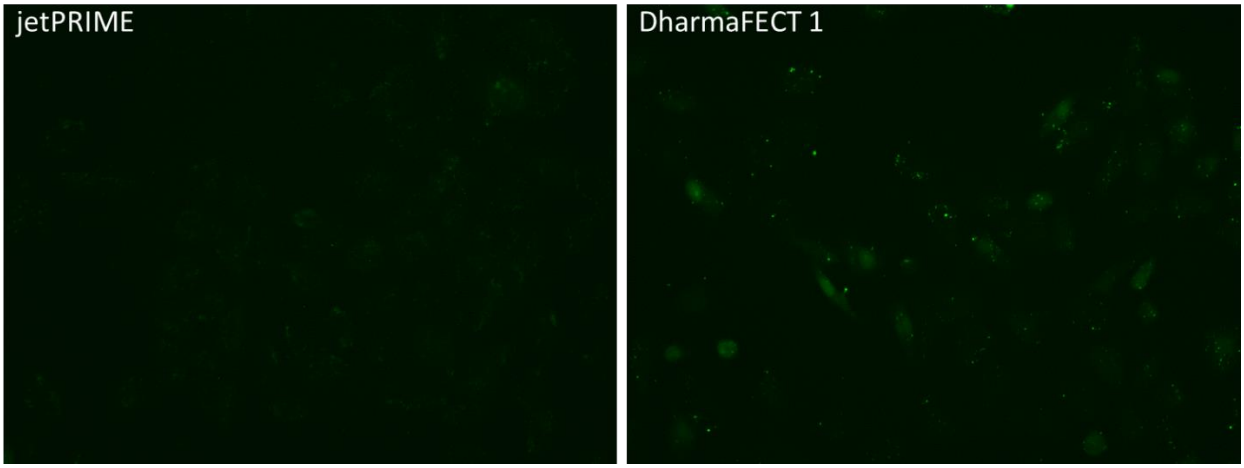

Figure 6.1 – Transfection of siGLO with DharmaFECT transfection reagent resulted in higher efficiency than transfection with jetPRIME. green fluorescence of MDA-MB-231 cells treated with siGLO fluorescent siRNA and either jetPRIME or DharmaFECT transfection reagents. Images captured with FLoid cell imaging station at 460X magnification and an excitation wavelength of 482/18, representative of n=2**.**

6.3.2 *ACBD3* Targeting siRNA Treatment

25nM *ACBD3* siRNA was not able to knockdown ACBD3 protein levels at 48 hours post transfection (Figure 6.2). PKCA siRNA was used as a positive control for the transfection and its inhibition by appropriate siRNA appeared to upregulate ACBD3 protein expression relative to untreated and transfection reagent only controls. in all siRNA assays, cells were treated twice at 24-hour intervals and cells were analysed 48 hours after the second treatment. ACBD3 expression varied between all cell conditions but was lowest in the transfection reagent-only and non-targeting siRNA conditions. There was also a large difference in ACBD3 expression between 2 independent pairs of untreated cells (lanes 1 and 2, 11 and 12, 2 biological replicates of 2 technical replicates each).

This experiment was repeated several times at 80nM *ACBD3* siRNA and 120nM siRNA without successful knockdown of ACBD3 protein (not shown, typical of results in Figure 6.2, with high variance in ACBD3 expression between conditions and between replicates). Ultimately attempts to downregulate ACBD3 were unsuccessful and instead work was focussed on overexpression and mutation of *ACBD3*.

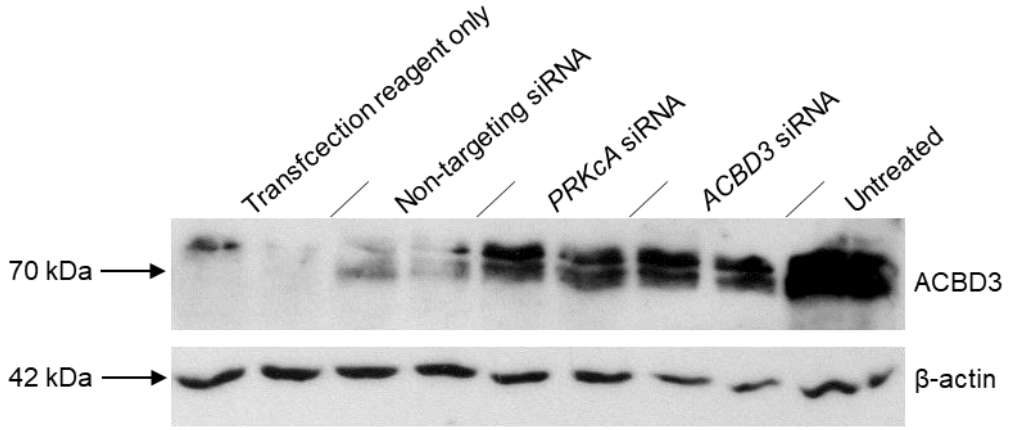

Figure 6.2 – 25nM ACBD3 targeting siRNA did not knockdown ACBD3 protein levels after 48 hours in the T47D breast cancer cell line. Each condition was assayed twice independently for n=2 (shown), all siRNA treatments at 25nM in medium. ACBD3 exposure time = 5 minutes, Beta actin was measured as a loading control (exposure time = 10 seconds).

6.3.3 Overexpression of ACBD3

ACBD3 protein was stably expressed in cell lines using a *pEGFP-C3 ACBD3* containing transfection vector. Appropriate concentration of the selection drug G418 was tested for the T47D parental and T47D-EveR cell lines using previous literature to inform initial trial concentrations. Cells were seeded at 50,000 per well in 6 well plates and treated with complete media and selection drug at various concentrations in duplicate for 14 days, media was changed every 3 days. After 14 days, all wells were checked for living cells and concentrations of G418 at or above 400µg/ml left no visible viable cells. Medium was then changed to complete medium with no selection agent and plates were incubated for a further 10 days to ensure no viable cells remained. The minimum concentration that killed all cells in 14 days was used as the selection concentration for stable transfection.

T47D parental and T47D everolimus resistant cell lines were transfected using lipofectamine 3000 reagent using the standard protocol in 24 well plates. After 48 hours, cell lines were checked for fluorescence and selection media was added. Controls included transfection reagent only, transfection with *pEGFP-C3* empty *vector*, and transfection with siGLO RNA. When cells appeared 80% confluent they were transferred into sequentially larger flasks. Recovery time for cells to grow at a

reasonable rate varied between cell line and between vectors but was generally 4 weeks.

Only the parental T47D cell line transfected with ACBD3 constructs was used for experimentation as maintaining everolimus resistance in the T47D-EveR cell line (100nM everolimus every third passage) in addition to transfection with *eGFP-C3-ACBD3* vector and maintenance with selection media added too many variables to experiments. The MDA-MB-361 cell line was also transfected with ACBD3 constructs but the cells failed to recover even up to six weeks post transfection. This was repeated with a larger starting number of MDA-MB-361 cells to transfect but these cells also failed to recover from the transfection and so could also not be used for experimentation. It appeared that these cells were dividing as evidenced by islands of cells that would reappear after dispersion by trypsin detachment but that cells were dying at approximately the same rate they were dividing. There was a previous attempt to create an everolimus resistant MDA-MB-361 cell line but these cells did not reach the same level of resistance as the T47D-EveR cell line (Hare 2018).

6.3.4 Characterising ACBD3 Overexpressing Cell Lines

Both the T47D parental and T47D-EveR cell lines were transfected with *pEGFP-C3 ACBD3* and both grew much slower initially than their non-transfected equivalents. Qualitatively, after 10 passages the T47D parental transfected cells grew almost as quickly as the non-transfected cells and T47D EveR transfected cells grew faster than the T47D-EveR non-transfected cell line. The T47D-EveR and T47D-EveR-ACBD3 cell lines were both treated with 100nM everolimus complete media every 3 passages to maintain resistance. The EveR-ACBD3 cells appeared to recover growth faster than the EveR cell line when transferred into complete medium without everolimus.

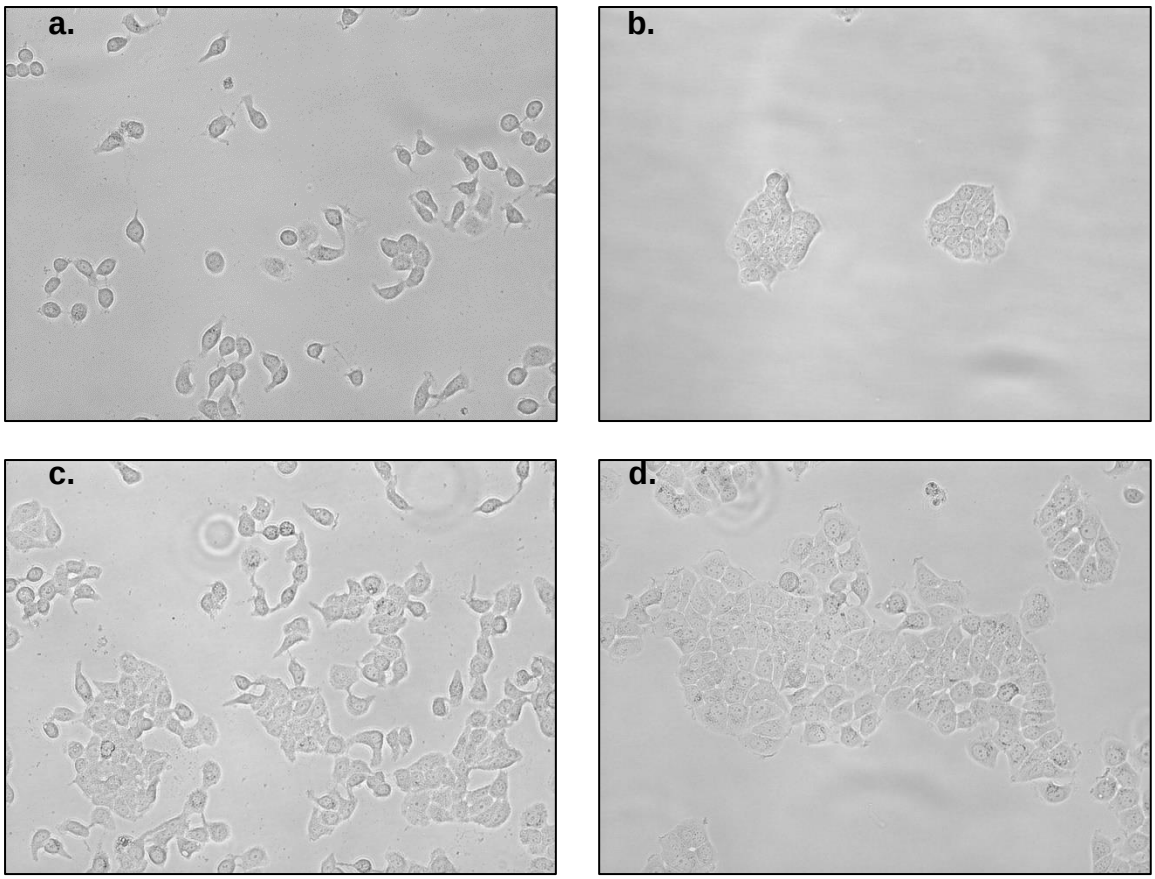

Figure 6.3 – Growth patterns of different T47D cell line variants change when stably transfected with eGFP-C3-ACBD3 vector and grown in complete media containing 400µg/ml G418 selection media. a) T47D parental cells. **b)** T47D-ACBD3 cells. **c)** T47D-EveR cells. **d)** T47D-EveR-ACBD3 cells. Transfection with ACBD3 caused cell lines to grow in larger tighter islands than their non-transfected equivalents. The T47D-EveR line grew in loose islands whereas the T47D parental cell line did not, ACBD3 overexpression caused T47D parental cells to grow in islands and T47D-EveR cells to grow in larger tighter islands.

The parental T47D cell line grows like many other typical breast cancer cell lines, cells are adherent and grow evenly across the plate and may form loose and very small islands of cells (Figure 6.3a). When transfected with *pEGFP-C3 ACBD3* and grown in selection media (G418 400µg/ml) cells formed small compact islands and were more strongly adherent taking several minutes longer to detach from flasks when using trypsin (Figure 6.3b). The everolimus resistant T47D cell line (T47D-EveR) grew somewhat evenly across the plate and formed loose small islands that are consistent with previous reports of this cell line (Figure 6.3c) (Hare 2018). When

transfected with ACBD3 and grown in selection media, the T47D-EveR cells grew in much larger islands of cells with lone cells being uncommon (Figure 6.3d).

The *pEGFP-C3-ACBD3* vector encodes ACBD3 with C-terminal conjugated green fluorescent protein meaning that the transfected ACBD3 protein fluoresces. The transfected cell lines had varying fluorescence and some cells fluoresced more than others suggesting that transfection efficiency varied. This may have relevance to findings that in 3D cell culture, ACBD3 overexpression led to side populations of cells (Huang, Y., Yang et al. 2018). If ACBD3 overexpression was causing T47D cells to form side populations of stem like cells they may be able to promote the growth of non-transfected cells or replace them in the selection media effectively creating a heterogeneous population of cells.

The *eGFP-C3* transfected T47D cells had a similar rate of growth to the T47D parental cells overall except at 168 hours where the mean cell number was less for the *eGFP-C3* transfected cells (262,222 cells) compared to the parental cells (465,556 cells) (Figure 6.4). The *eGFP-C3* had no mean increase in cell number between 120 hours and 168 hours but the high standard deviation of the *eGFP-C3* transfected cells at 168 hours meant that it was not statistically significantly different from the parental cells at the same time point (*P = .207656). *eGFP-C3* transfection was chosen as the control for relative cell number experiments where ACBD3 was overexpressed, and it was reassuring that empty vector transfection did not affect growth rate of the control cells relative to the parental cells. At the same time, the growth curve was not exactly the same between the parental cells and the eGFP-C3 transfected cells, highlighting the importance of an empty vector control as selection media could have an effect on cell growth.

Cell growth was increased in the *eGFP-C3-ACBD3* transfected cells compared to both the parental cells and the *eGFP-C3* transfected cell controls (Figure 6.4). The mean number of ACBD3 transfected cells was greater than the controls at all time points after seeding and was greater to a statistically significant degree at 168 hours (1,400,000 total cells for ACBD3 transfected cells, 262,222 total cells for control, *P = 0.008615).

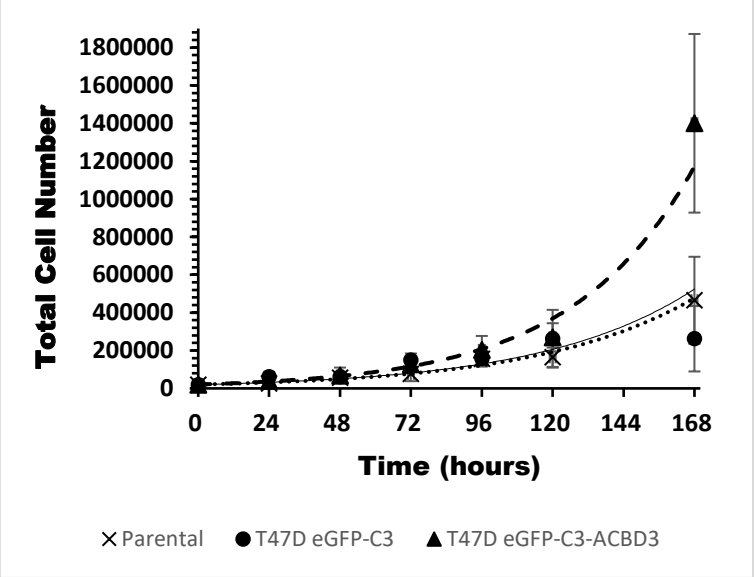

Figure 6.4 - Growth curves of: T47D parental cells (cross marker, dotted line), T47D *eGFP-C3* transfected cells (circle marker, solid line), and T47D *eGFP-ACBD3* transfected cells (triangle marker, dashed line) over 7 days (168 hours) starting from 20,000 cells seeded in 9.6cm^2 wells. Each time point was measured in 3 independent replicates (n=3),. Parental cell equation of trendline = $y=20000e^{0.0189x}$, *eGFP-C3* cells equation of trendline = $y=20000e^{0.0194x}$, *eGFP-C3-ACBD3* cells = $y=20000e^{0.0243x}$.

6.3.5 Mutation of Key ACBD3 Protein Interaction Sites

ACBD3 overexpression in cell lines is useful for modelling what happens when *ACBD3* is upregulated in cancer but tells us little about which ACBD3 functions play a role in any phenotypical changes. ACBD3 has an unusually diverse number of cellular functions and 3 distinct domains. I chose to mutate each domain using site directed mutagenesis (SDM) to prevent specific or general functions of ACBD3 and transfected mutants into cell lines as previously described. The ACBP domain was targeted based on literature for Acyl CoA inhibiting mutations in other ACB domain containing proteins (Kragelund, B. B., Andersen et al. 1993). This domain is highly conserved between ACBD protein family members, but it is not known how this domain is connected to ACBD3 function. Null mutation of this domain may lead to behaviour changes that give insight as to the function of ACB domain of ACBD3. If ACBD3 upregulation facilitates everolimus resistance then I would expect this mutant to rule in or out the role of the ACB domain in any resistance to everolimus.

The GOLD domain of ACBD3 contains several putative binding sites for other proteins but these are not all characterised, instead the GOLD domain contains many sites for Golgi interaction and because of this I decided to delete the entire domain and create a truncated ACBD3 protein missing the N-terminal 147 amino acids giving a weight of 43.5 kDa. A GOLD deletion mutant cannot bind Golgi but I would expect many of ACBD3s cytoplasmic roles and roles at the mitochondrial membrane to remain intact. Any behavioural differences between cells overexpressing the wildtype and cells expressing the truncated ACBD3 would therefore be down to the loss of ACBD3 at the Golgi and relative increase elsewhere. This may uncover which functions of ACBD3 are dependent on Golgi localisation and how delocalisation of ACBD3 effects breast cancer as deletion of this domain has previously been detected in 1 breast cancer tumour (Chapter 3 – Figure 3.3b).

Attempts were made to mutate the Q domain on residues F258 and Q259 to A and A based on previous literature showing that this abolishes interaction between ACBD3 and PI4Kβ (McPhail, Ottosen et al. 2017). Several revisions were made to the primer design and PCR procedure but a successful ACBD3 FQ258AA mutant could not be attained by the methodology.

6.3.6 Acyl-CoA Binding Domain Loss of Function Mutation ACBD3(KQ117AA)

As was discussed in the introduction, ACBD3 is part of the Acetyl CoA binding domain containing family of proteins but has not been shown to bind CoAs. To explore the role of the ACB domain in ACBD3, it was decided that the ACB domain should be mutated to inhibit speculative Acyl-CoA binding as based on its ACB domain structure; ACBD3 is predicted to bind palmitoyl-CoA (Fan, Liu et al. 2010). There are 5 possible amino acid targets to inhibit the ACB domain which is made up of 4 α-helices with conserved residues and motifs (Figure 6.5). Amino acids K117 and Q118 were chosen for mutation because they could both be mutated in one round of SDM PCR, were located on the second coil which is an inner coil of the domain that makes up an important part of the binding pocket, and are fully conserved between ACBP and ACBD3 (Figure 6.6) (Færgeman, Sigurskjold et al. 1996, Kragelund, Birthe B., Poulsen et al. 1999, Kragelund, Birthe B., Knudsen et al. 1999, Kragelund, B. B.,

Andersen et al. 1993). Mutating multiple essential residues made it more likely to achieve ACB functional inhibition.

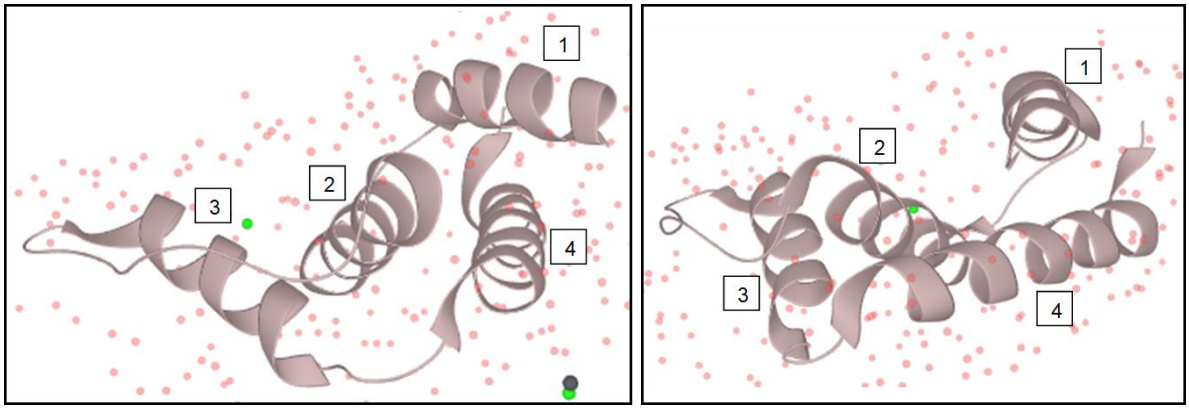

Figure 6.5 - Example ACB domain from ACBP shown from 2 different angles (90^{o} rotation) (https://www.uniprot.org/uniprot/P07108, adapted from (Taskinen, van Aalten et al. 2007). The ACB domain of ACBD3 is closely related to the ACB domain of ACBP shown above. There is no experimentally solved structure for the ACB domain whilst there is for ACBP. The ACB domain is made up of 4 coils (1-4) in both proteins and the residues that are required for function are well conserved between ACB domain containing proteins (Færgeman, Sigurskjold et al. 1996, Kragelund, Poulsen et al. 1999, Kragelund, Knudsen et al. 1999).

```
ACBD3       LEELYGLALRFFKEK---DGKAFHPTYEEKLKLVALHKQVLMGPYNPDTCPEVGFFDVLG 57
ACBP        ------SQAEFEKAAEEVRHLKTKPSDEEMLFIYGHYKQATVGDIN---TERPGMLDFTG 51
                  .* *          :*: ** * : . :**. :*  *     . *::*. *

ACBD3       NDRRREWAALGNMSKEDAMVEFVKLLNRCCHLFST  92
ACBP        KAKWDAWNELKGTSKEDAMKAYINKVEELKKKYGI  86
            : :   *  * . ******  ::: ::.  : :.
```

Figure 6.6 – Multiple sequence alignment between the ACB domains of ACBD3 and ACBP proteins. Asterisks represent conserved residues, colons represent highly similar residues, single dots represent weakly similar residues. The green arrows represent ACBD3 residues essential for speculative CoA binding (Kragelund, B. B., Andersen et al. 1993, Fan, Liu et al. 2010).

To engineer this mutant, 2 primers were created, primer 1 was created to be complementary to the sense strand with the centre of the primer over codons 117 and 118 (base 349-355 of the *ACBD3* transcript coding for lysine and glutamine) (Figure 6.7). The primer is non-complementary to codons 117 and 118 and instead contains the sequence CGCCG followed by the complementary base T. A second primer was designed to be fully complementary to the antisense strand binding immediately after primer 1 creating an origin of PCR.

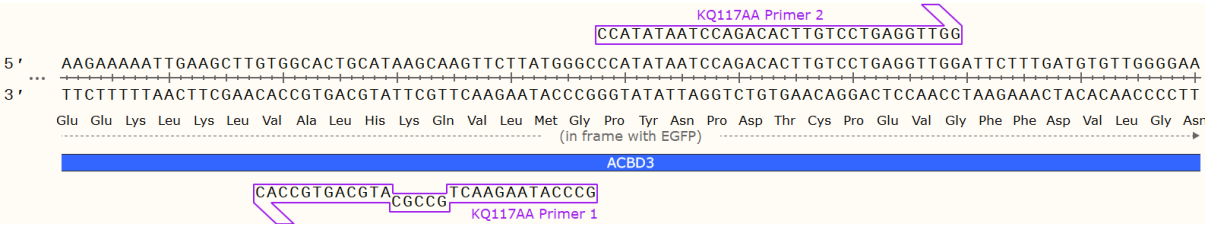

Figure 6.7 – Primer set to mutate *ACBD3* codons 117 and 118 (base pairs 349-355) from AAG (lysine) and CAA (glutamine) to GCG (alanine) and GCA (alanine) (created in snapgene). During PCR primers are extended on opposite strands of the pEGFP-C3-ACBD3 circular plasmid in opposite directions from a single point of origin. Note that primer 1 is the reverse complement and therefore the codons are inverted and complementary to the mutation being achieved.

During the first round of SDM PCR these primers are extended at the 3' end with a high-fidelity polymerase (Q5) causing amplification of the entire plasmid and introduces the CGCCG mutation from primer 1 to the newly synthesised linear antisense DNA strand. In subsequent PCR cycles an increasing amount of available template, in the form of linear PCR product with base changes from primer 1, was incorporated into these products and when primer 2 annealed to these products it was subsequently extended. As the antisense template strand has the desired mutation, this newly synthesised sense strand also contains the mutated sequence. In these products the very 5' end of the sense strand is complementary to primer 2 and the very 5' end of the antisense strand is complementary to primer 1 and from this point the reaction continues in the same way as a standard PCR. This causes all PCR product to contain the 117 and 118 codon changes from AAG CAA to GCG GCA.

a)

```
ACBD3wildtype       CAACTTATGAAGAAAAATTGAAGCTTGTGGCACTGCATAAGCAAGTTCTTATGGGCCCAT 370
ACBD3KQ117AA        CAACTTATGAAGAAAAATTGAAGCTTGTGGCACTGCATGCGGCAGTTCTTATGGGCCCAT 420
                    ************************************  *  ****************
```

b)

```
ACBD3wildtype       GEAAAGGAAEEARRLEQRWGFGLEELYGLALRFFKEKDGKAFHPTYEEKLKLVALHKQVL 120
ACBD3KQ117AA        GEAAAGGAAEEARRLEQRWGFGLEELYGLALRFFKEKDGKAFHPTYEEKLKLVALHAAVL 120
                    ************************************************************  **
```

Figure 6.8 – multiple sequence alignments of ACBD3 wildtype and mutated ACBD3-KQ117AA. a) DNA sequence and **b)** translated single letter amino acid sequence (Madeira, Park et al. 2019). Asterisks represent complementary alignment; the correct DNA mutations are confirmed here and no other mutations were introduced to the *ACBD3* transcript. The DNA mutations translate to the correct amino acid changes which were also aligned, in this case K117 and Q118 were each mutated to A (Gasteiger, Gattiker et al. 2003).

After PCR the linear products were treated with a kinase, ligase, DNase (KLD) mix to phosphorylate and subsequently blunt end clone the PCR product into a circular plasmid. The plasmid was grown in DH5α *E.Coli* and the template DNA is methylated, whilst DNA produced by PCR is not, the DNase only digests methylated DNA destroying the wildtype plasmid and leaving only the circularised mutant PCR product. Mutation in the plasmid was then confirmed by sanger sequencing using commercially available universal C3 plasmid primers (EGFP-C3 forward: 5' CATGGTCCTGCTGGAGTTCGTG 3', EGFP-C3 reverse: 5' GTTCAGGGGGAGGTGTG 3') that allow any DNA inserted into C3 multiple cloning site to be read from either end. The sequencing results were aligned with the wildtype sequence in the clustal omega tool confirm the mutation and to check that no other mutations had been introduced to the gene (Figure 6.8a) (Madeira, Park et al. 2019). The translated amino acid sequence (using the Expasy translate tool) was also aligned to ensure the right codon changes had been introduced (Figure 6.8b) (Gasteiger, Gattiker et al. 2003).

6.3.7 GOLD Domain Deletion – ACBD3(K381_R528*delins*XX)

It was decided that the GOLD domain should be deleted rather than mutated due to multiple protein-protein binding motifs and uncertainty around the roles of different sections of the domain. Making deletions using SDM differs from mutating

DNA, instead of using primers with non-complementary bases from a single point of origin, primers were designed to flank either side of the DNA sequence to be deleted. In this case transcription termination was required after codon 380 (coding for amino acid isoleucine) so a primer was designed that annealed the sense strand with additional noncomplementary bases that code for 2 stop codons (TAG TAA) (Figure 6.9).

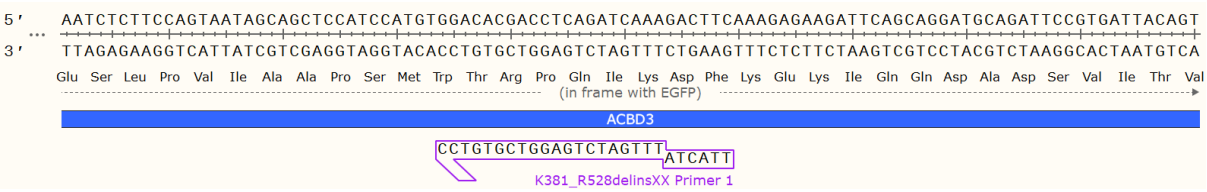

Figure 6.9 - Primer 1 to delete *ACBD3* codons 381 to 529 (base pairs 1144-1587) and bases downstream of the open reading frame and add ATC ATT complement to stop codons (XX).

The sequence of the full *pEGFP-C3-ACBD3* plasmid was not immediately available, so primer 2 was designed to be complementary to the plasmid sequence on the antisense strand after the KpnI restriction site of the multiple cloning site as it was previously reported that the *ACBD3* cDNA was inserted into the pEGFP-C3 plasmid using the SacI and KpnI endonucleases to engineer the *ACBD3* expressing vector (Figure 6.10) (Sbodio, Hicks et al. 2006).

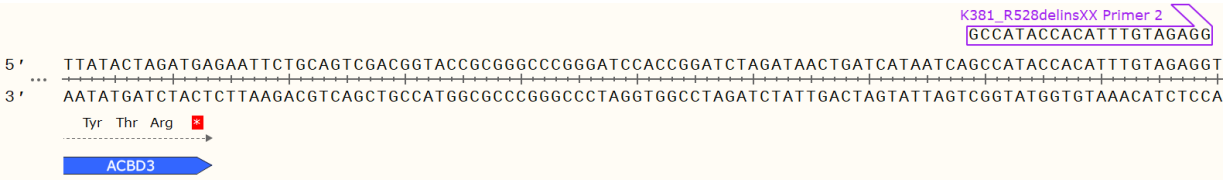

Figure 6.10 - Primer 2 to delete ACBD3 codons 381 to 529 (base pairs 1144-1587) and additional bases downstream of the ORF in the pEGFP-C3-ACBD3 plasmid (figure created in snapgene) After PCR and ligation, the 5' end of the sequence complementary to primer 1 and 5' end of the sequence complementary to primer 2 will be joined, removing the GOLD domain, the 5' end of primer 1 also adds 2 stop codons to terminate transcription at base pair 1143. The DNA sequence displayed is the pEGFP-C3-ACBD3 plasmid confirmed by sanger sequencing.

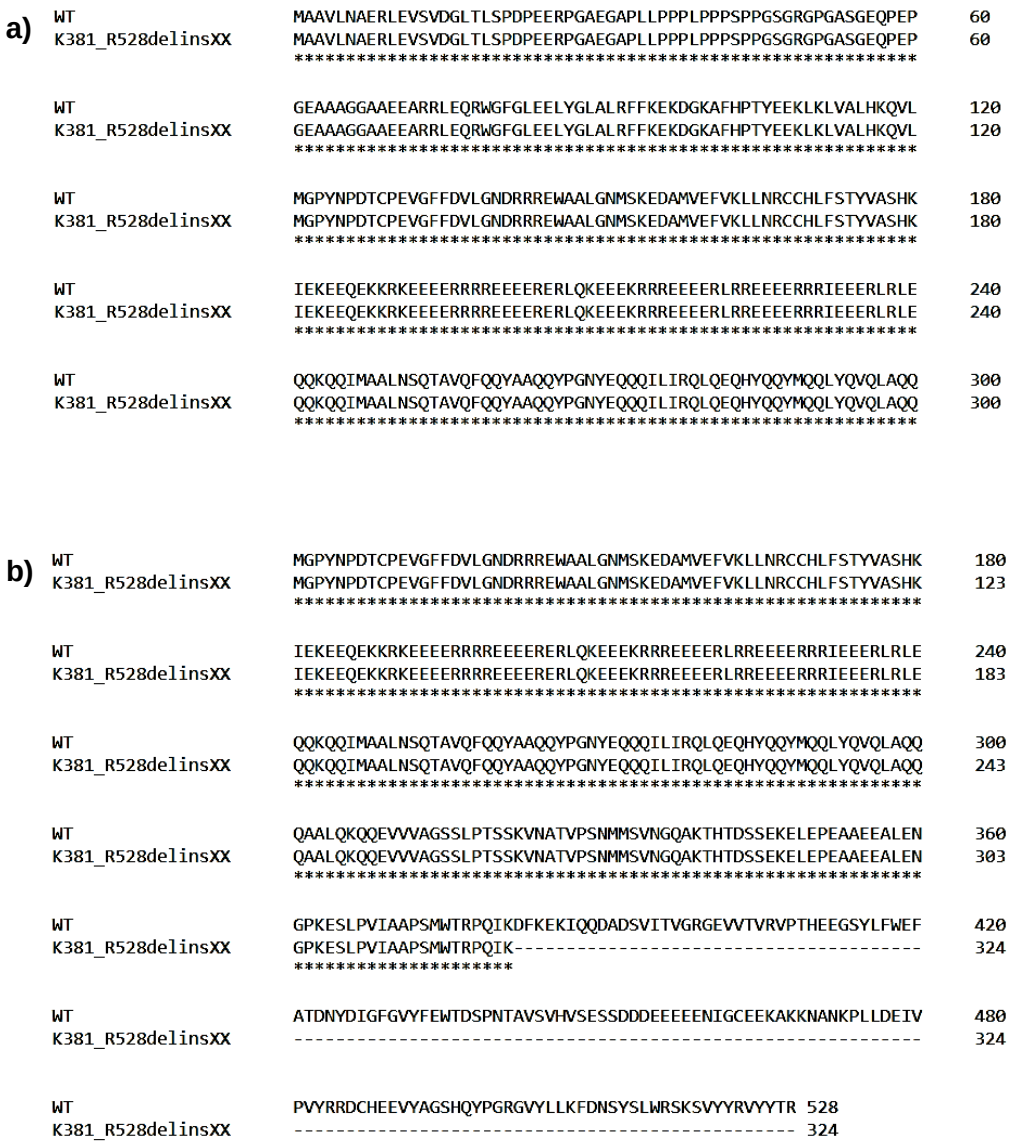

Figure 6.11 - Multiple sequence alignments of ACBD3 wildtype (WT) and mutated ACBD3-K381_R528delinsXX amino acid sequence. The mutated plasmid was sequenced, translated into amino acid sequence, and aligned. A) Forward read from the start of gene shows no base changes up to amino acid 300. B) reverse read shows no changes to sequence between amino acids 180 and 381. Codons 382 and 383 were successfully changed to stop codons. Sequence downstream of CBD3-K381_R528delinsXX termination matches the sequence of the C3 plasmid.

This primer pair and PCR program successfully deleted the GOLD domain without affecting other parts of the *ACBD3* sequence of DNA upstream or downstream of the insert (Figure 6.11). Subsequent sequencing of the wildtype and mutant C3 plasmids found that ACBD3 had been cloned into the vector differently than reported, most likely using XhoI and EcoRI restriction enzymes (Chapter 2 - Figure 2.1). Fortunately, the downstream sequence used to engineer K381_R528*delins*XX primer 2 anneals downstream of the EcoRI cut site so was still successful in creating a GOLD deletion mutant. The primers for all ACBD3 mutations are detailed in Table 6.1.

primer	sequence	Anneal temp
KQ117AA primer 1	5'- GCCCATAAGAACT **GC** C **GC** ATGCAGTGCCAC -3'	71°C
KQ117AA primer 2	5'- CCATATAATCCAGACACTTGTCCTGAGGTTGG -3'	
K381_R528*delins*XX primer 1	5'- **TTACTA** TTTGATCTGAGGTCGTGTCC -3'	56°C
K381_R528*delins*XX primer 2	5'- GCCATACCACATTTGTAGAGG -3'	

Table 6.1 – Primer pairs for creating *ACBD3* mutants. Green shaded and undelined bases signify a mismatch from the *ACBD3* wildtype DNA sequence and orange represents added bases. K381_R528*delins*XX primer 2 is the only primer that anneals downstream of the ACBD3 gene on the plasmid directly after the multiple cloning site.

6.3.8 Transfection Confirmation

Successful transfection of ACBD3 containing plasmids was confirmed by western blotting. Figure 6.12 is a western blot of T47D cell line lysates transfected with either eGFP-C3 or eGFP-C3 with one of the ACBD3 constructs (WT, KQ117AA, K381_R528delinsXX). The samples were taken one passage after the final experiment in this chapter to prove that expression of ACBD3 or ACBD3 mutant was maintained until the end of experimentation. Endogenous ACBD3 appeared to be upregulated in all ACBD3 transfected cell compared to the eGFP-C3 transfected cells (Figure 6.12a).

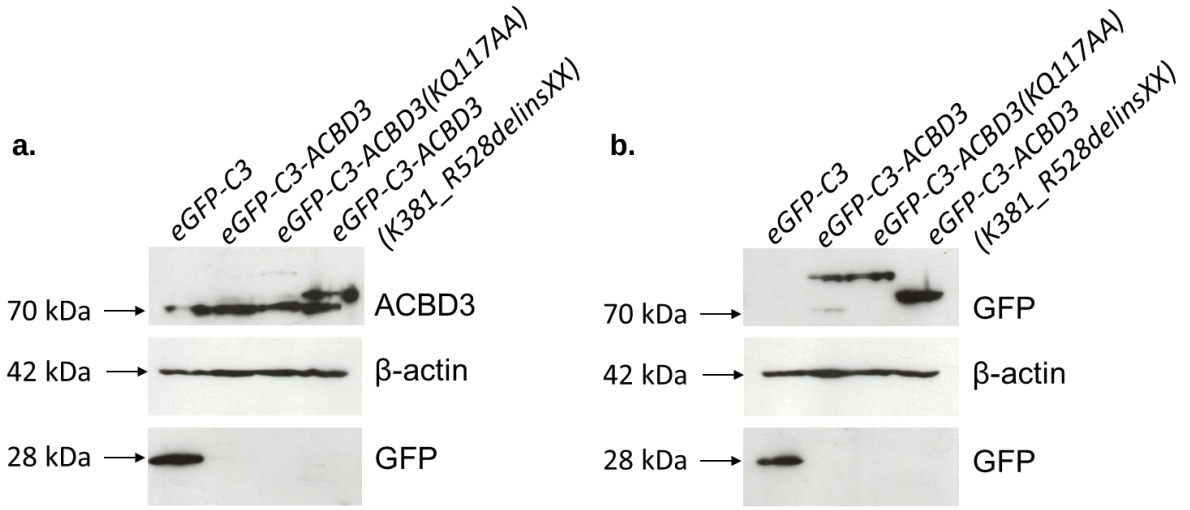

Figure 6.12 – T47D cells were successfully transfected with ACBD3 constructs and protein expression was maintained until the end of experimentation. Lysates of transfected T47D cells were taken one passage after the final experiment using these cells. each cell lysate was loaded in duplicate on one SDS-PAGE gel and stained for either ACBD3 or GFP in the 50-120 kDa size range. GFP staining was also carried out in the 0-35kDa size range. β-actin was used as a loading control in addition to cell counting immediately prior to lysis. **a)** unconjugated GFP (28kDa) was only detectable in T47D cells transfected with the *eGFP-C3* plasmid (lane 1). Endogenous ACBD3 (70kDa) was upregulated in *eGFP-C3-ACBD3*, *eGFP-C3-ACBD3(KQ117AA)* and *eGFP-C3-ACBD3(K381_R528delinsXX)* transfected cells (lanes 2 to 4) compared to *eGFP-C3* transfected cells (lane 1). GFP-ACBD3 and conjugate protein was not detectable by ACBD3 staining, the GFP-ACBD3(KQ117AA) protein was only weakly detected by ACBD3 antibosy and the GFP-ACBD3(K381_R528delinsXX) conjugate was readily detectable (lane 4, 75kDA). **b)** GFP-ACBD3 conjugate was detectable by GFP antibody for all ACBD3 constructs (lanes 2 to 4) and was of the expected size in all cases. As in Figure 6.11a, unconjugated GFP was only detectable in cells transfected with the *eGFP-C3* plasmid (lane 1). a and b were carried out as one blot (8 lanes), the uncropped blot is available in the appendix – Figure 9.2.

The ACBD3 antibody could not detect the GFP-ACBD3 and GFP-ACBD3(KQ117AA) conjugate protein was only weakly detected (Figure 6.12a, lanes two and three, top panel), ACBD3 antibody could detect the GFP-ACBD3(K381_R528delinsXX) protein (Figure 6.12a, lane four top panel) as visualised by the second higher weight band. Unconjugated GFP was only detected in the *eGFP-C3* transfected cells (Figure 6.12a, lane one, bottom panel) confirming that all the detected green fluorescence post transfection was due to GFP-ACBD3 protein in the ACBD3 transfected cells. ACBD3

is a loosely structured and flexible protein, it is possible the the GFP tap covers the antibody epitope in the wildtype and double point mutation mutant (KQ117AA) preventing detection by western blot. ACBD3(K381_R528delinsXX) has a much larger change (truncation by deletion of the GOLD domain) which may cause much larger structural change, allowing for exposure of the epitope sequence.

GFP staining in the expected size region of the GFP-ACBD3 conjugate protein produced bands of the expected size (ninety-eight kDa) for the GFP-ACBD3 wildtype (Figure 6.11b, lane two, top panel) and GFP-ACBD3(KQ117AA) (Figure 6.12b, lane three, top panel). The GFP-ACBD3(K381_R528delinsXX) has an expected molecular weight of 43.5 kDa as the protein is truncated with GOLD domain deleted and GFP tag added (71.5 kDa total). The wildtype ACBD3 protein consistently bands at approximately 8 kDa larger than expected on western blots so the expected band size for GFP-ACBD3(K381_R528delinsXX) was between 71.5 kDa and 79.5 kDa. GFP-ACBD3(K381_R528delinsXX) was detected by GFP antibody at approximately 75 kDa (Figure 6.12b, lane 4, top panel), this protein was also detected at the same size by the ACBD3 antibody in Figure 6.12a. This confirmed that GFP-ACBD3 was expressed at the protein level and that this expression was maintained until all experimentation was complete. Figure 6.12a also showed that endogenous ACBD3 expression was higher in the eGFP-ACBD3 (all constructs) transfected cells than in the eGFP only transfected cells.

PI4Kβ protein expression was compared between T47D cells transfected with different vectors. PI4Kβ protein expression was highest in the eGFP-C3-ACBD3 transfected cells, *eGFP-C3-ACBD3(KQ117AA)* and *eGFP-C3-ACBD3 (K381_R528delinsXX)* transfected cells also had higher PI4Kβ expression than the *eGFP-C3* transfected cells (Figure 6.13).

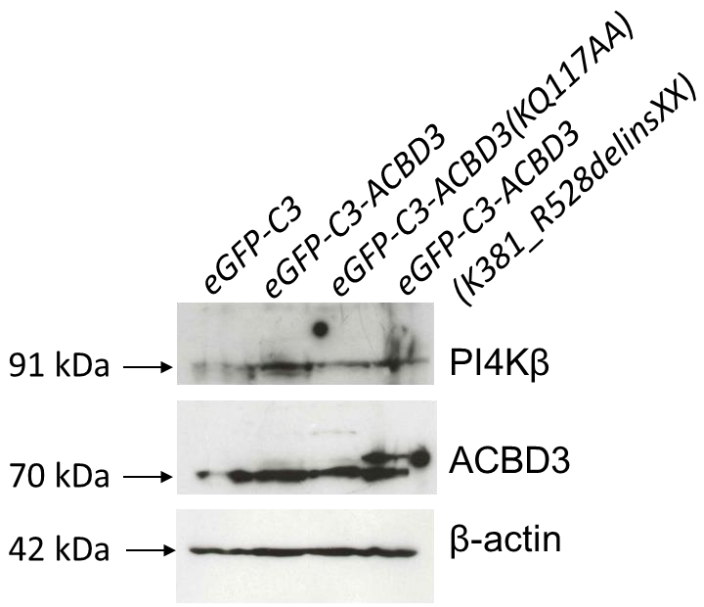

Figure 6.13 – PI4Kβ is upregulated in T47D overexpressing ACBD3, ACBD3(KQ117AA), or ACBD3(K381_R528del) protein relative to control. This western blot is the same as in Figure 6.12a with the addition of the PI4Kβ panel which was stained with anti PI4Kβ antibody.

6.3.9 Everolimus Resistance T47D Breast Cancer Cell Line Overexpressing ACBD3 or KQ117AA Mutant

ACBD3 was found to be upregulated at the mRNA level and protein level in the T47D everolimus cell line relative to the parental line (Chapter 5 – Figure 5.9, Figure 5.15). ACBD3 expression was not induced by everolimus treatment at the maintenance dose (100nM in medium) and so it was hypothesised that ACBD3 had a role in everolimus resistance. Everolimus tolerance was measured in the T47D parental, T47D *eGFP-C3*, T47D *eGFP*-C3-ACBD3, T47D eGFP-C3ACBD3(KQ117AA), and T47D-EveR cell lines by Sulforhodamine B (SRB) assay. Cells were treated with different concentrations of everolimus or DMSO only control for 72 hours and repeated 3 times independently for a total of n=3 with 6 technical replicates per condition per run. After 72 hours the cells were fixed and stained with SRB. Relative cell number (RCN) was calculated where the DMSO control mean optical density equalled one.

The T47D parental and T47D-EveR cell lines were first compared to corroborate the previous finding that the T47D-EveR cell line was everolimus resistant and had maintained that resistance (Hare 2018). The T47D-EveR cell line

was found to have higher relative cell number (RCN) at 0.1nM, 1nM, 10nM, and 1000nM everolimus treatment relative to the T47D parental cell line (*P = 0.018, 0.015, 0.02, 0.032 respectively) (Figure 6.14a). differences were smaller than previously reported but reached statistical significance. T47D cells transfected with *eGFP-C3* and the T47D parental cells had a very similar response to everolimus and RCN was not significantly different at any everolimus concentration. This provided evidence that *C3-eGFP* transfected cells were a good control for measuring resistance in other transfected T47D cells and that G418 selection media did not augment everolimus tolerance by measure of RCN.

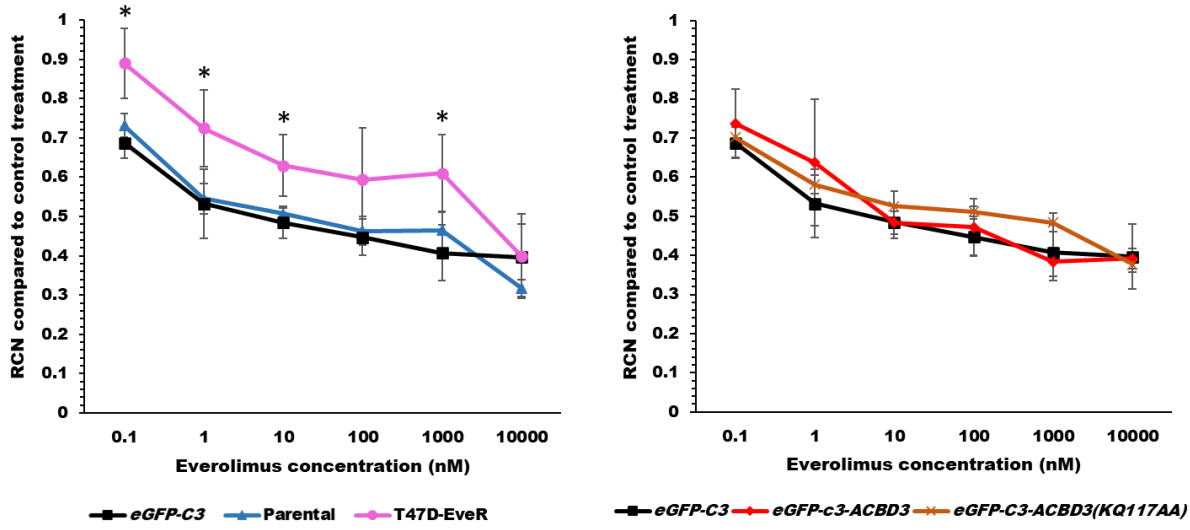

Figure 6.14 – The T47D-EveR cell line had increased everolimus resistance, T47D cells transfected with ACBD3 or ACBD3(KQ117AA) did not have increased everolimus resistance compared to controls. a) The T47D-EveR cell line had a higher relative cell number (RCN) after 72-hour everolimus treatment compared to the T47D parental cell line at 0.1nM, 1nM, 10nM, and 1000nM treatment. There was no significant difference between the T47D parental cells and cells transfected with *eGFP-C3*. **b)** T47D parental cells transfected with *eGFP-C3-ACBD3* or *eGFP-C3-ACBD3(KQ117aa)* had no increased resistance to everolimus compared to control cells transfected with *eGFP-C3* at any concentration. Cells transfected with *eGFP-C3-ACBD3(KQ117aa)* had a statistically higher RCN than cells transfected with *eGFP-C3-ACBD3* at 1000nM everolimus treatment (*P = 0.006879). error bars represent the standard deviation.

T47D cells transfected with *eGFP-C3-ACBD3* or *eGFP-C3-KQ117AA* did not have any additional resistance to everolimus compared to cells transfected with

eGFP-C3 control at any concentration of everolimus treatment (Figure 6.14b). increasing concentrations of everolimus resulted in decreasing RCN and no concentration of everolimus increased cell number. There was a statistically significant difference between *eGFP-C3-ACBD3* and *eGFP-C3-KQ117AA* transfected cells at 1000nM everolimus treatment (0.384 RCN and 0.484 RCN respectively, **P* = 0.006879).

6.3.10 Anoikis resistance in ACBD3 overexpressing T47D cells

The purpose of this thesis has been to further characterise ACBD3, uncover regulators or expression and determine why ACBD3 has a negative effect on breast cancer outcomes. ACBD3 overexpression has been associated with cancer stem cell maintenance, which is associated with recurrence, and worse prognosis for breast cancer patients (Huang, Y., Yang et al. 2018, Peitzsch, Tyutyunnykova et al. 2017). Metastasis, where cancer cells can break through the basal lamina of their immediate environment and overcome anoikis to move to distant sites in the body, accounts for the most cancer deaths. A role for ACBD3 in escaping the immediate environment could explain why its overexpression is associated with worse patient prognosis.

Anoikis is a form of programmed cell death when cells lose adhesion (*in vivo* this is loss of adhesion to the extracellular membrane) (Frisch, Francis 1994, Kim, Y. N., Koo et al. 2012). The ability of T47D cells to resist anoikis when transfected with vectors encoding ACBD3 or ACBD3 mutants was measured by coating culture plates with poly-2-hydroxyethyl methacrylate (polyHEMA) to prevent adhesion. After 24 hours cells were stained with trypan blue and counted to assess viability.

T47D cells transfected with *eGFP-C3-ACBD3* had 18% less resistance to anoikis than control cells transfected with *eGFP-C3* and this reached statistical significance (**P* = 0.020437) (Figure 6.15). *eGFP-C3-ACBD3(KQ117AA)* and *eGFP-C3-ACBD3 (K381_R528delinsXX)* transfected cells also had decreased anoikis resistance compared to controls (12% decrease, **P* = 0.002776 and 18% decrease **P* = 0.004062 respectively).

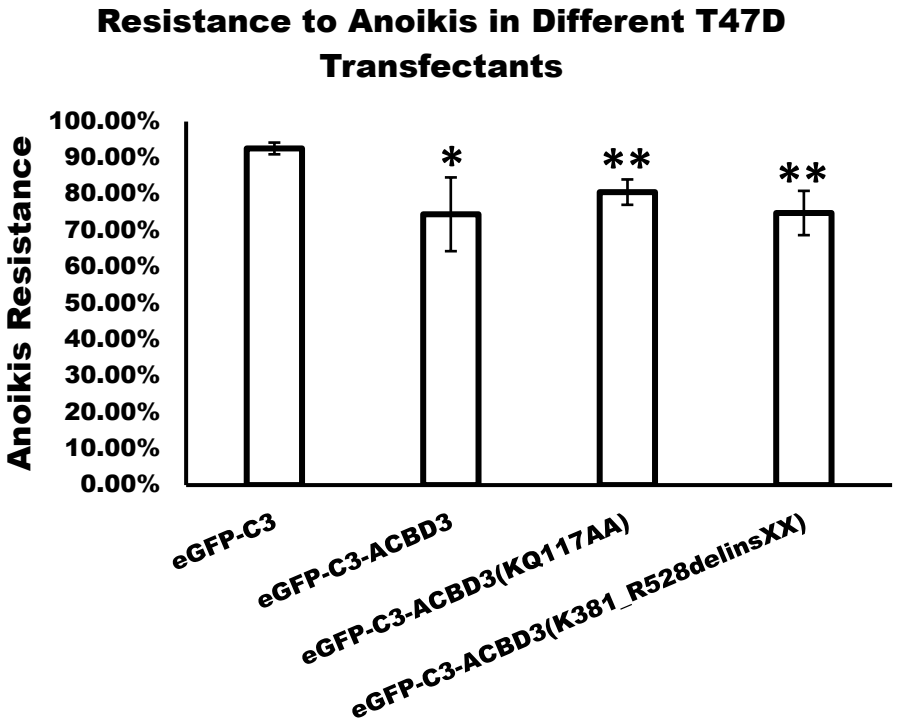

Figure 6.15 – T47D cells transfected with wildtype *ACBD3* or *ACBD3* mutants have less anoikis resistance than T47D cells transfected with an empty vector control. After 24 hours incubation in suspension culture, there was a small but statistically significant decrease in anoikis resistance for cells transfected with: *eGFP-C3-ACBD3* (74.49%, **P* = 0.020437), *eGFP-C3-ACBD3(KQ117AA)* (80.58%, **P* = 0.002776) *eGFP-C3-ACBD3 (K381_R528delinsXX)* (74.84%, **P* = 0.004062) compared to control cells transfected with *eGFP-C3* (92.6%). Anoikis was measured in 3 biological replicates per condition (n=3), error bars represent the standard deviation.

6.3.11 Oncogenic protein Expression Changes in the ACBD3 Overexpressing T47D Breast Cancer Cell Line

Overexpression of ACBD3 did not lead to increased everolimus resistance but led to decreased anoikis resistance (Figures 6.14 and 6.15). To probe the effect of ACBD3 expression, an array to determine the relative expression of a series of onco-proteins was performed on ACBD3 and ACBD3(K381_R528del) overexpressing T47D cells relative to an empty vector control (Figure 6.16). Proteins that had at least a 2-fold change in expression in the ACBD3 and/or ACBD3(K381_R528del) overexpressing cells are briefly described. Proteins with at least a 1.5-fold change in expression are summarised in Table 6.2 and 6.3

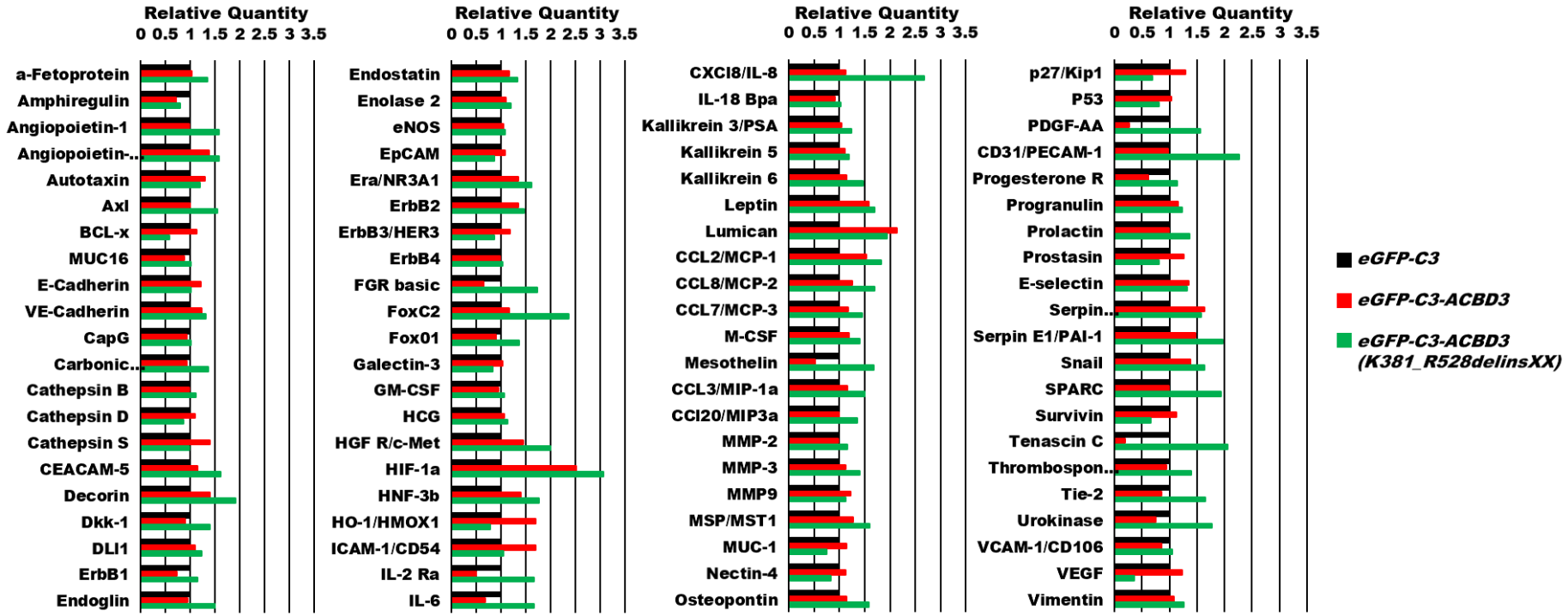

Figure 6.16 – comparison of oncoprotein expression in T47D cells overexpressing ACBD3 or ACBD3(K381_R528delinsXX) relative to an empty vector control. A human oncology array of 84 oncoproteins was performed and array spots were analysed with ImageJ software to determine pixel density. Control spots were used to normalise total loading between different arrays and the pixel density of the control (T47D cells transfected with *eGFP-C3*) for each protein was reported as 1 and pixel density was then reported for T47D cells transfected with *eGFP-C3-ACBD3* or green for T47D cells transfected with *eGFP-C3-ACBD3(K381_R528delinsXX)* relative to the controls. The relative amount of protein expression is represented in red for T47D cells transfected with *eGFP-C3-ACBD3* and green for T47D cells transfected with *eGFP-C3-ACBD3(K381_R528delinsXX)*. Each sample was measured in duplicate with a mean average taken, n=1. Proteins with fold changes larger than 1.5 are detailed in Table 6.2 for ACBD3 overexpressing cells and Table 6.3 for ACBD3(K381_R528del) overexpressing cell

Protein	Fold change	Protein	Fold change
HIF-1a	2.53-fold increase	Lumican	2.13-fold increase
FGR basic	1.52-fold decrease	MCP-1	1.52-fold increase
HO-1	1.71-fold increase	Mesothelin	1.95-fold decrease
c-MET	1.45-fold increase	PDGF-AA	3.82-fold decrease
ICAM-1	1.7 fold decrease	Progesterone Receptor	1.63-fold decrease
IL-2 Ra	2.02-fold decrease	Serpin B5	1.63-fold increase
IL-6	1.47-fold decrease	Tenascin C	5.13-fold decrease
Leptin	1.59-fold increase		

Table 6.2 – Oncogenic proteins that had at least a 1.5-fold change in expression in ACBD3 overexpressing T47D cells relative to control. Fold changes of 1.95 or more are highlighted in green for increases and red for decreases.

Hypoxia inducible factor 1-α was 2.53-fold upregulated in the ACBD3 overexpressing T47D cell line and 3.07-fold upregulated in the ACBD3(K381_R528del) expressing cell line. It is a member of the bHLH-PAS super family of proteins and contains a basic helix-loop-helix that binds DNA and PER-ARNT-SIM domain (Scheuermann, Yang et al. 2007). This domain allows for hetero-dimerization with HIF-1b which subsequently allows its activity as a transcription factor (Dengler, Galbraith et al. 2014).

Interleukin-2 receptor α (IL-2 Ra, also known as CD25) was 2.02-fold downregulated in the ACBD3 overexpressing cells. IL-2 Ra expression is associated with node invasion and worse prognosis for breast cancer patients (Kuhn, Dou 2005).

Lumican is an extracellular matrix protein and was found to be 2.13-fold upregulated in ACBD3 overexpressing cells and 1.95-fold upregulated in ACBD3(K381_R528del) expressing cells.

Mesothelin is a cell surface glycoprotein associated with immunogenicity and was 1.95-fold downregulated in ACBD3 overexpressing cells (Zhenjiang, Rao et al. 2017). Mesothelin was 1.67-fold upregulated in the ACBD3(K381_R528del) expressing cells.

Platelet derived growth factor-AA (PDGF-AA) is decreased by pro inflammatory cytokines and was 3.82-fold downregulated in ACBD3 overexpressing cells (Kose, Xie et al. 1996). It was 1.67-fold upregulated in ACBD3(K381_R528del) expressing cells.

Tenascin C was 5.13-fold downregulated in ACBD3 overexpressing cells and 2.06-fold upregulated in the ACBD3(K381_R528del) overexpressing cells.

Protein	**Fold change**	**Protein**	**Fold change**
Angiopoietin-1	1.58-fold increase	Lumican	1.95-fold increase
Angiopoietin-like 4	1.58-fold increase	MCP-1	1.83-fold increase
Axl	1.54-fold increase	MCP-2	1.69-fold increase
BCL-x	1.75-fold decrease	Mesothelin	1.67-fold increase
CEACAM-5	1.62-fold increase	MST1	1.60-fold increase
Decorin	1.90-fold increase	Osteopontin	1.58-fold increase
Endoglin	1.50-fold increase	PDGF-AA	1.56-fold increase
ERα	1.62-fold increase	PECAM-1	2.27-fold increase
FGR basic	1.73-fold increase	Serpin B5	1.57-fold increase
Fox C2	2.37-fold increase	Serpin E1	1.97-fold increase
c-Met	2.01-fold increase	Snail	1.64-fold increase
HIF1a	3.07-fold increase	SPARC	1.93-fold increase
Fox A2	1.78-fold increase	Survivin	1.51-fold decrease
IL-2 Ra	1.67-fold increase	Tenascin C	2.06-fold increase
IL-6	1.67-fold increase	Tie-2	1.65-fold increase
IL-8	2.68-fold increase	Urokinase	1.77-fold increase
Leptin	1.69-fold increase	VEGF	2.82-fold decrease

Table 6.3 – oncogenic proteins that had at least a 1.5-fold change in expression in ACBD3(K381_R528del) overexpressing T47D cells relative to control. Fold changes of 1.95 or more are highlighted in green for increased and red for decreases.

Foxhead Box C2 (FoxC2) protein was 2.37-fold upregulated in the ACBD3(K381_R528del) overexpressing cells. FOXC2 is a transcription factor that may have a role in the development of mesenchymal tissues (Hollier, Tinnirello et al. 2013).

c-MET (Hepatocyte growth factor receptor) is a tyrosine kinase receptor that is expressed in epithelial cells and was 2.01-fold upregulated in ACBD3(K381_R528del)-overexpressing cells. In cancer it promotes angiogenesis and has been found to be deregulated in breast cancer (You, McDonald 2008, Chaudhary, Choudhary et al. 2020).

Interleukin-8 (CXLCl8/IL-8) is expressed by macrophages and epithelial cells. IL-8 can induce chemotaxis (cell movement) and angiogenesis and is associated with cellular inflammation and oxidant stress (Bickel 1993, Heidemann, Ogawa et al. 2003). It was 2.68-fold upregulated in ACBD3(K381_R528del) overexpressing cells.

Platelet endothelial cell adhesion molecule (PECAM-1) was 2.27-fold upregulated in ACBD3(K381_R528del) overexpressing cells.

Plasminogen activator inhibitor-1 (SERPIN E1) is a serine protease inhibitor that inhibits Plasmin formation and matrix metalloproteinases, ultimately inhibiting fibrinolysis or extracellular membrane breakdown (Lee, E., Vaughan et al. 1996, Flevaris, Vaughan 2017). It was 1.97-fold upregulated in ACBD3(K381_R528del) overexpressing cells.

Vascular endothelial growth factor (VEGF) was 2.82 fold downregulated in ACBD3(K381_R528del) overexpressing cells. VEGF promotes angiogenesis and high expression is associated with poor prognosis in breast cancer (Liu, Y., Tamimi et al. 2011, Shibuya 2011). NUMB prevents VEGF degradation (van Lessen, Nakayama et al. 2015).

6.4 Discussion

ACBD3 was previously found to be upregulated in the everolimus resistant T47D cell line and it was hypothesised that this upregulation may contribute to the resistance. To determine if this was the case, ACBD3 was overexpressed in the T47D cell line and several mutant constructs of ACBD3 were also engineered. As well as everolimus resistance, cells overexpressing ACBD3 were also assayed for growth

rate, anoikis resistance, and changes in oncoprotein expression to determine if ACBD3 might have other, currently unexplored, roles in breast cancer.

PI4Kβ was overexpressed in all the ACBD3 transfects relative to the empty vector control. A mutant to abolish ACBD3-PI4Kβ interactions was unsuccessful so the effect of a non PI4Kβ binding ACBD3 mutant could not be determined. The Acyl-CoA binding inhibiting mutant (KQ117AA) expressing cells had less PI4Kβ protein expression than WT or K381-R528del ACBD3 expressing cells.

ACBD3 overexpression did not increase everolimus resistance in the T47D cell line relative to the empty vector (*eGFP-C3*) control and neither did the ACB domain mutant (KQ117AA). KQ117AA and WT ACBD3 overexpressing cells had significantly different RCN at 1000nM everolimus treatment. Mean RCN was not very different from other concentrations, but smaller errors (measured by standard deviation) meant that the results reached a statistical significance (*P = 0.006879). The WT ACBD3 overexpressing line performed the worst out of all lines assayed at 10,000nM everolimus treatment, but this did not reach statistical significance relative to any other cell line treated with the same concentration. The empty vector control and parental cells had a very similar response to everolimus treatment proving that the empty vector cells were a good control for this experiment and that the vector and the G418 selection drug did not affect everolimus tolerance.

ACBD3 monoclonal antibodies failed to stain for GFP-ACBD3 but did stain the endogenous wildtype ACBD3. Conjugated GFP may cover the epitope in the introduced ACBD3. GFP-ACBD3(K381_R528del) could be detected by both ACBD3 and GFP antibodies. ACBD3 containing C3 vector was different than expected based on previous reports. Based on the position of ACBD3 within the multiple cloning site, it was almost certainly spliced in using XhoI and EcoRI restriction enzymes as opposed to the Kpn1 and SacI enzyme previously reported (Sbodio, Hicks et al. 2006). It is possible that multiple constructs were made by the group.

6.4.1 ACBD3 Overexpression

MDA-MB-361 cells transfected with WT ACBD3, or any of the ACBD3 mutants failed to recover even 8 weeks post transfection. The C3 empty vector transfected cells also had a slow growth rate but grew noticeably faster than the ACBD3 transfects. Unfortunately, A large enough cell number to perform cell growth assays

was never reached. MDA-MB-361 cells also reached a lower maximum everolimus resistance in the work that established the T47D-EveR cell line (Hare 2018).

Everolimus resistance was maintained from previous reports although the difference between T47D-EveR and T47D parental cells everolimus was smaller (this still reached statistical significance at 0.1nM, 1nM, 10nM, and 1000nM treatment. It was not disclosed whether the T47D-EveR cells were assayed for resistance one or two passages after maintenance treatment with 100nM everolimus, all tolerance experiments in this work were performed 2 passages after the maintenance treatment which may be the source of reported resistance differences.

ACBD3 overexpression did not increase cell number at any concentration of everolimus treatment relative to cell transfected with an empty vector control. Expression of the ACBD3(KQ117AA) mutant in the same cell line also resulted in no increased resistance to everolimus. The ACBD3(K381_R528) (GOLD deletion mutant) was not ready at the time of the SRB assays and performing the assay separately and later for these cells would have introduced too many sources of error. As WT ACBD3 and Acyl-CoA binding mutant ACBD3 did not affect everolimus resistance, it is unlikely that the truncated form of ACBD3 would result in any increase in tolerance.

Based on this, the hypothesis that ACBD3 is causative of everolimus resistance must be rejected. ACBD3 may still have a role in everolimus resistance in the T47D-EveR cell line, or may be a marker of other changes that are causative. Another possible candidate for the mechanism or resistance is PI4Kβ which was also upregulated at the mRNA level (Chapter 5 – Figure 5.7) and protein level (Chapter 5 – Figure 5.13) in the T47D-EveR cell line, and mRNA expression was induced by everolimus treatment (Chapter 5 – Figure 5.8).

ACBD3 overexpression also resulted in cells that grew in tighter islands much like the phenotypical change seen in the T47D cells when they were engineered to be everolimus resistant (Hare 2018). ACBD3 transfection of T47D-EveR cells was qualitatively observed to recover growth after everolimus maintenance treatment more quickly suggesting either less inhibition of growth or less lag time in growth after media change. Whilst ACBD3 could not affect everolimus resistance, it may be a consequence of resistance or contribute to some other feature of the resistant cell line.

6.4.2 Oncogenic Protein Expression Changes

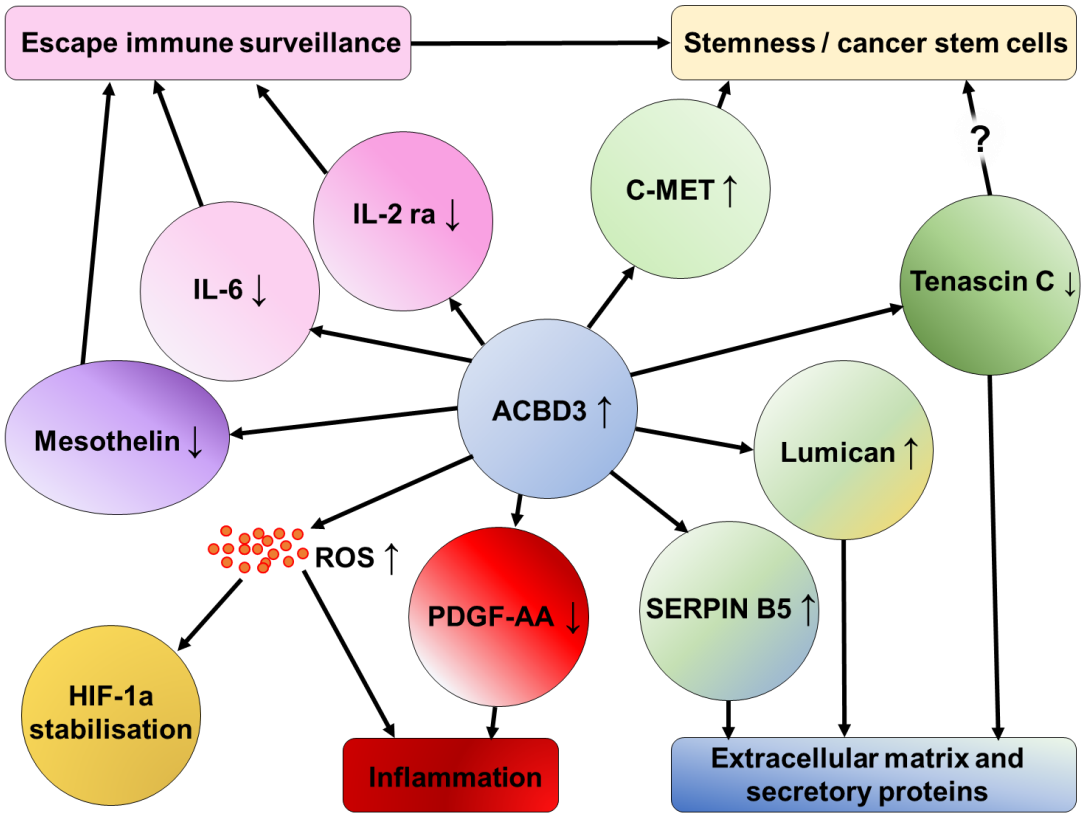

Figure 6.17 – Network analysis of protein level changes in the T47D breast cancer cell line when ACBD3 was overexpressed. Arrows next to proteins show upregulation or downregulation in response to ACBD3 upregulation. The way in which these expression changes may alter breast cancer cells is then given in shaded boxes. The roles of these proteins and how their differential expression might affect breast cancer cells is detailed below. ROS = reactive oxygen species.

ACBD3 expression was previously correlated with increased cancer stem cells and cancer stem cells effectively avoid the immune system for years after cancer treatments (Huang, Y., Yang et al. 2018). Mesothelin is a cell surface glycoprotein associated with immunogenicity and was downregulated in ACBD3 overexpressing cells at approximately half the level of control cells. ACBD3 overexpression also resulted in down regulation of CD54/ICAM1and IL6 (1.7-fold and 1.47-fold respectively), in addition to previously described IL-2, presenting an argument that ACBD3 overexpression reduces the immunogenicity of breast cancer cells, an important characteristic of CSCs which must evade the immune system.

Tenascin C was 5.1-fold downregulated in ACBD3 overexpressing cells and 2.1-fold upregulated in the ACBD3(K381_R528del) expressing cells. Tenascin C is a glycoprotein expressed in the extracellular matrix and in neurodevelopment promotes differentiation of cells (Wiese, Karus et al. 2012, Guo, M., Jan et al. 1996, Verdi, Schmandt et al. 1996). Tenascin C positively regulates NOTCH and enhances expression of LGR5, a target of Wnt (Oskarsson, Acharyya et al. 2011). ACBD3 is known to inhibit NOTCH signalling during mitosis in embryonic development giving it an opposing action. If ACBD3 promotes stemness in cancer in the same way that it does in neurogenesis then positive regulators of NOTCH (such as Tenascin C) may need to be downregulated. The ACBD3(K381_R528del) mutant cannot bind the Golgi and therefore mimics cytosolic mitotic ACBD3. It is not therefore surprising to find that a positive regulator of NOTCH signalling has very different protein expression between control cells, cells overexpressing ACBD3, and cells expressing ACBD3(K381_R528del). ACBD3 overexpression was also previously reported to affect the beta-catenin/Wnt signalling pathway (Huang, Y., Yang et al. 2018).

Snail (SNAI1) was 1.64-fold upregulated when ACBD3(K381_R528del) was expressed. SNAI1 is promoted by Wnt signalling and represses E-Cadherin to regulate EMT. c-MET was 2.07-fold increased when ACBD3(K381_R528del) was expressed. c-MET is usually only expressed by stem cells and progenitor cells, ACBD3 maintains stem cell pools by a signalling role it can perform during mitosis when the Golgi breaks down releasing ACBD3 into the cytosol. The ACBD3(K381_R528del) protein is lacking a Golgi dynamics (GOLD) domain and is therefore constitutively found in the cytosol and this may allow it to signal for stemness factors to a higher level than wildtype ACBD3. c-MET was upregulated to a lesser extent when ACBD3 was overexpressed (1.5-fold).

Many of the oncogenic proteins that had 2-fold change or more in expression when wildtype ACBD3 was overexpressed were immunogenic proteins and/or involved in inflammation. There were also several changes to proteins that regulate the extracellular membrane or angiogenesis. These changes support a role for ACBD3 in both stemness (decreased detection by immune system and ability to migrate) and as a marker of progression as inflammation promotes a cancer microenvironment and angiogenesis is essential for tumour growth beyond the scale of millimetres (Hanahan, Weinberg 2011).

HIF1a is a transcription factor and master regulator of hypoxia response. HIF1a expression predicts poor response to primary chemotherapy in breast cancer (Generali, Berruti et al. 2006). Reactive oxygen species stabilise HIF-1a and lead to its accumulation (Quintero, Brennan et al. 2006, Bonello, Zähringer et al. 2007) and in hepatocellular carcinoma HIF-1a promoted EMT and this was enhanced by Wnt/B-catenin (Zhang, Q., Bai et al. 2013). ACBD3 overexpression has been shown to increase Wnt/B-catenin and its overexpression may confer an advantage when HIF-1a is upregulated as HIF-1a enhances EMT. ACBD3 is also involved in redox stress and the related increased in reactive oxygen species (ROS) might stabilise HIF-1a (Gatliff, East et al. 2017, Liu, J., Rone et al. 2006, Shoshan-Barmatz, Krelin et al. 2018). Increased ROS may account for the increased HIF1a protein levels in ACBD3 overexpressing T47D cells. The ACBD3(K381_R528del) overexpressing cells had even higher levels of HIF-1a protein expression. This mutant form of ACBD3 cannot bind to the Golgi but ACBD3 mediates redox stress at the mitochondria by interaction with TSPO (Gatliff, East et al. 2017). The mechanism by which ACBD3 binds TSPO is not known but ACBD3 contains a C-terminal proline rich domain that is typical of protein-protein interaction sites and this domain is intact in the ACBD3(K381_R528del) mutant. The inability of ACBD3(K381_R528del) to be retained by the Golgi would also mean more protein is available to make interactions at the mitochondria.

HIF1a is associated with PR negativity in breast cancer (Gruber, Greiner et al. 2004, Laughner, Taghavi et al. 2001, Xu, Zhou et al. 2017), ACBD3 protein expression was significantly higher in PR- breast cancer patient samples compared to PR+++ patients (Chapter 4, Figure 4.10b), and ACBD3 was found to interact with the PR co-chaperone UNC45A (Chapter 3 – Figure 3.8). ACBD3 may negatively regulate the progesterone receptor and may regulate HIF-1a directly or via regulation of PR. Progesterone receptor expression was 1.63-fold less when ACBD3 was overexpressed (Table 6.2). HIF1a promotes metastasis in breast cancer and whilst ACBD3 expression has been reported to increase with more advanced cancer stage, the finding was not corroborated by ACBD3 immunohistochemical staining of patient samples (Huang, Y., Yang et al. 2018, Liu, Z. J., Semenza et al. 2015).

Interleukin-2 receptor α (IL-2) is associated with node invasion in breast cancer and was downregulated in T47D cells when ACBD3 was overexpressed (García-Tuñón, Ricote et al. 2003). ACBD3 expression was not different between primary

breast cancer and lymph node breast cancer patient samples, and it is not surprising that ACBD3 expression does not upregulate proteins associated with invasiveness (Chapter 4, Figure 4.10a). Conversely, in cells expressing ACBD3(K381_R528del) IL-2 was 1.67-fold upregulated compared to controls (3.69-fold upregulated compared to wildtype ACBD3 overexpressing cells) suggesting that downregulation of IL-2 may be linked to ACBD3 Golgi function as IL-2ra is post-translationally processed by the Golgi.

Overall ACBD3 appeared to increase inflammatory potential and simultaneously decreased proteins associated with immunogenicity. Several proteins associated with CSCs also underwent changes in expression supporting evidence that ACBD3 promotes CSC formation. Other proteins with expression changes were involved in Wnt signalling which was the proposed mechanism by which ACBD3 promotes CSC formation (Huang, Y., Yang et al. 2018). Whilst ACBD3 overexpression did not increase resistance to everolimus, it did cause cells to grow faster, suggesting it could be a proliferative marker. The oncoarray findings support the previously suggested role for ACBD3 as an activator of Wnt signalling and further found proteins related to stemness were altered when ACBD3 was overexpressed. Since the first publication concerning ACBD3 and breast cancer, I have hypothesised that ACBD3 had a role beyond Wnt signalling so to find other cancer related pathways what have protein level changes when ACBD3 was overexpressed has been validating. The implications of these protein level changes and how they might fit in with results from other chapters are commented on further in Chapter 7 – Discussion.

Chapter 7

Discussion

7.1 Key Findings

78% of female breast cancer patients survive for over ten years meaning that breast cancer has one of the best prognoses of all cancers, but new treatments are in decline and triple negative breast cancer patients have fewer therapy options with little improvement in patient outcomes for decades (Won, Spruck 2020). Breast cancer incidence in the UK is increasing for females; it currently causes over 11,000 deaths per year in the UK and without improved treatment there will be more deaths per year in the future (Cancer Research UK 2017). Understanding of breast cancer development and progression is better defined than most cancers with several receptors known to play key roles, several alleles known to be risk factors, and many oncoproteins known to drive the disease (National Institute for Health and Care Excellence 2017, Filippini, Vega 2013, Ngeow, Sesock et al. 2017, Ciriello, Gatza et al. 2015, Ross-Innes, Stark et al. 2012, Papa, Pezzino et al. 1990, Chi, Singhal et al. 2019, Rostoker, Abelson et al. 2015, Lamb, Vanzulli et al. 2019, Deshmukh, Srivastava et al. 2019). The picture however is not complete and there may be many more factors and roles left to uncover that have differing degrees of importance in breast cancer progression and therefore treatment. Targeted treatments are essential for increasing efficacy of chemotherapies whilst simultaneously reducing off target effects and are the focus of a whole generation of drug development in cancer and elsewhere.

This work sought to determine whether ACBD3 expression affected breast cancer cell behaviour. Through broad research using breast cancer cell lines and breast cancer patient data I can conclude that *ACBD3* tumour expression did have an effect on breast cancer patient outcomes with high *ACBD3* mRNA expression correlating with worse outcomes. ACBD3 mRNA and protein expression were higher in breast cancer cell lines compared to a normal like breast cell control and ACBD3 protein expression was highest in oestrogen receptor positive (ER+) cell lines. This suggested ACBD3 as a marker of poor prognosis and of ER positivity. Novel

transcriptional effectors of ACBD3 were found that further suggest ACBD3 expression as a marker of ER reprogramming and differential signalling.

ACBD3 was upregulated in an everolimus resistant cell line and it was hypothesised that ACBD3 facilitated this chemotherapeutic resistance. ACBD3 overexpression in a naïve cell line did not result in increased resistance to everolimus, but the ACBD3 overexpressing cells did undergo phenotypical changes as well as fold level changes in expression of oncoproteins involved in extracellular matrix, immune presentation, inflammation and angiogenesis. From this it was hypothesised that high ACBD3 expression may promote tumorigenesis through increased inflammation and reduced immunogenicity of cells.

Iron is one of few known regulators of ACBD3, but this has only been observed in duodenum cells of rats (Okazaki, Ma et al. 2012). Iron treatment of breast cancer cells was found to increase ACBD3 protein expression, the opposite of what was expected. Increased intracellular iron can increase redox stress, and ACBD3 also contributes to redox stress by participating in a complex with PKA to prevent calcium export from the mitochondria by VDAC1 (Li, H., Degenhardt et al. 2001, Gatliff, East et al. 2017, Shoshan-Barmatz, Krelin et al. 2018). ACBD3 facilitated iron import and subsequent ACBD3 upregulation in breast cells may form a positive feedback loop of escalating redox stress and inflammation in addition to the ACBD3 role in mitochondrial redox stress. The rationale for an ACBD3-iron redox causing feedback loop is supported by Huntington's disease research and these findings support the hypothesis that ACBD3 promotes tumorigenesis by increasing inflammation (Rosas, Chen et al. 2012, Baiamonte, Lee et al. 2013, Sbodio, Paul et al. 2013).

Phosphatidylinositol 4-kinase beta (PI4Kβ) is dependent on ACBD3 interaction for its activity and was also studied throughout this work. ACBD3 protein expression positively correlated with PI4Kβ protein expression across breast cell lines and overexpression of ACBD3 protein also led to increased PI4Kβ protein expression. Treatment of breast cancer cells with the PI4Kβ enzymatic activity inhibitor BQR695 did not result in changes to ACBD3 protein expression. in breast cancer cell lines, PI4Kβ mRNA expression was high in breast cancer cell lines derived from adenocarcinomas and low in cells derived from invasive ductal carcinomas.

7.2 Graphical Overview of ACBD3 Functions

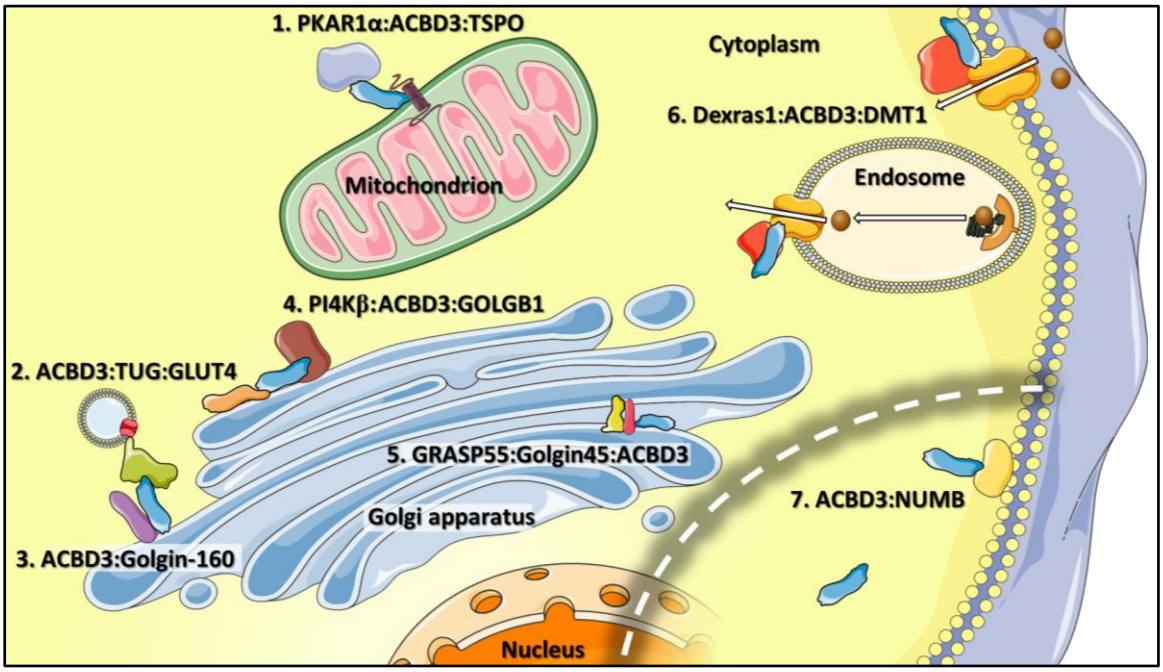

Figure 7.1 – Graphical overview of ACBD3 function. ACBD3 has functions at the Golgi, Mitochondria, cell membrane, transferrin containing endosomes, and in the cytoplasm during mitosis. **1.** ACBD3 (blue) localises to the mitochondria by binding TPSO (purple coil), ACBD3 can then recruit PKA via the PKAR1α subunit (grey) which phosphorylates VDAC to prevent calcium import into the mitochondria signalling redox stress and subsequent inflammation. PKA also phosphorylates StAR on the mitochondria which allows cholesterol import into the mitochondria for steroid synthesis. **2.** ACBD3 binds TUG (green) at the Golgi and together they retain GLUT4 (pink) storage vesicles at the Golgi in the absence of insulin signalling. **3.** ACBD3 binds Golgin-160 which also binds TUG protein if TUG has been acetylated. Golgin-160 is cleaved by Caspases during apoptosis and ACBD3 has higher binding affinity for the caspase 3 generated Golgin-160 fragment over the full-length peptide. **4.** ACBD3 localises PI4Kβ to Golgi membranes increasing the rate of conversion of PI into PI(4)P by tethering PI4Kβ to the site of its substrate. GOLGB1 (maroon) also binds ACBD3 and stabilises it at the Golgi. **5.** ACBD3 binds Golgin45 (pink) at the Golgi which binds GRASP55 (yellow) and all play a structural role in the assembly, stacking and maintenance of the Golgi. **6.** ACBD3 tethers Dexras1 (red) to DMT1 (orange) and stimulates DMT1 to import iron into the cell. Transferrin binds the transferrin receptor and is endocytosed into the cell with DMT1. Acidification causes release of iron from transferrin and the iron is then imported to the cytoplasm by DMT1 stimulated by ACBD3 and Dexras1. **7.** During mitosis the Golgi fragments and ACBD3 is released into the cytoplasm. In neural development ACBD3 binds NUMB (yellow) and they synergistically inhibit NOTCH signalling to specify neuronal stem cell fate.

7.3 ACBD3 as a Marker in Breast Cancer

ACBD3 mRNA and protein expression were higher in breast cancer cell lines compared to a normal like breast cell line (MCF12A). mRNA expression was highest in the HER2+ SKBR3 breast cancer cell line at 5.8-fold the level of the MCF12A cell line, with protein levels being the highest in the PMC42, T47D, and MDA-MB-361 cell lines which were all ER+. High *ACBD3* mRNA expression was consistently detrimental to breast cancer patient outcomes across different tumour subtypes, receptor status and the cohort as a whole. There were no instances where high *ACBD3* expression was associated with improved patient outcomes. In isolation, this suggests that *ACBD3* expression is a marker of poor prognosis in patients and particularly a marker of distant metastasis risk in breast cancer. An increased risk of metastases subsequently decreases survival, as 90% of cancer deaths are caused my metastatic tumours (Peitzsch, Tyutyunnykova et al. 2017).

Staining of breast cancer cores for ACBD3 protein expression showed tissue specific staining, particularly of breasts ducts, where ACBD3 expression was often higher than surrounding cells. A common feature of normal and cancerous tissue was high ACBD3 staining of luminal epithelial and myoepithelial basal cells of ducts. Ductal cells sometimes had a mosaic pattern where ACBD3 was high or very low in neighbouring cells of the same type (luminal/myoepithemial/basal). Luminal B intrinsic subtype breast cancer patients had the largest decrease in relapse free survival when ACBD3 was expressed above the median level. The luminal B intrinsic subtype has a similar gene expression profile to luminal breast cells and the subtype is associated with ER expression. Patients with luminal B breast cancers have a worse prognosis than those with luminal A with higher expression of proliferative markers but is otherwise similar to the luminal A subtype (Ciriello, Gatza et al. 2015, Cancer Research UK 2017).

ACBD3 may be another proliferative marker that distinguishes the luminal B subtype from luminal A. Differentiating luminal A from luminal B is largely dependent on tumour grade and proliferation rate where luminal B breast cancers are higher in both aspects (Inic, Zegarac et al. 2014). High ACBD3 mRNA expression was associated with worse prognosis, just as patient with luminal B cancers have worse prognosis than those with luminal A. The T47D cell line is a model for luminal A breast cancer and T47D cells that overexpressed ACBD3 grew faster than controls certainly suggesting that it increased proliferation in Luminal A-type cells. There were also

increases in inflammatory proteins when ACBD3 was overexpressed which can be promotive of a tumour microenvironment and therefore progressive. ACBD3 protein levels were high in ER+ breast cell lines further associating its expression with luminal breast cancer subtypes.

As an essential protein in Golgi structure and function, it would be expected to find high protein expression of ACBD3 in secretory cells (Xihua, Mengjing et al. 2017, Liao, J., Guan et al. 2019, Shinoda, Fujita et al. 2012, Yue, Qian et al. 2019, Truschel, Zhang et al. 2012, Xiang, Wang 2010, Sohda, Misumi et al. 2001). Myoepithelial cells have secretory properties and are responsible for milk ejection as well as the other secretory proteins including Serpin B5 (Tamazato Longhi, Magalhães et al. 2016). ACBD3 overexpression in T47D cells, or expression of the ACBD3(K381_R528) GOLD domain deletion mutant, resulted in a 1.6-fold increase in Serpin B5 expression, supporting a role for ACBD3 in epithelial breast cell secretion, and a possible explanation for its high expression in the epithelial cells of the ducts.

70-80% of breast cancers are invasive ductal carcinomas that derive from epithelial cells (Cancer Research UK 2017), ACBD3 staining was noted to be particularly high in epithelial ductal cells and cells that infiltrated ducts of breast cancer cores. This may explain ACBD3 staining was scored lower overall in adjacent breast tissue cores compared to cancerous tissue cores but did not appear high when viewed in the context of whole breast cores. When cores were viewed as a whole (including connective tissue, adipose tissue, and non-cancerous tissue), ACBD3 was not higher overall but the cells that formed the IDCs were. High ACBD3 protein staining in luminal epithelial cells is also a concern in the context of Luminal B type breast cancer patients who were found to have the largest decrease in RFS when *ACBD3* mRNA expression was high. ACBD3 may be a driver of luminal type breast cancers or a marker of aggressiveness.

When breast cancer cores were stained for ACBD3 protein, there was no significant difference in ACBD3 staining between non-metastatic breast cancer cores and cores from metastatic breast cancer of the lymph node suggesting that ACBD3 expression at the protein level does not correlate with metastasis. It was also observed with invasive ductal carcinomas that there were often many invasive cells in the lobules that had low staining for ACBD3, but some cells embedded in them had very high staining. ACBD3 overexpression in breast cancer cell lines was previously found to increase side populations of breast cancer stem cells in culture that

resembled CSCs (Huang, Y., Yang et al. 2018). CSCs are often slower growing more dormant cells (Peitzsch, Tyutyunnykova et al. 2017), so an association between ACBD3 expression and lymph node invasion was not necessarily expected. Selective staining of only some invasive cells in lobules could be, in effect, staining cancer stem cells or cells that may become them as the heterogenous tumour evolves. Supporting evidence for ACBD3 in CSC formation and maintenance are discussed further in later sections and ACBD3 expression cannot be ruled out as a marker for CSCs.

7.3.1 ACBD3 and the Human Epidermal Growth Factor Receptor 2 (HER2)

In breast cancer cell lines, *ACBD3* mRNA expression was highest in the HER2+ SKBR3 breast cancer cell line (Also ER+). Both mRNA and protein expression of ACBD3 were high in the HER2+ MDA-MB-361 cell line. HER2 protein was 1.36-fold upregulated when ACBD3 was overexpressed in T47D cells and 1.46-fold upregulated when ACBD3(K381_R528) (ACBD3 GOLD domain deletion mutant) was expressed (. The T47D breast cancer cell line is not considered HER2 positive, increased HER2 expression in ACBD3 overexpressing T47D cells therefore supports a potential interplay between ACBD3 expression and HER2 expression. In breast cancer patients, tumour *ACBD3* mRNA expression above the median resulted in lower relapse free survival, lower overall survival, and lower distant metastasis free survival for HER2- breast cancer patients which matched the trend for patient outcomes overall when *ACBD3* was expressed above the median level.

ACBD3 mRNA levels were also found to be statistically higher in tumours that were non-responsive to anti-HER2 therapies. Currently only patients with HER2 3+ tumours are offered anti HER2 therapies, so looking at response to anti-HER2 therapy is already selecting for patients with high HER2-expressing tumours. Patients with HER--low breast cancer are not currently offered anti HER2 therapy but there is a growing consensus of preclinical data that new generation trastuzumab derivatives (such as trastuzumab-duocarmazine) and novel anti-HER2 drugs may be effective in killing HER2-low breast cancer cells (van der Lee, Groothuis et al. 2015, Eiger, Agostinetto et al. 2021).

ACBD3 staining of a breast cancer core array found that ACBD3 protein was significantly higher in HER2 negative cores compared to HER2 1+ cores. Breast cancer patients with tumours graded 2+ or 3+ had higher mean expression of ACBD3

compared to patients with HER2 1+ graded tumours but this did not reach statistical significance. If a comparison can one day be made between responders and non-responders to trastuzumab-duocarmazine when patients have low HER2 expression (1+), a larger difference in ACBD3 expression may be seen as I found the base level of ACBD3 to be lower in HER2 1+ tumours.

IGFIR can phosphorylate and activate the HER2 receptor to negate the effects of anti-HER2 therapies in breast cancer cell lines and anti-IGFIR drugs re-sensitize trastuzumab resistant cell lines to trastuzumab (Lu, Y., Zi et al. 2001, Lu, Y., Zi et al. 2004, Nahta, Yuan et al. 2005). HER2 heterodimerisation is one of the most common mechanisms of anti-HER2 resistance in cancers (Pohlmann, Mayer et al. 2009). *ACBD3* transcription was found to be induced by X10, an insulin analogue that activates the IGF and insulin receptors. ACBD3 is involved in glucose transporter 4 vesicle cycling and subsequent glucose import in response to insulin, so it is logical that the insulin signalling pathway could regulate *ACBD3* expression (Belman, Bian et al. 2015, Bogan, Rubin et al. 2012).

Higher expression of *ACBD3* in non-responders to trastuzumab may be an indicator of the increased IGF signalling that sustains HER2 activation and signalling in the presence of trastuzumab. It is conceivable that upregulation of ACBD3, induced by IGF1R signalling, would subsequently increase the pool of available GLUT4 containing vesicles and therefore increase glucose import and energy for the proliferating cancer cells.

Lapatinib (anti-HER2 therapy) leads to downregulation of GLUT4 in HER2+ breast cancers (Acharya, Xu et al. 2016). This lends evidence to a hypothesis that there is interplay between insulin signalling, HER2+ breast cancers, and ACBD3 expression. This also supports an argument that overexpression of ACBD3 increases resistance to anti-HER2 therapies through increases in expression and activity of insulin related pathways.

7.3.2 ACBD3 and the Oestrogen Receptor (ER)

ACBD3 protein levels were highest in the PMC42, T47D, and MDA-MB-361 cell lines which were all ER+ but GNST and 17βE2 (activators of ER signalling pathway) were found to repress *ACBD3* transcription by at least 2-fold. FOXA1 was found to be a positive *ACBD3* transcription factor in normal breast tissue and FOXA1 is

associated with ER expression in breast cancer and ER signal reprogramming (Thorat, Marchio et al. 2008). It is conceivable that ER signalling negatively regulates ACBD3 expression in healthy breast tissue, but that in breast cancer FOXA1 expression contributes to the reprogramming of ER binding and signalling in breast cancer (Ross-Innes, Stark et al. 2012), cancelling out the negative impact of GNST and 17βE2-mediated ER transcriptional repression of ACBD3. This would explain why distant metastasis-free survival was worse for ER+ patients when *ACBD3* expression was high.

Differential responses to oestrogen have been reported in breast cancer to the extent where normal and cancerous breast cells could be differentiated between depending on their cistrome (Chi, Singhal et al. 2019). The oestrogen induced tumour suppressor Rho GTPase-activating protein 7 is induced by oestrogen in normal breast tissue but not in ER+ breast cancer cells and ACBD3 may follow the inverse to this pattern, repressed by oestrogen normally but not in ER+ breast cancers (Chi, Singhal et al. 2019). This further suggests ACBD3 expression could be a marker of a reprogrammed oestrogen receptor signalling pathway that no longer represses *ACBD3* transcription. ER reprogramming is associated with breast cancer metastasis and therapy resistance (Ross-Innes, Stark et al. 2012, Achinger-Kawecka, Valdes-Mora et al. 2020), ACBD3 expression was also found to be associated with increased risk of metastasis and small but significant increases in resistance to some chemotherapies.

In the T47D breast cancer cell line, ERα protein was upregulated 1.35-fold when ACBD3 was overexpressed and 1.61-fold when ACBD3(K381_R528) was expressed. There is possibly cross-regulation between ACBD3 and ER; certainly increased ACBD3 has the potential to increase output from the Golgi, either by increasing Golgi size or activity, and as a nuclear receptor, the ER is post translationally processed by the Golgi. Bisphenol A was also discovered as a positive *ACBD3* transcriptional regulator, it is an oestrogen mimic found in plastic bottles, receipts, and other common products and has been associated with breast cancer and other cancers (Wang, Z., Liu et al. 2016, Jalal, Surendranath et al. 2017, Sengupta, Obiorah et al. 2013, Acconcia, Pallottini et al. 2015).

Breast cancer core staining for ACBD3 found that the highest mean ACBD3 protein scoring was found in ER+, PR-, HER2-, breast cancer patients, but this difference did not reach statistical significance compared to patients with other

combinations of receptor status. A larger dataset may find that this observation reaches statistical significance. The potential interplay between ACBD3 and ER is also supported when survival in ER negative patients is considered. Overall survival and distant metastasis free survival were not significantly different in ER- breast cancer patients when divided by *ACBD3* expression (Appendix – Figure 9.3), *ACBD3* overexpression had more influence on relapse free survival and overall survival in patients whose tumours expressed ER.

7.3.3 ACBD3 and the Progesterone Receptor (PR)

ACBD3 protein staining was significantly higher in PR- breast cancer cores compared to PR 3+ cores. ACBD3 interacts with the progesterone receptor chaperone UNC45A, a regulatory component of the progesterone receptor/heat shock protein 90 chaperoning complex which functions in the assembly and folding of the progesterone receptor (Chadli, Graham et al. 2006a). UNC45A expression limits PR chaperoning and an ACBD3-UNC45A interaction could have a negative effect on PR nuclear expression. As ACBD3 is known to regulate the expression of the GLUT4 receptor by retaining it at the Golgi, it could contribute to PR nuclear localisation regulation in a similar way (Belman, Bian et al. 2015, Bogan, Rubin et al. 2012). It is possible that PR signalling-dependent breast cancers may be under selection pressure to downregulate ACBD3 protein relative to PR- breast cancers.

7.4 ACBD3 and Breast Cancer Therapy

ACBD3 mRNA expression varied between different breast cancer cell lines and was 2.1-fold to 5.8-fold higher in breast cancer cell lines compared to the MCF12A cell line, mRNA expression did not correlate with protein expression. This suggests that ACBD3 protein levels are regulated post transcriptional and/or post translation and this is supported by the finding that the ACBD3 reading frame is hypomethylated and not regulated by methylation at the stage of transcription in normal breast or breast cancer. Any targeting of ACBD3 may be reliant on finding protein level regulators.

ACBD3 is directly involved in iron transport into the cell where it binds DMT1 iron transporter and the positive regulator Dexras1, and ACBD3 protein expression is

downregulated by high levels of iron in the duodenum via negative feedback to maintain iron homeostasis (Okazaki, Ma et al. 2012, Okazaki, Glass 2017). There is no direct evidence for negative feedback in other tissues but isoforms of DMT1 are present in most tissues and it was expected that ACBD3 would have a similar role in all tissues and therefore be similarly regulated by iron (Lis, Barone et al. 2004). It was unexpected then to find that supplementing iron in cell culture medium as ferric ammonium citrate increased ACBD3 protein expression at 179nM and 89.53μM ferric ammonium citrate concentration in the MDA-MB-231 cell line. This means that intracellular iron was not found to negatively regulate ACBD3 in this breast cancer cell line.

Whilst changes in ACBD3 expression varied between the T47D parental and everolimus resistant cell lines, ACBD3 expression was either higher or not different at the mRNA level in the T47D-EveR cells at all seeding densities and higher in the T47D-EveR cells at the protein level at all time points after seeding. Increased expression of ACBD3 in the T47D-EveR cell line suggested that it could have a role in promoting or maintaining everolimus resistance in the cells.

Direct upregulation of *ACBD3* by everolimus treatment was ruled out by treating T47D cells with everolimus and this led to the hypothesis that ACBD3 upregulation caused the everolimus resistance. Work by a previous student who engineered the T47D-EveR cell line found that β-catenin protein was upregulated in that cell line (Hare 2018) combined with the knowledge that ACBD3 overexpression in breast cancer has been shown to increase β-catenin activity (Huang, Yang et al. 2018), provides a further possible link between ACBD3 and everolimus resistance in breast cancer.

ACBD3 overexpression did not increase cell number at any concentration of everolimus treatment relative to cell transfected with an empty vector control. Expression of the ACBD3(KQ117AA) mutant in the same cell line also resulted in no increased resistance to everolimus. Based on this, the hypothesis that ACBD3 is causative of everolimus resistance must be rejected. ACBD3 may still have a role in everolimus resistance in the T47D-EveR cell line or may be a marker of other changes that are causative of resistance. One possibility is that ACBD3 upregulation is a marker of stemness in the T47D-EveR cells. Hare (2018) found that Wnt signalling and ALDH signalling were upregulated in the T47D-EveR, both markers of stemness (Hare 2018, Ginestier, Hur et al. 2007, Reya, Clevers 2005).

Another possible candidate for the mechanism of everolimus resistance is PI4Kβ which was also upregulated at the mRNA and protein level in the T47D-EveR cell line, and mRNA expression was induced by everolimus treatment.

7.5 PI4KB, and its Interaction with ACBD3

PI4Kβ is the main binding partner of ACBD3 and like ACBD3 it is located on chromosome 1q (1q21.3). *PI4Kβ* expression was previously found to be a marker for breast cancer recurrence and is upregulated in 20% of breast tumours (Goh, Feng et al. 2017, Tan, Brill 2014, Morrow, Alipour et al. 2014). These two factors informed the decision to measure PI4Kβ expression simultaneously to ACBD3 expression in most instances but discussion around results from PI4Kβ have remained brief until now to focus on ACBD3.

At the mRNA level there was a clear and statistically significant difference in *PI4Kβ* expression between cell lines derived from adenocarcinomas (high expression) and cell lines derived from invasive ductal carcinomas (low expression). Only the MDA-MB-231 cell line (triple negative, adenocarcinoma derived) had higher *PI4Kβ* expression than the MCF12A control cells to a statistically significant level. PI4Kβ protein expression was higher in breast cancer cell lines compared to the normal-like control, with the exception of the MDA-MB-436 cell line which had lower PI4Kβ protein expression. The MDA-MB-436 cell line also had the lowest *PI4Kβ* mRNA expression.

ACBD3 and PI4Kβ protein expression positively correlated but this was absent at the mRNA level. *ACBD3* mRNA levels also did not correlate well with ACBD3 protein levels: T47D and MDA-MB-361 cells had high levels of ACBD3 protein expression but second and third lowest expression of *ACBD3* mRNA respectively, (not including the normal like MCF12A line). In contrast, PI4Kβ mRNA and protein levels did positively correlate between cell lines.

PI4Kβ mRNA expression was increased in the T47D-EveR cell line compared to parental cells and by a larger fold change than for *ACBD3* expression. *PI4Kβ* mRNA was induced by 100μM everolimus treatment and PI4Kβ protein expression also increased following 72 hours of everolimus treatment. This suggests that it may in fact be PI4Kβ that contributes to everolimus resistance in the T47D-EveR cell line,

and as ACBD3 and PI4Kβ protein expression positively correlate than upregulated ACBD3 may simply be a marker of upregulated PI4Kβ.

PI4Kβ has previously been found to have a role in breast cancer but treating MDA-MB-231 cells with the reported IC50 of a PI4Kβ specific inhibitor had no statistical effect on cell growth, it took a much larger dose of the treatment to cause significant cell number decrease (50-100μM). The 0nM treatment had large variance making it hard to perform statistical analysis against it. It's possible that as a combined therapy that BQR695 could have a value in breast cancer treatment but would appear to be a poor candidate as a single treatment due to the high dose required to reach the GI50 in the MDA-MB-231 breast cancer cell line.

PI4Kβ activity is dependent on the presence of ACBD3 *in vitro*, was pulled down by ACBD3 in 293T cells and recruited by ACBD3 in Vero cells (Klima, Tóth et al. 2016, Sasaki, Ishikawa et al. 2012). It was hypothesised that this relationship could be reciprocal with PI4Kβ activity affecting ACBD3 expression. The PI4Kβ inhibitor BQR695 did not consistently affect the protein expression of ACBD3 in the MDA-MB-231 cell line suggesting that PI4Kβ activity is not a regulator of ACBD3 protein expression. Inhibition of PI4Kβ was assayed as an inhibitor of MDA-MB-231 cell growth and treatment only resulted in a statistical reduction in cell number at 50μM and 100μM (555-fold and 1111-fold the reported IC50 respectively).

PI4Kβ was overexpressed in ACBD3 overexpressing T47D cells relative to the empty vector control. This is in agreement with previous findings where there was positive correlation between ACBD3 and PI4Kβ protein expression across breast cancer cell lines. A mutant to abolish ACBD3-PI4Kβ interactions was unsuccessful so the effect of a non PI4Kβ binding ACBD3 mutant could not be determined. The Acyl-CoA binding inhibiting mutant (KQ117AA) expressing cells had less PI4Kβ protein expression than WT or K381-R528del ACBD3 expressing cells.

In summary, PI4Kβ may have a role in resistance to everolimus and the expression of ACBD3 protein appears to affect the expression of PI4Kβ protein, which may be reciprocal.

7.6 Future Work

I believe There is still much research to be done concerning ACBD3 and breast cancer. Results in this work indicate that ACBD3 may be a reliable biomarker for relapse risk and for stemness, and I hypothesised that ACBD3 expression may be a marker of oestrogen receptor reprogramming which is itself associated with drug resistance and metastasis (Achinger-Kawecka, Valdes-Mora et al. 2020).

ACBD3 overexpression in normal like breast cell lines and analysis of secretions from ACBD3 overexpressing cells were two experiments that unfortunately could not be carried out. Based on the upregulation of several extracellular and secretory proteins when ACBD3 was overexpressed I would expect to find similar changes in media secretions and a global increase in total secreted proteins due to the role of ACBD3 in the functioning of the Golgi. ACBD3 protein expression in luminal B cell models could not be obtained and this may be important in determining if ACBD3 is a marker of or contributor to the Luminal B subtype. Assessing luminal B specific markers when ACBD3 is overexpressed in Luminal A cells (such as Ki67) would provide valuable evidence to determine if this is the case (As was carried out on T47D Luminal A model cells in this project).

ACBD3 can induce redox stress by promoting phosphorylation of VDAC1 at the mitochondria which prevents mitochondrial calcium import (Gatliff, East et al. 2017). The level of reactive oxygen species (ROS) in a cell can be measured and it would be interesting to determine what happens to these levels when ACBD3 is overexpressed in normal and cancerous breast cells (Wu, D., Yotnda 2011). HIF-1a protein expression was higher when ACBD3 was overexpressed and measuring ROS may help to determine if ACBD3 directly upregulates HIF-1a or if it is stabilised by ROS generated by ACBD3 overexpression. Similarly, specific research on ACBD3 expression and inflammation in breast tissue may have a high value for breast cancer insight or even be translational to Huntington's disease research and therapy.

In the background of this work, PI4Kβ expression has also been examined in cell lines and in everolimus resistant cells and may have a causative role in the latter. The ACBD3-PI4Kβ interaction should not be ignored in future work concerning ACBD3 and breast cancer. PI4Kβ functional inhibition was not found to influence ACBD3 expression in this work but they were found to be co-expressed across cell lines at the protein level, and PI4Kβ was upregulated when ACBD3 was

overexpressed. I hope that oncoprotein expression change data when ACBD3 was overexpressed will aid in asking more specific questions and designing more targeted experiments concerning ACBD3 in breast cancer and help elucidate any addition role for ACBD3 in breast cancer cell behaviour.

7.6 Concluding Remarks

There were a very limited number of publications relating to ACBD3 at the start of this project (42 research articles primarily concerning ACBD3 and 3 review articles, as of October 1st 2017), of which only one paper made a correlation between ACBD3 and cancer (Liu, Jun, Matyakhina et al. 2003), and none made a specific link between ACBD3 and breast cancer or normal breast tissue. The inception of this project was based on unpublished data showing increased ACBD3 protein expression in breast cancer cell lines and upon assessing the literature ACBD3 became an appealing protein to study with contextual roles in the cell and roles that could be applicable to multiple hallmarks of cancer.

In this thesis, higher ACBD3 expression has been associated with breast cancer, worse prognosis for breast cancer patients, and increased inflammatory markers. An important next step will be in repeating this methodology for ACBD3 protein expression with a large dataset as mRNA and protein expression did not correlate in breast cancer cell lines. ER+ breast cancer patient cores were found to have the highest ACBD3 protein staining, matching cell line data, but the IHC core data did not reach statistical significance. Other evidence highlighting a relationship between ACBD3 and ER positivity suggests that a larger dataset may reach statistical significance.

When viewing breast cancer cores stained for ACBD3 at high magnification it was apparent that ACBD3 expression was highest in luminal epithelial cells and cells surrounding ducts in breast core samples. The association between ACBD3 and epithelial breast cells that may be based on the requirement of ACBD3 expression for Golgi function and therefore secretion. Patients with Luminal B type cancers had the largest decrease in relapse free survival when ACBD3 was high and like Luminal type cancers ACBD3 expression was found to be associated with ER positivity.

I have hypothesised that ACBD3 overexpression in breast cancer contributes to an inflammatory microenvironment whilst simultaneously supressing detection by

the immune system. In Huntington's disease, ACBD3 protein is overexpressed in the corpus striatum and iron levels are also dysregulated suggesting that ACBD3 is not negatively regulated by iron in the brain either (Sbodio, Paul et al. 2013, Rosas, Chen et al. 2012). ACBD3 overexpression has been shown to increase iron import, and resultant redox stress may even form a positive feedback loop that exacerbates Huntington's disease (Rosas, Chen et al. 2012, Sbodio, Paul et al. 2013, Falk, Pierfrancesco et al. 1999). Any feedback loop that increases redox stress has implications in cancer as redox stress can cause inflammation which can promote a tumour microenvironment (Hanahan, Weinberg 2011). Overexpression of ACBD3-GFP also led to increased endogenous ACBD3 protein supporting a positive feedback loop for ACBD3 expression in breast cancer.

The effect of ACBD3 on breast cancer behaviour has been both interesting and fruitful. I can conclude that ACBD3 affects cancer related pathways in a breast cell line and has clinical relevance for patients. More work is necessary to elucidate the mechanisms by which ACBD3 expression affects breast cancer patients, and I was limited, largely, by the small base of knowledge from which to start. I hope that the breast core staining and oncoprotein array data, in particular, will help in informing future experiments into ACBD3 and breast cancer behaviour.

Chapter 8

References list

ACCONCIA, F. and MARINO, M., 2016. Steroid Hormones: Synthesis, Secretion, and Transport. In: A. BELFIORE and D. LEROITH, eds, *Principles of Endocrinology and Hormone Action.* Cham: Springer International Publishing, pp. 1-31.

ACCONCIA, F., PALLOTTINI, V. and MARINO, M., 2015. Molecular Mechanisms of Action of BPA. *Dose-response : a publication of International Hormesis Society,* **13**(4), pp. 1559325815610582-1559325815610582.

ACHARYA, S., XU, J., WANG, X., JAIN, S., WANG, H., ZHANG, Q., CHANG, C.C., BOWER, J., ARUN, B., SEEWALDT, V. and YU, D., 2016. Downregulation of GLUT4 contributes to effective intervention of estrogen receptor-negative/HER2-overexpressing early stage breast disease progression by lapatinib. *American journal of cancer research,* **6**(5), pp. 981-995.

ACHINGER-KAWECKA, J., VALDES-MORA, F., LUU, P., GILES, K.A., CALDON, C.E., QU, W., NAIR, S., SOTO, S., LOCKE, W.J., YEO-TEH, N., GOULD, C.M., DU, Q., SMITH, G.C., RAMOS, I.R., FERNANDEZ, K.F., HOON, D.S., GEE, J.M.W., STIRZAKER, C. and CLARK, S.J., 2020. Epigenetic reprogramming at estrogen-receptor binding sites alters 3D chromatin landscape in endocrine-resistant breast cancer. *Nature Communications,* **11**(1), pp. 320.

ALEXANDER, J.J., CHAPMAN, L., PALLANSCH, M., STEPHENSON, W. and ANDERSON, L., 1993. Coxsackievirus B2 infection and aseptic meningitis: a focal outvreak among members of a high school football team. *The Journal of Infectious Diseases,* **167**(5), pp. 1201-1205.

ALPY, F. and TOMASETTO, C., 2005. Give lipids a START: the StAR-related lipid transfer (START) domain in mammals. *Journal of cell science,* **118**(13), pp. 2791.

ALTMAN, D.G. and BLAND, J.M., 1983. Measurement in Medicine: The Analysis of Method Comparison Studies. *Journal of the Royal Statistical Society.Series D (The Statistician),* **32**(3), pp. 307-317.

AMIN, M.B., EDGE, S., GREENE, F., BYRD, D.R., BROOKLAND, R.K., WASHINGTON, M.K., GERSHENWALD, J.E., COMPTON, C.C., HESS, K.R., SULLIVAN, D.C., JESSUP, J.M., BRIERLEY, J.D., GASPAR, L.E., SCHILSKY, R.L., BALCH, C.M., WINCHESTER, D.P., ASARE, E.A., MADERA, M., GRESS, D.M. and MEYER, L.R., 2017. *AJCC Cancer Staging Manual.* 8th edn. American Joint Committe on Cancer.

ARAKANE, F., KING, S.R., DU, Y., KALLEN, C.B., WALSH, L.P., WATARI, H., STOCCO, D.M. and STRAUSS, J.F., 1997. Phosphorylation of Steroidogenic Acute Regulatory Protein (StAR) Modulates Its Steroidogenic Activity. *Journal of Biological Chemistry,* **272**(51), pp. 32656-32662.

ARTAVANIS-TSAKONAS, S., RAND, M.D. and LAKE, R.J., 1999. Notch Signaling: Cell Fate Control and Signal Integration in Development. *Science,* **284**(5415), pp. 770.

ATLANTE, A., CALISSANO, P., BOBBA, A., GIANNATTASIO, S., MARRA, E. and PASSARELLA, S., 2001. Glutamate neurotoxicity, oxidative stress and mitochondria. *FEBS letters,* **497**(1), pp. 1-5.

AULMANN, S., BLÄKER, H., PENZEL, R., RIEKER, R.J., OTTO, H.F. and SINN, H.P., 2003. CTCF gene mutations in invasive ductal breast cancer. *Breast cancer research and treatment,* **80**(3), pp. 347-352.

BACHMEIER, B.E., ALBINI, A., VENÉ, R., BENELLI, R., NOONAN, D., WEIGERT, C., WEILER, C., LICHTINGHAGEN, R., JOCHUM, M. and NERLICH, A.G., 2005. Cell density-dependent regulation of matrix metalloproteinase and TIMP expression in differently tumorigenic breast cancer cell lines. *Experimental cell research,* **305**(1), pp. 83-98.

BACHMEIER, B.E., VENÉ, R., IANCU, C.M., PFEFFER, U., MAYER, B., NOONAN, D., ALBINI, A., JOCHUM, M. and NERLICH, A.G., 2005. Transcriptional control of cell density dependent regulation of matrix metalloproteinase and TIMP expression in breast cancer cell lines. *Thrombosis and haemostasis,* **93**(4), pp. 761-769.

BAIAMONTE, B.A., LEE, F.A., BREWER, S.T., SPANO, D. and LAHOSTE, G.J., 2013. Attenuation of Rhes activity significantly delays the appearance of behavioral symptoms in a mouse model of Huntington's disease. *PloS one,* **8**(1), pp. e53606.

BANG, S., STEENSTRA, C. and KIM, S.F., 2012. Striatum specific protein, Rhes regulates AKT pathway. *Neuroscience letters,* **521**(2), pp. 142-147.

BARBOSA, M.A. and MARTEL, F., 2020. *Targeting Glucose Transporters for Breast Cancer Therapy: The Effect of Natural and Synthetic Compounds.*

BARR, F.A., PUYPE, M., VANDEKERCKHOVE, J. and WARREN, G., 1997. GRASP65, a Protein Involved in the Stacking of Golgi Cisternae. *Cell,* **91**(2), pp. 253-262.

BASELGA, J., CAMPONE, M., PICCART, M., BURRIS, H.A., RUGO, H.S., SAHMOUD, T., NOGUCHI, S., GNANT, M., PRITCHARD, K.I., LEBRUN, F., BECK, J.T., ITO, Y., YARDLEY, D., DELEU, I., PEREZ, A., BACHELOT, T., VITTORI, L., XU, Z., MUKHOPADHYAY, P., LEBWOHL, D. and HORTOBAGYI, G.N., 2012. Everolimus in Postmenopausal Hormone-Receptor–Positive Advanced Breast Cancer. *N Engl J Med,* **366**(6), pp. 520-529.

BAUMANN, C.A., RIBON, V., KANZAKI, M., THURMOND, D.C., MORA, S., SHIGEMATSU, S., BICKEL, P.E., PESSIN, J.E. and SALTIEL, A.R., 2000. CAP defines a second signalling pathway required for insulin-stimulated glucose transport. *Nature,* **407**(6801), pp. 202-207.

BAYLIN, S.B. and HERMAN, J.G., 2000. DNA hypermethylation in tumorigenesis: epigenetics joins genetics. *Trends in genetics : TIG,* **16**(4), pp. 168-174.

BAZZARO, M., SANTILLAN, A., LIN, Z., TANG, T., LEE, M.K., BRISTOW, R.E., SHIH, I. and RODEN, R.B., 2007. Myosin II co-chaperone general cell UNC-45 overexpression is associated with ovarian cancer, rapid proliferation, and motility. *The American journal of pathology,* **171**(5), pp. 1640-1649.

BEAVER, J.A. and PARK, B.H., 2012. The BOLERO-2 trial: the addition of everolimus to exemestane in the treatment of postmenopausal hormone receptor-positive advanced breast cancer. *Future oncology (London, England),* **8**(6), pp. 651-657.

BELMAN, J.P., BIAN, R.R., HABTEMICHAEL, E.N., LI, D.T., JURCZAK, M.J., ALCÁZAR-ROMÁN, A., MCNALLY, L.J., SHULMAN, G.I. and BOGAN, J.S., 2015. Acetylation of TUG Protein Promotes the Accumulation of GLUT4 Glucose Transporters in an Insulin-responsive Intracellular Compartment. *Journal of Biological Chemistry,* **290**(7), pp. 4447-4463.

BERNARDO, G.M., LOZADA, K.L., MIEDLER, J.D., HARBURG, G., HEWITT, S.C., MOSLEY, J.D., GODWIN, A.K., KORACH, K.S., VISVADER, J.E., KAESTNER, K.H., ABDUL-KARIM, F.W., MONTANO, M.M. and KERI, R.A., 2010. FOXA1 is an essential determinant of ERalpha expression and mammary ductal morphogenesis. *Development (Cambridge, England),* **137**(12), pp. 2045-2054.

BERRIDGE, M.V. and TAN, A.S., 1993. Characterization of the Cellular Reduction of 3-(4,5-dimethylthiazol-2-yl)-2,5-diphenyltetrazolium bromide (MTT): Subcellular Localization, Substrate Dependence, and Involvement of Mitochondrial Electron Transport in MTT Reduction. *Archives of Biochemistry and Biophysics,* **303**(2), pp. 474-482.

BICKEL, M., 1993. The role of interleukin-8 in inflammation and mechanisms of regulation. *Journal of periodontology,* **64**(5 Suppl), pp. 456-460.

BIÈCHE, I., CHAMPÈME, M. and LIDEREAU, R., 1995. Loss and gain of distinct regions of chromosome 1q in primary breast cancer. *Clinical Cancer Research,* **1**(1), pp. 123-127.

BJORNSTI, M. and HOUGHTON, P.J., 2004. The tor pathway: a target for cancer therapy. *Nature Reviews Cancer,* **4**(5), pp. 335-348.

BOGAN, J.S., RUBIN, B.R., YU, C., LÖFFLER, M.G., ORME, C.M., BELMAN, J.P., MCNALLY, L.J., HAO, M. and CRESSWELL, J.A., 2012. Endoproteolytic Cleavage of TUG Protein Regulates GLUT4 Glucose Transporter Translocation. *Journal of Biological Chemistry,* **287**(28), pp. 23932-23947.

BONELLO, S., ZÄHRINGER, C., BELAIBA, R.S., DJORDJEVIC, T., HESS, J., MICHIELS, C., KIETZMANN, T. and GÖRLACH, A., 2007. Reactive oxygen species activate the HIF-1alpha promoter via a functional NFkappaB site. *Arteriosclerosis, Thrombosis, and Vascular Biology,* **27**(4), pp. 755-761.

BOURAS, E., KARAKIOULAKI, M., BOUGIOUKAS, K.I., AIVALIOTIS, M., TZIMAGIORGIS, G. and CHOURDAKIS, M., 2019. Gene promoter methylation and cancer: An umbrella review. *Gene,* **710**, pp. 333-340.

BREASTED, J.H., 1930. *The Edwin Smith Surgical Papyrus: published in facsimile and hieroglyphic transliteration with translation and commentary in two volumes.* Chic. UP.

BRISARD, D., ECKERDT, F., MARSH, L.A., BLYTH, G.T., JAIN, S., CRISTOFANILLI, M., HORIUCHI, D. and PLATANIAS, L.C., 2018. Antineoplastic effects of selective CDK9 inhibition with atuveciclib on cancer stem-like cells in triple-negative breast cancer. *Oncotarget,* **9**(99), pp. 37305-37318.

BROWN, K.F., RUMGAY, H., DUNLOP, C., RYAN, M., QUARTLY, F., COX, A., DEAS, A., ELLISS-BROOKES, L., GAVIN, A., HOUNSOME, L., HUWS, D., ORMISTON-SMITH, N., SHELTON, J., WHITE, C. and PARKIN, D.M., 2018. The fraction of cancer attributable to modifiable risk factors in England, Wales, Scotland, Northern Ireland, and the United Kingdom in 2015. *British journal of cancer,* **118**(8), pp. 1130-1141.

BUNIELLO, A., MACARTHUR, J.A.L., CEREZO, M., HARRIS, L.W., HAYHURST, J., MALANGONE, C., MCMAHON, A., MORALES, J., MOUNTJOY, E., SOLLIS, E., SUVEGES, D., VROUSGOU, O., WHETZEL, P.L., AMODE, R., GUILLEN, J.A., RIAT, H.S., TREVANION, S.J., HALL, P., JUNKINS, H., FLICEK, P., BURDETT, T., HINDORFF, L.A., CUNNINGHAM, F. and PARKINSON, H., 2019. The NHGRI-EBI GWAS Catalog of published genome-wide association studies, targeted arrays and summary statistics 2019. *Nucleic acids research,* **47**(D1), pp. D1005-D1012.

BURTON, M., ROSE, T., FÆRGEMAN, N. and KNUDSEN, J., 2005. Evolution of the acyl-CoA binding protein (ACBP). *Biochemical Journal,* **392**, pp. 299-307.

CAILLEAU, R., OLIVÉ, M. and CRUCIGER, Q.V.J., 1978. Long-term human breast carcinoma cell lines of metastatic origin: Preliminary characterization. *In vitro,* **14**(11), pp. 911-915.

CALAUTTI, E., GROSSI, M., MAMMUCARI, C., AOYAMA, Y., PIRRO, M., ONO, Y., LI, J. and DOTTO, G.P., 2002. Fyn tyrosine kinase is a downstream mediator of Rho/PRK2 function in keratinocyte cell–cell adhesion. *Journal of Cell Biology,* **156**(1), pp. 137-148.

CANCER RESEARCH UK, 2020-last update, About breast cancer staging and grade. Available: https://www.cancerresearchuk.org/about-cancer/breast-cancer/stages-types-grades/about-breast-cancer-staging-grades [04/20, 2021].

CANCER RESEARCH UK, 2017-last update, Breast Cancer Statistics. Available: https://www.cancerresearchuk.org/health-professional/cancer-statistics/statistics-by-cancer-type/breast-cancer [04/21, 2020].

CAREY, L.A., PEROU, C.M., LIVASY, C.A., DRESSLER, L.G., COWAN, D., CONWAY, K., KARACA, G., TROESTER, M.A., TSE, C.K., EDMISTON, S., DEMING, S.L., GERADTS, J., CHEANG, M.C., NIELSEN, T.O., MOORMAN, P.G., EARP, H.S. and MILLIKAN, R.C., 2006. Race, breast cancer subtypes, and survival in the Carolina Breast Cancer Study. *Jama,* **295**(21), pp. 2492-2502.

CERAMI, E., GAO, J., DOGRUSOZ, U., GROSS, B.E., SUMER, S.O., AKSOY, B.A., JACOBSEN, A., BYRNE, C.J., HEUER, M.L., LARSSON, E., ANTIPIN, Y., REVA, B., GOLDBERG, A.P., SANDER, C. and SCHULTZ, N., 2012. The cBio Cancer Genomics Portal: An Open Platform for Exploring Multidimensional Cancer Genomics Data. *CANCER DISCOVERY,* **2**(5), pp. 401.

CHADLI, A., GRAHAM, J.D., ABEL, M.G., JACKSON, T.A., GORDON, D.F., WOOD, W.M., FELTS, S.J., HORWITZ, K.B. and TOFT, D., 2006a. GCUNC-45 is a novel regulator for the progesterone receptor/hsp90 chaperoning pathway. *Molecular and cellular biology,* **26**(5), pp. 1722-1730.

CHADLI, A., GRAHAM, J.D., ABEL, M.G., JACKSON, T.A., GORDON, D.F., WOOD, W.M., FELTS, S.J., HORWITZ, K.B. and TOFT, D., 2006b. GCUNC-45 is a novel regulator for the

progesterone receptor/hsp90 chaperoning pathway. *Molecular and cellular biology,* **26**(5), pp. 1722-1730.

CHAN, J.Y., LAPARA, K. and YEE, D., 2016. Disruption of insulin receptor function inhibits proliferation in endocrine-resistant breast cancer cells. *Oncogene,* **35**(32), pp. 4235-4243.

CHAN, J.Y., HACKEL, B.J. and YEE, D., 2017. Targeting Insulin Receptor in Breast Cancer Using Small Engineered Protein Scaffolds. *Mol Cancer Ther,* **16**(7), pp. 1324.

CHANDRASHEKAR, D.S., BASHEL, B., BALASUBRAMANYA, S.A.H., CREIGHTON, C.J., PONCE-RODRIGUEZ, I., CHAKRAVARTHI, B.V.S.K. and VARAMBALLY, S., 2017. UALCAN: A Portal for Facilitating Tumor Subgroup Gene Expression and Survival Analyses. *Neoplasia (New York, N.Y.),* **19**(8), pp. 649-658.

CHAUDHARY, S.S., CHOUDHARY, S., RAWAT, S., AHIR, G., BILGRAMI, A.L. and ASHRAF, G.M., 2020. Chapter 11 - c-Met as a potential therapeutic target in triple negative breast cancer. In: S.P. GUPTA, ed, *Cancer-Leading Proteases.* Academic Press, pp. 295-326.

CHEAH, J.H., KIM, S.F., HESTER, L.D., CLANCY, K.W., PATTERSON, S.E., PAPADOPOULOS, V. and SNYDER, S.H., 2006. NMDA Receptor-Nitric Oxide Transmission Mediates Neuronal Iron Homeostasis via the GTPase Dexras1. *Neuron,* **51**(4), pp. 431-440.

CHEN, Y., PATEL, V., BANG, S., COHEN, N., MILLAR, J. and KIM, S.F., 2012. Maturation and Activity of Sterol Regulatory Element Binding Protein 1 Is Inhibited by Acyl-CoA Binding Domain Containing 3. *PLOS ONE,* **7**(11), pp. e49906.

CHENG, X., HUBER, T.L., CHEN, V.C., GADUE, P. and KELLER, G.M., 2008. NUMB Mediates the Interaction between Wnt and Notch to Modulate Primitive Erythropoietic Specification from the Hemangioblast. *Development (Cambridge, England),* **135**(20), pp. 3447-3458.

CHI, D., SINGHAL, H., LI, L., XIAO, T., LIU, W., PUN, M., JESELSOHN, R., HE, H., LIM, E., VADHI, R., RAO, P., LONG, H., GARBER, J. and BROWN, M., 2019. Estrogen receptor signaling is reprogrammed during breast tumorigenesis. *Proc Natl Acad Sci USA,* **116**(23), pp. 11437.

CHINTAMANI, SINGH, J.P., MITTAL, M.K., SAXENA, S., BANSAL, A., BHATIA, A. and KULSHRESHTHA, P., 2005. Role of p-glycoprotein expression in predicting response to neoadjuvant chemotherapy in breast cancer-a prospective clinical study. *World Journal of Surgical Oncology,* **3**(1), pp. 61.

CHOI, B.-., BANG, S., CHEN, Y., CHEAH, J.H. and KIM, S.F., 2013. PKA modulates iron trafficking in the striatum via small GTPase, Rhes. *Neuroscience,* **253**, pp. 214-220.

CIRIELLO, G., GATZA, M.L., BECK, A.H., WILKERSON, M.D., RHIE, S.K., PASTORE, A., ZHANG, H., MCLELLAN, M., YAU, C., KANDOTH, C., BOWLBY, R., SHEN, H., HAYAT, S., FIELDHOUSE, R., LESTER, S.C., TSE, G.M., FACTOR, R.E., COLLINS, L.C., ALLISON, K.H., CHEN, Y.Y., JENSEN, K., JOHNSON, N.B., OESTERREICH, S., MILLS, G.B., CHERNIACK, A.D., ROBERTSON, G., BENZ, C., SANDER, C., LAIRD, P.W., HOADLEY, K.A., KING, T.A., TCGA RESEARCH NETWORK and PEROU, C.M., 2015. Comprehensive Molecular Portraits of Invasive Lobular Breast Cancer. *Cell,* **163**(2), pp. 506-519.

CLAYTON, E.L., MINOGUE, S. and WAUGH, M.G., 2013. Mammalian phosphatidylinositol 4-kinases as modulators of membrane trafficking and lipid signaling networks. *Progress in lipid research,* **52**(3), pp. 294-304.

COGLIANO, V.J., BAAN, R., STRAIF, K., GROSSE, Y., LAUBY-SECRETAN, B., EL GHISSASSI, F., BOUVARD, V., BENBRAHIM-TALLAA, L., GUHA, N., FREEMAN, C., GALICHET, L. and WILD, C.P., 2011. Preventable Exposures Associated With Human Cancers. *JNCI: Journal of the National Cancer Institute,* **103**(24), pp. 1827-1839.

COLALUCA, I.N., TOSONI, D., NUCIFORO, P., SENIC-MATUGLIA, F., GALIMBERTI, V., VIALE, G., PECE, S. and DI FIORE, P.P., 2008. NUMB controls p53 tumour suppressor activity. *Nature,* **451**(7174), pp. 76-80.

COLANZI, A. and CORDA, D., 2007. Mitosis controls the Golgi and the Golgi controls mitosis. *Current opinion in cell biology; Membranes and organelles,* **19**(4), pp. 386-393.

CORSO, G., INTRA, M., TRENTIN, C., VERONESI, P. and GALIMBERTI, V., 2016. CDH1 germline mutations and hereditary lobular breast cancer. *Familial cancer,* **15**(2), pp. 215-219.

COSSON, P. and LETOURNEUR, F., 1997. Coatomer (COPI)-coated vesicles: role in intracellular transport and protein sorting. *Current opinion in cell biology,* **9**(4), pp. 484-487.

COSTELLO, J.L., CASTRO, I.G., SCHRADER, T.A., ISLINGER, M. and SCHRADER, M., 2017a. Peroxisomal ACBD4 interacts with VAPB and promotes ER-peroxisome associations. *Cell Cycle,* **16**(11), pp. 1039-1045.

COSTELLO, J.L., CASTRO, P.G., HACKER, C., SCHRADER, T.A., METZ, J., ZEUSCHNER, D., AZADI, A.S., GODINHO, L.F., COSTINA, V., FINDEISEN, P., MANNER, A., ISLINGER, M. and SCHRADER, M., 2017b. ACBD5 and VAPB mediate membrane associations between peroxisomes and the ER. *The Journal of cell biology,* **216**(2), pp. 331-342.

DAMASCHKE, N.A., GAWDZIK, J., AVILLA, M., YANG, B., SVAREN, J., ROOPRA, A., LUO, J., YU, Y.P., KELES, S. and JARRARD, D.F., 2020. CTCF loss mediates unique DNA hypermethylation landscapes in human cancers. *Clinical Epigenetics,* **12**(1), pp. 80.

DANNO, S., KUBOUCHI, K., MEHRUBA, M., ABE, M., NATSUME, R., SAKIMURA, K., EGUCHI, S., OKA, M., HIRASHIMA, M., YASUDA, H. and MUKAI, H., 2017. PKN2 is essential for mouse embryonic development and proliferation of mouse fibroblasts. *Genes to cells : devoted to molecular & cellular mechanisms,* **22**(2), pp. 220-236.

DAUTRY-VARSAT, A., CIECHANOVER, A. and LODISH, H.F., 1983. pH and the recycling of transferrin during receptor-mediated endocytosis. *Proc Natl Acad Sci USA,* **80**(8), pp. 2258.

DE JOUSSINEAU, C., SAHUT-BARNOLA, I., TISSIER, F., DUMONTET, T., DRELON, C., BATISSE-LIGNIER, M., TAUVERON, I., POINTUD, J., LEFRANÇOIS-MARTINEZ, A., STRATAKIS, C.A., BERTHERAT, J., VAL, P. and MARTINEZ, A., 2014. mTOR pathway is activated by PKA in adrenocortical cells and participates in vivo to apoptosis resistance in primary pigmented nodular adrenocortical disease (PPNAD). *Human molecular genetics,* **23**(20), pp. 5418-5428.

DENGLER, V.L., GALBRAITH, M. and ESPINOSA, J.M., 2014. Transcriptional regulation by hypoxia inducible factors. *Critical reviews in biochemistry and molecular biology,* **49**(1), pp. 1-15.

DESHMUKH, S.K., SRIVASTAVA, S.K., POOSARLA, T., DYESS, D.L., HOLLIDAY, N.P., SINGH, A.P. and SINGH, S., 2019. Inflammation, immunosuppressive microenvironment and breast cancer: opportunities for cancer prevention and therapy. *Annals of translational medicine,* **7**(20), pp. 593.

DOCQUIER, F., KITA, G.X., FARRAR, D., JAT, P., O'HARE, M., CHERNUKHIN, I., GRETTON, S., MANDAL, A., ALLDRIDGE, L. and KLENOVA, E., 2009. Decreased poly(ADP-ribosyl)ation of CTCF, a transcription factor, is associated with breast cancer phenotype and cell proliferation. *Clinical cancer research : an official journal of the American Association for Cancer Research,* **15**(18), pp. 5762-5771.

DOROBANTU, C.M., FORD-SILTZ, L.A., SITTIG, S.P., LANKE, K.H., BELOV, G.A., VAN KUPPEVELD, F.J. and VAN DER SCHAAR, H.M., 2015. GBF1- and ACBD3-independent recruitment of PI4KIIIβ to replication sites by rhinovirus 3A proteins. *Journal of virology,* **89**(3), pp. 1913-1918.

DOROBANTU, C.M., VAN DER SCHAAR, H.,M., FORD, L.A., STRATING, J.R.P.M., ULFERTS, R., FANG, Y., BELOV, G. and VAN KUPPEVELD, F.,J.M., 2014. Recruitment of PI4KIIIÎ² to coxsackievirus B3 replication organelles is independent of ACBD3, GBF1, and Arf1. *Journal of virology,* **88**(5), pp. 2725-2736.

DORRIS, J.R.,3rd and JONES, S., 2014. Everolimus in Breast Cancer: The Role of the Pharmacist. *The Annals of Pharmacotherapy,* **48**(9), pp. 1194-1201.

DREJER, K., 1992. The bioactivity of insulin analogues from in vitro receptor binding to in vivo glucose uptake. *Diabetes/metabolism reviews,* **8**(3), pp. 259-285.

DUFFY, M.J., SYNNOTT, N.C. and CROWN, J., 2018. Mutant p53 in breast cancer: potential as a therapeutic target and biomarker. *Breast cancer research and treatment,* **170**(2), pp. 213-219.

DUMITRU, I., NEITZ, A., ALFONSO, J. and MONYER, H., 2017. *Diazepam Binding Inhibitor Promotes Stem Cell Expansion Controlling Environment-Dependent Neurogenesis.*

DUPREZ, E., TONG, J., DÃ©RRÃ©, J., CHEN, S., BERGER, R., CHEN, Z. and LANOTTE, M., 1997. JEM-1, a novel gene encoding a leucine-zipper nuclear factor upregulated during retinoid-induced maturation of NB4 promyelocytic leukaemia. *Oncogene,* **14**, pp. 1563.

EIGER, D., AGOSTINETTO, E., SAÚDE-CONDE, R. and DE AZAMBUJA, E., 2021. The Exciting New Field of HER2-Low Breast Cancer Treatment. *Cancers,* **13**(5), pp. 1015. doi: 10.3390/cancers13051015.

EISA, N.H., JILANI, Y., KAINTH, K., REDD, P., LU, S., BOUGRINE, O., ABDUL SATER, H., PATWARDHAN, C.A., SHULL, A., SHI, H., LIU, K., ELSHERBINY, N.M., EISSA, L.A., EL-SHISHTAWY, M.M., HORUZSKO, A., BOLLAG, R., MAIHLE, N., ROIG, J., KORKAYA, H., COWELL, J.K. and CHADLI, A., 2019. The co-chaperone UNC45A is essential for the

expression of mitotic kinase NEK7 and tumorigenesis. *The Journal of biological chemistry,* **294**(14), pp. 5246-5260.

ELUSTONDO, P., MARTIN, L.A. and KARTEN, B., 2017. Mitochondrial cholesterol import. *Biochimica et Biophysica Acta (BBA) - Molecular and Cell Biology of Lipids; Lipids of Mitochondria,* **1862**(1), pp. 90-101.

EPPING, M.T., MEIJER, L.A., BOS, J.L. and BERNARDS, R., 2009. UNC45A confers resistance to histone deacetylase inhibitors and retinoic acid. *Molecular cancer research : MCR,* **7**(11), pp. 1861-1870.

FÆRGEMAN, N.J. and KNUDSEN, J., 1997. Role of long-chain fatty acyl-CoA esters in the regulation of metabolism and in cell signalling. *Biochem J,* **323**(1), pp. 1.

FÆRGEMAN, N.J., SIGURSKJOLD, B.W., KRAGELUND, B.B., ANDERSEN, K.V. and KNUDSEN, J., 1996. Thermodynamics of Ligand Binding to Acyl-Coenzyme A Binding Protein Studied by Titration Calorimetry. *Biochemistry,* **35**(45), pp. 14118-14126.

FALK, J.D., PIERFRANCESCO, V., FOYE, P.E., HIROSHI, U., JULIO, P., DANIELSON, P.E., LERNER, D.L., JUAN, B. and GREGOR, S.J., 1999. Rhes: A striatal-specific Ras homolog related to Dexras1. *Journal of neuroscience research,* **57**(6), pp. 782-788.

FAN, J., LIU, J., CULTY, M. and PAPADOPOULOS, V., 2010. Acyl-coenzyme A binding domain containing 3 (ACBD3; PAP7; GCP60): An emerging signalling molecule. *Progress in lipid research,* **49**(3), pp. 218-234.

FECCHI, K., VOLONTE, D., HEZEL, M.P., SCHMECK, K. and GALBIATI, F., 2006. Spatial and temporal regulation of GLUT4 translocation by flotillin-1 and caveolin-3 in skeletal muscle cells. *FASEB journal : official publication of the Federation of American Societies for Experimental Biology,* **20**(6), pp. 705-707.

FEKETE, J.T. and GYŐRFFY, B., 2019. ROCplot.org: Validating predictive biomarkers of chemotherapy/hormonal therapy/anti-HER2 therapy using transcriptomic data of 3,104 breast cancer patients. *International journal of cancer,* **145**(11), pp. 3140-3151.

FERDINANDUSSE, S., FALKENBERG, K.D., KOSTER, J., MOOYER, P.A., JONES, R., VAN ROERMUND, C.,W.T., PIZZINO, A., SCHRADER, M., WANDERS, R.J.A., VANDERVER, A. and WATERHAM, H.R., 2017. ACBD5 deficiency causes a defect in peroxisomal very long-chain fatty acid metabolism. *J Med Genet,* **54**(5), pp. 330.

FERRÉ, P. and FOUFELLE, F., 2007. SREBP-1c Transcription Factor and Lipid Homeostasis: Clinical Perspective. *Hormone Research in Paediatrics,* **68**(2), pp. 72-82.

FILIPPINI, S.E. and VEGA, A., 2013. Breast cancer genes: beyond BRCA1 and BRCA2. *Frontiers in bioscience (Landmark edition),* **18**, pp. 1358-1372.

FINLAY-SCHULTZ, J., JACOBSEN, B.M., RILEY, D., PAUL, K.V., TURNER, S., FERREIRA-GONZALEZ, A., HARRELL, J.C., KABOS, P. and SARTORIUS, C.A., 2020. New generation breast cancer cell lines developed from patient-derived xenografts. *Breast Cancer Research,* **22**(1), pp. 68.

FISHILEVICH, S., NUDEL, R., RAPPAPORT, N., HADAR, R., PLASCHKES, I., INY STEIN, T., ROSEN, N., KOHN, A., TWIK, M., SAFRAN, M., LANCET, D. and COHEN, D., 2017. GeneHancer: genome-wide integration of enhancers and target genes in GeneCards. *Database : the journal of biological databases and curation,* **2017**, pp. 10.1093/database/bax028.

FLEVARIS, P. and VAUGHAN, D., 2017. The Role of Plasminogen Activator Inhibitor Type-1 in Fibrosis. *Seminars in thrombosis and hemostasis,* **43**(2), pp. 169-177.

FRAILE, E.A., CHAVDOULA, E., LALIOTIS, G.I., ANASTAS, V., SEREBRENNIKOVA, O., PARASKEVOPOULOU, M.D. and TSICHLIS, P.N., 2020. The inhibition of KDM2B promotes the differentiation of basal-like breast cancer cells via the posttranslational destabilization of SLUG. *bioRxiv,* , pp. 2020.05.21.109819.

FRISCH, S.M. and FRANCIS, H., 1994. Disruption of epithelial cell-matrix interactions induces apoptosis. *The Journal of cell biology,* **124**(4), pp. 619-626.

FRITTOLI, E., PALAMIDESSI, A., MARIGHETTI, P., CONFALONIERI, S., BIANCHI, F., MALINVERNO, C., MAZZAROL, G., VIALE, G., MARTIN-PADURA, I., GARRÉ, M., PARAZZOLI, D., MATTEI, V., CORTELLINO, S., BERTALOT, G., DI FIORE, P.P. and SCITA, G., 2014. A RAB5/RAB4 recycling circuitry induces a proteolytic invasive program and promotes tumor dissemination. *The Journal of cell biology,* **206**(2), pp. 307-328.

FUMAGALLI, S., TOTTY, N.F., HSUAN, J.J. and COURTNEIDGE, S.A., 1994. A target for Src in mitosis. *Nature,* **368**(6474), pp. 871-874.

GAO, J., AKSOY, B.A., DOGRUSOZ, U., DRESDNER, G., GROSS, B., SUMER, S.O., SUN, Y., JACOBSEN, A., SINHA, R., LARSSON, E., CERAMI, E., SANDER, C. and SCHULTZ, N., 2013. Integrative analysis of complex cancer genomics and clinical profiles using the cBioPortal. *Science signaling,* **6**(269), pp. pl1.

GARCÍA-HEREDIA, J.M., VERDUGO SIVIANES, E.M., LUCENA-CACACE, A., MOLINA-PINELO, S. and CARNERO, A., 2016. Numb-like (NumbL) downregulation increases tumorigenicity, cancer stem cell-like properties and resistance to chemotherapy. *Oncotarget,* **7**(39), pp. 63611-63628.

GARCÍA-TUÑÓN, I., RICOTE, M., RUIZ, A., FRAILE, B., PANIAGUA, R. and ROYUELA, M., 2003. Interleukin-2 and its receptor complex (α, β and γ chains) in in situand infiltrative human breast cancer: an immunohistochemical comparative study. *Breast Cancer Research,* **6**(1), pp. R1.

GARRIDO, P., OSORIO, F.G., MORÃ¡N, J., CABELLO, E., ALONSO, A., FREIJE, J.M. and GONZÃ¡LEZ, C., 2015. Loss of GLUT4 induces metabolic reprogramming and impairs viability of breast cancer cells. *Journal of cellular physiology,* **230**(1), pp. 191-198.

GASTEIGER, E., GATTIKER, A., HOOGLAND, C., IVANYI, I., APPEL, R.D. and BAIROCH, A., 2003. ExPASy: The proteomics server for in-depth protein knowledge and analysis. *Nucleic acids research,* **31**(13), pp. 3784-3788.

GATLIFF, J., EAST, D.A., SINGH, A., ALVAREZ, M.S., FRISON, M., MATIC, I., FERRAINA, C., SAMPSON, N., TURKHEIMER, F. and CAMPANELLA, M., 2017. A role for TSPO in

mitochondrial Ca2+ homeostasis and redox stress signaling. *Cell Death &Amp; Disease,* **8**, pp. e2896.

GEISBRECHT, B.V., ZHANG, D., SCHULZ, H. and GOULD, S.J., 1999. Characterization of PECI, a Novel Monofunctional Î”3,Î”2-Enoyl-CoA Isomerase of Mammalian Peroxisomes. *Journal of Biological Chemistry,* **274**(31), pp. 21797-21803.

GENERALI, D., BERRUTI, A., BRIZZI, M.P., CAMPO, L., BONARDI, S., WIGFIELD, S., BERSIGA, A., ALLEVI, G., MILANI, M., AGUGGINI, S., GANDOLFI, V., DOGLIOTTI, L., BOTTINI, A., HARRIS, A.L. and FOX, S.B., 2006. Hypoxia-inducible factor-1alpha expression predicts a poor response to primary chemoendocrine therapy and disease-free survival in primary human breast cancer. *Clinical cancer research : an official journal of the American Association for Cancer Research,* **12**(15), pp. 4562-4568.

GINESTIER, C., HUR, M.H., CHARAFE-JAUFFRET, E., MONVILLE, F., DUTCHER, J., BROWN, M., JACQUEMIER, J., VIENS, P., KLEER, C.G., LIU, S., SCHOTT, A., HAYES, D., BIRNBAUM, D., WICHA, M.S. and DONTU, G., 2007. ALDH1 is a marker of normal and malignant human mammary stem cells and a predictor of poor clinical outcome. *Cell stem cell,* **1**(5), pp. 555-567.

GOH, J.Y., FENG, M., WANG, W., OGUZ, G., YATIM, S.M.J.M., LEE, P.L., BAO, Y., LIM, T.H., WANG, P., TAM, W.L., KODAHL, A.R., LYNG, M.B., SARMA, S., LIN, S.Y., LEZHAVA, A., YAP, Y.S., LIM, A.S.T., HOON, D.S.B., DITZEL, H.J., LEE, S.C., TAN, E.Y. and YU, Q., 2017. Chromosome 1q21.3 amplification is a trackable biomarker and actionable target for breast cancer recurrence. *Nature medicine,* **23**, pp. 1319.

GOVERS, R., 2014. Cellular regulation of glucose uptake by glucose transporter GLUT4. *Advances in clinical chemistry,* **66**, pp. 173-240.

GRENINGER, A.L., KNUDSEN, G.M., BETEGON, M., BURLINGAME, A.L. and DERISI, J.L., 2013. *ACBD3 interaction with TBC1 domain 22 protein is differentially affected by enteroviral and kobuviral 3A protein binding.*

GRIMM, S.L. and ROSEN, J.M., 2003. The Role of C/EBPβ in Mammary Gland Development and Breast Cancer. *Journal of mammary gland biology and neoplasia,* **8**(2), pp. 191-204.

GRUBER, G., GREINER, R.H., HLUSHCHUK, R., AEBERSOLD, D.M., ALTERMATT, H.J., BERCLAZ, G. and DJONOV, V., 2004. Hypoxia-inducible factor 1 alpha in high-risk breast cancer: an independent prognostic parameter? *Breast cancer research : BCR,* **6**(3), pp. R191-8.

GUIDOTTI, A., FORCHETTI, C.M., CORDA, M.G., KONKEL, D., BENNETT, C.D. and COSTA, E., 1983. Isolation, characterization, and purification to homogeneity of an endogenous polypeptide with agonistic action on benzodiazepine receptors. *Proceedings of the National Academy of Sciences of the United States of America,* **80**(11), pp. 3531-3535.

GUO, H., ZHANG, C., LIU, Q., LI, Q., LIAN, G., WU, D., LI, X., ZHANG, W., SHEN, Y., YE, Z., LIN, S. and LIN, S., 2012. The Axin/TNKS complex interacts with KIF3A and is required for insulin-stimulated GLUT4 translocation. *Cell research,* **22**, pp. 1246.

GUO, M., JAN, L.Y. and JAN, Y.N., 1996. Control of Daughter Cell Fates during Asymmetric Division: Interaction of Numb and Notch. *Neuron,* **17**(1), pp. 27-41.

GUO, W., CHEN, D., FAN, Z. and EPSTEIN, H.F., 2011. Differential turnover of myosin chaperone UNC-45A isoforms increases in metastatic human breast cancer. *Journal of Molecular Biology,* **412**(3), pp. 365-378.

HAIKARAINEN, T., KRAUSS, S. and LEHTIO, L., 2014. Tankyrases: structure, function and therapeutic implications in cancer. *Current pharmaceutical design,* **20**(41), pp. 6472-6488.

HALSTED, W.S., 1907. The results of radical operations for the cure of cancer of the breast. *Trans Am Surg Assoc,* **25**, pp. 61-79.

HAMATANI, K., EGUCHI, H., KOYAMA, K., MUKAI, M., NAKACHI, K. and KUSUNOKI, Y., 2014. A novel RET rearrangement (ACBD5/RET) by pericentric inversion. *inv(10)(p12.1;q11.2), in papillary thyroid cancer from an atomic bomb survivor exposed to high-dose radiation.{Oncology} {Reports},* (32),.

HAN, X., DIAO, L., XU, Y., XUE, W., OUYANG, T., LI, J., WANG, T., FAN, Z., FAN, T., LIN, B. and XIE, Y., 2014. Association between the HER2 Ile655Val polymorphism and response to trastuzumab in women with operable primary breast cancer. *Annals of oncology : official journal of the European Society for Medical Oncology,* **25**(6), pp. 1158-1164.

HANAHAN, D. and WEINBERG, R.A., 2011. Hallmarks of Cancer: The Next Generation. *Cell,* **144**(5), pp. 646-674.

HANAHAN, D. and WEINGBERG, R., 2000. The hallmarks of cancer. *Cell,* **100**(1), pp. 57-70.

HARE, S.H., 2018. *The Development and Characterisation of Everolimus Resistant Breast Cancer Cells.* PhD edn. Uxbridge, London, UK: Brunel University London.

HARE, S.H. and HARVEY, A.J., 2017. *mTOR function and therapeutic targeting in breast cancer.*

HARRISON, L.M., 2012. Rhes: A GTPâ€“Binding Protein Integral to Striatal Physiology and Pathology. *Cellular and molecular neurobiology,* **32**(6), pp. 907-918.

HE, J., KALLIN, E.M., TSUKADA, Y. and ZHANG, Y., 2008. The H3K36 demethylase Jhdm1b/Kdm2b regulates cell proliferation and senescence through p15(Ink4b). *Nature structural & molecular biology,* **15**(11), pp. 1169-1175.

HEIDEMANN, J., OGAWA, H., DWINELL, M.B., RAFIEE, P., MAASER, C., GOCKEL, H.R., OTTERSON, M.F., OTA, D.M., LUGERING, N., DOMSCHKE, W. and BINION, D.G., 2003. Angiogenic effects of interleukin 8 (CXCL8) in human intestinal microvascular endothelial cells are mediated by CXCR2. *The Journal of biological chemistry,* **278**(10), pp. 8508-8515.

HOLLIER, B.G., TINNIRELLO, A.A., WERDEN, S.J., EVANS, K.W., TAUBE, J.H., SARKAR, T.R., SPHYRIS, N., SHARIATI, M., KUMAR, S.V., BATTULA, V.L., HERSCHKOWITZ, J.I., GUERRA, R., CHANG, J.T., MIURA, N., ROSEN, J.M. and MANI, S.A., 2013. FOXC2 expression links epithelial-mesenchymal transition and stem cell properties in breast cancer. *Cancer research,* **73**(6), pp. 1981-1992.

HOROVA, V., LYOO, H., RÓŻYCKI, B., CHALUPSKA, D., SMOLA, M., HUMPOLICKOVA, J., STRATING, J.R.P.M., VAN KUPPEVELD, F.,J.M., BOURA, E. and KLIMA, M., 2019. Convergent evolution in the mechanisms of ACBD3 recruitment to picornavirus replication sites. *PLoS pathogens,* **15**(8), pp. e1007962-e1007962.

HORTOBAGYI, G.N., 2015. *Everolimus Plus Exemestane for the Treatment of Advanced Breast Cancer: A Review of Subanalyses from BOLERO-2.*

HOUGHTON-GISBY, J. and HARVEY, A.J., 2020. ACBD3, its Cellular Interactors, and its role in Breast Cancer. *Cancer Studies and Therapeutics,* **5**(2), pp. 1-7.

HOWE, L.R. and BROWN, A.M., 2004. Wnt signaling and breast cancer. *Cancer biology & therapy,* **3**(1), pp. 36-41.

HUANG, S.A., MISHINA, Y.M., LIU, S., CHEUNG, A., STEGMEIER, F., MICHAUD, G.A., CHARLAT, O., WIELLETTE, E., ZHANG, Y., WIESSNER, S., HILD, M., SHI, X., WILSON, C.J., MICKANIN, C., MYER, V., FAZAL, A., TOMLINSON, R., SERLUCA, F., SHAO, W., CHENG, H., SHULTZ, M., RAU, C., SCHIRLE, M., SCHLEGL, J., GHIDELLI, S., FAWELL, S., LU, C., CURTIS, D., KIRSCHNER, M.W., LENGAUER, C., FINAN, P.M., TALLARICO, J.A., BOUWMEESTER, T., PORTER, J.A., BAUER, A. and CONG, F., 2009. Tankyrase inhibition stabilizes axin and antagonizes Wnt signalling. *Nature,* **461**(7264), pp. 614-620.

HUANG, Y., YANG, L., PEI, Y., WANG, J., WU, H., YUAN, J. and WANG, L., 2018. Overexpressed ACBD3 has prognostic value in human breast cancer and promotes the self-renewal potential of breast cancer cells by activating the Wnt/beta-catenin signaling pathway. *Experimental cell research,* **363**(1), pp. 39-47.

HVID, H., BLOUIN, M.J., BIRMAN, E., DAMGAARD, J., POULSEN, F., FELS, J.J., FLEDELIUS, C., HANSEN, B.F. and POLLAK, M., 2013. Treatment with insulin analog X10 and IGF-1 increases growth of colon cancer allografts. *PloS one,* **8**(11), pp. e79710.

INIC, Z., ZEGARAC, M., INIC, M., MARKOVIC, I., KOZOMARA, Z., DJURISIC, I., INIC, I., PUPIC, G. and JANCIC, S., 2014. Difference between Luminal A and Luminal B Subtypes According to Ki-67, Tumor Size, and Progesterone Receptor Negativity Providing Prognostic Information. *Clinical Medicine Insights.Oncology,* **8**, pp. 107-111.

ITKONEN, H.M., BROWN, M., URBANUCCI, A., TREDWELL, G., HO LAU, C., BARFELD, S., HART, C., GULDVIK, I.J., TAKHAR, M., HEEMERS, H.V., ERHO, N., BLOCH, K., DAVICIONI, E., DERUA, R., WAELKENS, E., MOHLER, J.L., CLARKE, N., SWINNEN, J.V., KEUN, H.C., REKVIG, O.P. and MILLS, I.G., 2017. Lipid degradation promotes prostate cancer cell survival. *Oncotarget,* **8**(24), pp. 38264-38275.

IVELL, R. and BALVERS, M., 2001. The evolution of the endozepine-like peptide (ELP) in the mammalian testis. *Zucht hygeine (Reproduction in domestic animals),* **36**(3-4), pp. 153-6.

IVELL, R., PUSCH, W., BALVERS, M., VALENTIN, M., WALTHER, N. and WEINBAUER, G., 2000. Progressive inactivation of the haploid expressed gene for the sperm-specific endozepine-like peptide (ELP) through primate evolution. *Gene,* **255**(2), pp. 335-345.

JALAL, N., SURENDRANATH, A.R., PATHAK, J.L., YU, S. and CHUNG, C.Y., 2017. Bisphenol A (BPA) the mighty and the mutagenic. *Toxicology reports,* **5**, pp. 76-84.

KAKUTA, K., ORINO, K., YAMAMOTO, S. and WATANABE, K., 1997. High Levels of Ferritin and its Iron in Fetal Bovine Serum. *Comparative Biochemistry and Physiology Part A: Physiology,* **118**(1), pp. 165-169.

KELLEY, L.A., MEZULIS, S., YATES, C.M., WASS, M.N. and STERNBERG, M.J.E., 2015. The Phyre2 web portal for protein modeling, prediction and analysis. *Nature Protocols,* **10**, pp. 845.

KEYDAR, I., CHEN, L., KARBY, S., WEISS, F.R., DELAREA, J., RADU, M., CHAITCIK, S. and BRENNER, H.J., 1979. Establishment and characterization of a cell line of human breast carcinoma origin. *European journal of cancer,* **15**(5), pp. 659-670.

KHALIL, B., TAÏB, B., LIONEL, B., SHANGANG, Z., DEMETRA, R., DITTE, N., SUSANNE, M., FAERGEMAN, N.J. and THIERRY, A., 2015. A novel role for central ACBP/DBI as a regulator of longâ€• chain fatty acid metabolism in astrocytes. *Journal of neurochemistry,* **133**(2), pp. 253-265.

KIM, H.S., LEE, K., KIM, S., CHO, S., SHIN, H.J., KIM, C. and KIM, J., 2018. Arrayed CRISPR screen with image-based assay reliably uncovers host genes required for coxsackievirus infection. *Genome research,* **28**(6), pp. 859-868.

KIM, M.K., 2018. Novel insight into the function of tankyrase. *Oncology letters,* **16**(6), pp. 6895-6902.

KIM, Y.N., KOO, K.H., SUNG, J.Y., YUN, U.J. and KIM, H., 2012. Anoikis resistance: an essential prerequisite for tumor metastasis. *International journal of cell biology,* **2012**, pp. 306879.

KIRCHNER, G.I., MEIER-WIEDENBACH, I. and MANNS, M.P., 2004. Clinical Pharmacokinetics of Everolimus. *Clinical pharmacokinetics,* **43**(2), pp. 83-95.

KLIMA, M., CHALUPSKA, D., RÓŻYCKI, B., HUMPOLICKOVA, J., REZABKOVA, L., SILHAN, J., BAUMLOVA, A., DUBANKOVA, A. and BOURA, E., 2017. Kobuviral Non-structural 3A Proteins Act as Molecular Harnesses to Hijack the Host ACBD3 Protein. *Structure,* **25**(2), pp. 219-230.

KLIMA, M., TÓTH, D.,J., HEXNEROVA, R., BAUMLOVA, A., CHALUPSKA, D., TYKVART, J., REZABKOVA, L., SENGUPTA, N., MAN, P., DUBANKOVA, A., HUMPOLICKOVA, J., NENCKA, R., VEVERKA, V., BALLA, T. and BOURA, E., 2016. Structural insights and in vitro reconstitution of membrane targeting and activation of human PI4KB by the ACBD3 protein. *Scientific Reports,* **6**, pp. 23641.

KOO, T.K. and LI, M.Y., 2016. A Guideline of Selecting and Reporting Intraclass Correlation Coefficients for Reliability Research. *Journal of chiropractic medicine,* **15**(2), pp. 155-163.

KOREISHI, M., GNIADEK, T.J., YU, S., MASUDA, J., HONJO, Y. and SATOH, A., 2013. The golgin tether giantin regulates the secretory pathway by controlling stack organization within Golgi apparatus. *PloS one,* **8**(3), pp. e59821.

KOSE, K.N., XIE, J.F., CARNES, D.L. and GRAVES, D.T., 1996. Pro-inflammatory cytokines downregulate platelet derived growth factor-alpha receptor gene expression in human osteoblastic cells. *Journal of cellular physiology,* **166**(1), pp. 188-197.

KOTTAKIS, F., FOLTOPOULOU, P., SANIDAS, I., KELLER, P., WRONSKI, A., DAKE, B.T., EZELL, S.A., SHEN, Z., NABER, S.P., HINDS, P.W., MCNIEL, E., KUPERWASSER, C. and TSICHLIS, P.N., 2014. NDY1/KDM2B functions as a master regulator of polycomb complexes and controls self-renewal of breast cancer stem cells. *Cancer research,* **74**(14), pp. 3935-3946.

KRAGELUND, B.B., ANDERSEN, K.V., MADSEN, J.C., KNUDSEN, J. and POULSEN, F.M., 1993. Three-dimensional structure of the complex between acyl-coenzyme A binding protein and palmitoyl-coenzyme A. *Journal of Molecular Biology,* **230**(4), pp. 1260-1277.

KRAGELUND, B.B., KNUDSEN, J. and POULSEN, F.M., 1999. *Acyl-coenzyme A binding protein (ACBP).*

KRAGELUND, B.B., POULSEN, K., ANDERSEN, K.V., BALDURSSON, T., KRØLL, J.B., NEERGÅRD, T.B., JEPSEN, J., ROEPSTORFF, P., KRISTIANSEN, K., POULSEN, F.M. and KNUDSEN, J., 1999. Conserved Residues and Their Role in the Structure, Function, and Stability of Acyl-Coenzyme A Binding Protein. *Biochemistry,* **38**(8), pp. 2386-2394.

KRISHNA, B.M., CHAUDHARY, S., PANDA, A.K., MISHRA, D.R. and MISHRA, S.K., 2018. Her2 (Ile)655(Val) polymorphism and its association with breast cancer risk: an updated meta-analysis of case-control studies. *Scientific reports,* **8**(1), pp. 7427-018-25769-y.

KRUEGER, K.E. and PAPADOPOULOS, V., 1990. Peripheral-type benzodiazepine receptors mediate translocation of cholesterol from outer to inner mitochondrial membranes in adrenocortical cells. *Journal of Biological Chemistry,* **265**(25), pp. 15015-15022.

KUCHENBAECKER, K.B., HOPPER, J.L., BARNES, D.R., PHILLIPS, K., MOOIJ, T.M., ROOS-BLOM, M., JERVIS, S., VAN LEEUWEN, F.E., MILNE, R.L., ANDRIEU, N., GOLDGAR, D.E., TERRY, M.B., ROOKUS, M.A., EASTON, D.F., ANTONIOU, A.C. and AND THE BRCA1 AND BRCA2,COHORT CONSORTIUM, 2017. Risks of Breast, Ovarian, and Contralateral Breast Cancer for BRCA1 and BRCA2 Mutation Carriers. *JAMA,* **317**(23), pp. 2402-2416.

KUHN, D.J. and DOU, Q.P., 2005. The role of interleukin-2 receptor alpha in cancer. *Frontiers in bioscience : a journal and virtual library,* **10**, pp. 1462-1474.

KUMAR, A., MUZIK, O., SHANDAL, V., CHUGANI, D., CHAKRABORTY, P. and CHUGANI, H.T., 2012. Evaluation of age-related changes in translocator protein (TSPO) in human brain using 11C-R]-PK11195 PET. *Journal of Neuroinflammation,* **9**(1), pp. 232.

KURZEJAMSKA, E., JOHANSSON, J., JIRSTRÖM, K., PRAKASH, V., ANANTHASESHAN, S., BOON, L., FUXE, J. and RELIGA, P., 2014. C/EBPβ expression is an independent predictor of overall survival in breast cancer patients by MHCII/CD4-dependent mechanism of metastasis formation. *Oncogenesis,* **3**(11), pp. e125-e125.

LACHMANN, S., JEVONS, A., DE RYCKER, M., CASAMASSIMA, A., RADTKE, S., COLLAZOS, A. and PARKER, P.J., 2011. Regulatory Domain Selectivity in the Cell-Type Specific PKN-Dependence of Cell Migration. *PLOS ONE,* **6**(7), pp. e21732.

LAIRD, P.W., 2003. The power and the promise of DNA methylation markers. *Nature Reviews Cancer,* **3**(4), pp. 253-266.

LAMB, C.A., VANZULLI, S.I. and LANARI, C., 2019. Hormone receptors in breast cancer: more than estrogen receptors. *Medicina,* **79**(Spec 6/1), pp. 540-545.

LAN, Y., ZHANG, N., LIU, H., XU, J. and JIANG, R., 2016. Golgb1 regulates protein glycosylation and is crucial for mammalian palate development. *Development (Cambridge, England),* **143**(13), pp. 2344-2355.

LANFRAY, D., CARON, A., ROY, M., LAPLANTE, M., MORIN, F., LEPRINCE, J., TONON, M. and RICHARD, D., 2016. *Involvement of the Acyl-CoA binding domain containing 7 in the control of food intake and energy expenditure in mice.*

LANFRAY, D. and RICHARD, D., 2017. Emerging Signaling Pathway in Arcuate Feeding-Related Neurons: Role of the Acbd7. *Frontiers in Neuroscience,* **11**, pp. 328.

LASFARGUES, E.Y., COUTINHO, W.G. and REDFIELD, E.S., 1978. Isolation of two human tumor epithelial cell lines from solid breast carcinomas. *Journal of the National Cancer Institute,* **61**(4), pp. 967-978.

LASFARGUES, E.Y. and OZZELLO, L., 1958. Cultivation of Human Breast Carcinomas. *Journal of the National Cancer Institute,* **21**(6), pp. 1131-1147.

LAUGHNER, E., TAGHAVI, P., CHILES, K., MAHON, P.C. and SEMENZA, G.L., 2001. HER2 (neu) signaling increases the rate of hypoxia-inducible factor 1alpha (HIF-1alpha) synthesis: novel mechanism for HIF-1-mediated vascular endothelial growth factor expression. *Molecular and cellular biology,* **21**(12), pp. 3995-4004.

LEE, D.S., YOON, S.Y., LOOI, L.M., KANG, P., KANG, I.N., SIVANANDAN, K., ARIFFIN, H., THONG, M.K., CHIN, K.F., MOHD TAIB, N.A., YIP, C.H. and TEO, S.H., 2012. Comparable frequency of BRCA1, BRCA2 and TP53 germline mutations in a multi-ethnic Asian cohort suggests TP53 screening should be offered together with BRCA1/2 screening to early-onset breast cancer patients. *Breast cancer research : BCR,* **14**(2), pp. R66.

LEE, E., VAUGHAN, D.E., PARIKH, S.H., GRODZINSKY, A.J., LIBBY, P., LARK, M.W. and LEE, R.T., 1996. Regulation of Matrix Metalloproteinases and Plasminogen Activator Inhibitor-1 Synthesis by Plasminogen in Cultured Human Vascular Smooth Muscle Cells. *Circulation research,* **78**(1), pp. 44-49.

LEE, S.C., HOU, M.F., HSIEH, P.C., WU, S.H., HOU, L.A., MA, H., TSAI, S.M. and TSAI, L.Y., 2008. A case-control study of the HER2 Ile655Val polymorphism and risk of breast cancer in Taiwan. *Clinical biochemistry,* **41**(3), pp. 121-125.

LI, H., DEGENHARDT, B., TOBIN, D., YAO, Z., TASKEN, K. and PAPADOPOULOS, V., 2001. Identification, Localization, and Function in Steroidogenesis of PAP7: A Peripheral-Type

Benzodiazepine Receptor- and PKA (RIalpha)-Associated Protein. *Molecular Endocrinology,* **15**(12), pp. 2211-2228.

LI, J., HOUSEKNECHT, K.L., STENBIT, A.E., KATZ, E.B. and CHARRON, M.J., 2000. Reduced glucose uptake precedes insulin signaling defects in adipocytes from heterozygous GLUT4 knockout mice. *The FASEB Journal,* **14**(9), pp. 1117-1125.

LIAO, J., GUAN, Y., CHEN, W., SHI, C., YAO, D., WANG, F., LAM, S.M., SHUI, G. and CAO, X., 2019. ACBD3 is required for FAPP2 transferring glucosylceramide through maintaining the Golgi integrity. *Journal of molecular cell biology,* **11**(2), pp. 107-117.

LIAO, J., ZENG, S.X., ZHOU, X. and LU, H., 2012. Global Effect of Inauhzin on Human p53-Responsive Transcriptome. *PLoS ONE,* **7**(12), pp. e52172.

LIMAME, R., DE BEECK, K.O., VAN LAERE, S., CROES, L., DE WILDE, A., DIRIX, L., VAN CAMP, G., PEETERS, M., DE WEVER, O., LARDON, F. and PAUWELS, P., 2014. *Expression profiling of migrated and invaded breast cancer cells predicts early metastatic relapse and reveals KrÃ¼ppel-like factor 9 as a potential suppressor of invasive growth in breast cancer.*

LIPSA, A., KOWTAL, P. and SARIN, R., 2019. Novel germline STK11 variants and breast cancer phenotype identified in an Indian cohort of Peutz-Jeghers syndrome. *Human molecular genetics,* **28**(11), pp. 1885-1893.

LIS, A., BARONE, T.A., PARADKAR, P.N., PLUNKETT, R.J. and ROTH, J.A., 2004. Expression and localization of different forms of DMT1 in normal and tumor astroglial cells. *Brain research.Molecular brain research,* **122**(1), pp. 62-70.

LIU, J., RONE, M.B. and PAPADOPOULOS, V., 2006. Protein-protein interactions mediate mitochondrial cholesterol transport and steroid biosynthesis. *The Journal of biological chemistry,* **281**(50), pp. 38879-38893.

LIU, J., MATYAKHINA, L., HAN, Z., SANDRINI, F., BEI, T., STRATAKIS, C.A. and PAPADOPOULOS, V., 2003. Molecular cloning, chromosomal localization of human peripheral-type benzodiazepine receptor and PKA regulatory subunit type 1A (PRKAR1A)-associated protein PAP7, and studies in PRKAR1A mutant cells and tissues. *The FASEB Journal,* **17**(9), pp. 1189-1191.

LIU, S. and STORRIE, B., 2012. Are Rab proteins the link between Golgi organization and membrane trafficking? *Cellular and Molecular Life Sciences,* **69**(24), pp. 4093-4106.

LIU, Y., TAMIMI, R.M., COLLINS, L.C., SCHNITT, S.J., GILMORE, H.L., CONNOLLY, J.L. and COLDITZ, G.A., 2011. The association between vascular endothelial growth factor expression in invasive breast cancer and survival varies with intrinsic subtypes and use of adjuvant systemic therapy: results from the Nurses' Health Study. *Breast cancer research and treatment,* **129**(1), pp. 175-184.

LIU, Y., KAHN, R.A. and PRESTEGARD, J.H., 2014. Interaction of Fapp1 with Arf1 and PI4P at a membrane surface: an example of coincidence detection. *Structure,* **22**(3), pp. 421-430.

LIU, Z.J., SEMENZA, G.L. and ZHANG, H.F., 2015. Hypoxia-inducible factor 1 and breast cancer metastasis. *Journal of Zhejiang University.Science.B,* **16**(1), pp. 32-43.

LU, H., LEI, Z., LU, Z., LU, Q., LU, C., CHEN, W., WANG, C., TANG, Q. and KONG, Q., 2013. Silencing tankyrase and telomerase promotes A549 human lung adenocarcinoma cell apoptosis and inhibits proliferation. *Oncology Reports,* **30**(4), pp. 1745-1752.

LU, L., GAO, Y., ZHANG, Z., CAO, Q., ZHANG, X., ZOU, J. and CAO, Y., 2015. Kdm2a/b Lysine Demethylases Regulate Canonical Wnt Signaling by Modulating the Stability of Nuclear β-Catenin. *Developmental cell,* **33**(6), pp. 660-674.

LU, Y., ZI, X. and POLLAK, M., 2004. Molecular mechanisms underlying IGF-I-induced attenuation of the growth-inhibitory activity of trastuzumab (Herceptin) on SKBR3 breast cancer cells. *International journal of cancer,* **108**(3), pp. 334-341.

LU, Y., ZI, X., ZHAO, Y., MASCARENHAS, D. and POLLAK, M., 2001. Insulin-like growth factor-I receptor signaling and resistance to trastuzumab (Herceptin). *Journal of the National Cancer Institute,* **93**(24), pp. 1852-1857.

LUNKES, A. and MANDEL, J., 1998. A Cellular Model That Recapitulates Major Pathogenic Steps of Huntington's Disease. *Human molecular genetics,* **7**(9), pp. 1355-1361.

LV, H., ZHANG, M., SHANG, Z., LI, J., ZHANG, S., LIAN, D. and ZHANG, R., 2017. Genome-wide haplotype association study identify the FGFR2 gene as a risk gene for acute myeloid leukemia. *Oncotarget,* **8**(5), pp. 7891-7899.

LYOO, H., VAN DER SCHAAR, HILDE M., DOROBANTU, C.M., RABOUW, H.H., STRATING, J.R.P.M. and VAN KUPPEVELD, FRANK J. M., 2019. ACBD3 Is an Essential Pan-enterovirus Host Factor That Mediates the Interaction between Viral 3A Protein and Cellular Protein PI4KB. *mBio,* **10**(1), pp. e02742-18.

MAAG, R.S., MANCINI, M., ROSEN, A. and MACHAMER, C.E., 2005. Caspase-resistant Golgin-160 disrupts apoptosis induced by secretory pathway stress and ligation of death receptors. *Molecular biology of the cell,* **16**(6), pp. 3019-3027.

MADEIRA, F., PARK, Y.M., LEE, J., BUSO, N., GUR, T., MADHUSOODANAN, N., BASUTKAR, P., TIVEY, A.R.N., POTTER, S.C., FINN, R.D. and LOPEZ, R., 2019. The EMBL-EBI search and sequence analysis tools APIs in 2019. *Nucleic acids research,* **47**, pp. W636-W641.

MANCINI, M., MACHAMER, C.E., ROY, S., NICHOLSON, D.W., THORNBERRY, N.A., CASCIOLA-ROSEN, L. and ROSEN, A., 2000. Caspase-2 Is Localized at the Golgi Complex and Cleaves Golgin-160 during Apoptosis. *J Cell Biol,* **149**(3), pp. 603.

MASCIARI, S., LARSSON, N., SENZ, J., BOYD, N., KAURAH, P., KANDEL, M.J., HARRIS, L.N., PINHEIRO, H.C., TROUSSARD, A., MIRON, P., TUNG, N., OLIVEIRA, C., COLLINS, L., SCHNITT, S., GARBER, J.E. and HUNTSMAN, D., 2007. Germline E-cadherin mutations in familial lobular breast cancer. *Journal of medical genetics,* **44**(11), pp. 726-731.

MCLAUGHLIN, R.P., HE, J., VAN DER NOORD, VERA E., REDEL, J., FOEKENS, J.A., MARTENS, J.W.M., SMID, M., ZHANG, Y. and VAN DE WATER, B., 2019. A kinase inhibitor

screen identifies a dual cdc7/CDK9 inhibitor to sensitise triple-negative breast cancer to EGFR-targeted therapy. *Breast Cancer Research,* **21**(1), pp. 77.

MCLEAN, E., COGSWELL, M., EGLI, I., WOJDYLA, D. and DE BENOIST, B., 2009. Worldwide prevalence of anaemia, WHO Vitamin and Mineral Nutrition Information System, 1993-2005. *Public health nutrition,* **12**(4), pp. 444-454.

MCNAMARA, C.W., LEE, M.C., LIM, C.S., LIM, S.H., ROLAND, J., SIMON, O., YEUNG, B.K., CHATTERJEE, A.K., MCCORMACK, S.L., MANARY, M.J., ZEEMAN, A.M., DECHERING, K.J., KUMAR, T.S., HENRICH, P.P., GAGARING, K., IBANEZ, M., KATO, N., KUHEN, K.L., FISCHLI, C., NAGLE, A., ROTTMANN, M., PLOUFFE, D.M., BURSULAYA, B., MEISTER, S., RAMEH, L., TRAPPE, J., HAASEN, D., TIMMERMAN, M., SAUERWEIN, R.W., SUWANARUSK, R., RUSSELL, B., RENIA, L., NOSTEN, F., TULLY, D.C., KOCKEN, C.H., GLYNNE, R.J., BODENREIDER, C., FIDOCK, D.A., DIAGANA, T.T. and WINZELER, E.A., 2013. Targeting Plasmodium PI(4)K to eliminate malaria. *Nature,* **504**(7479), pp. 248-253.

MCPHAIL, J.A., OTTOSEN, E.H., JENKINS, M.L. and BURKE, J.E., 2017. The Molecular Basis of Aichi Virus 3A Protein Activation of Phosphatidylinositol 4 Kinase IIIÎ², PI4KB, through ACBD3. *Structure,* **25**(1), pp. 121-131.

MENENDEZ, J.A. and LUPU, R., 2007. Fatty acid synthase and the lipogenic phenotype in cancer pathogenesis. *Nature Reviews Cancer,* **7**, pp. 763.

MILAZZO, G., SCIACCA, L., PAPA, V., GOLDFINE, I.D. and VIGNERI, R., 1997. ASPB10 insulin induction of increased mitogenic responses and phenotypic changes in human breast epithelial cells: evidence for enhanced interactions with the insulin-like growth factor-I receptor. *Molecular carcinogenesis,* **18**(1), pp. 19-25.

MILLER, W.L., 2013. Steroid hormone synthesis in mitochondria. *Molecular and cellular endocrinology; Mitochondrial endocrinology â€“ Mitochondria as key to hormones and metabolism,* **379**(1), pp. 62-73.

MILLER, W.L. and AUCHUS, R.J., 2011. The Molecular Biology, Biochemistry, and Physiology of Human Steroidogenesis and Its Disorders. *Endocrine reviews,* **32**(1), pp. 81-151.

MIRINOV, A.A. and BEZNOUSSENKO, G.V., 2011. Molecular mechanisms responsible for formation of Golgi ribbon. *Histology and Histopathology,* **26**(1), pp. 117-133.

MOHAN, S., SHEENA, A., POULOSE, N. and ANILKUMAR, G., 2010. Molecular Dynamics Simulation Studies of GLUT4: Substrate-Free and Substrate-Induced Dynamics and ATP-Mediated Glucose Transport Inhibition. *PLOS ONE,* **5**(12), pp. e14217.

MOLINARI, A., CIANFRIGLIA, M., MESCHINI, S., CALCABRINI, A. and ARANCIA, G., 1994. P-glycoprotein expression in the Golgi apparatus of multidrug-resistant cells. *International journal of cancer,* **59**(6), pp. 789-795.

MONTGOMERY, K.G., GERTIG, D.M., BAXTER, S.W., MILNE, R.L., DITE, G.S., MCCREDIE, M.R.E., GILES, G.G., SOUTHEY, M.C., HOPPER, J.L. and CAMPBELL, I.G., 2003. The ***HER2*** I655V Polymorphism and Risk of Breast Cancer in Women < Age 40 Years. *Cancer Epidemiol Biomarkers Prev,* **12**(10), pp. 1109.

MOOG-LUTZ, C., TOMASETTO, C., RÉGNIER, C.H., WENDLING, C., LUTZ, Y., MULLER, D., CHENARD, M., BASSET, P. and RIO, M., 1997. MLN64 exhibits homology with the steroidogenic acute regulatory protein (STAR) and is over-expressed in human breast carcinomas. *International Journal of Cancer,* **71**(2), pp. 183-191.

MORAN, O., NIKITINA, D., ROYER, R., POLL, A., METCALFE, K., NAROD, S.A., AKBARI, M.R. and KOTSOPOULOS, J., 2017. Revisiting breast cancer patients who previously tested negative for BRCA mutations using a 12-gene panel. *Breast cancer research and treatment,* **161**(1), pp. 135-142.

MORROW, A.A., ALIPOUR, M.A., BRIDGES, D., YAO, Z., SALTIEL, A.R. and LEE, J.M., 2014. The Lipid Kinase PI4KIIIB Is Highly Expressed in Breast Tumors and Activates Akt in Cooperation with Rab11a. *Mol Cancer Res,* **12**(10), pp. 1492.

MOYER, B.D. and BALCH, W.E., 2001. 1 - Structural Basis for Rab Function: An Overview. In: W.E. BALCH, C.J. DER and A. HALL, eds, *Methods in Enzymology.* Academic Press, pp. 3-6.

MURPHY, S., MARTIN, S. and PARTON, R.G., 2009. Lipid droplet-organelle interactions; sharing the fats. *Biochimica et Biophysica Acta (BBA) - Molecular and Cell Biology of Lipids; Lipid Droplets as dynamic organelles connecting influx, efflux and storage of lipids,* **1791**(6), pp. 441-447.

MUSTAFA, M., LEE, J.Y. and KIM, M.H., 2015. CTCF negatively regulates HOXA10 expression in breast cancer cells. *Biochemical and biophysical research communications,* **467**(4), pp. 828-834.

NAGY, A., LÁNCZKY, A., MENYHÁRT, O. and GYŐRFFY, B., 2018. Validation of miRNA prognostic power in hepatocellular carcinoma using expression data of independent datasets. *Scientific Reports,* **8**(1), pp. 9227.

NAHTA, R., YUAN, L.X., ZHANG, B., KOBAYASHI, R. and ESTEVA, F.J., 2005. Insulin-like growth factor-I receptor/human epidermal growth factor receptor 2 heterodimerization contributes to trastuzumab resistance of breast cancer cells. *Cancer research,* **65**(23), pp. 11118-11128.

NANAYAKKARA, A.K., VOGEL, P.D. and WISE, J.G., 2019. Prolonged inhibition of P-glycoprotein after exposure to chemotherapeutics increases cell mortality in multidrug resistant cultured cancer cells. *PLOS ONE,* **14**(6), pp. e0217940.

NATIONAL INSTITUTE FOR HEALTH AND CARE EXCELLENCE, 2018. *Early and locally advanced breast cancer: diagnosis and management.*

NATIONAL INSTITUTE FOR HEALTH AND CARE EXCELLENCE, 2017. *Advanced breast cancer: diagnosis and treatment.*

NGEOW, J., SESOCK, K. and ENG, C., 2017. Breast cancer risk and clinical implications for germline PTEN mutation carriers. *Breast cancer research and treatment,* **165**(1), pp. 1-8.

NHS ENGLAND, 2018-last update, Chemotherapy protocol, Breast cancer, Everolimus and Exemestane. Available:

https://www.uhs.nhs.uk/Media/SUHTExtranet/Services/Chemotherapy-SOPs/Breastcancer/Everolimus-Exemestane.pdf [04/21, 2020].

OCHSNER, S., ABRAHAM, D., MARTIN, K., DING, W., MCOWITI, A., WANG, Z., ANDREANO, K., HAMILTON, R.A., CHEN, Y., HAMILTON, A., GANTNER, M.L., DEHART, M., QU, S., HILSENBECK, S.G., BECNEL, L.B., BRIDGES, D., MA'AYAN, A., HUSS, J.M., STOSSI, F., FOULDS, C.E., KRALLI, A., MCDONNELL, D.P. and MCKENNA, N.J., 2018. The Signaling Pathways Project: an integrated 'omics knowledgebase for mammalian cellular signaling pathways. *bioRxiv,* , pp. 401729.

OH, S., OH, C. and YOO, K.H., 2017. Functional roles of CTCF in breast cancer. *BMB reports,* **50**(9), pp. 445-453.

OKAZAKI, Y. and GLASS, J., 2017. Protoporphyrin IX regulates peripheral benzodiazepine receptor associated protein 7 (PAP7) and divalent metal transporter 1 (DMT1) in K562 cells. *Biochemistry and Biophysics Reports,* **10**, pp. 26-31.

OKAZAKI, Y., MA, Y., YEH, M., YIN, H., LI, Z., YEH, K. and GLASS, J., 2012. DMT1 (IRE) expression in intestinal and erythroid cells is regulated by peripheral benzodiazepine receptor-associated protein 7. *American Journal of Physiology-Gastrointestinal and Liver Physiology,* **302**(10), pp. G1180-G1190.

ORSETTI, B., NUGOLI, M., CERVERA, N., LASORSA, L., CHUCHANA, P., ROUGÉ, C., URSULE, L., NGUYEN, C., BIBEAU, F., RODRIGUEZ, C. and THEILLET, C., 2006. Genetic profiling of chromosome 1 in breast cancer: mapping of regions of gains and losses and identification of candidate genes on 1q. *British journal of cancer,* **95**, pp. 1439.

OSKARSSON, T., ACHARYYA, S., ZHANG, X.H.-., VANHARANTA, S., TAVAZOIE, S.F., MORRIS, P.G., DOWNEY, R.J., MANOVA-TODOROVA, K., BROGI, E. and MASSAGUÉ, J., 2011. Breast cancer cells produce tenascin C as a metastatic niche component to colonize the lungs. *Nature medicine,* **17**(7), pp. 867-874.

PANARELLA, A., BEXIGA, M.G., GALEA, G., O' NEILL, E.D., SALVATI, A., DAWSON, K.A. and SIMPSON, J.C., 2016. A systematic High-Content Screening microscopy approach reveals key roles for Rab33b, OATL1 and Myo6 in nanoparticle trafficking in HeLa cells. *Scientific Reports,* **6**, pp. 28865.

PAPA, V., GLIOZZO, B., CLARK, G.M., MCGUIRE, W.L., MOORE, D., FUJITA-YAMAGUCHI, Y., VIGNERI, R., GOLDFINE, I.D. and PEZZINO, V., 1993. Insulin-like growth factor-I receptors are overexpressed and predict a low risk in human breast cancer. *Cancer research,* **53**(16), pp. 3736-3740.

PAPA, V., PEZZINO, V., COSTANTINO, A., BELFIORE, A., GIUFFRIDA, D., FRITTITTA, L., VANNELLI, G.B., BRAND, R., GOLDFINE, I.D. and VIGNERI, R., 1990. Elevated insulin receptor content in human breast cancer. *The Journal of clinical investigation,* **86**(5), pp. 1503-1510.

PAPLOMATA, E. and O'REGAN, R., 2014. The PI3K/AKT/mTOR pathway in breast cancer: targets, trials and biomarkers. *Medical Oncology,* **6**(4), pp. 154-166.

PEITZSCH, C., TYUTYUNNYKOVA, A., PANTEL, K. and DUBROVSKA, A., 2017. Cancer stem cells: The root of tumor recurrence and metastases. *Seminars in cancer biology; Progress in Biological Understanding of Cancer Metastasis,* **44**, pp. 10-24.

PERCY, L., MANSOUR, D. and FRASER, I., 2017. Iron deficiency and iron deficiency anaemia in women. *Best practice & research.Clinical obstetrics & gynaecology,* **40**, pp. 55-67.

PERILLO, B., DI DONATO, M., PEZONE, A., DI ZAZZO, E., GIOVANNELLI, P., GALASSO, G., CASTORIA, G. and MIGLIACCIO, A., 2020. ROS in cancer therapy: the bright side of the moon. *Experimental & molecular medicine,* **52**(2), pp. 192-203.

PETERSEN, P.H., ZOU, K., HWANG, J.K., JAN, Y.N. and ZHONG, W., 2002. Progenitor cell maintenance requires numb and numblike during mouse neurogenesis. *Nature,* **419**, pp. 929.

PETRIDIS, C., SHINOMIYA, I., KOHUT, K., GORMAN, P., CANEPPELE, M., SHAH, V., TROY, M., PINDER, S.E., HANBY, A., TOMLINSON, I., TREMBATH, R.C., ROYLANCE, R., SIMPSON, M.A. and SAWYER, E.J., 2014. Germline CDH1 mutations in bilateral lobular carcinoma in situ. *British journal of cancer,* **110**(4), pp. 1053-1057.

PFAU, R., TZATSOS, A., KAMPRANIS, S.C., SEREBRENNIKOVA, O.B., BEAR, S.E. and TSICHLIS, P.N., 2008. Members of a family of JmjC domain-containing oncoproteins immortalize embryonic fibroblasts via a JmjC domain-dependent process. *Proceedings of the National Academy of Sciences of the United States of America,* **105**(6), pp. 1907-1912.

PINTO, D., VASCONCELOS, A., COSTA, S., PEREIRA, D., RODRIGUES, H., LOPES, C. and MEDEIROS, R., 2004. HER2 polymorphism and breast cancer risk in Portugal. *European journal of cancer prevention : the official journal of the European Cancer Prevention Organisation (ECP),* **13**(3), pp. 177-181.

POHLMANN, P.R., MAYER, I.A. and MERNAUGH, R., 2009. Resistance to Trastuzumab in Breast Cancer. *Clinical cancer research : an official journal of the American Association for Cancer Research,* **15**(24), pp. 7479-7491.

PUPUTTI, M., SIHTO, H., ISOLA, J., BUTZOW, R., JOENSUU, H. and NUPPONEN, N.N., 2006. Allelic imbalance of HER2 variant in sporadic breast and ovarian cancer. *Cancer genetics and cytogenetics,* **167**(1), pp. 32-38.

PUSCH, W., BALVERS, M., HUNT, N. and IVELL, R., 1996. A novel endozepine-like peptide (ELP) is exclusively expressed in male germ cells. *Molecular and cellular endocrinology,* **122**(1), pp. 69-80.

QUINTERO, M., BRENNAN, P.A., THOMAS, G.J. and MONCADA, S., 2006. Nitric oxide is a factor in the stabilization of hypoxia-inducible factor-1alpha in cancer: role of free radical formation. *Cancer research,* **66**(2), pp. 770-774.

RABOUILLE, C., MISTELI, T., WATSON, R. and WARREN, G., 1995. Reassembly of Golgi stacks from mitotic Golgi fragments in a cell-free system. *The Journal of cell biology,* **129**(3), pp. 605-618.

RAJAPAKSHA, M., KAUR, J., BOSE, M., WHITTAL, R.M. and BOSE, H.S., 2013. Cholesterol-Mediated Conformational Changes in the Steroidogenic Acute Regulatory Protein Are Essential for Steroidogenesis. *Biochemistry,* **52**(41), pp. 7242-7253.

RAZAVI, P., CHANG, M.T., XU, G., BANDLAMUDI, C., ROSS, D.S., VASAN, N., CAI, Y., BIELSKI, C.M., DONOGHUE, M.T.A., JONSSON, P., PENSON, A., SHEN, R., PAREJA, F., KUNDRA, R., MIDDHA, S., CHENG, M.L., ZEHIR, A., KANDOTH, C., PATEL, R., HUBERMAN, K., SMYTH, L.M., JHAVERI, K., MODI, S., TRAINA, T.A., DANG, C., ZHANG, W., WEIGELT, B., LI, B.T., LADANYI, M., HYMAN, D.M., SCHULTZ, N., ROBSON, M.E., HUDIS, C., BROGI, E., VIALE, A., NORTON, L., DICKLER, M.N., BERGER, M.F., IACOBUZIO-DONAHUE, C.A., CHANDARLAPATY, S., SCALTRITI, M., REIS-FILHO, J.S., SOLIT, D.B., TAYLOR, B.S. and BASELGA, J., 2018. The Genomic Landscape of Endocrine-Resistant Advanced Breast Cancers. *Cancer cell,* **34**(3), pp. 427-438.e6.

REEDIJK, M., ODORCIC, S., CHANG, L., ZHANG, H., MILLER, N., MCCREADY, D.R., LOCKWOOD, G. and EGAN, S.E., 2005. High-level coexpression of JAG1 and NOTCH1 is observed in human breast cancer and is associated with poor overall survival. *Cancer research,* **65**(18), pp. 8530-8537.

RESNICK, R.J., TAYLOR, S.J., LIN, Q. and SHALLOWAY, D., 1997. Phosphorylation of the Src substrate Sam68 by Cdc2 during mitosis. *Oncogene,* **15**(11), pp. 1247-1253.

RESNIK, J.L., REICHART, D.B., HUEY, K., WEBSTER, N.J. and SEELY, B.L., 1998. Elevated insulin-like growth factor I receptor autophosphorylation and kinase activity in human breast cancer. *Cancer research,* **58**(6), pp. 1159-1164.

REYA, T. and CLEVERS, H., 2005. Wnt signalling in stem cells and cancer. *Nature,* **434**(7035), pp. 843-850.

REYER, H., SHIRALI, M., PONSUKSILI, S., MURANI, E., VARLEY, P.F., JENSEN, J. and WIMMERS, K., 2017. Exploring the genetics of feed efficiency and feeding behaviour traits in a pig line highly selected for performance characteristics. *Molecular Genetics and Genomics,* **292**(5), pp. 1001-1011.

RHEINBAY, E., PARASURAMAN, P., GRIMSBY, J., TIAO, G., ENGREITZ, J.M., KIM, J., LAWRENCE, M.S., TAYLOR-WEINER, A., RODRIGUEZ-CUEVAS, S., ROSENBERG, M., HESS, J., STEWART, C., MARUVKA, Y.E., STOJANOV, P., CORTES, M.L., SEEPO, S., CIBULSKIS, C., TRACY, A., PUGH, T.J., LEE, J., ZHENG, Z., ELLISEN, L.W., IAFRATE, A.J., BOEHM, J.S., GABRIEL, S.B., MEYERSON, M., GOLUB, T.R., BASELGA, J., HIDALGO-MIRANDA, A., SHIODA, T., BERNARDS, A., LANDER, E.S. and GETZ, G., 2017. Recurrent and functional regulatory mutations in breast cancer. *Nature,* **547**(7661), pp. 55-60.

RICHARDSON, D.R. and PONKA, P., 1997. The molecular mechanisms of the metabolism and transport of iron in normal and neoplastic cells. *Biochimica et Biophysica Acta (BBA) - Reviews on Biomembranes,* **1331**(1), pp. 1-40.

ROCHE, S., FUMAGALLI, S. and COURTNEIDGE, S.A., 1995. Requirement for Src family protein tyrosine kinases in G2 for fibroblast cell division. *Science (New York, N.Y.),* **269**(5230), pp. 1567-1569.

ROSAS, H.D., CHEN, Y.I., DOROS, G., SALAT, D.H., CHEN, N., KWONG, K.K., BUSH, A., FOX, J. and HERSCH, S.M., 2012. Alterations in Brain Transition Metals in Huntington Disease: An Evolving and Intricate Story. *Archives of Neurology,* **69**(7), pp. 887-893.

ROSS-INNES, C.S., STARK, R., TESCHENDORFF, A.E., HOLMES, K.A., ALI, H.R., DUNNING, M.J., BROWN, G.D., GOJIS, O., ELLIS, I.O., GREEN, A.R., ALI, S., CHIN, S.F., PALMIERI, C., CALDAS, C. and CARROLL, J.S., 2012. Differential oestrogen receptor binding is associated with clinical outcome in breast cancer. *Nature,* **481**(7381), pp. 389-393.

ROSTOKER, R., ABELSON, S., BITTON-WORMS, K., GENKIN, I., BEN-SHMUEL, S., DAKWAR, M., ORR, Z.S., CASPI, A., TZUKERMAN, M. and LEROITH, D., 2015. Highly specific role of the insulin receptor in breast cancer progression. *Endocrine-related cancer,* **22**(2), pp. 145-157.

RUBY, M.A., RIEDL, I., MASSART, J., ÅHLIN, M. and ZIERATH, J.R., 2017. Protein kinase N2 regulates AMP kinase signaling and insulin responsiveness of glucose metabolism in skeletal muscle. *American journal of physiology.Endocrinology and metabolism,* **313**(4), pp. E483-E491.

RUSSO, J. and RUSSO, I.H., 2006. The role of estrogen in the initiation of breast cancer. *The Journal of steroid biochemistry and molecular biology,* **102**(1-5), pp. 89-96.

SARAN, U., FOTI, M. and DUFOUR, J., 2015. Cellular and molecular effects of the mTOR inhibitor everolimus. *Clinical science,* **129**(10), pp. 895-914.

SARITAS-YILDIRIM, B., PLINER, H.A., OCHOA, A. and SILVA, E.M., 2015. Genome-Wide Identification and Expression of Xenopus F-Box Family of Proteins. *PloS one,* **10**(9), pp. e0136929-e0136929.

SASAKI, J., ISHIKAWA, K., ARITA, M. and TANIGUCHI, K., 2012. ACBD3 mediated recruitment of PI4KB to picornavirus RNA replication sites. *EMBO J,* **31**(3), pp. 754.

SBODIO, J.I., HICKS, S.W., SIMON, D. and MACHAMER, C.E., 2006. GCP60 Preferentially Interacts with a Caspase-generated Golgin-160 Fragment. *Journal of Biological Chemistry,* **281**(38), pp. 27924-27931.

SBODIO, J.I. and MACHAMER, C.E., 2007. Identification of a Redox-sensitive Cysteine in GCP60 That Regulates Its Interaction with Golgin-160. *Journal of Biological Chemistry,* **282**(41), pp. 29874-29881.

SBODIO, J.I., PAUL, B.D., MACHAMER, C.E. and SNYDER, S.H., 2013. Golgi protein ACBD3 mediates neurotoxicity associated with Huntington's disease. *Cell reports,* **4**(5), pp. 890-897.

SCHEUERMANN, T.H., YANG, J., ZHANG, L., GARDNER, K.H. and BRUICK, R.K., 2007. Hypoxia-inducible factors Per/ARNT/Sim domains: structure and function. *Methods in enzymology,* **435**, pp. 3-24.

SCHLAFSTEIN, A.J., WITHERS, A.E., RUDRA, S., DANELIA, D., SWITCHENKO, J.M., MISTER, D., HARARI, S., ZHANG, H., DADDACHA, W., EHDAIVAND, S., LI, X., TORRES, M.A. and YU, D.S., 2018. CDK9 Expression Shows Role as a Potential Prognostic Biomarker in Breast Cancer Patients Who Fail to Achieve Pathologic Complete Response after

Neoadjuvant Chemotherapy. *International journal of breast cancer,* **2018**, pp. 6945129-6945129.

SCHMIDT, A., DURGAN, J., MAGALHAES, A. and HALL, A., 2007. Rho GTPases regulate PRK2/PKN2 to control entry into mitosis and exit from cytokinesis. *The EMBO journal,* **26**(6), pp. 1624-1636.

SEIMIYA, H., MURAMATSU, Y., OHISHI, T. and TSURUO, T., 2005. Tankyrase 1 as a target for telomere-directed molecular cancer therapeutics. *Cancer Cell,* **7**(1), pp. 25-37.

SENGUPTA, S., OBIORAH, I., MAXIMOV, P.Y., CURPAN, R. and JORDAN, V.C., 2013. Molecular mechanism of action of bisphenol and bisphenol A mediated by oestrogen receptor alpha in growth and apoptosis of breast cancer cells. *British journal of pharmacology,* **169**(1), pp. 167-178.

SEWER, M.B. and LI, D., 2008. Regulation of steroid hormone biosynthesis by the cytoskeleton. *Lipids,* **43**(12), pp. 1109-1115.

SHEN, W., AZHAR, S. and KRAEMER, F.B., 2015. Lipid Droplets and Steroidogenic Cells. *Experimental cell research,* **340**(2), pp. 209-214.

SHIBUYA, M., 2011. Vascular Endothelial Growth Factor (VEGF) and Its Receptor (VEGFR) Signaling in Angiogenesis: A Crucial Target for Anti- and Pro-Angiogenic Therapies. *Genes & cancer,* **2**(12), pp. 1097-1105.

SHIN, H.J., KU, K.B., KIM, S., KIM, H.S., KIM, Y.S., KIM, B.T., KIM, S.J. and KIM, C., 2021. A Crucial Role of ACBD3 Required for Coxsackievirus Infection in Animal Model Developed by AAV-Mediated CRISPR Genome Editing Technique. *Viruses,* **13**(2), pp. 237. doi: 10.3390/v13020237.

SHINODA, Y., FUJITA, K., SAITO, S., MATSUI, H., KANTO, Y., NAGAURA, Y., FUKUNAGA, K., TAMURA, S. and KOBAYASHI, T., 2012. Acyl-CoA binding domain containing 3 (ACBD3) recruits the protein phosphatase PPM1L to ER-Golgi membrane contact sites. *FEBS letters,* **586**(19), pp. 3024-3029.

SHORT, B., PREISINGER, C., KÖRNER, R., KOPAJTICH, R., BYRON, O. and BARR, F.A., 2001. A GRASP55-rab2 effector complex linking Golgi structure to membrane traffic. *J Cell Biol,* **155**(6), pp. 877.

SHORTER, J., WATSON, R., GIANNAKOU, M., CLARKE, M., WARREN, G. and BARR, F.A., 1999. GRASP55, a second mammalian GRASP protein involved in the stacking of Golgi cisternae in a cellâ€• free system. *EMBO J,* **18**(18), pp. 4949.

SHOSHAN-BARMATZ, V., KRELIN, Y. and SHTEINFER-KUZMINE, A., 2018. VDAC1 functions in Ca2+ homeostasis and cell life and death in health and disease. *Cell calcium; Ca2+-transport systems and their implication in cell death & survival,* **69**, pp. 81-100.

SLAMON, D.J., CLARK, G.M., WONG, S.G., LEVIN, W.J., ULLRICH, A. and MCGUIRE, W.L., 1987. Human breast cancer: correlation of relapse and survival with amplification of the HER-2/neu oncogene. S. *Science,* **235**(4785), pp. 177-182.

SLAMON, D.J., LEYLAND-JONES, S., SHAK, S., PATON, V., BAJAMONDE, A., FLEMING, T., EIERMANN, W., WOLTER, J., BASELGA, J. and NORTON, L.W., 1998. Addition of Herceptin (humanized anti-HER2 antibody) to first line chemotherapy for HER2 overexpressing metastatic breast cancer (HER2+/MBC) markedly increases anti-cancer activity: a randomised multinational controlled phase III trial. . *Procedings of the American Society of Clinical Oncology,* **16**, pp. 377.

SLAMON, D.J., LEYLAND-JONES, B., SHAK, S., FUCHS, H., PATON, V., BAJAMONDE, A., FLEMING, T., EIERMANN, W., WOLTER, J., PEGRAM, M., BASELGA, J. and NORTON, L., 2001. Use of Chemotherapy plus a Monoclonal Antibody against HER2 for Metastatic Breast Cancer That Overexpresses HER2. *N Engl J Med,* **344**(11), pp. 783-792.

SMIRAGLIA, D.J. and PLASS, C., 2002. The study of aberrant methylation in cancer via restriction landmark genomic scanning. *Oncogene,* **21**(35), pp. 5414-5426.

SOHDA, M., MISUMI, Y., YAMAMOTO, A., YANO, A., NAKAMURA, N. and IKEHARA, Y., 2001. Identification and Characterization of a Novel Golgi Protein, GCP60, That Interacts with the Integral Membrane Protein Giantin. *Journal of Biological Chemistry,* **276**(48), pp. 45298-45306.

SOLOVIEV, M., ESTEVES, M.P., AMIRI, F., CROMPTON, M.R. and RIDER, C.C., 2013. Elevated transcription of the gene QSOX1 encoding quiescin Q6 sulfhydryl oxidase 1 in breast cancer. *PloS one,* **8**(2), pp. e57327.

SOUPENE, E., KAO, J., CHENG, D.H., WANG, D., GRENINGER, A.L., KNUDSEN, G.M., DERISI, J.L. and KUYPERS, F.A., 2016. Association of NMT2 with the acyl-CoA carrier ACBD6 protects the N-myristoyltransferase reaction from palmitoyl-CoA. *Journal of lipid research,* **57**(2), pp. 288-298.

SOUPENE, E., SERIKOV, V. and KUYPERS, F.A., 2008. Characterization of an acyl-coenzyme A binding protein predominantly expressed in human primitive progenitor cells. *Journal of lipid research,* **49**(5), pp. 1103-1112.

SOUPENE, E., WANG, D. and KUYPERS, F.A., 2014. Remodeling of host phosphatidylcholine by Chlamydia acyltransferase is regulated by acyl-CoA binding protein ACBD6 associated with lipid droplets. *MicrobiologyOpen,* **4**(2), pp. 235-251.

SPELL, C., KÖLSCH, H., LÜTJOHANN, D., KERKSIEK, A., HENTSCHEL, F., DAMIAN, M., VON BERGMANN, K., RAO, M.L., MAIER, W. and HEUN, R., 2004. SREBP-1a Polymorphism Influences the Risk of Alzheimer's Disease in Carriers of the ApoE4 Allele. *Dementia and geriatric cognitive disorders,* **18**(3-4), pp. 245-249.

STENMARK, H., 2009. Rab GTPases as coordinators of vesicle traffic. *Nature Reviews Molecular Cell Biology,* **10**, pp. 513.

STORZ, P., 2005. Reactive oxygen species in tumor progression. *Frontiers in bioscience : a journal and virtual library,* **10**, pp. 1881-1896.

STRUSHKEVICH, N., MACKENZIE, F., CHERKESOVA, T., GRABOVEC, I., USANOV, S. and PARK, H., 2011. Structural basis for pregnenolone biosynthesis by the mitochondrial

monooxygenase system. *Proceedings of the National Academy of Sciences of the United States of America,* **108**(25), pp. 10139-10143.

STYLIANOU, S., CLARKE, R.B. and BRENNAN, K., 2006. Aberrant Activation of Notch Signaling in Human Breast Cancer. *Cancer Res,* **66**(3), pp. 1517.

SVENDSEN, A.M., WINGE, S.B., ZIMMERMANN, M., LINDVIG, A.B., WARZECHA, C.B., SAJID, W., HORNE, M.C. and DE MEYTS, P., 2013. Down-regulation of cyclin G2 by insulin, IGF-I (insulin-like growth factor 1) and X10 (AspB10 insulin): role in mitogenesis. *Biochemical Journal,* **457**(1), pp. 69-77.

TAMAZATO LONGHI, M., MAGALHÃES, M., REINA, J., MORAIS FREITAS, V. and CELLA, N., 2016. EGFR Signaling Regulates Maspin/SerpinB5 Phosphorylation and Nuclear Localization in Mammary Epithelial Cells. *PloS one,* **11**(7), pp. e0159856.

TAN, J. and BRILL, J.A., 2014. Cinderella story: PI4P goes from precursor to key signaling molecule. *Critical reviews in biochemistry and molecular biology,* **49**(1), pp. 33-58.

TANG, D., YUAN, H., VIELEMEYER, O., PEREZ, F. and WANG, Y., 2012. Sequential phosphorylation of GRASP65 during mitotic Golgi disassembly. *Biology Open,* **1**(12), pp. 1204.

TANG, Z., LI, C., KANG, B., GAO, G., LI, C. and ZHANG, Z., 2017. GEPIA: a web server for cancer and normal gene expression profiling and interactive analyses. *Nucleic acids research,* **45**, pp. W98-W102.

TASKINEN, J.P., VAN AALTEN, D.,M., KNUDSEN, J. and WIERENGA, R.K., 2007. High resolution crystal structures of unliganded and liganded human liver ACBP reveal a new mode of binding for the acyl-CoA ligand. *Proteins,* **66**(1), pp. 229-238.

TAYLOR, S.J. and SHALLOWAY, D., 1994. An RNA-binding protein associated with Src through its SH2 and SH3 domains in mitosis. *Nature,* **368**(6474), pp. 867-871.

THORAT, M.A., MARCHIO, C., MORIMIYA, A., SAVAGE, K., NAKSHATRI, H., REIS-FILHO, J.S. and BADVE, S., 2008. Forkhead box A1 expression in breast cancer is associated with luminal subtype and good prognosis. *Journal of clinical pathology,* **61**(3), pp. 327-332.

TOMASETTO, C., RÉGNIER, C., MOOG-LUTZ, C., MATTEI, M.G., CHENARD, M.P., LIDEREAU, R., BASSET, P. and RIO, M.C., 1995. Identification of Four Novel Human Genes Amplified and Overexpressed in Breast Carcinoma and Localized to the q11-q21.3 Region of Chromosome 17. *Genomics,* **28**(3), pp. 367-376.

TONG, J.H., FANT, X., DUPREZ, E., BENOIT, G., UPHOFF, C.C., DREXLER, H.G., PLA, J.C., LOFVENBERG, E. and LANOTTE, M., 1998. Expression patterns of the JEM-1 gene in normal and tumor cells: ubiquity contrasting with a faint, but retinoid-induced, mRNA expression in promyelocytic NB4 cells. *Leukemia.,* **12**(11), pp. 1733-1740.

TOWNSEND, D.M., HE, L., HUTCHENS, S., GARRETT, T.E., PAZOLES, C.J. and TEW, K.D., 2008. NOV-002, a glutathione disulfide mimetic, as a modulator of cellular redox balance. *Cancer research,* **68**(8), pp. 2870-2877.

TOYOKUNI, S., OKAMOTO, K., YODOI, J. and HIAI, H., 1995. Persistent oxidative stress in cancer. *FEBS letters,* **358**(1), pp. 1-3.

TREGEI, S., YI, S., NGOZI, W. and BRIAN, S., 2010. Rab33b and Rab6 are Functionally Overlapping Regulators of Golgi Homeostasis and Trafficking. *Traffic,* **11**(5), pp. 626-636.

TRUSCHEL, S.T., ZHANG, M., BACHERT, C., MACBETH, M.R. and LINSTEDT, A.D., 2012. Allosteric Regulation of GRASP Protein-dependent Golgi Membrane Tethering by Mitotic Phosphorylation. *Journal of Biological Chemistry,* **287**(24), pp. 19870-19875.

TUNG, N., LIN, N.U., KIDD, J., ALLEN, B.A., SINGH, N., WENSTRUP, R.J., HARTMAN, A.R., WINER, E.P. and GARBER, J.E., 2016. Frequency of Germline Mutations in 25 Cancer Susceptibility Genes in a Sequential Series of Patients With Breast Cancer. *Journal of clinical oncology : official journal of the American Society of Clinical Oncology,* **34**(13), pp. 1460-1468.

TZENG, H. and WANG, Y., 2016. Rab-mediated vesicle trafficking in cancer. *Journal of Biomedical Science,* **23**, pp. 70.

UEMURA, T., SHEPHERD, S., ACKERMAN, L., JAN, L.Y. and JAN, Y.N., 1989. numb, a gene required in determination of cell fate during sensory organ formation in Drosophila embryos. *Cell,* **58**(2), pp. 349-360.

UGHACHUKWU, P. and UNEKWE, P., 2012. Efflux pump-mediated resistance in chemotherapy. *Annals of medical and health sciences research,* **2**(2), pp. 191-198.

UJJAINWALA, A.L., COURTNEY, C.D., RHOADS, S.G., RHODES, J.S. and CHRISTIAN, C.A., 2018. Genetic loss of diazepam binding inhibitor in mice impairs social interest. *Genes, Brain and Behavior,* **17**(5), pp. e12442.

ULLRICH, O., STENMARK, H., ALEXANDROV, K., HUBER, L.A., KAIBUCHI, K., SASAKI, T., TAKAI, Y. and ZERIAL, M., 1993. Rab GDP dissociation inhibitor as a general regulator for the membrane association of rab proteins. *Journal of Biological Chemistry,* **268**(24), pp. 18143-18150.

VAN DER LEE, M.M., GROOTHUIS, P.G., UBINK, R., VAN DER VLEUTEN, M.A., VAN ACHTERBERG, T.A., LOOSVELD, E.M., DAMMING, D., JACOBS, D.C., ROUWETTE, M., EGGING, D.F., VAN DEN DOBBELSTEEN, D., BEUSKER, P.H., GOEDINGS, P., VERHEIJDEN, G.F., LEMMENS, J.M., TIMMERS, M. and DOKTER, W.H., 2015. The Preclinical Profile of the Duocarmycin-Based HER2-Targeting ADC SYD985 Predicts for Clinical Benefit in Low HER2-Expressing Breast Cancers. *Molecular cancer therapeutics,* **14**(3), pp. 692-703.

VAN LESSEN, M., NAKAYAMA, M., KATO, K., KIM, J.M., KAIBUCHI, K. and ADAMS, R.H., 2015. Regulation of vascular endothelial growth factor receptor function in angiogenesis by numb and numb-like. *Arteriosclerosis, Thrombosis, and Vascular Biology,* **35**(8), pp. 1815-1825.

VAN RAAMSDONK, J.M., MURPHY, Z., SELVA, D.M., HAMIDIZADEH, R., PEARSON, J., PETERSÉN, Á, BJÖRKQVIST, M., MUIR, C., MACKENZIE, I.R., HAMMOND, G.L., VOGL, A.W., HAYDEN, M.R. and LEAVITT, B.R., 2007. Testicular degeneration in Huntington disease. *Neurobiology of disease,* **26**(3), pp. 512-520.

VAN WEEGHEL, M., TE BRINKE, H., VAN LENTHE, H., KULIK, W., MINKLER, P.E., STOLL, M.S.K., SASS, J., JANSSEN, U., STOFFEL, W., SCHWAB, K.O., WANDERS, R.J.A., HOPPEL, C.L. and HOUTEN, S.M., 2012. Functional redundancy of mitochondrial enoyl-CoA isomerases in the oxidation of unsaturated fatty acids. *The FASEB Journal,* **26**(10), pp. 4316-4326.

VERDI, J.M., SCHMANDT, R., BASHIRULLAH, A., JACOB, S., SALVINO, R., CRAIG, C.G., PROGRAM, A.E.S.T., LIPSHITZ, H.D. and MCGLADE, C.J., 1996. Mammalian NUMB is an evolutionarily conserved signaling adapter protein that specifies cell fate. *Current Biology,* **6**(9), pp. 1134-1145.

WALT, A., AJ, S., BROOKS, S. and CORTEZ, A., 1976. The surgical implications of estrophile protein estimation in carcinoma of the breast. *Surgery,* **80**, pp. 506-12.

WANG, J.B., ERICKSON, J.W., FUJI, R., RAMACHANDRAN, S., GAO, P., DINAVAHI, R., WILSON, K.F., AMBROSIO, A.L., DIAS, S.M., DANG, C.V. and CERIONE, R.A., 2010. Targeting mitochondrial glutaminase activity inhibits oncogenic transformation. *Cancer cell,* **18**(3), pp. 207-219.

WANG, Z., LIU, H. and LIU, S., 2016. Low-Dose Bisphenol A Exposure: A Seemingly Instigating Carcinogenic Effect on Breast Cancer. *Advanced science (Weinheim, Baden-Wurttemberg, Germany),* **4**(2), pp. 1600248-1600248.

WATROWSKI, R., CASTILLO-TONG, D.C., WOLF, A., SCHUSTER, E., FISCHER, M.B., SPEISER, P. and ZEILLINGER, R., 2015. HER2 Codon 655 (Ile/Val) Polymorphism and Breast Cancer in Austrian Women. *Anticancer Research,* **35**(12), pp. 6667-6670.

WAUGH, M.G., 2014. Amplification of Chromosome 1q Genes Encoding the Phosphoinositide Signalling Enzymes PI4KB. *AKT3, {PIP}5K1A and {PI}3KC2B in Breast Cancer.Journal of Cancer,* **5**(9), pp. 790-796.

WEI, L.L., SHERIDAN, P.L., KRETT, N.L., FRANCIS, M.D., TOFT, D.O., EDWARDS, D.P. and HORWITZ, K.B., 1987. Immunologic analysis of human breast cancer progesterone receptors. 2. Structure, phosphorylation, and processing. *Biochemistry,* **26**(19), pp. 6262-6272.

WESSELS, E., NOTEBAART, R.A., DUIJSINGS, D., LANKE, K., VERGEER, B., MELCHERS, W.J.G. and VAN KUPPEVELD, FRANK J. M., 2006. Structure-Function Analysis of the Coxsackievirus Protein 3A: IDENTIFICATION OF RESIDUES IMPORTANT FOR DIMERIZATION, VIRAL RNA REPLICATION, AND TRANSPORT INHIBITION. *Journal of Biological Chemistry,* **281**(38), pp. 28232-28243.

WHITEHEAD, R.H., BERTONCELLO, I., WEBBER, L.M. and PEDERSEN, J.S., 1983. A New Human Breast Carcinoma Cell Line (PMC42) With Stem Cell Characteristics. I. Morphologic Characterization. *JNCI: Journal of the National Cancer Institute,* **70**(4), pp. 649-661.

WIESE, S., KARUS, M. and FAISSNER, A., 2012. Astrocytes as a source for extracellular matrix molecules and cytokines. *Frontiers in pharmacology,* **3**, pp. 120-120.

WILLIAMSON, E.A., WOLF, I., O'KELLY, J., BOSE, S., TANOSAKI, S. and KOEFFLER, H.P., 2006. BRCA1 and FOXA1 proteins coregulate the expression of the cell cycle-dependent kinase inhibitor p27(Kip1). *Oncogene,* **25**(9), pp. 1391-1399.

WON, K.A. and SPRUCK, C., 2020. Triple-negative breast cancer therapy: Current and future perspectives (Review). *International journal of oncology,* **57**(6), pp. 1245-1261.

WORLD CANCER RESEARCH FUND / AMERICAN INSTITUTE FOR CANCER RESEARCH, 2018. *Diet, Nutrition, Physical activity and Breast Cancer.*

WU, D. and YOTNDA, P., 2011. Production and detection of reactive oxygen species (ROS) in cancers. *Journal of visualized experiments : JoVE,* **(57):3357. doi**(57), pp. 10.3791/3357.

WU, Y., YE, H., LIU, J., MA, Q., YUAN, Y., PANG, Q., LIU, J., KONG, C. and LIU, M., 2020. Prevalence of anemia and sociodemographic characteristics among pregnant and non-pregnant women in southwest China: a longitudinal observational study. *BMC Pregnancy and Childbirth,* **20**(1), pp. 535.

XIANG, Y. and WANG, Y., 2010. GRASP55 and GRASP65 play complementary and essential roles in Golgi cisternal stacking. *The Journal of cell biology,* **188**(2), pp. 237-251.

XIAO, X., LEI, X., ZHANG, Z., MA, Y., QI, J., WU, C., XIAO, Y., LI, L., HE, B. and WANG, J., 2017. Enterovirus 3A facilitates viral replication by promoting PI4KB-ACBD3 interaction. *Journal of virology,* .

XIE, X., TANG, S., CAI, Y., PI, W., DENG, L., WU, G., CHAVANIEU, A. and TENG, Y., 2016. Suppression of breast cancer metastasis through the inactivation of ADP-ribosylation factor 1. *Oncotarget,* **7**(36), pp. 58111-58120.

XIHUA, Y., MENGJING, B., ROMAIN, C., SIYANG, L., JIA, M., LIANHUI, Z., FEIFEI, M., QIANG, Y., PANPAN, Z., SHUAIYANG, J., ROTHMAN, J.E., YI, Q. and INTAEK, L., 2017. ACBD3 functions as a scaffold to organize the Golgi stacking proteins and a Rab33b-GAP. *FEBS letters,* **591**(18), pp. 2793-2802.

XU, W., ZHOU, W., CHENG, M., WANG, J., LIU, Z., HE, S., LUO, X., HUANG, W., CHEN, T., YAN, W. and XIAO, J., 2017. Hypoxia activates Wnt/β-catenin signaling by regulating the expression of BCL9 in human hepatocellular carcinoma. *Scientific Reports,* **7**(1), pp. 40446.

YAN, M., YANG, X., WANG, H. and SHAO, Q., 2018. The critical role of histone lysine demethylase KDM2B in cancer. *American journal of translational research,* **10**(8), pp. 2222-2233.

YANG, M. and PARK, J.Y., 2012. DNA methylation in promoter region as biomarkers in prostate cancer. *Methods in molecular biology (Clifton, N.J.),* **863**, pp. 67-109.

YING, M., TILGHMAN, J., WEI, Y., GUERRERO-CAZARES, H., QUINONES-HINOJOSA, A., JI, H. and LATERRA, J., 2014. Kruppel-like Factor-9 (KLF9) Inhibits Glioblastoma Stemness through Global Transcription Repression and Integrin Î±6 Inhibition. *Journal of Biological Chemistry,* **289**(47), pp. 32742-32756.

YIN-MURPHY, M. and ALMOND, J., 1996. Picornaviruses. In: S. BARON, ed, *Medical Microbiology.* 4th edition edn. Texas: University of Texas Medical Branch at Galveston, pp. Chapter 53.

YOU, W. and MCDONALD, D.M., 2008. The hepatocyte growth factor/c-Met signaling pathway as a therapeutic target to inhibit angiogenesis. *BMB reports,* **41**(12), pp. 833-839.

YU, X., LIU, M. and HOLDEN, D.W., 2016. *Salmonella Effectors SseF and SseG Interact with Mammalian Protein ACBD3 (GCP60) To Anchor Salmonella-Containing Vacuoles at the Golgi Network.*

YUE, X., QIAN, Y., GIM, B. and LEE, I., 2019. Acyl-CoA-Binding Domain-Containing 3 (ACBD3; PAP7; GCP60): A Multi-Functional Membrane Domain Organizer. *International journal of molecular sciences,* **20**(8), pp. 2028.

ZACHAROPOULOU, N., TSAPARA, A., KALLERGI, G., SCHMID, E., TSICHLIS, P.N., KAMPRANIS, S.C. and STOURNARAS, C., 2018. The epigenetic factor KDM2B regulates cell adhesion, small rho GTPases, actin cytoskeleton and migration in prostate cancer cells. *Biochimica et Biophysica Acta (BBA) - Molecular Cell Research,* **1865**(4), pp. 587-597.

ZAHNOW, C.A., 2009. CCAAT/enhancer-binding protein beta: its role in breast cancer and associations with receptor tyrosine kinases. *Expert reviews in molecular medicine,* **11**, pp. e12.

ZHANG, J., SHAO, X., SUN, H., LIU, K., DING, Z., CHEN, J., FANG, L., SU, W., HONG, Y., LI, H. and LI, H., 2016. NUMB negatively regulates the epithelial-mesenchymal transition of triple-negative breast cancer by antagonizing Notch signaling. *Oncotarget,* **7**(38), pp. 61036-61053.

ZHANG, Q., BAI, X., CHEN, W., MA, T., HU, Q., LIANG, C., XIE, S., CHEN, C., HU, L., XU, S. and LIANG, T., 2013. Wnt/β-catenin signaling enhances hypoxia-induced epithelial–mesenchymal transition in hepatocellular carcinoma via crosstalk with hif-1α signaling. *Carcinogenesis,* **34**(5), pp. 962-973.

ZHANG, Y., LIU, S., MICKANIN, C., FENG, Y., CHARLAT, O., MICHAUD, G.A., SCHIRLE, M., SHI, X., HILD, M., BAUER, A., MYER, V.E., FINAN, P.M., PORTER, J.A., HUANG, S.A. and CONG, F., 2011. RNF146 is a poly(ADP-ribose)-directed E3 ligase that regulates axin degradation and Wnt signalling. *Nature cell biology,* **13**, pp. 623.

ZHAO, J., LI, B., HUANG, X., MORELLI, X. and SHI, N., 2017. Structural Basis for the Interaction between Golgi Reassembly-stacking Protein GRASP55 and Golgin45. *The Journal of biological chemistry,* **292**(7), pp. 2956-2965.

ZHENG, Q., FAN, H., MENG, Z., YUAN, L., LIU, C., PENG, Y., ZHAO, W., WANG, L., LI, J. and FENG, J., 2018. Histone demethylase KDM2B promotes triple negative breast cancer proliferation by suppressing p15INK4B, p16INK4A, and p57KIP2 transcription. *Acta Biochimica et Biophysica Sinica,* **50**(9), pp. 897-904.

ZHENJIANG, L., RAO, M., LUO, X., SANDBERG, E., BARTEK, J.,Jr, SCHOUTROP, E., VON LANDENBERG, A., MENG, Q., VALENTINI, D., POIRET, T., SINCLAIR, G., PEREDO, I.H.,

DODOO, E. and MAEURER, M., 2017. Mesothelin-specific Immune Responses Predict Survival of Patients With Brain Metastasis. *EBioMedicine,* **23**, pp. 20-24.

ZHOU, Y., ATKINS, J.B., ROMPANI, S.B., BANCESCU, D.L., PETERSEN, P.H., TANG, H., ZOU, K., STEWART, S.B. and ZHONG, W., 2007. The Mammalian Golgi Regulates Numb Signaling in Asymmetric Cell Division by Releasing ACBD3 during Mitosis. *Cell,* **129**(1), pp. 163-178.

Chapter 9

Appendix

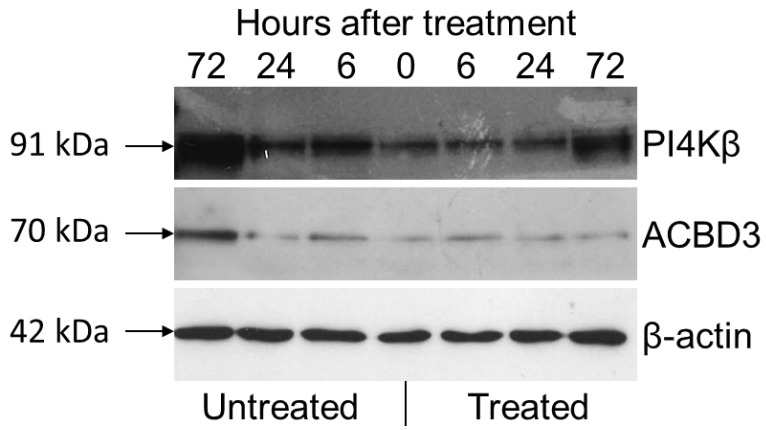

Figure 9.1 - ACBD3 protein did not change over time following everolimus treatment in the T47D cell line but did increase over time in the DMSO only controls. PI4Kβ protein expression increased at 72 hours everolimus treatment but also increased over time in the controls**.** β-actin protein staining was used as a loading control in addition to cell counting before lysis. β-actin exposure = 10 seconds, ACBD3 exposure = 2 minutes, PI4Kβ exposure = 1 minute. Representative blot from n=2. Un cropped version of Figure 5.9.

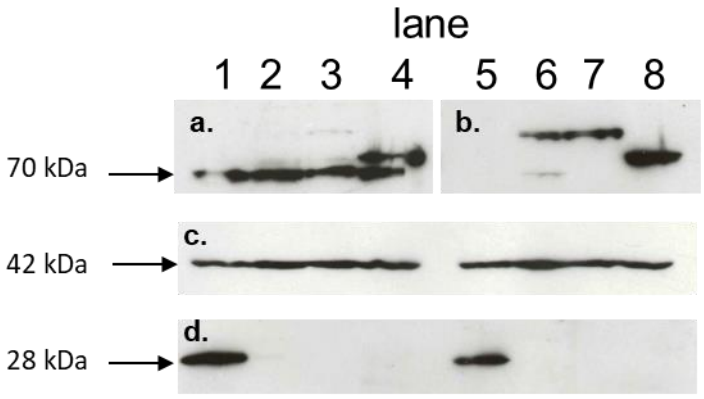

Figure 9.2 – T47D cells were successfully transfected with ACBD3 constructs and protein expression was maintained until the end of experimentation. Uncropped blot from Figure 6.12. All samples on this blot were loaded into one gel and transferred to one nitrocellulose membrane. After blocking the membrane was divided into 4 sections (a-d) for staining with different antibodies. samples were loaded in duplicate (same biological replicate) as follows: lanes 1 and 5 – T47D cells transfected with *eGFP-C3* empty vector, lanes 2 and 6 – T47D cells transfected with *eGFP-C3-ACBD3* vector, lanes 3 and 7 – T47D cells transfected with *eGFP-C3-ACBD3(KQ117AA)* vector, lanes 4 and 8 – T47D cells transfected with *eGFP-C3-ACBD3(K381_R528delinsXX)* vector.

Staining was then carried out as follows: section **a.** anti-ACBD3 antibody, **b.** anti-GFP antibody, **c.** anti- β-actin antibody, **d.** anti GFP-antibody.

note: there is a blank lane between samples 4 and 5.

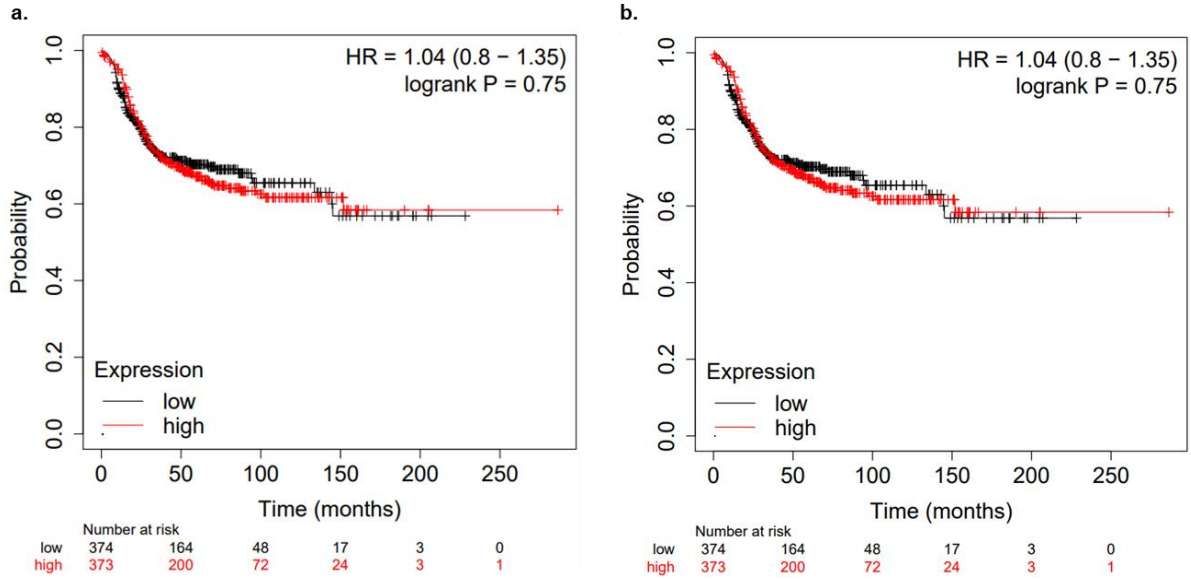

Figure 9.3 – KMplotter results for ER- breast cancer patients when *ACBD3* mRNA expression was above the median (high, red line) or below the median (low, black line). a. Overall survival, and **b.** Distant metastasis free survival**.**